UNIVERSITÉ DE STRASBOURG

ÉCOLE DOCTORALE MATHEMATIQUES, SCIENCES DE L'INFORMATION ET DE L'INGENIEUR

Laboratoire des Sciences de l'Ingénieur, de l'Informatique et de l'Imagerie

THÈSE présentée par :

Loïc MAURER

soutenue le : **17 septembre 2020**

pour obtenir le grade de : **Docteur de l'Université de Strasbourg**

Discipline/ Spécialité : Génie de l'environnement

Mécanismes de transfert et dynamique d'accumulation d'un large spectre de micropolluants au sein de l'écosystème des filtres plantés et de zones de rejet végétalisées associées

THÈSE dirigée par :

Pr. WANKO NGNIEN Adrien	Professeur, ICube - ENGEES
Dr. HEINTZ Dimitri	Ingénieur de recherche - HDR, IBMP

RAPPORTEURS :

Dr. PINEAU Charles	Directeur de recherche, BIOSIT / Université de Rennes 1
Pr. GARCIA Joan	Professeur, GEMMA / Universitat Politècnica de Catalunya Barcelona Tech

---

AUTRES MEMBRES DU JURY :

Pr. HOLLENDER Juliane	Professeure, EAWAG
Pr. BERNIER François	Professeur, IBMP

INVITE :

M. VENANDET Nicolas	Chargé d'études, Assainissement - Eau et Nature en Ville, Agence de l'Eau Rhin Meuse

ACKNOWLEDGEMENT

First of all, I would like to thank Juliane Hollender, Joan Garcia, Charles Pineau and François Bernier for accepting and validating this thesis. It was a great honor that all of you accepting to be part of my thesis jury. I would like to thank you for your feedbacks to improve these research works.

I would also thank l'Agence de l'Eau Rhin Meuse for its financial support and more specifically M. Nicolas Venandet for its engagement in this topic and its help to support our research works at l'Agence de l'Eau Rhin Meuse.

I also wish to express my deepest gratitude and appreciation to my two thesis supervisors Adrien Wanko and Dimtri Heintz. I would like to say that it was a great honor to work with you. I would like to thank you for your patience, the trust placed in me, your scientific knowledge transmitted and all the other great moments. A special thanks for Dimitri and all the great discussion, we had about Alsace-Lorraine (RCSA, FCM etc…) and everything that you have done for me during this thesis.

Claire, I would like to thank you for these last three years. You have been a wonderful help to me during these years and I am very grateful for your engagement in my PhD works, all your advices, the time spent in the lab and for my manuscript. I am very grateful for everything you have done for me during this PhD works.

I would also like to thank all the members of my two teams Julie, Arnaud, Julien, Paul for all the good times during this thesis, their advices and their engagement in my thesis and all the teams of Icube/ENGEES and IBMP.

I would like to thank the PhD students of my teams Elena, Pulchérie, Eloïse, Julie, Mohammad, Lee-Anh, Juan for all this good time in the labs.

Nicolas and Xavier, I am very grateful for all your advices in numerical modelling, your help to resolve my simulations and all the drinks that we have shared during the last six years.
I would like to thank Marie, Martin and Carole for their support in all my experiments in the study field.

I would also like to express my gratitude to my friends Anne-Laure, Audrey, Elisabeth, Eva, Gwen, Floriane, Marie, Morgane, Cyril, Elio, Greg, Loïc, Nico, Thomas, Xavier… I have a special thanks for Audrey and Thomas, for all you have done for me over the years.

Finally, I would like to thank my family for their support over the years. More precisely to my grandparents, my brother Thomas and my parents. I know all the sacrifices you have made to ensure my academic success and I am deeply grateful to you. All your support has been the most precious thing I have ever had.

Summary (in French) of the thesis

La qualité des masses d'eau est devenue une problématique majeure au cours des dernières décennies. En effet, la mise en place de réglementations internationales et nationales pour protéger ces masses d'eau et limiter les risques pour l'environnement et la santé humaine souligne cette importance. Les polluants, et plus particulièrement les micropolluants retrouvés dans l'environnement, peuvent avoir différentes origines, mais les eaux urbaines sont la source la plus mentionnée dans la littérature. Les stations d'épuration des eaux usées ont été mises en place pour traiter ces eaux usées, tout d'abord dans les zones urbaines puis les zones rurales. Or le traitement des eaux usées dans ces zones rurales pose des problèmes spécifiques. Ainsi les filtres plantés de roseaux sont devenus la filière de traitement privilégiée pour répondre à cette problématique dans cet environnement. En effet, ces filtres plantés de roseaux vont utiliser des fonctions naturelles pour traiter les eaux usées (sorption, filtration, biodégradation). En outre, pour compléter ces traitements, des systèmes tels que les zones de rejet végétalisées peuvent être mis en place. Ainsi l'ensemble de cette filière de traitement a prouvé son efficacité pour la dépollution des matières en suspension, des polluants carbonés, azotés et phosphorés, mais n'a pas été conçue en considérant la problématique des micropolluants. Cependant, des études ont montré leur efficacité sur l'abattement d'un certain nombre d'entre eux. Ces études restent néanmoins concentrées sur un nombre restreint de molécules et ne prennent que rarement en considération l'ensemble de l'écosystème. Ainsi l'objectif de l'étude menée vise à décrire et comprendre la distribution et le devenir d'un large spectre de micropolluants en analysant l'ensemble de l'écosystème du filtre planté et de la zone de rejet végétalisée. Pour cela, ce projet de recherche s'est concentré sur trois axes majeurs permettant de répondre à cette problématique :

- une analyse non ciblée des micropolluants au sein de l'écosystème en utilisant la spectrométrie de masse à haute résolution couplée à la chromatographie liquide (LC-HRMS/MS),

- une localisation spécifique des micropolluants au sein des tissus des plantes à l'aide de l'imagerie par spectrométrie de masse (IMS),

- une modélisation numérique de l'écoulement dans les zones de rejet végétalisées par Computational Fluids Dynamic (CFD) couplée à une analyse non ciblée pour comprendre la distribution des micropolluants au sein des différents écoulements.

La première partie de cette thèse est consacrée à l'analyse d'un spectre large des micropolluants dans l'écosystème d'un filtre planté et d'une zone de rejet végétalisée. Ainsi l'eau, les sédiments et les plantes de ce système ont été analysés. Cette analyse s'est tout d'abord concentrée sur une phase de développement. En effet, une méthode d'extraction et d'analyse des micropolluants au sein des différentes matrices a été développée. Cette méthode, basée sur la sublimation et l'extraction liquide, a été optimisée pour l'identification des micropolluants. Ensuite, l'identification des micropolluants a été réalisée par spectrométrie de masse (spectrométrie de masse à haute résolution couplée à la chromatographie liquide (LC-HRMS/MS)) et spectrométrie de masse couplée à la chromatographie en phase gazeuse (GC-MS/MS). L'identification en LC-HRMS/MS ou l'annotation des micropolluants a été effectuée en générant des formules brutes et en suivant la classification mentionnée dans Schymanski et al., 2014. Pour cela, une base de données locale a été produite en collectant les données d'une dizaine de bases de données concernant ces polluants.
Les résultats obtenus montrent que les micropolluants représentent entre 30 % et 50 % du profil métabolique annoté sur les différents compartiments. Cette proportion de micropolluants est également accompagnée par une large distribution des micropolluants au sein de l'écosystème. De plus, une distribution similaire peut être observée entre le filtre planté de roseau et la zone de rejet végétalisé, soulignant cette large diffusion des micropolluants et de leurs produits de dégradation au sein des différents compartiments de l'environnement.
En parallèle, cette analyse non ciblée a également été effectuée sur un profil vertical du sol composant le filtre planté, afin d'évaluer la migration potentielle des micropolluants vers les couches inférieures. À travers cette étude, il a ainsi pu être constaté que les micropolluants vont se diffuser au sein des différents horizons de sol. Au sein de cette distribution, un nombre plus conséquent de composés est détecté dans l'horizon supérieur. À l'opposé, l'horizon inférieur contiendra de manière préférentielle des composés hydrophobes. La couche supérieure (10 premiers centimètres) étant celle séquestrant la plus grande partie des micropolluants, celle-ci joue un rôle clé dans les interactions et contaminations potentielles.

Or, cette distribution ne peut être expliquée sans un questionnement sur le devenir des molécules mères. En effet, la transformation des molécules mères par biodégradation lorsqu'elles sont organiques est souvent mentionnée dans la littérature. Or, ces systèmes composés d'organismes vivants tels que les plantes favorisent cette transformation des composés. Ainsi la seconde partie de cette thèse a porté sur la distribution et la dégradation de micropolluants au sein des plantes. En effet, les plantes se développant au sein du filtre planté ou sur les berges d'une zone humide de traitement tertiaire sont exposées de manière chronique aux micropolluants. Ainsi, cette étude a été réalisée en utilisant l'imagerie par spectrométrie de masse (Matrix-Assisted Laser Desorption/Ionization-Imaging (SolariX) (FT ICR)) sur des plantes poussant au sein des ouvrages de dépollution ou se développant à proximité de ceux-ci. Ce mode d'analyse a également entrainé un développement et une optimisation de la préparation d'échantillons (coupe d'échantillons de plantes).
Ainsi cette distribution a été analysée au sein de différentes plantes. Tout d'abord, la distribution des micropolluants a été étudiée dans les feuilles d'un peuplier noir (*Populus nigra*). En effet, le peuplier est une espèce spontanée qui pousse sur les berges des rivières en Europe. Dans cette étude, une distribution spatiale spécifique des micropolluants au sein des feuilles peut être soulignée. En effet, les micropolluants semblent être stockés préférentiellement dans les régions

périphériques des feuilles de peuplier. Ces résultats suggèrent un mécanisme de stockage au sein de la plante pour la gestion et le confinement de ces polluants.
Cette distribution de micropolluants a ensuite été mise en évidence au sein des feuilles de *Salix alba* (saule, autre plante fréquemment retrouvée au sein des zones de rejet végétalisées). L'objectif de cette seconde étude portait sur le devenir des micropolluants et de leurs métabolites (produits de dégradations et produits conjugués). En effet, un mécanisme de biotransformation semble être observé au sein des feuilles de saules. Ces produits de dégradation n'étant pas retrouvés au sein des échantillons d'eau et de sol, il semble qu'un processus *in planta* apparait. Ce processus est mentionné dans la littérature sous la dénomination de « green liver » en comparaison de ceux se déroulant au sein du foie chez les animaux.
Après avoir étudié la distribution des micropolluants et leurs métabolites dans des feuilles de plantes qui poussent dans des zones de rejets, l'étude s'est concentrée enfin sur la distribution des micropolluants sur une plante entière. En effet, l'imagerie par spectrométrie de masse a été employée sur le profil d'une plante (*Phragmites australis :* roseau, plante référence dans les ouvrages de traitement des eaux usées par les plantes) afin de comprendre la répartition de ces micropolluants au sein des différents organes.

La dernière partie de cette thèse a porté sur les corrélations entre les écoulements hydrodynamiques à travers une zone de rejet végétalisée et la distribution des micropolluants. Pour cela, les écoulements des eaux usées dans la zone de rejet végétalisée ont été simulés en utilisant un modèle numérique 3D (OpenFoam) basé sur la CFD (computational fluid dynamics). Ce modèle 3D a été construit à partir des données GPS collectées sur le site de l'étude et permettant de représenter finement le site d'étude. En parallèle, le débit d'eau d'entrée a été mesuré pendant 2 ans afin de simuler les cas les plus représentatifs. Les modèles d'écoulement puis de transport scalaire ont été validés à l'aide d'expériences de traçage *in situ* réalisées à différentes saisons.
La création du modèle numérique et les résultats de ces simulations ont mis en évidence la présence de zones d'écoulement préférentielles ainsi que des régions à écoulements lents, voire stagnants, au sein de la zone de rejet végétalisée. En considérant ces différentes zones, des échantillons de sédiments (vision intégrative de la pollution) ont été collectés afin d'analyser leur contenu en micropolluants. Cette analyse a été effectuée selon la méthode développée dans la première partie de cette thèse. Les résultats obtenus ont mis mettre en évidence l'influence de l'hydraulique sur la distribution et le devenir des micropolluants.

Table of content

List of abbreviations

AERM: Agence de l'Eau Rhin Meuse

ATC: Anatomic Therapeutic Chemical

BOD_5: Biochemical Oxygen Demand during a period of 5 days

CFD: Computational Fluid Dynamics

CHCA: alpha-Cyano-4-HydroxyCinnamic Acid

COD: Chemical Oxygen Demand

CW: Constructed Wetland

DESI: Desorption ElectroSpray Ionization

DHA: 2,6-DiHydroxyAcetophenone

DHB: 2,5-DiHydroxyBenzoic acid

EI: Electronic Impact

ESI: ElectroSpray Ionization

FT ICR: Fourier Transform—Ion Cyclotron Resonance

GC: Gas Chromatography

GC-MS/MS: Gas Chromatography- tandem Mass Spectrometry

HRMS: High Resolution Mass Spectrometry

IMS: Imagerie par Spectrométrie de Masse

IT: Information Technology

IT: Ion Trap

LAESI: Laser Ablation ElectroSpray Ionization

LC: Liquid Chromatography

LC-HRMS/MS: Liquid Chromatography- tandem High Resolution Mass Spectrometry

LES: Large Eddy Scale

LD_{50}: median Lethal Dose

MALDI: Matrix-Assisted Laser Desorption/Ionization

MS: Mass Spectrometry

MSI: Mass Spectrometry Imaging

PAH: Polycyclic Aromatic Hydrocarbons

RANS: Reynolds Average Navier Stokes

SA: Sinapic Acid

SIMS: Secondary Ion Mass Spectrometry

SPE: Solid Phase Extraction

TKN: Total Kjeldahl Nitrogen

TOF: Time Of Flight

TP: Total Phosphorus

TSS: Total Suspended Solids

VFCW: Vertical Flow Constructed Wetland

WFD: Water Framework Directive

WHO: World Health Organization

WWTP: Waste Water Treatment Plant

List of figures

List of tables

List of supplementary files

General Introduction

Anthropogenic activities and more particularly industrial activities, and our lifestyle have fostered the emergence of contaminants in the environment. All compounds released to the environment, which could generate a risk, or an issue could be called contaminants or pollutants. To deal with the increasing discharge of pollutants into the environment, several treatment systems have been set up in recent decades. But the pollutants concern has also been studied in water for centuries. Indeed, water, due to its multiple uses has always been a resource causing tensions. On the other hand, a large part of contaminants has been released to water since the Antiquity. The main objective of these first sewer systems was to remove stagnant and wastewater pollution from residential areas. This evacuation and concentration at local point to release wastewater have also led to large environmental pollution.

In France and in Europe, national and international regulations to protect water resources were only established in the second half of the twentieth century. The wastewater treatment plant (WWTP) setting up began in the 1960s–1970s years and the contaminants removal objectives were only defined in the French water law in 1992. Besides, these WWTPs were first set up in urban areas, which represent the main pollutants flow released to the environment. However, Water Framework Directive (WFD), adopted in 2000 by the European Commission, which determine the water quality objectives to be reached in the countries of the European Union, has led to the setting up of WWTPs in areas. But the rural context has also its drawbacks. Low cost systems should be implemented, and this context has led to the introduction of extensive water treatment systems. Furthermore, all these WWTPs were generally designed to remove carbon, nutrients and suspended solids pollution, which were the main pollutants issues in the twentieth century, but not designed for micropollutants removal.

In France, most of the WWTPs are well adapted to remove these "conventional" pollutants, but these systems are now facing two main challenges: the sustainability and the emergent contaminants. These emergent contaminants or micropollutants cover a wide compounds variety. But they can be defined as compounds that could have adverse effects on the environment or the human health even in low concentration (ppm, ppb). These micropollutants issues and the potential risks generated, have led to new regulations. The example of Watch lists in the European legislation could well illustrate this new regulation.

Micropollutants can reach the environment using several flow paths (runoffs from agriculture or urban areas, accidental releases…). But in developed countries, urban wastewater (household or industry) remains one of the major points where micropollutants were detected (Ternes and Joss, 2007; Michael et al., 2013; Eggen et al., 2014), WWTPs are one of the main release points

to aquatic environment. To deal with these micropollutants, several processes could be used such as ozonation processes or activated carbon, etc. Nonetheless, the high costs and energy consumption do not fit with extensive treatment systems developed in rural areas. In the local context, the Agence de l'Eau Rhin-Meuse (AERM) promotes the constructed wetland set up and especially tertiary treatment wetlands at the outlet of the WWTPs. These tertiary treatment wetlands could not be considered as treatment systems according to the French law, but have several benefits:

- an alternative to pipes to connect the WWTP to the environment,
- a buffer effect to reduce peak flow downstream for the environment release,
- a complementary treatment.

These systems being a sustainable alternative could also be partly efficient to remove some micropollutants from the aqueous phase. Indeed, in a previous PhD project (Nuel, 2017), the system efficiency to remove drugs was studied. It has been demonstrated that this system could partly remove drugs but the efficiency could be impacted by the seasons. On the other hand, drugs distribution was also investigated in the other compartments (plants, macroinvertebrates and sludge) and showed that compounds specificity could be detected. Nevertheless, this study was only performed using LC-MS/MS target analysis with one micropollutant type: the drugs with 86 compounds. The behavior of these 86 compounds do not necessarily provide a global overview of micropollutants fate in this system. A study focused on selected compounds could bias the general results obtained. But in recent years, the technology advances and more precisely in liquid chromatography coupled in high resolution mass spectrometry (LC-HRMS) have led to screening a vast diversity of micropollutants even at very low concentrations. These advances will be helpful to understand the mechanisms involved in this kind of system. Therefore, this research project has been focused on a large screening of micropollutants in a constructed wetland (CW) and the associated tertiary treatment wetland. This investigation and distribution analysis was conducted considering the following concerns:

- micropollutants large screening development in the main environment compartment (water, sludge, plants),

- micropollutants spatial distribution in the different compartments using MALDI Imaging,
- micropollutants distribution coupled with water flow modeling using Computational Fluid Dynamics (CFD).

In this way, the manuscript will be structured following these axes. Indeed, the first part of the manuscript will be dedicated to the state of the art. In this first chapter, the urban wastewater context, the micropollutants types, their origins and fate in the environment, and the methods used to find or understand their behavior will be detailed. Then the second chapter will be dedicated to the distribution of a micropollutants large screening within the different compartments of the wetlands. The method developed to detect these micropollutants and all the metabolomic workflow will be introduced and commented. Three main examples will be chosen to illustrate this method. Indeed, the environment compartments (water, sludge, plants) in the constructed wetland and the tertiary wetland have been investigated, as the vertical sludge profile of the constructed wetland. The third chapter will be devoted to the micropollutants spatial distribution using mass spectrometry imaging. Non-target screening could provide a general overview of the contaminants, but spatial distribution could also be crucial to understand some bioprocesses. In this chapter, the main interest will focus on the understanding of spatial distribution in living organisms (plants) but also in sludge.
The use of mass spectrometry imaging could help to understand some biological processes and the mechanisms occurring in plants to deal with this stress. But water remains the major vector of micropollutants to the environment. Therefore, the relationship between micropollutants distribution and water flow process should be investigated. The last chapter is dedicated to this relationship. This chapter will be focused on the prediction of water flow areas in an artificial pond wetland using a CFD model and the understanding of water flow influence on micropollutants distribution (using a non-targeted approach). This manuscript will end with a general conclusion which takes up the main ideas detailed in this thesis.

Chapter 1:

State of art

1.1. Urban wastewater and waste water treatment system

1.1.1. Urban wastewater treatment: a gradual improvement to limit the impact of human activities

While being one of the most crucial resources for mankind, water has been one of the first resources polluted by the human activities. The sedentary lifestyle development has raised the fate of waste and specifically the feces.

Since the Antiquity, different civilizations tried to remove these feces from the resident areas. For example, the Minoan civilization (Corrigan 1932) or the Harappa cities (Jansen 1989) illustrate this sanitation beginning. But the prime example is the *Cloaca Maxima* set up in Roma. It was probably the first sewer system in a big city (Hopkins 2007). These systems will reappear in the nineteenth century after the cholera outbreaks. Indeed, John Snow demonstrated that cholera outbreaks in London were linked to polluted water. Therefore, sewer emergence took place gradually in the big cities (London, Paris with Belgrand and Haussman). Nevertheless, the wastewater disposal had to be combined with treatment system to prevent the health risks. Therefore, water treatment before the release into the environment, was gradually introduced for wastewater collected. One of the main examples is probably the development of activated sludge process by Arden and Lockett in 1914.

The first urban wastewater concern was focused on sanitation with health issues and therefore has been associated with the wastewater coming from the domestic activities (urines and feces). But urban wastewater could not be restricted to this aspect. Indeed, domestic activities also generate graywater. This graywater is not directly in contact with feces but could contain some contaminants coming from other domestic activities (shower, washing machines, sink…). Besides domestic activities are not the only source of urban wastewater. Stormwater could also be considered as a part of urban wastewater. For example, rainfall dripping on roofs, or road could be collected in combined sewers and become a part of this urban wastewater. Nevertheless, in the recent years the national authorities tried to separate domestic wastewater from stormwater and promote specific treatment for storm water near the areas where they were generated, as shown by the separative sewer networks development in the new city districts. Finally, urban wastewater could also cover industrial effluents, which contain a wide variety of chemical contaminants. These effluents with new chemical contaminants have led national authorities to set up water treatment before their release in the sewer and the environment.

Nevertheless, these water treatment systems spread widely only in the second half of the twentieth century in Europe. The development of industrial activities has also generated new effluents with chemicals contaminations and led to the water treatment system development.

Indeed, the European directive in 1991 (European Directive 91/271/C.E.E. May 21th 1991) defines the resource objectives and then WWTPs were introduced in the main urban areas. But the performances results were only established in 2000 with the WFD (Directive: 2000/60/C.E.E. October 23rd 2000). The WFD aims for good water quality (surface and ground water) in the European Union and have promoted the WWTPs setting up.

This WWTP setting up has been significantly impacted by these legislation changes. First WWTPs were set up in urban areas with the main pollutants flow. Then, the performance objective introduced in the WFD generated WWTP installations throughout the country and small communities. However, these small communities do not have the same issues and resources than urban areas. In this way, the treatment system used for big cities as activated sludge, most common treatment system, is not well adapted to the rural context. These specific problems and resources should be considered to define the water treatment fitting with the context.

1.1.2. Constructed Wetlands (CWs): wastewater treatment system applied to small communities

The rural specificities have led to the development of wastewater treatment systems adapted to this context. Indeed, low cost and low energy consuming systems have been set up. These extensive systems, as opposed to intensive systems (as activated sludge), were based on natural processes found in the environment.

These systems could be named using the terms of ecological engineering, introduced by Mitsch (Mitsch 2012). One of its definitions mentioned ecological engineering as the use of the surrounding ecosystems to reduce or solve pollution issues. According to this definition, different treatment systems could be set up to clean water without chemical input or high energy consumption (ponds, ditches, bed filters). Kadlec and Wallace define wetlands as “land areas that are wet during part or all of the year because of their location in the landscape” (Kadlec and Wallace, 2009). They define these areas as transition land between terrestrial systems and aquatic systems. Constructed wetlands (CWs) are man-made systems designed in non-wetland

site to treat stormwater or wastewater using the high biological activities found in their ecosystems to improve the pollutant removal abilities (Kadlec and Wallace, 2009). In this way, CWs are fully in line with this approach. As natural wetlands, the CWs are composed of water, plants and a media (soil, gravel…) (Kadlec and Wallace, 2009).

CWs were created during the 1950s in Germany with the experiments of Käthe Seidel (Vymazal 2010) and the CW set up to clean wastewater began in the 1970s (Kickuth 1970). Besides their efficiency to remove pollutants in moderate climates, these systems show their adaptation to all climate types. Indeed, CW are used around the world to treat several effluents (domestics, industrial, stormwater…), as the literature underlines their set up in all the continents (García et al., 2010).

These CWs could be distinguished by the hydraulics modes. The two main CWs types are surface flow and subsurface flow wetlands (Kadlec and Wallace, 2009). The surface flow wetlands mimics natural systems such as ponds or marshes and are mainly used as polishing/ and/or tertiary treatment of effluent from previous water treatment systems (Kadlec and Wallace, 2009). These surface wetlands could also be clustered according to the plant type growing in the wetland (Brix, 1994):

- free-floating macrophyte-based systems,
- emergent macrophyte-based systems,
- submerged macrophyte-based system.

These surface flow wetlands could be compared to the subsurface wetlands. The subsurface wetlands do not have a surfacing water and wastewater flows beneath the surface of the media around the plants rhizomes (Kadlec and Wallace, 2009). This kind of wetlands could be clustered as horizontal subsurface wetlands and vertical flow wetland depending on the hydraulics mode applied. In the horizontal subsurface wetland, a continuous and horizontal water flow is set up. The horizontal subsurface wetland is used as a single-family or small communities water treatment system and it is well adapted for the denitrification processes (Wallace and Knight, 2006). On the other hand, wastewater treatment could also be performed by vertical flow constructed wetlands (VFCWs). This system is widely used in Europe and more particularly in France as a wastewater treatment system for small communities (lower than 2,000 peoples). Therefore, this CW type will be detailed in the next sections. Briefly, water will percolate through the different soil types (organic matter, sand, gravel…) (Kadlec and Wallace, 2009), and in the rhizosphere area to remove carbon, nutrients or total suspended solids by biological processes or filtration.

Finally, these systems mentioned in the literature as traditional CW could be combined to generate hybrid systems. For example, a combination of two VFCWs with a horizontal flow CWs could be used for effluent denitrification in sensitive areas. Besides, these traditional CWs are distinguished from enhanced CW with facilities (ventilation, baffles…). An overview of the different CWs is proposed in the **Figure 1**.

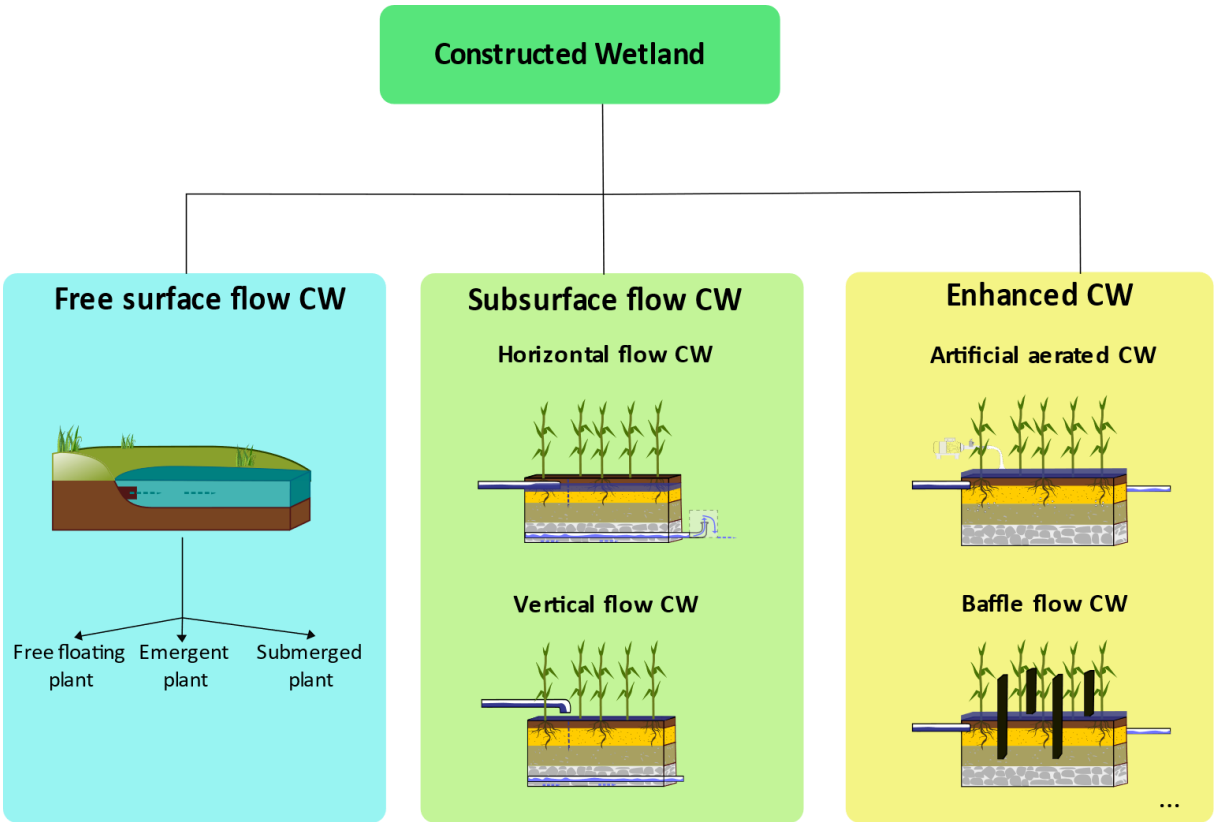

Figure 1: CWs types mentioned in the literature (Kadlec and Wallace, 2009). The traditional CWs without any input are opposed to enhanced CW using facilities (artificial and baffle). Concerning the traditional CWs the hydraulics mode influence could be visualized with the different CW type (subsurface, free surface and vertical flow).

The pollutants removal in these wetlands are based on a combination of physical, chemical, and biological processes. Thus the main processes are sedimentation, adsorption, plant uptake and biological degradation (Brix, 1994; Reddy and D'Angelo, 1997).

These mechanisms could be distinguished in two ways. The pollutants transfers and the biotransformation. Physicochemical mechanisms such as sedimentation, adsorption or volatilization underline the transfers of pollutants from the liquid phase to the gas or solid phase. These transfers could be characterized by several parameters (Henry constant for volatilization, Kow or Kd for sorption, …). A higher log Kow coefficient will indicate a higher hydrophobicity behavior and then a higher ability to be sorbed (Rogers, 1996). Nevertheless, the sorption could

also be influenced by the media characteristics, and the environmental conditions (pH, redox, …) or organic matter (Cottin and Merlin, 2008; Brunsch et al., 2018; Biel-Maeso et al., 2019).

Indeed, biodegradation could be setting up in the different living organisms growing in these systems. The degradation of "conventional" pollutants (carbon, nitrogen or phosphorus) could be performed by the microorganism's metabolism or plant degradation. Nonetheless, the micropollutants could also be degraded by these living organisms. For example, ibuprofen degradation has been shown in reed (He et al., 2017) but also with the combination of microorganisms growing in the media and associated to the plants. Concerning the degradation by microorganisms, micropollutants will be used for co-metabolism due to their low concentration (Luo et al., 2014; Singhal and Perez-Garcia, 2016).

Besides, all these mechanisms could be influenced by several environmental parameters. First to obtain comparable results in the inlet and outlet wastewater and be able to conclude on the system efficiency, the water budget should be established. (Kadlec and Wallace, 2009). Indeed, as these systems mimic the natural processes, they are also influenced by the environmental conditions. Therefore, rainfall, evaporation, evapotranspiration, infiltration and solar radiations should be considered to evaluate wetland efficiency. Besides, these environmental parameters could also influence physico-chemical processes (radiation with the photodegradation, pH for the sorption, …) (Rühmland et al., 2015) and biological processes (temperature, pH, dissolved oxygen, redox potential for the microorganisms communities growing in these systems) (Hijosa-Valsero et al., 2011). On the other hand, the wetland characteristic should also affect these processes. Indeed, hydraulic load rate, water volume (for surface flow wetland) and media characteristics could also alter the mechanisms (Kadlec and Wallace, 2009). The media type (porous or impermeable) could impact water flow inside the wetland and different hydraulics equations will govern the water in these two types of media. Furthermore, media size and porosity are also crucial points concerning the subsurface flow as a non-adapted media could generate clogging in these systems.

In France, more than 70% of the cities have fewer than 1,000 inhabitants. Regarding this population distribution, it seems that VFCWs are well adapted to treat wastewater in these cities with small communities. The CW are not inexpensive treatment systems, but comparatively to other technologies (activated sludge, sequencing batch reactors, …), they represent a low-cost solution (Kadlec and Wallace, 2009) well adapted to the rural context. Besides, the vertical flow constructed wetlands (VFCWs) have become the most popular systems used in France.

Therefore, this state of art will now be focused on VFCW and more precisely on VFCW adapted to the French context.

In France, the environment ministry (ministère de la Transition écologique et solidaire) results underline that CWs represent 4,200 WWTP in 2018. The increases of CWs set up could be observed in **Figure 2** and highlight the impact of WFD and the growing importance of this kind of system in France ("Portail d'informations sur l'assainissement communal - Services en ligne," visited on 01/02/ 2020).

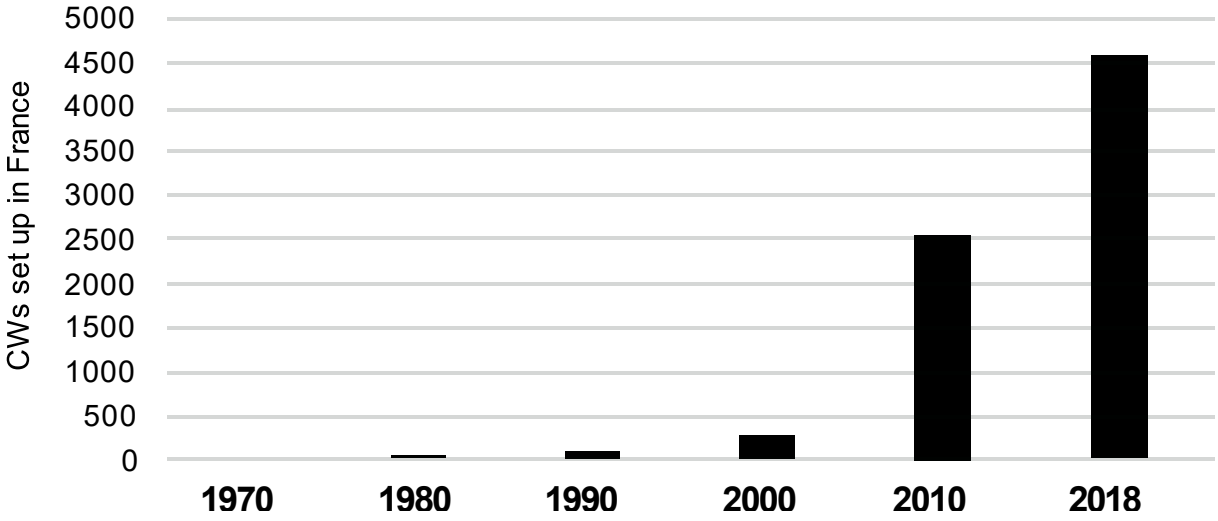

Figure 2: CWs operating in France between 1970 and 2018 ("Portail d'informations sur l'assainissement communal - Services en ligne," visited on 01/02/ 2020).

On the other hand, these CWs can be clustered according to the hydraulics that manages the water treatment. CWs could distinguish those with a horizontal flow and vertical flow constructed wetlands (VFCW). The flow applied in the CW play a key role in the degradation processes that could occur in the CW.

The horizontal flow CW maintains a constant water level. The CW will be partly saturated with water, and anoxic conditions could be observed. These conditions could for example boost the denitrification. On the other hand, VFCWs are bed filters planted with *Phragmites australis*. These beds are alternatively feeding by large batches of wastewater (Kadlec and Wallace, 2009). Then water will percolate in the different soil layers. This percolation will engender aerobic conditions, promoting organic matter degradation, as the bed filters are drained. The VFCWs could also remove total suspended solids (TSS), by filtration process, but they are less efficient for the denitrification process. This system is not only popular in France but also in

several countries in Europe (Austria, Denmark, Germany, United Kingdom) to deal with the pollution sources from small communities (Kadlec and Wallace, 2009).

In France, the classical wastewater treatment system is based on a two-stage VFCWs, where water percolates through the layers as shown in **Figure 3**. This system could be completed with a horizontal flow CW or a pond to refine water treatment particularly for nitrates.

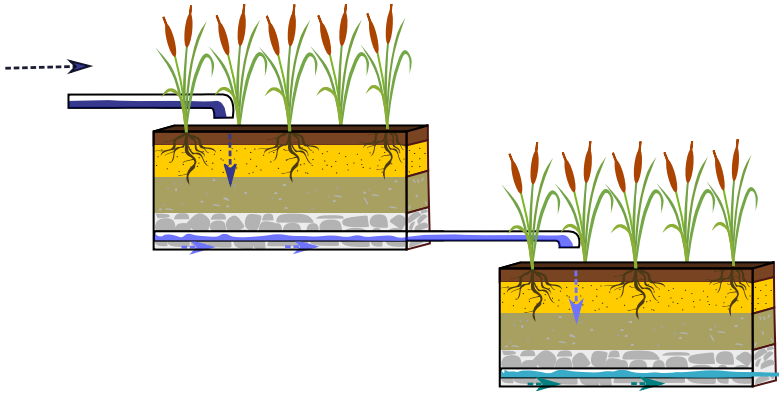

Figure 3: Two stage VFCW system. The main system used in France to treat wastewater.

According to the French law, their expected performances obey the regulation of TSS, biochemical oxygen demand during a period of 5 days (BOD_5), chemical oxygen demand (COD) and total Kjeldahl nitrogen (TKN) (Ruiz 2017). Nevertheless, these WWTP could be located dozen meters from the environment and pipes should be added to connect WWTP to the environment. Nevertheless, more sustainable alternatives could be set up such as tertiary treatment wetland implementation.

1.1.3. Tertiary treatment wetlands

In the French context, these tertiary treatment wetlands could be considered as surface flow wetlands. Connecting the WWTP to the environment, the tertiary treatment wetland could not be considered as a treatment system according to the regulation at the opposite of VFCWs Arrêté du 22 juin 2007 (*Arrêté du 22 juin 2007 relatif à la collecte, au transport et au traitement des eaux usées des agglomérations d'assainissement ainsi qu'à la surveillance de leur fonctionnement et de leur efficacité, et aux dispositifs d'assainissement non collectif recevant une charge brute de pollution organique supérieure à 1,2 kg/j de DBO5.*, 2007). In this way, no regulation defines the removal performance of these systems. Besides, non-conventional design and the lack of procedures have led to different tertiary treatment wetlands. The wetland

design is mainly defined by the site constraints (Nuel 2017). Nevertheless, three main models could be observed in France. These three main classes are

- meadows wetlands,
- pond wetland,
- ditch wetland.

Wetland using other materials (gravels, geomembrane…) could also be mentioned. The three main classes could be observed in **Figure 4**.

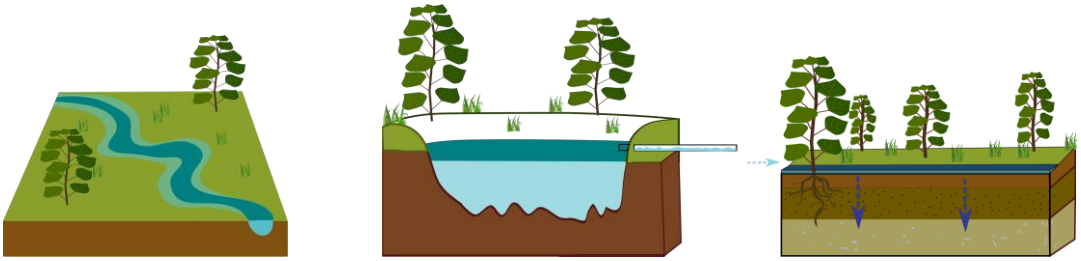

A B C

Figure 4: The main wetland classes used as tertiary treatment in France **A)** Ditches wetland, **B)** Ponds wetland, **C)** Meadows wetland.

The meadow wetland has large flood areas with a gentle slope to the environment and will infiltrate water. On the other hand, pond wetlands were generated by excavating the site. The digging will generate a natural pond where water could flow. The final cluster, ditches wetlands, are similar to pond wetlands, but the length to width ratio is higher and the water depth lower. (Prost-boucle and Boutin, 2012).

All the systems were set up to enhance some processes. The CWs and the tertiary treatment wetlands were designed to improve the quality of water released, considering the carbon, nitrogen and phosphorus. Nevertheless, these systems are chronically exposed to new emergent contaminants and were not designed to treat them.

1.2. Micropollutants: a large panel of molecules with an increasing interest

1.2.1. A continually evolving definition

Micropollutants or emerging contaminants definition covers a wide variety of compounds and this definition have been modified over the years. Moriarty defined micropollutants as

compounds from anthropogenic activities (xenobiotics) detected in higher proportion than naturally occurring amount (Moriarty 1983). Nevertheless, this definition is questionable, as micropollutants remain contaminants with adverse effects, even if they were found naturally in the environment. Therefore, another definition most adapted to our context and widely used in the environmental study introduces micropollutants as all compounds with adverse effects on the environment or human health even in very low concentration (µg/L or ng/L) (Ministère de la transition ecologique, 2015).

The micropollutants could be clustered as inorganic micropollutants (the heavy metals) and organic micropollutants (pesticides, drugs, personal care products, …). According to the European Union, micropollutants could represent more than 110,000 compounds with diverse properties (Ministère de la transition ecologique, 2015).

Compounds found in this definition have changed over the years. Indeed, a better knowledge of the impacts of chemical products and the advances in technology have led the addition of xenobiotics included in this definition. In this way, the different classes were progressively considered over the last decades. The first micropollutants studies were focused on heavy metals, metalloids from industry pollution during the 1970s. Then, pesticides, drugs or personal care products were investigated. This approach has also influenced the scientist literature. Indeed, heavy metals are still the main micropollutants studied, even if an increase of pesticides or drugs studies could be observed in the environmental field. On the other hand, personal care products, considered as a more recent subject area, is only emerging these recent years. An example of this evolution could be illustrated in the **Figure 5** with the progression of published articles focused on the different micropollutants classes in wastewater from 1970 to 2020. The results could be obtained using the keywords “wastewater” + micropollutants classes (for example “drugs” in the title and the keywords) in ScienceDirect.

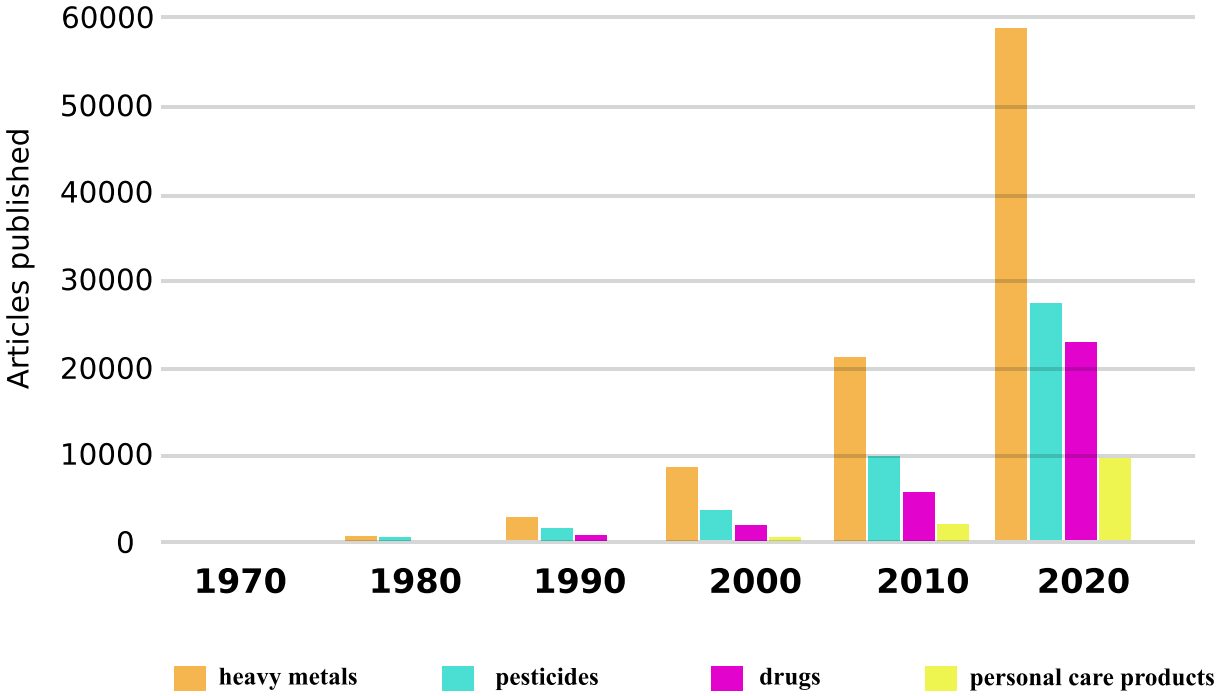

Figure 5: Articles published from 1970 to 2020 with the keywords wastewater and heavy metals or pesticides or drugs or personal products according to the results found in ScienceDirect.

1.2.2. Micropollutants types

The technology development has led to increase the analytical capabilities. Indeed, the advances in LC-HRMS in the recent years have promoted the screening of a vast diversity of micropollutants. On the other hand, the micropollutants concern has also led to new European or national regulations to consider this issue. As mentioned in the introduction, the WFD has defined strategies to restore the waterbodies quality. This WFD has generated different priority substances lists ((*Decision No 2455/2001/EC of the European Parliament and of the Council of 20 November 2001 establishing the list of priority substances in the field of water policy and amending Directive 2000/60/EC (Text with EEA relevance)*, 2001)), which has been extended in 2015 (*Commission Implementing Decision (EU) 2015/495 of 20 March 2015 establishing a watch list of substances for Union-wide monitoring in the field of water policy pursuant to Directive 2008/105/EC of the European Parliament and of the Council (notified under document C (2015) 1756) Text with EEA relevance*, 2015). The limits on concentrations of the priority substances have been defined in (*Directive 2008/105/EC of the European Parliament and of the Council of 16 December 2008 on environmental quality standards in the field of water policy, amending and subsequently repealing Council Directives 82/176/EEC, 83/513/EEC, 84/156/EEC, 84/491/EEC, 86/280/EEC and amending Directive 2000/60/EC of*

the European Parliament and of the Council, 2008). These Watch list and emergent substances screening were also incorporated in the French legislation. A national screening of emergent and hazardous substances in the effluent was carried out in France between 2002 and 2007 (RSDE action Rejets de substances Dangereuses dans les Eaux). Then environment quality concentrations were defined in the French legislation, based on their environmental impact and following the Circulaire du 7 mai 2007 (*Circulaire du 7 mai 2007 DCE/23 définissant les "normes de qualité environnementale provisoires (NQEp)" des 41 substances impliquées dans l'évaluation de l'état chimique des masses d'eau ainsi que des substances pertinentes du programme national de réduction des substances dangereuses dans l'eau*). But most of the compounds investigated did not have any environment quality concentration due to the lack of data on their potential impacts. All these lists or the compound screenings in the aquatic environment raise the origins of these compounds in wastewater. The micropollutants have several origins as micropollutants classes are existing. In this research project, five main classes were detected and are among the main classes found in the literature concerning the municipal wastewater (Deblonde et al., 2011; Luo et al., 2014; Margot et al., 2015; Wang et al., 2017). In this way, these main classes, i.e., polycyclic aromatic hydrocarbons (PAHs), pesticides, drugs, personal care products and heavy metals will be introduced in this section.

1.2.2.1. Hydrocarbon micropollutants: PAHs

PAHs are described as a compound class with carbons and hydrogen and at least two aromatic rings (Abdel-Shafy and Mansour, 2016). They are a part of the non-saturated hydrocarbons and belong to the aromatic hydrocarbons class, which could be divided into monocyclic aromatic hydrocarbons (benzene, toluene, ethylbenzene and xylen (BTEX)) and PAHs. These PAHs could be found in different environment compartments due to their physico-chemicals properties. Generally, most of the PAHs found in the environment are those with 2 to 7 rings (Neff 1979). They represent more than 100 chemical persistent compounds which could be naturally found in the environment.

In the literature, PAHs are mainly studied using the priority list defined by the United States environmental protection agency (US EPA) in 1976 (Keith 2015). The list could be found in the **Figure 6**.

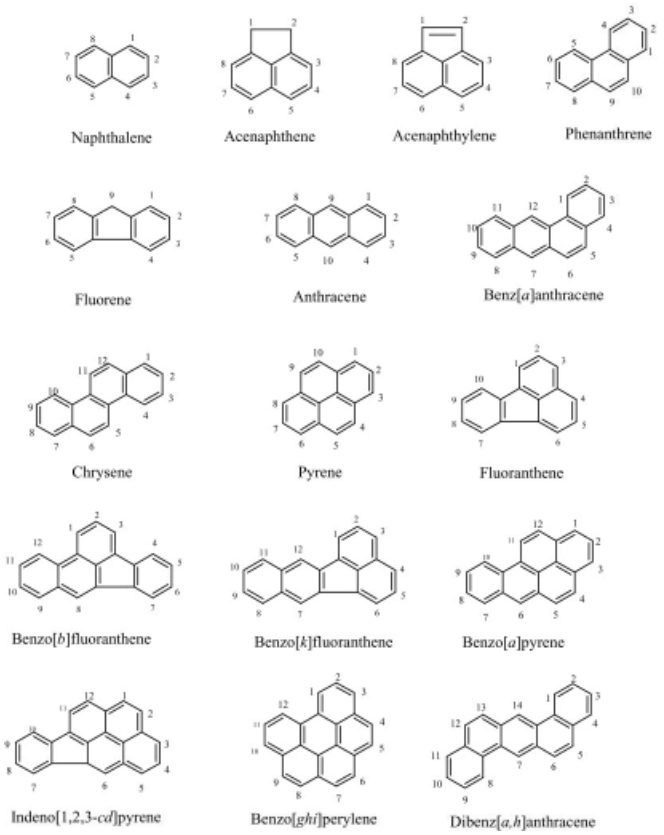

Figure 6: PAHs priority list from the US EPA (Yan, et al., 2014).

In the literature, this list combined to the total hydrocarbon is widely used to determine the PAHs contamination found in the environment and is used for worldwide comparison. Nevertheless, these compounds were listed in the 1970s or 1980s (Andersson and Achten, 2015). But the analytical methods and studies advances have improved our knowledge of these PAHs, and underline the lacks of the identification of some of the most toxic PAHs (Andersson and Achten, 2015).

Different classifications using a broader spectrum of PAHs could be found in the literature. First, the PAHs could be clustered according to their structure (ring numbers). In this way, three main classes are described (Marçais 2017):

- "light" PAHs (fewer than three rings),
- "intermediate" PAHs (four rings),
- "heavy" PAHs (more than four rings).

On the other hand, PAHs could also be grouped according to the pathways (Neff 1979):

- pyrogenic,
- petrogenic biogenic (Grice et al., 2009; Wilcke et al., 2002).

However, most PAHs found in the environment are pyrogenic PAHs, resulting from incomplete burning of organic matter (Kouzayha 2011). Indeed, PAHs are mainly detected due to anthropogenic activities (for example heating or driving) or the fossil fuels burning (Baek et al., 1991; Besombes et al., 2001; Masclet et al., 1986). Depending on the region studied, natural emissions of PAHs could also be noticed with forest fires or volcanic eruptions (Nikolaou et al., 1984).

1.2.2.2. Pesticides: substances controlling organisms harmful to crops

According to the World Health Organization (WHO) definition, pesticide is a general term used for chemical compounds intended for controlling any organism considered harmful to crops. To protect crops, different compounds with diverse pesticides action could be found. This variety of pesticides actions could be illustrated by the examples of isoproturon that inhibits photosynthesis or pendimethalin that blocks the cell division.

As PAHs, the pesticides have also been classified. The international organizations such as European Union or WHO have clustered pesticides following different criteria. For example, pesticides could be clustered as biocide compounds or phytopharmaceutical compounds according to the European regulation (Directive 91/414/CEE du Conseil, du 15 juillet 1991, concernant la mise sur le marché des produits phytopharmaceutiques). The WHO, clustered the pesticides according to the lethal dose (LD_{50}) and then the risk for human health (World Health Organization 2010). Nevertheless, this classification is barely mentioned in the literature. The main clusters used are based on the pesticides target or the chemical structure. The target pesticides classification is focused on the targeted organisms and defines three main classes:

- insecticides,
- herbicides,
- fungicides.

In these different classes, herbicides represent the highest pesticides sales increases in the last dedaces (Carvalho, 2017). Nevertheless, the pesticides use and widespread is depending on the continent considered. Indeed in North America or in Europe herbicides are widely used, due to intensive agriculture, while in Asia a high use of insecticide could be noticed (Carvalho, 2017).

The second classification is based on the pesticides chemical structure. Pesticides could be clustered from the origins (mineral, plant or synthetic compound). This last cluster only used the chemical structure to distinguish compounds. The main classes are

- organochlorines,
- organophosphates,
- carbamates,
- phoenix,
- pyrethroid.

1.2.2.3. Drugs and personal care products: micropollutants linked to domestic activities

Drugs could also present a wide compound diversity, used for human and animals' health. The French Public Health Code defines drugs as all compounds with preventive or curative properties for human or animal health ("Code de la santé publique | Legifrance"). This common objective is one of the few similarities found for all these compounds (Taylor and Senac, 2014). Besides, all the legal compounds found had undergone a marketing authorization process. This process is based on three main steps to validate a drug for a commercial use of an active substance (Lechat 2006):

- the preclinical stage to define the toxicity,
- the first stage with the pharmaco kinetic study,
- the second stage with the dose response and the pharmaco kinetic parameters.

The drugs commercially used could, then, be clustered according to the Anatomic Therapeutic Chemical (ATC) systems and following the WHO recommendations (World Health Organization Collaborating Centre for Drug Statistics Methodology 1996). Nevertheless, this classification is not mainly used by French doctors and the scientist literature. Drugs are mainly classified using the therapeutic classes as anti-inflammatories, analgesics, antidepressants, beta blockers or antibiotics. After their application, drugs will be only partially degraded and excreted in urine, generating a pollution source for wastewater.

On the other hand, domestic activities would also generate a large part of micropollutants found in the environment. Indeed, all these compounds used for the body, beautification or cleaning are found in our daily life and could be gathered in the detergent or personal care products. Toothpaste, shampoo, soap and all cosmetic products are examples of this class of compounds,

which are daily used. But most of them are released in the “gray” water and then in the sewer and the WWTP.

1.2.2.4. Heavy metals and metalloids

The last category mentioned in this manuscript will be the heavy metals and the metalloids. The heavy metals term is a loose term used to define all the metal compounds with adverse effect on the environment (Hodson, 2004). This loose term has generated different definitions based on the density or other properties of these compounds (Hodson, 2004).

This compounds with density higher than 5,000 kg/m^3 are naturally found in the environment (Tchounwou et al., 2012). Heavy metals could also be described as metal elements found between the copper and lead in the Mendeleïev classification. However, these compounds are mainly used in anthropogenic activities such as industry activities or domestic activities. The main activities generating heavy metals are fossil fuels burning, metallurgy, textile, plastic or electronic, electrochemistry, industry and reach the environment through road runoffs or industrial effluents (Cotran et al., 1990; Fergusson, 1990; Hong et al., 1994; Candelone et al., 1995; Freyssinet et al., 2002; Callender, 2003; Sukandar et al., 2006).

Besides, heavy metals could be found in different compounds used in our daily life (painting, flame retardants, electronics) and could be found in the sewer such as personal care products.

Therefore, this section has underlined that diverse micropollutants could be in the environment. Besides the diversity and the number of micropollutants are increasing over the years, by the development of anthropogenic activities. This large variety raises the question of fate and origins of micropollutants found in the environment.

1.3. Origins and fate of micropollutants in the wastewater treatment systems and the environment

1.3.1. Micropollutants emission and potential degradation process

Micropollutants found in the environment result from diverse processes. Some micropollutants such as heavy metals could result from natural processes (eruption, forest fires, rock alteration) (Masindi and Muedi, 2018) and others such as personal care products are coming from anthropogenic activities. Nevertheless, human activities generate the main metals or organic

micropollutants flow to the environment (Ravindra et al., 2008; Warner et al., 2019). This activity development has widely impacted the environment quality.

1.3.1.1. Micropollutants sources

Micropollutants diversity found in the environment could have several origins, due to the variety of classes. For example, volatile compounds can easily disperse in the air and atmospheric transfers and the rainfalls could spread them to the environment. Besides, these volatiles compounds are found in several micropollutants compounds (Abdel-Shafy and Mansour, 2016; Pimentel, 1995), generating a spread to environment. Therefore, the use of this kind of compounds could cause a global environmental issue. The contamination by atmospheric transfers could be described according to three main ways:

- the atmospheric dispersion,
- the rainfalls,
- the rainfall with soil leaching.

The atmospheric dispersion could be illustrated by the example of fuel burning creating hydrocarbons emission or pesticides application in agriculture fields. This transfer to the environment is highly correlated to weather (wind, rain, …) (Gil and Sinfort, 2005). And even if the pesticides should not be applied in windy weather, the contamination by atmospheric transfers should not be neglected. On the other hand, the rainfall could also impact the environment. Indeed, volatile compounds such as PAHs or pesticides will pollute the environment during rainfall events directly or by soil leaching. Rainfall could transfer micropollutants found in the soil after pesticides application or atmospheric deposits to the environment (Marçais 2017). Therefore, the runoffs and the infiltration will contaminate both surface and groundwater.

The leaching could also impact drugs distribution in the environment. Indeed drugs are found in the sewage sludge applied as soil improvement on the agriculture field (Ivanová et al., 2018). Studies have already shown the ability of sludge to sorbe micropollutants (Petrović et al., 2005; Verlicchi et Zambello 2015; Ivanová et al., 2018; Y.-S. Lee et al., 2019; Liu et al., 2019; Pérez-Lemus et al., 2019). Finally, these micropollutants could be released with the soil leaching. Leaching could cause runoffs and will diffuse micropollutants to the environment (Lapworth et

al., 2012). On the other hand, Gros et al., 2019 have underlined that veterinary drugs found in slurry, used as soil improvement, could be infiltrated through different soil layers.

Nevertheless, this pollution characterized as diffuse pollution has generally a lower impact than local micropollutant emission point. The main sources of drugs and all micropollutants from domestic activities are correlated to this local emission point (Eggen, Moeder, et Arukwe 2010). The specific point could represent several activities and the key examples are

- landfills, where unused drugs or personal care products could be found. These micropollutants could be released to the environment due to leaching, percolation and other water infiltration. (Buszka et al., 2009; Eggen et al., 2010; Holm et al., 1995),

- farming or aquaculture where animals could be treated using antibiotics. The use of these drugs could generate direct or indirect environmental contamination near the farms (Haya et al., 2005; Cabello 2006; Burkholder et al., 2007),

- accidental spill with the hydrocarbons could be released to the environment (Le Bihanic 2013),

- septic tanks or on-site sewage facilities when the system is permeable (Blum et al., 2017; Conn et al., 2010; Godfrey et al., 2007; Gros et al., 2017).

Wastewater treatment systems and urban wastewater which are mentioned as the major point where micropollutants were released to the environment (Kasprzyk-Hordern et al., 2009; Luo et al., 2014; Petrie et al., 2015; Phillips et al., 2012; Verlicchi et al., 2012). Indeed, all the domestic activities (cleaning, hygiene, clothes washing, healthcare…) will generate gray water mixed with wastewater and sometimes with storm water, which is released to the WWTP. Nevertheless, these WWTPs were not designed to treat micropollutants. In this way, WWTP became one of the major points where micropollutants can be released to the environment.

The **Figure 7** summarized the various processes that cause the environmental micropollutants contamination.

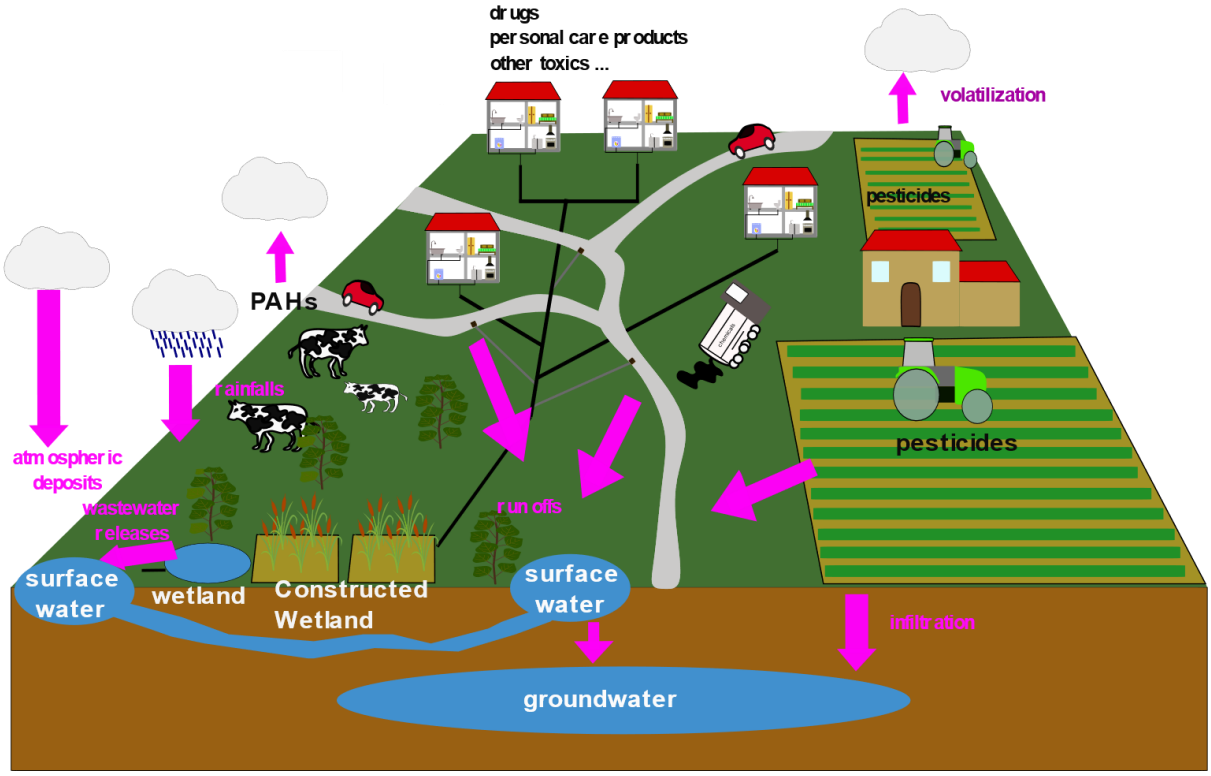

Figure 7: Potential sources of micropollutants found in the environment. The diffuse and the local emission release point are mentioned (WWTP, agriculture activities, domestic activities, leaching…). Besides the different mechanisms occurring in micropollutants transfers could be found (runoffs, volatilization, atmospheric deposits, rainfalls…).

Nevertheless, the micropollutants investigation which only focus on parent compounds underestimate the micropollutants release to the environment. Indeed, the parent compounds could be partly degraded using some metabolization processes generating degradation products called metabolites. These metabolites (catabolite, conjugated or deconjugated compounds) could be found in higher quantity in the environment and could generate a higher toxic risk than the parent compounds (Kosjek et Heath 2008; Kern et al., 2011; Wang et Lin 2012; Herrmann et al., 2015; Yin et al., 2017). For example, Marsik et al., 2017, have demonstrated that ibuprofen (parent compound) represents less than 1% of all the ibuprofen forms found in plants. These results highlight the fact that all the different metabolites should be considered to understand the fate of drugs in the environment.

1.3.1.2. Micropollutants fate

The catabolites and conjugates of organic micropollutants after metabolization cover various compounds coming from transformation processes. Biotic (like digestion) and abiotic (like photodegradation) processes could occur to transform the parent compounds. Furthermore, a spatial and temporal difference could be observed in the metabolites detected. Indeed, this transformation could be performed before the release into the environment, during micropollutants transfers or once it has been caught in an environment compartment. The drugs example could illustrate the transformation before their release. These metabolization processes are highly considered for pharmaceuticals applications. Once the drugs have been absorbed and reach the target organs, it would be removed from the organism. Enzymatic reactions found in the organs and more particularly in liver cells will metabolize the compound (Lechat 2006).

Cytochrome P450 and aryl sulfatase or UDP glucuronyl transferase are the main enzymes involved degrading drugs in the organism. Cytochrome P450 will generate a compound oxidation (Phase I) then a conjugation process (phase II) which could be performed using aryl sulfate or UDP-glucuronyl transferase (Meunier et al., 2004). The main degradation process could be found in **Figure 8**.

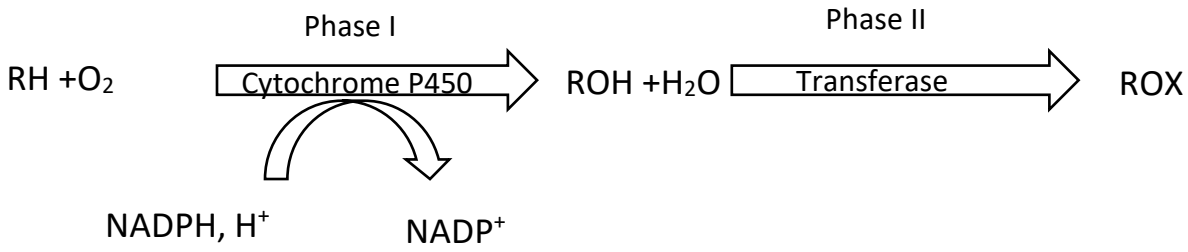

RH : drugs
ROH : metabolites
ROX : sulfate or glucuronic residues

Figure 8: Drugs enzymatic degradation in human body adapted from Meunier et al., 2004 (Meunier, de Visser, et Shaik 2004).

On the other hand, these transformations are compound-dependent, and compounds are not always fully degraded in the organisms. Therefore, parent compounds and their metabolites will be excreted in the urine then found in wastewater.

Furthermore, this transformation resulting from human or animal metabolism is only part of the micropollutants transformation, and it could be only related to some micropollutants classes. Indeed, during the wastewater transport or treatment and release to the environment other metabolization processes could occur. Two main metabolization processes could be distinguished in two groups. First the micropollutants metabolization could be linked to biological activities and then to physico-chemical reactions.

Organic micropollutants degradation using microbial consortium metabolism in the water treatment systems or in the environment has already been studied in the literature (Singhal and Perez-Garcia, 2016). Indeed, Singhal et Perez-Garcia indicate that the use of microorganisms with specific metabolic capabilities such as - heterotrophic sulfate reduction (Zhang and Wang, 2014) autotrophic sulfur-oxidizing denitrification (Hao et al., 2014; Pokorna and Zabranska, 2015) anaerobic methane-oxidation denitrification (Raghoebarsing et al., 2006), partial nitrite reduction to nitrous oxide for energy generation (D. Scherson et al., 2013) and electron shuttle redox biotransformation (Van der Zee and Cervantes, 2009) - will be helpful to promote micropollutants removal. Besides, Singhal et Perez-Garcia show that two-enzyme classes, cytochromes P450 and laccases are classically used to degrade drugs in the organisms and micropollutants in enzyme assays (Harms et al., 2011; Lah et al., 2011; Singhal and Perez-Garcia, 2016). Nevertheless, these micropollutants are mainly used in the co-metabolization due to their low concentration (Singhal and Perez-Garcia, 2016). Besides, this co-metabolization is dependent on the bioavailability (complex structure or function group) (Luo et al., 2014).

On the other hand, these micropollutants could also be caught by plant in the environment or in wastewater treatment systems using plants such as CW, as it has been described for metals. (Verbruggen et al., 2009). Besides plant could also have a key role in this metabolization and the environment detoxification. Indeed, the metabolic processes occurring in plants exposed to micropollutants have already been studied (C. Huber et al., 2009; He et al., 2017; Marsik et al., 2017; Klampfl 2019). Furthermore Marsik et al., (2017), have demonstrated that the

metabolites represent more than 99% and 18 compounds (considering Phase I metabolites) of the organic micropollutants detected.

This detoxification process with three phases has already been described. The first phase (phase I) introduces functional groups and prepare the conjugation occurring in the phase II by oxidation or hydrolysis (Komives and Gullner, 2005). The reactions occurring in the phase I are mainly managed by cytochrome P450 in the endoplasmic reticulum (He et al., 2017; Klampfl 2019). Then the second phase (phase II) deactivates the micropollutants using some transferases. Finally, compounds are stored in specific plant compartments (part of the phytoextraction). In this way, this process working similarly to animal liver has been described as "green liver" in the literature (Sandermann 1999).

On the other hand, physico-chemical reactions could also create micropollutants metabolites. Ozonation process is mainly used to treat micropollutants in water (M. M. Huber et al., 2005; Hollender et al., 2009; Nakada et al., 2007; Zimmermann et al., 2011; Y. Lee et al., 2013) and transform micropollutants.

This process has shown its efficiency but as any degradation processes, it could generate more toxic by-products (Sonntag et Gunten 2012). Furthermore, this system could not be set up in rural areas due to their high costs. However, other physico-chemical processes as photodegradation could occur in these systems. Indeed, the photodegradation is also efficient to degrade micropollutants in wastewater (Mathon et al., 2019; Rühmland et al., 2015) and generate some metabolites.

All the processes could help to degrade the parent compounds but even if degradation products are generated, these WWTPs remain the major point of micropollutants releases.

But this degradation process concerns only organic micropollutants and therefore, inorganic micropollutants will only be transferred in other compartments. As mentioned previously, the plant uptake is one transfer way mentioned in the literature. But for conventional wastewater treatment system, sorption is one of the most mentioned mechanisms explaining their fate (Batool and Saleh, 2020; Kumar et al., 2020). These transfers to the solid phase could also be depending on the metals nature as the sorption differs according to the metals considered (Karvelas et al., 2003).

1.3.2. Wastewater treatment systems: systems degrading micropollutants but also a release point

Micropollutants found in freshwater have become one of the major concerns in the last decades (Schwarzenbach et al., 2006; Richardson, 2009; Margot et al., 2015; Geissen et al., 2015; Busch et al., 2016). And the wastewater treatment systems effluent releases have been described as one of the main sources of these micropollutants in surface water (Huber et al., 2005; Kasprzyk-Hordern et al., 2009; Kolpin et al., 2002). Therefore, studies investigated micropollutants presence in WWTP. These micropollutants are found in both urban and rural areas (Matamoros et al., 2005; Nakada et al., 2007) underling this global issue. Indeed, several national studies were carried out in France such as AMPERES (2006-2009) or ECHIBIOTEB (2010) and indicate this global issue. For example, the AMPERES project suggests that no micropollutants removal efficiency difference could be observed between WWTP or CW systems, when these systems were designed to treat the same conventional pollutants (carbon or carbon and nutrients). More than 10% of the selected compounds and 90% of drugs were found in the effluents with concentrations higher than 100 ng/L pointing up the impact of water treatment system on the micropollutants release. However, the AMPERES project suggests that less substances were quantified in wastewater from rural areas than in urban areas. Even if these systems have been widely described as micropollutants release sources, processes have been set up to improve the micropollutants removal. This process could for example, be based on advanced oxidation processes (ozonation, UV, photo irradiation, Fenton oxidation…) (Singhal and Perez-Garcia, 2016). Nevertheless, these systems could have high costs and would not be adapted to the rural context. The most adapted solution in rural area is to use wetlands with high residence time (Singhal and Perez-Garcia, 2016). Although CW as any water treatment system could release micropollutants, the micropollutant removal study in CW have also highlighted their efficiency to treat some micropollutants (Hijosa-Valsero et al., 2010; Matamoros et al., 2016, 2008, 2005; Nuel et al., 2018). Besides long sludge residence time and hydraulics residence time would have a positive impact of micropollutants removal (Harb et al., 2019).

Nevertheless, a wide diversity of micropollutants removal rate or concentration could be found in these systems. (Nuel et al., 2018; Pereira et al., 2015). Some micropollutants could be released in higher concentrations in outlet water than inlet water. This phenomenon could be partly explained by drugs deconjugaison that could occur during the water transport (Verlicchi and Zambello, 2015). On the other hand, the variety of micropollutants removal rate could be influenced by biotic and abiotic parameters. Indeed a seasonal effect could be found for some

drugs as described in Nuel et al., 2018. Temperature (Hijosa-Valsero et al., 2011), sunlight and photodegradation (Andreozzi et al., 2003) could influence the degradation process by enhancing the bacterial activities, increasing indirectly the hydraulic residence time or at the opposite reducing the degradation with less sunlight. Finally, the physicochemical properties (log Know, pka, Henry constant, solubility…) are mentioned explaining micropollutants removal from the liquid phase. Nevertheless, these parameters cannot fully be exampling the micropollutants distribution in the different environment compartment.

1.3.3. Micropollutants distribution in the different CW compartments

Micropollutants initially found in wastewater will be distributed in the different compartments, during their transport and according to some of their properties. For example, volatile compounds will be found in air compartment too. On the other hand, some of them could be sorbed to solid particles and accumulated in soil/sediment matrices in wetlands or in the environment (Azaroff et al., 2020; Gruchlik et al., 2018). In the literature, it is mentioned that hydrophobic compounds are easily sorbed in solid matrices (Gruchlik et al., 2018). For example, PAHs properties will improve their sorption in solid particles. This sorption capacity is partly depending on the molecular weight. Indeed, heavy PAHs will be sorbed easily in solid matrices (Le Bihanic 2013). On the other hand, micropollutants could also be absorbed by animals, especially in the lipidic tissues, then be accumulated along the food chain (Chevreuil et al., 1995; Derco et al., 2013; Yao et al., 2018), generating a potential human health risk.

Besides, in the wetland such as in river, plants are also growing in this polluted environment. Their capabilities to store micropollutants using different processes have already been mentioned and are described in the **Figure 9**. Indeed, the use of plants combined to microorganisms to remove, degrade or isolate micropollutants or other toxic compounds from contaminated soil has been described as phytoremediation (Chaney et al., 1997; Gadd 2001; Favas et al., 2014). This approach was first focused on metal removal with the use of hyperaccumulating plants. But the role of plants could not be restricted to metal uptake as various compounds could be caught by plants (Favas et al., 2014). Plants have different strategies to remove micropollutants from contaminated environment. The main strategies mentioned are

- phytodegradation that metabolizes contaminants inside plant cells using specific enzymes (mentioned in the section 3.1.2),

- phytoextraction that stores contaminants in specific parts of plants,
- phytostabilization that limits the diffusion of contaminants in soil by trapping and catching them in root cells or humus,
- phytovolatilization that volatilizes and releases compounds into the atmosphere after their transformation (Favas et al., 2014).

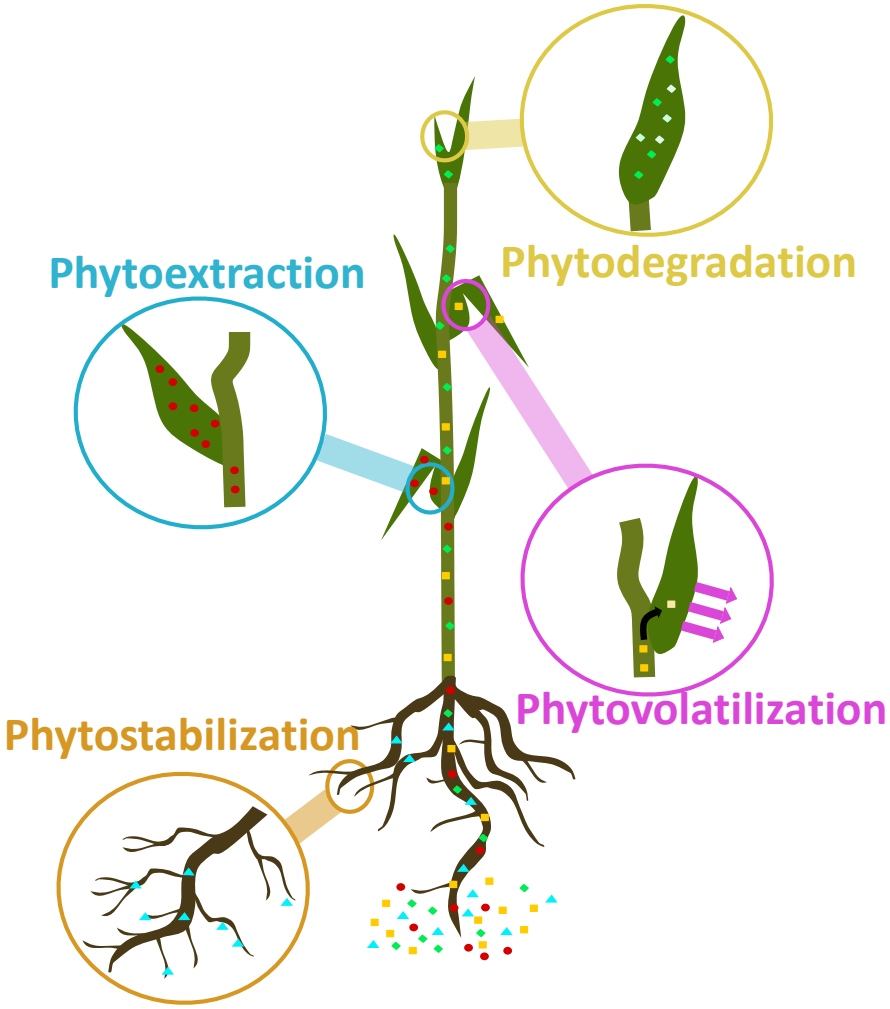

Figure 9: Phytoremediation strategies found in the environment adapted from (Favas et al., 2014). Phytovolatilization, phytostabilization, phytodegradation and phytoextraction are the main mechanisms occurring in plants.

Nevertheless, as mentioned in the previous sections, micropollutants cover a large diversity of compounds. The diversity of compounds analysis has long been a challenge, and the micropollutants detection has involved the analytical tools development. Besides, the increase of this concern has also generated a technological breakthrough to be able to perform non-target screening and obtain an overview of micropollutants in the different environmental matrices.

1.4. Large micropollutants screening in the environment compartments

This section will be focused on the screening in the different compartments of the environment and the different analytical instruments used to detect micropollutants, then the non-target screening of micropollutants using high-resolution mass spectrometry will be developed and finally the use of mass spectrometry imaging to obtain spatial distribution in samples will be described.

1.4.1. Micropollutants screening in the different compartments of the environment and wetland

The analyses found in the 1970s and 1980s were mainly focused on river water (Literáthy, 1975; Meijers and van der Leer, 1976). Nevertheless, the large widespread of micropollutants into the other compartments were also considered. Micropollutants analyses were also performed in the different compartments such as sediments (Literáthy 1975) or in animals like fish (Koli et al., 1980) to understand their toxic effect on the organisms. At the same time, hyperaccumulating plants were studied to remove heavy metals from contaminated soil (Reeves and Brooks, 1983; Wither and Brooks, 1977).

As waste water was identified as one of the major sources, studies were also focused on WWTP to understand the release and the potential removal of micropollutants in this treatment system. (Carballa et al., 2004; Castiglioni et al., 2006; Lindqvist et al., 2005; Radjenović et al., 2009; Ternes, 1998; Vogelsang et al., 2006) but also in sewage sludge produced (Ivanová et al., 2018; Martín et al., 2015). Indeed, this sludge used as soil improvement could also be considered as a potential pollutant source. In the same vein, this approach was also conducted for water treatment adapted to the rural context. Therefore, natural wetlands and constructed wetlands were also investigated to understand their removal performance (Chen et al., 2016; Dordio et al., 2010; Hijosa-Valsero et al., 2011; Matamoros et al., 2008; Matamoros and Bayona, 2006; Petrie et al., 2018; Rühmland et al., 2015).

On the other hand, over the last decades, the advances in technology have generated a breakthrough in micropollutants detection. Several analytical tools could be used to detect emergent contaminants in samples (UV, fluorescence detectors…). Nevertheless, the main technology used is mass spectrometry (MS). In environmental studies MS in tandem with gas chromatography (GC) or with liquid chromatography (LC) is widely used to identify them.

Indeed, the tandem chromatography and MS based on the separation and measurement of mass-to-charge ratio (m/z) of individuals and ionized molecules and their fragmentation products provide high sensitivity and selectivity to detect this kind of compound. Mass spectrometer is characterized by three main elements: the ion sources, analyzer and the detectors as shown in **Figure 10**.

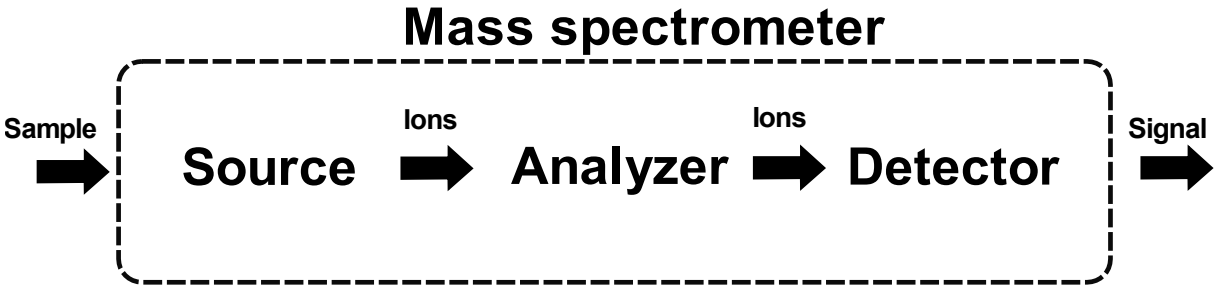

Figure 10: Mass spectrometer composition with the three main components.

The ion source is used to ionize and volatilize compounds. The types of source is based on a different physical principle and the operator should choose the most adapted source according to the characteristics of the molecule to be analyzed (thermal stability, chemical lability, volatile compound, chemical function, molecules size, MS in tandem with GC or LC). In the literature, several sources are mentioned, but the main representatives are

- Electronic Impact (EI) (hard ionization),
- Electrospray Ionization (ESI) (soft ionization),
- Atmospheric Pressure Photoionization (APPI) (soft ionization),
- Matrix Assisted Laser Desorption Ionization (MALDI) (soft ionization).

The second part of the spectrometer concerns the analyzer, which will measure the mass-to-charge ratio (m/z). As mentioned in the sources, different analyzers could be used. The main analyzers found in the mass spectrometer are

- Q: quadrupole mass filter,
- IT: Ion Trap,
- TOF: Time-Of-Flight,
- FT ICR: Fourier Transform—Ion Cyclotron Resonance.

Furthermore, several analyzers (MS-MS and MSn) can be coupled together to perform multidimensional mass spectrometry by successively using the separating power of each

analyzer (TQ, QTOF…). Finally, the chemical signals due to the ions are converted in electrical signals in the detectors and can be used by the operators with computer tools.

In the environmental studies, GC-MS (or GC-MS/MS) or LC-MS (MS/MS) were mainly used to analyze micropollutants. First the analyses were performed using GC-MS, which is well adapted to detect volatile, apolar compounds, PCB (polychlorinated biphenyl), PAHs or some pesticides. Nevertheless, the challenge of pesticides and drugs analysis, with more polar compounds have modified analytical methods. Indeed, the LC-MS using an ESI source is better suited to this kind of compounds. Besides, to obtain a wider range of compounds, the literature mentioned the combination of different sources as ESI and APPI (Chiaia-Hernandez et al., 2013).

In this way, micropollutants could be detected in high precision and with a lower limit of detection threshold thanks to the development of mass spectrometry and the combination of different analyzers (for example triple quadrupole…). Nonetheless, a large part of the environmental study are mainly focused on few numbers of micropollutants or some classes, as TQ are not well adapted for large screening and the detection of unknowns (Chiaia-Hernandez et al., 2013; Krauss et al., 2010). However, the analysis of a restricted number of molecules bias the vision of the contamination and the potential impact on the environment. Indeed, a large part of persistent micropollutants are not eliminated by conventional water treatment systems (Clara et al., 2005; Hug et al., 2014). Therefore, non-target screening of micropollutants was performed using high-resolution mass spectrometry to obtain a large overview of the contaminations found in the compartment considered.

1.4.2. High resolution mass spectrometry and large screening of micropollutants

The high resolution mass spectrometry (HRMS) improvement is based on two technological improvements, the multidimensional chromatography (GCxGC or LCxLC) and the trapping method (TOF, FT ICR, orbitrap…). (Pleil et Isaacs 2016). The capability to detect a large scale of compounds has been improved by this technological change. Indeed, thousands of features could be currently detected in biological or environmental samples (Gago-Ferrero et al., 2016; Pleil and Isaacs, 2016). The results obtained using HRMS will generate large data then different strategy of data interpretation should be performed (Krauss et al., 2010; Schymanski et al., 2015, 2014). In their study Schymanski et al., have mentioned the different strategy applied to identify compounds:

- target screening,
- suspect screening,
- non-target screening.

The target screening used reference standards to confirm compounds detection using retention time, exact mass and MS/MS. This method is well adapted for the analysis of a limited number of compounds.

To analyze a broader spectrum of compounds, suspect and non-target screening could be performed using LC-HRMS. The difference of these two analyses is based on the potential prior information obtained. Indeed, for suspect screening compounds information are available (molecular formula, structure…) and exact mass could be calculated and compared with data found in the spectra. The suspect screening procedure is described in **Figure 11**.

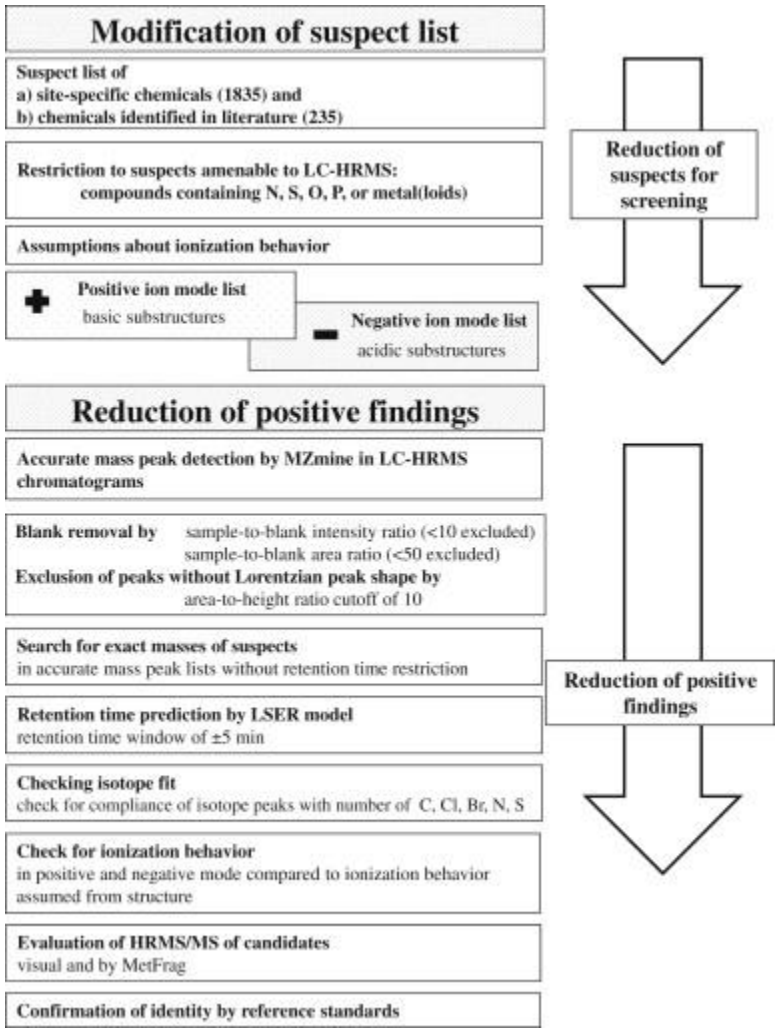

Figure 11: Suspect screening procedure using compound information to identify the analyte of interest as described in Hug et al., 2014.

On the other hand, when no prior data are available and the identification starts from the exact mass, isotopic pattern, adduct (Schymanski et al., 2014), non-target screening approach is applied using automated peak detection and spectra deconvolution algorithms (Hug et al., 2014). Then molecular formula are generated from the exact mass and isotope pattern and several candidate structure could be found (Hug et al., 2014). Therefore, several strategies with list of compounds (confirmed by standards, spectral libraries…) could be carried out to identify the compounds (Hug et al., 2014). The non-target screening procedure is described in **Figure 12.**

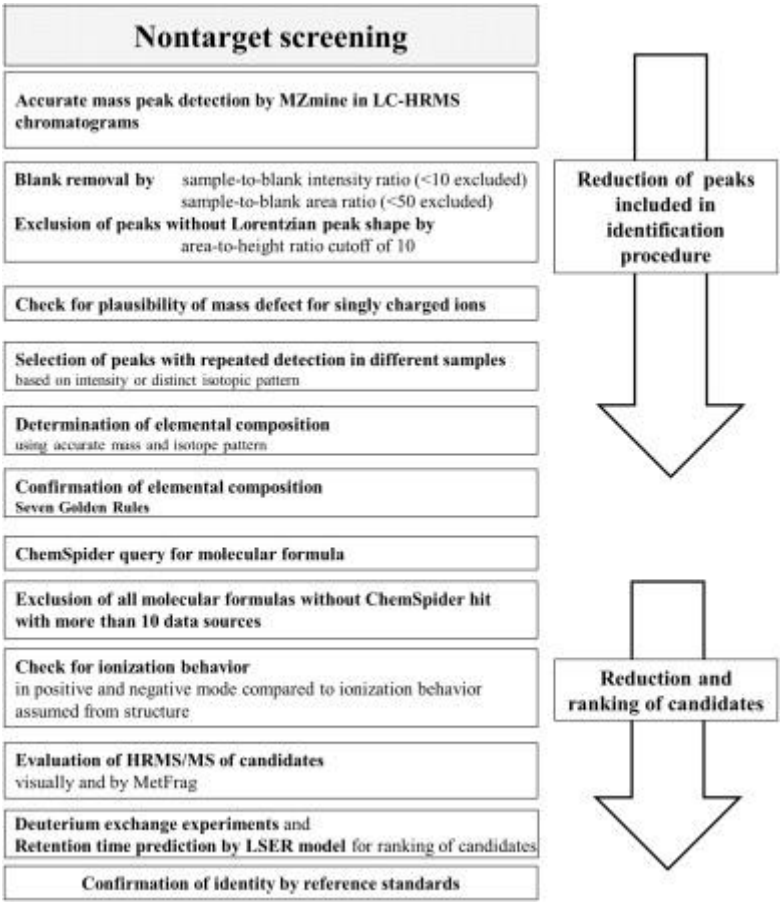

Figure 12: Non target screening procedure using compound information to identify the analyte of interest as described in Hug et al., 2014.

The **Figure 13** highlights the different strategies.

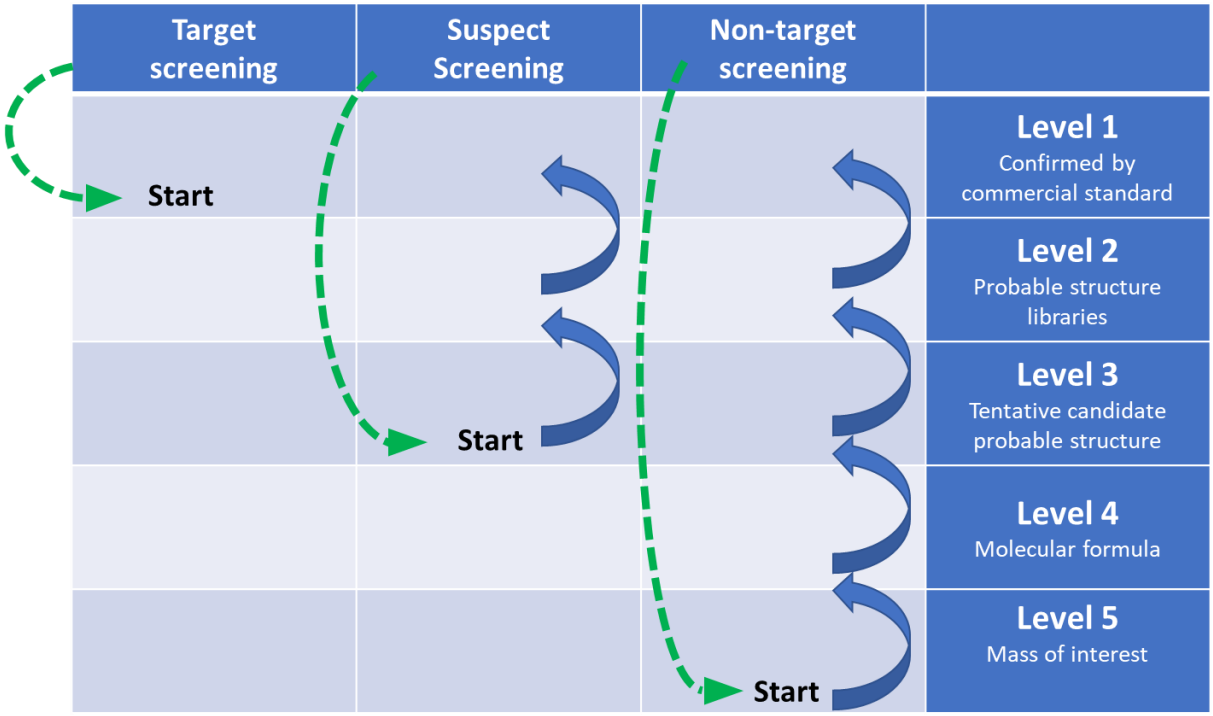

Figure 13: Compounds identification strategy and identification level of confidence (adapted from Schymanski et al., 2014). The green arrows indicate the start point of the screening approach considered. The blue arrows indicate the increasing confidence identification after each level confirmation.

This development has led to publications using this non-target screening in the environmental field to obtain the micropollutants distribution overview and understand their fate (Albergamo et al., 2019; Schollée et al., 2016). Therefore, the fate of micropollutants is now one of the major concerns. Indeed, this fate with transformation products has long been underestimated due to the lack of reference material for transformation products, analytical tools not well adapted and most transformation products are unknown (Kiefer et al., 2019). Therefore, conjugates or degradation products were poorly studied in the different matrices. However, some degradation products have already been detected in the environment and have serious toxic effect. The use of non-target screening will be very helpful to detect these degradation products in aquatic environment or water treatment. Indeed, several studies mentioned non-target screening to find transformation products or unknowns in the environment or after water treatment (ozonation) (Chiaia-Hernandez et al., 2014; Bletsou et al., 2015; Schollée et al., 2018).

This non-target approach could provide a broader overview of the micropollutants found in a sample. Nevertheless, these micropollutants are extracted by solvent from their original matrix. This extraction could generate some dilution and no spatial distribution could be observed for biological (plants, animals, …) samples. Yet, as it has been applied for medical approach,

spatial distribution could be crucial to understand bioprocesses and reactions occurring in organisms that have absorbed these pollutants. Therefore, the use of mass spectrometry imaging (MSI) will be crucial to understand the reactions of organisms exposed to these micropollutants.

1.4.3. MALDI Mass spectrometry imaging: The *in situ* location of pollutants in tissues

MSI could provide spatial distribution of compounds in samples surfaces, based on desorption-ionization phenomena (Pól et al., 2010). This method is becoming increasingly popular as shown by the number of articles on this topic. This method combines molecular analysis and spatial information and thus has a definite interest for biological applications. Every time the laser beam hits the sample, a mass spectrum will be recorded at the impact point and define the spatial resolution (pixel). MALDI principle is described in **Figure 14.**

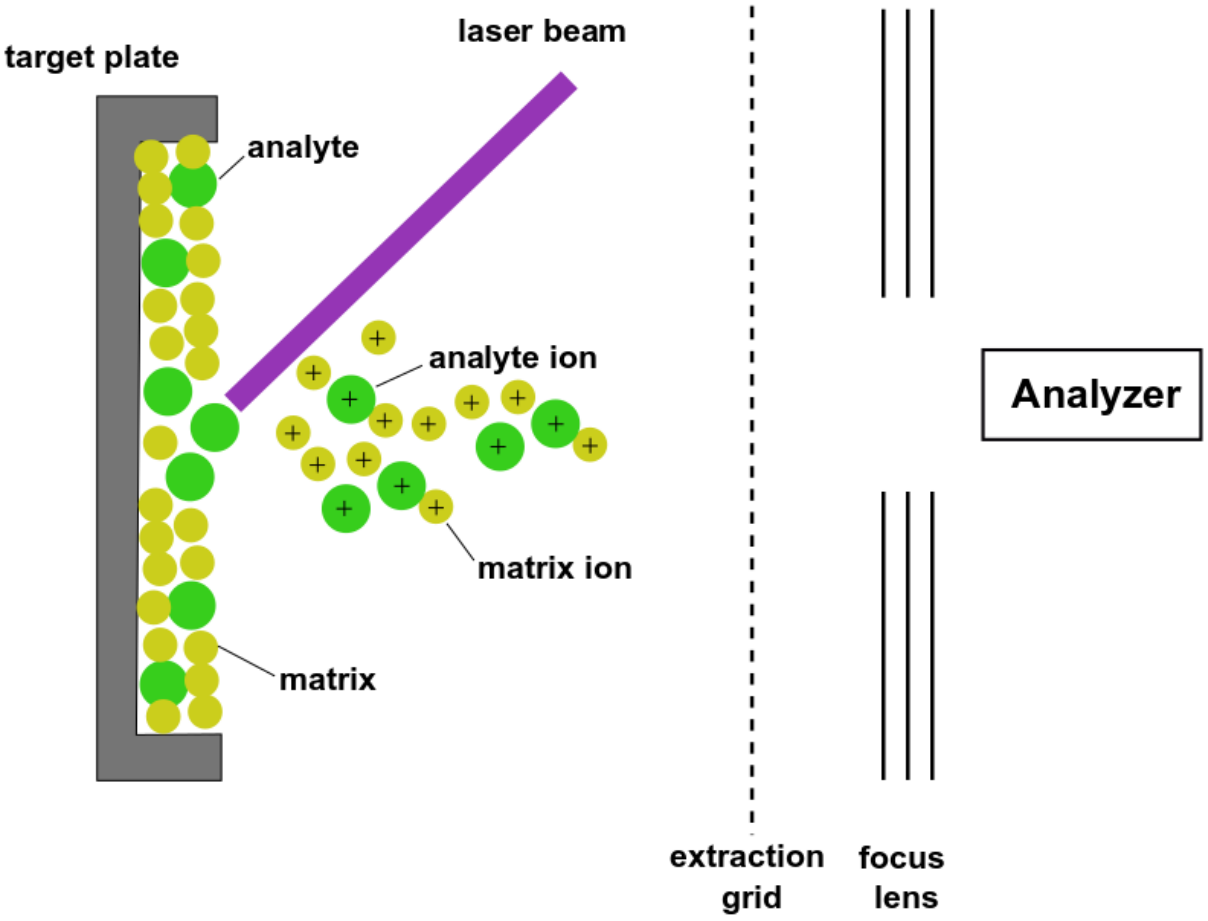

Figure 14: MALDI source principles adapted from Mendis, 2016.

Generally, the spatial resolution found is between 10 and 500 µm (and can reach the 5 µm resolution). But some instruments could have a higher resolution and work on the single cell. Finally, each pixel could be converted to obtain the mass spectra and find the distribution of compounds of interest in the samples. Several techniques are applied to perform MSI. In the literature, the most mentioned are

- Secondary Ion Mass Spectrometry (SIMS),
- Matrix Assisted Laser Desorption Ionization (MALDI),
- Laser desorption ionization,
- Desorption ElectroSpray Ionization (DESI),
- Laser Ablation ElectroSpray Ionization (LAESI).

The different techniques each have their benefits and drawbacks, but this section will only be focused on the MALDI—Imaging. This method was developed in the 1990s based on the works of Caprioli et al., (Caprioli, Farmer, et Gile 1997) and facilitates the MSI use for life science (Pól et al., 2010). This method based on soft ionization use was initially developed for proteins and lipids analysis (Caprioli et al., 1997) but now a wide range of applications could be mentioned such as drugs distribution (Cornett et al., 2008; Hsieh et al., 2007), plant metabolites (Jung et al., 2010).

On the other hand, the analysis performed using MALDI-MSI is really dependent of the sample's quality. Therefore, the most crucial part of the analysis is probably the sample preparation. Indeed, to preserve the spatial location, the tissue integrity should also be protected. Thus, the samples are generally snap-frozen after the collection using liquid nitrogen then stored at -80 °C. (Römpp and Spengler, 2013). To protect their integrity, the samples are then cryo-sectioned. In this crucial step, embedding materials which are compatible with MSI as described in Römpp et Spengler 2013, could be used. Then the slices are deposited on a microscope slide coated with indium-tin oxide (ITO) and MALDI matrix could be applied. This matrix will be used to extract the analytes of interest without impacting their spatial distribution. Besides, the matrix will absorb the laser wavelength and induce electronic transitions, and then generate ions. Several matrices and their deposition (robotic spotting, Electrospray deposition, spray coating, sublimation) methods are mentioned in the literature and the main matrices used are

- alpha-Cyano-4-HydroxyCinnamic Acid (CHCA),

- 2,6-DihHdroxyAcetophenone (DHA),
- 2,5-DiHydroxyBenzoic acid (DHB),
- Sinapic Acid (SA).

The matrix choice is depending on the analyte nature. For example, DHB is more adapted for compounds with high molecular weight and CHCA for small molecules. The matrix deposit is also a crucial part of the sample preparation. Indeed, the spatial resolution (depending on the droplets size or the analytes extraction are depending on the matrix choice and deposit (heterogeneity). Besides the deposition methods used (manual, spraying or sublimation) could also influence the spatial distribution.

Once the matrix applied, the sample and its matrix will be irradiated by a laser beam to desorbe and ionize compounds caught in the matrix. This ionization could be considered as a soft ionization and will generate mainly $[M+H]^+$, $[M+Na]^+$, $[M+K]^+$ in positive mode and $[M-H]^-$ in negative mode. The spatial resolution found in the tissue is depending on the laser spot size and then pixel size generated.

MALDI imaging is often used with TOF detectors. However, the mass resolution and accuracy could be improved using a FT ICR mass spectrometer. Indeed, FT ICR is based on the principle of charged particles circular movement (due to the Lorentz law) in a magnetic field. The cyclotron frequency will be proportional to the mass-to-charge ratio (m/z) and will be independent from the initial kinetic energy [1].

$$\omega = \frac{zB}{m} \text{ [1]}$$

Where ω the frequency, z the charge, m the mass and B the magnetic.

The ions will be trapped in an ICR (ion cyclotron resonance) cell radially by the magnetic field and axially by an electric field. To detect the different m/z, an excitation step followed by a detection step is necessary to measure the cyclotron frequencies. These steps will generate a sinusoidal signal that could be digitalized and amplified. To find the m/z in our samples this signal will be transformed using the Fourier Transform.

As it has been mentioned previously, MSI has several applications. A large part of the literature is focused on the clinical applications and pharmacology applications but few studies are

focused on environmental issues. The few studies focused on this topic evaluated the impacts of micropollutants on human health or in animals/plants distribution as environmental applications are an emerging topic (Lagarrigue et al., 2016).

This distribution could also be investigated with a broader view. Indeed, in environmental systems as well as water treatment systems (and CWs), the water distribution could influence the potential contamination in the environment of wetland systems. Therefore, a detailed knowledge of hydraulics will be very helpful to predict the potential area mainly contaminated.

1.5. Computational Fluid Dynamics for water flow process understanding in treatment systems

Numerical modeling could be very helpful to understand the WWTP processes. Indeed, physical, chemical, or biological processes but also hydraulics and their combination could be modeled to better understand the WWTP performances (Wicklein et al., 2016). Several approaches have been used to model treatment systems processes. Among these different approaches, the development of Computational Fluid Dynamics (CFD) over the last 50 years (Blocken and Gualtieri, 2012) has improved the capabilities to solve complex flow problems. Even if the governing equations are known since the 19th century, they required the development of numerical solutions to be solved on complex geometry using numerical schemes to find numerical solutions to partial derivatives that have no analytical solution (López-Jiménez et al., 2015 ; Samstag et al., 2016). Therefore, CFD has been increasingly used to solve water treatment problems in the recent years (Wicklein et al., 2016). The main applications of CFD models in water treatment systems are designed for treatment systems:

- position of key structures (agitators, baffles…),
- diagnosis of existing system,
- optimization of the existing system (impact of system modification) (Laurent 2016).

Nevertheless, few documents as guides for users detailing the CFD in water treatment applications are available, even if many works on the CFD fundamentals (Andersson 2012) could be found in the literature (Laurent 2016).

1.5.1. Water flow in complex geometry numerical modeling: the key steps

CFD could be used to solve the fundamental equations of fluid dynamics: the continuity and momentum equations (Navier-Stokes equations) using numerical schemes (Samstag et al., 2016). These equations do not have any analytical solutions and need hypothesis to be solved. Therefore, this section will introduce the key steps of the CFD model, mentioned in Blocken et Gualtieri 2012.

All CFD projects should start with the definition of the purposes and the context of modeling. Then the model must be conceptualized and will be structured using several hypotheses and science knowledge (Blocken and Gualtieri, 2012). This hypothesis concerns the dimension (2 or 3D), the water flow regimes (steady state or transient), the phases considered (air, water, particles) and their properties (Laurent 2016). For example, a 3D model could be useful for complex, heterogenous geometry without symmetries but will be more time consuming. On the other hand, water flow regime is depending on the boundary conditions. Indeed, for constant boundary conditions, a steady state simulation seems to be appropriated, at the opposite if the boundary conditions are not constant a transient simulate fits better (Laurent 2016). Then depending on the project, several phases could be considered, and multiphasic models could be set up for example for sedimentation process simulation. In this research project only, monophasic simulation will be considered.

Then the system geometry of the CFD model should be created. This geometry should include the details impacting the water flow process. Nevertheless, the details should be balanced with the calculation time consumption. Then this geometry should be meshed to solve the equations. In the same way, an accurate meshing should be performed in the region of interest and loose meshes should be done in other regions to limit calculation time consumptions. The meshing will be developed in the next section. Then the turbulence model and the boundary conditions could be set up. Next the equations could be solved using iterative methods to find a converged and stable solution. To evaluate this convergence, the difference in the sum of the errors between two successive iterations called residuals could be used (Laurent 2016). The final steps are focused on the calibration and the validation of the model to verify the solution quality with experimental data. The **Figure 15** introduces the different step used for a CFD model building.

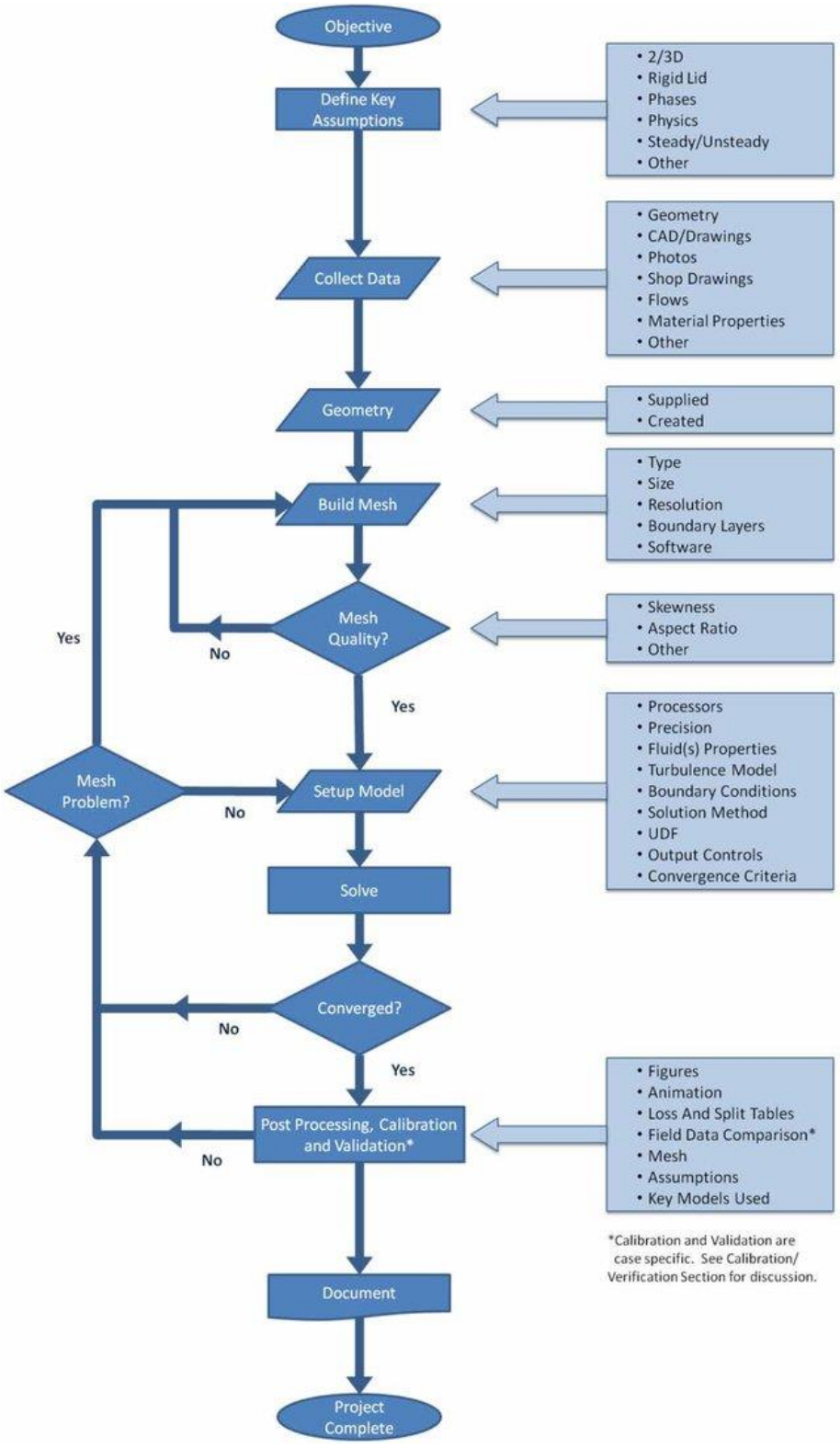

Figure 15: Following steps used for CFD model building (Wicklein et al. 2016).

1.5.2. Numerical model building

Once the general scheme introduced, some steps could be developed to introduce the numerical model development.

1.5.2.1. Governing equations in complex geometry for transient incompressible water flow

A numerical model is set up to bring a numerical solution to a physical problem. Therefore, the engineering problem should be transposed to a mathematical problem. In this way, the hypothesis as well as the equations governing the phenomena to solve should be identified, after the system limits definition (for example coordinates collected on field). In our case, the main object of the study concerns the water flow in the pond system. As water is considered as a Newtonian fluid (its viscosity is stressing independent), the Navier-Stokes equations could be used to simulate the flow. These equations are based on two equations: the continuity and momentum equations [2] [3].

$$\frac{\partial p}{\partial t} + \nabla.(pu) = 0 \qquad [2]$$

$$\frac{\partial pu}{\partial t} + \nabla(puu) + \nabla.\tau = -\nabla p + g \qquad [3]$$

Considering water as an incompressible fluid (density independent of the pressure changes). These equations can be used according to the following formulations [4] [5].

$$\nabla.u = 0 \qquad [4]$$

$$\frac{\partial u}{\partial t} + u.\nabla u = -\nabla p + \nu\Delta u \qquad [5]$$

These equations well known in the literature are detailed in several articles or books such as in Versteeg and Malalasekera 2007.

1.5.2.2. Turbulence

These equations applied in sewer systems, or WWTP generally used turbulent conditions. In this way, the fluid motion will be characterized by velocity and pressure changes. The turbulent condition could be characterized using Reynolds criteria described in the following equation [6].

$$Re = \frac{pUL}{\mu} \qquad [6]$$

ρ water density (kg/m^3), U: velocity (m/s), L: length (m) and μ dynamic viscosity.

When the Re is lower than 2000, a laminar flow could be noticed (no disruption or change in velocity and pressure) at the opposite a turbulent flow is observed when the Re is higher than 4000. The current IT technology could not resolve these equations for real applications using a Direct Numerical Simulation. Therefore, the turbulent model should be simplified using different hypotheses (Andersson 2012). The large—Eddy simulation (LES) could resolve the turbulence at large scale. But the most popular method for engineering issues is the one based on Reynolds Average Navier-Stokes (RANS) mentioned in **Figure 16**. This method calculates the turbulent fluctuations as time-averaged (Andersson 2012). This property reduces the calculation time, but some flow properties could not be solved.

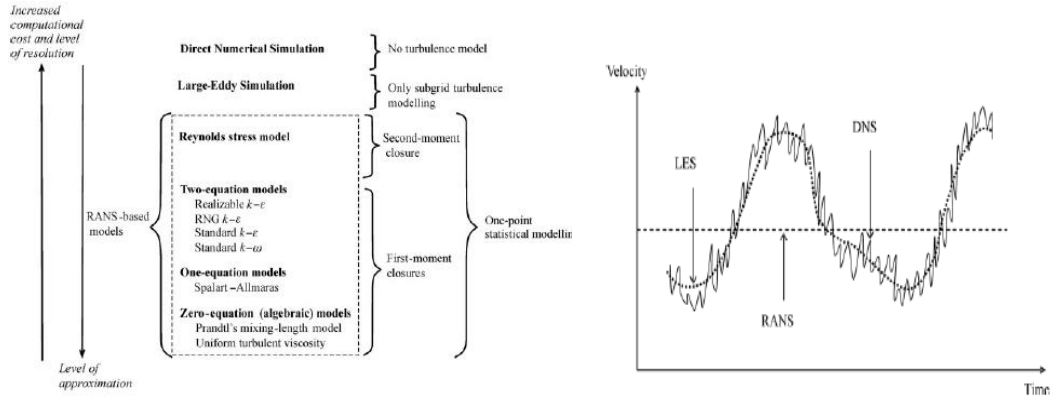

Figure 16: Turbulence models found to solve Navier-Stokes equations in CFD (Andersson 2012). Direct Numerical Simulation, Large Eddy Simulation and RANS are the different models used to solve Navier Stokes equation.

Besides different models could be used to represent the turbulence in a system. The main models found in the literature are k-Ɛ, k-ω or k-ω SST. Diverse articles and works have introduced these different models, but in CFD, the most conventional method used to consider the turbulence is the one based on RANS and k-Ɛ model (Samstag et al., 2016).

1.5.2.3. Boundary conditions

Boundary conditions should be implemented in the model to solve the different equations. These conditions could be clustered following two clusters:

- the Dirichlet conditions with a fixed value,
- the Neumann conditions with a gradient (Isenmann 2016).

The main conditions applied on the system's limits (inlet, outlet, walls) concern velocity, k-Ɛ parameters, and pressure. Velocity and turbulence parameters are generally filled for the inlet, an atmospheric pressure could be applied at the outlet (Isenmann 2016). Then concerning the walls, a zero velocity (no slip) could be applied or constrained velocity with the absence of roughness (slip). Finally, a free surface could be considered using a symmetry (no vertical flow) in the area considered.

1.5.2.4. Discretization

To solve the Navier-Stokes equation, the partial derivatives should be discretized. This discretization will transform the partial derivation into algebraic equation. The main method used in CFD is the finite volume method (Andersson 2012). The CFD model is split in "small

volume" called cells and considered small enough to calculate the fluid movement. This discretization could be performed using the Gauss theorem. Indeed Navier-Stokes equation could be written using a generic transport equation of a variable ∅ (Versteeg et Malalasekera 2007). The equation is described below [7].

$$\frac{\partial \rho \emptyset}{\partial t} + \nabla.(\rho \emptyset u) - \nabla.[\rho \Gamma_{\emptyset} \nabla \emptyset] = S_{\emptyset}(\emptyset) \quad [7]$$

The equation could be written using the integral form [8].

$$\int_{Vp} \rho \frac{\partial \emptyset}{\partial t} dV + \int_{Vp} \rho \frac{\partial U \emptyset}{\partial x} dV = \int_{Vp} \frac{\partial}{\partial x}\left(\Gamma \frac{\partial \emptyset}{\partial x}\right) dV + \int_{Vp} S_{\emptyset}\, dV \quad [8]$$

Advection Diffusion

Then using the Gauss theorem, the volume integral could be transformed into surface integral [9].

$$\int_{Vp} \nabla.A dV = \int_{S} A dS \quad [9]$$

And finally these equations could be linearized (Isenmann 2016).

On the other hand, several schemes could be used to discretize the CFD systems. A first-order scheme has been applied for the spatial discretization and concerning the temporal discretization 3 main schemes are generally used in the literature Implict Euler, Crank-Nicolson and Explicit Euler. In this study the numerical scheme applied has the first order scheme Implicit Euler described in the following equation. [10]

$$F\left(u_{xi,tj+1}\right) = \frac{u_{xi,tj+1} + u_{xi,tj}}{\Delta t} \quad [10]$$

1.5.2.5. Convergence calibration and validation

The final step of the CFD concerns the result verification. The first step is dedicated to the result convergence. Indeed, a result could be considered as converged if no changes could be observed in the velocity or a scalar field. To evaluate this change, it is recommended to monitor the residuals and check that differences is lower than the threshold. Finally, to ensure that the model represents the desired flow, it is necessary to compare the numerical results with experimental data, such as the residence time distribution found in Coggins et al., 2017.

1.5.3. CFD applied to water treatment systems

The final section concerning the CFD will be focused on its use on water treatment systems and more specifically in pond systems, which are similar to our study site. Indeed, CFD has widely been used to optimize WWTP units or in sewer systems (Dufresne et al., 2009; K Mohanarangam and D W Stephens, 2009) but also in more extensive systems like waste stabilization pond (Alvarado et al., 2013; Coggins et al., 2017; Ouedraogo et al., 2016).
Concerning this last cluster, the first studies were focused on the pond design parameters (Persson 2000; Sweeney et al., 2003; Shilton et al., 2003). The main objectives were to understand the water flow process through some complex geometry and then to optimize the pond design to improve the hydraulic performance.

Then studies were more generally focused on the processes optimization with some facilities (baffle for example) to improve this hydraulic performance in the systems (Rengers et al., 2016). On the other hand, some studies are interested in the pollutant removal rate improvement. To improve the removal, it has been suggested adding complementary aerators. For example, Alvarado et al., 2013, have studied the implementation of aerators in ponds.

But several studies have already used CFD in pond systems to evaluate their performance and the impact of ageing in this system. Indeed, ponds are naturally subject to sedimentation. This sedimentation could highly impact the hydraulic performance by reducing the residence time and create short circuits. Therefore, this issue has been studied in the recent years. For example, Coggins et al., 2017 have studied the impact of sludge accumulation on hydraulic performance for a pond system. Their study shows the impact of sludge accumulated over the months on the residence time. The area accumulating the sludge will generate a short circuit then reduce the residence and the hydraulic performance. According to their results, the residence time reduction is proportional to the sludge accumulated. Besides the sludge accumulation then the impact of hydraulic performances is linked to the system configuration. In the same way, other studies like the one performed by Ouedraogo et al., 2016 have also investigated the impact of sludge accumulation on hydraulic performance (Ouedraogo et al., 2016).

This section has shown that the CFD approach could be very helpful to understand the water flow and then to optimize some treatment system performance. Nevertheless, these

performances are mainly focused on the hydraulic, carbon or nitrogen removal. But the link with micropollutants distribution seems to be less obvious.

1.6. Objectives of the thesis

As it has been mentioned in this state of art, the micropollutants distribution in the environment has become a major concern. This micropollutants analysis is an interesting challenge for the mud or sediments accumulated over the years in the environment or constructed wetlands. It has been demonstrated that this compartment could accumulate micropollutants. Nevertheless, a study focused only on this compartment would ignore the interactions. The wastewater must be investigated to understand the potential origins of micropollutants in this system. Furthermore, these wetlands are systems containing living organisms and it is well known that micropollutants could be transformed or transported by these organisms. Therefore, the plants growing in these areas were also investigated to understand the fate of the micropollutants. In this way, the main objective of this PhD project is focused on the large scale micropollutants screening in the constructed wetland ecosystems and aims to understand their distribution and their fate. Therefore, this research project was structured in three specific main objectives:

- non-target micropollutants screening in LC-HRMS/MS in the different compartments of the constructed wetland,
- specific location of micropollutants *in planta* using mass spectrometry imaging,
- numerical modeling of water flow in wetland ecosystems and the correlation with micropollutants distribution.

After the investigation of the state of art, the manuscript will be structured following three main axes. The first part of this PhD project, presented in the chapter 2, investigated the micropollutants large scale screening in wetland ecosystem. In this way, water, sediments and plants were analyzed in constructed wetland and in the associated tertiary treatment wetland to obtain an overview of the metabolic profile of each compartment. This large screening will help to understand the wide spread of micropollutants in the ecosystem and the potential interactions between these compartments.

To obtain this large screening, a method has been developed from sample preparation to data analysis. However, the fate of micropollutants could not be restricted to their transfer to the

other compartments. Indeed, the micropollutants detected in mud or water could also be biodegraded, bio transformed, or transformed by physico-chemical reactions (oxidations). These phenomena are mainly due to the living organisms. Therefore, they were studied in plants growing in these polluted areas. Nevertheless, to understand these bioprocesses, a spatial distribution should be performed. This spatial distribution could be crucial to understand the mechanisms occurring in the organisms and then to understand the fate of these micropollutants.

Therefore, MSI will be used in this PhD project and developed in the third chapter. Indeed, the spatial distribution in sediment samples could also be studied using MSI. On the other hand, plants growing in constructed wetland or on the banks of a tertiary treatment wetland are chronically exposed to micropollutants. Therefore, micropollutants investigation was performed using mass spectrometry imaging (MALDI-Imaging (SolariX) (FT ICR)) on plants growing near the wastewater. In this section, all the MSI method development will be mentioned and then will be applied in three plants growing near wastewater. First, micropollutants distribution was studied in a black poplar (*Populus nigra*) leaves, then the fate of micropollutants and their metabolites was investigated in willow leaves (*Salix alba)*. Finally, a whole plant (reed, *Phragmites australis)* has been analyzed using mass spectrometry imaging to study the distribution in the different organs.

Nevertheless, in the constructed wetland, water flow could influence micropollutants distribution and then their fate. Therefore, the last part of this PhD project investigated waterflow influence on micropollutants distribution in a wetland system. The aim of this study was to link micropollutants distribution and water flow modeling. This section will be dedicated to the development of a numerical modeling for a study site. The results from water flow modeling will be used to define a sampling strategy and analyze micropollutants in sediments to visualize if a link between micropollutants distribution and water flow is existing. The results could underline the influence of hydraulics on micropollutants distribution.
Finally, this manuscript will end with a general conclusion containing the main results and ideas developed in this PhD project.

Chapter 2:
Non-target screening of micropollutants in the constructed wetlands' ecosystems

This thesis aimed at understanding micropollutants distribution in a constructed wetland ecosystem to optimize their management. Therefore, different tools and approaches have been used as it has been described in the objectives of the thesis. Micropollutants represent a wide diversity of compounds, as it has been mentioned in the state of art. Besides, this micropollutants diversity generates diverse behaviors (removal, adsorption, degradation). In this way, target analysis on micropollutants cannot provide a global overview of the potential contamination, distribution and spreading into the environment. Therefore, this global overview could only be obtained using a non-target approach, without any bias introduced by compounds selected. One of the major concerns in water treatment is focused on the fate of sludge accumulated over the years, in WWTP but also for the small communities. Indeed, their treatment could generate high costs. To reduce their costs and find the most adapted treatment systems, their content must be analyzed. Micropollutants content analysis will help to understand their potential toxicity, their potential release to the environment, and the potential reuse of sludge as agriculture soil improvement. However, as mentioned in the objectives of the thesis, the analysis of sludge could not be dissociated from the other compartments. Indeed, wastewater should be analyzed to understand the potential origins of these micropollutants. On the other hand, as plants are growing in these water treatment systems, they should be investigated to understand the fate of the micropollutants (uptake and transformation). This chapter will thus be focused on this non-target screening in the three compartments mentioned. First, the material and the methods used and developed to obtain this large screening of micropollutants will be described. This section will introduce the sampling strategy defined, the extraction method optimization, the non-target analysis method and then the data treatment optimization. Then this large scale micropollutants screening will be used for two applications in the environment ecosystem. First, a large-scale micropollutants screening in wetlands (tertiary treatment wetland and constructed wetlands) ecosystems then a large screening in a vertical profile of sediment layers in a constructed wetland.

2.1. Materials and Methods

In this materials and methods section, the environmental metabolomic workflow applied to this study is developed. This environmental metabolomic workflow is described in **Figure 17** with its key steps.

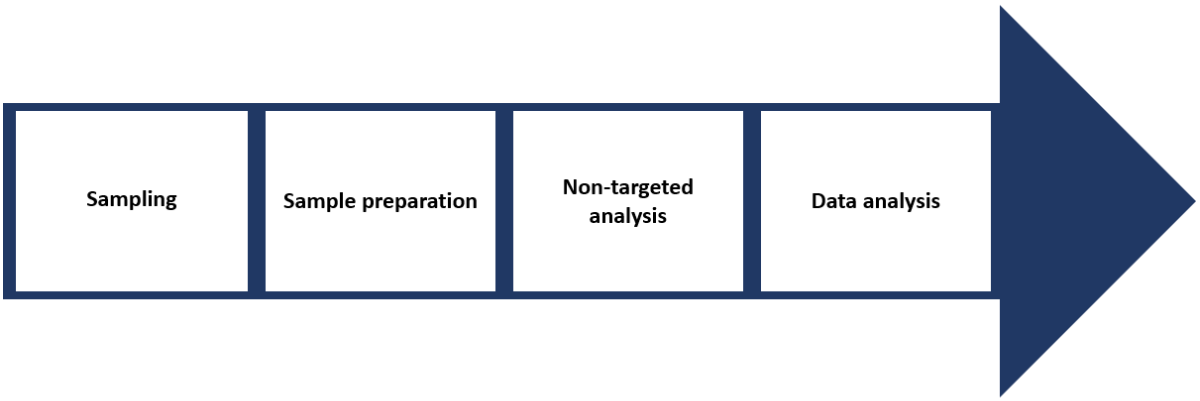

Figure 17: Environmental metabolomic workflow applied in this study with its key steps (sampling, sample preparation, non-target analysis and data analysis).

This material and methods will also be structured following this metabolomic workflow. Indeed, this section will introduce first the study site, environment compartments analyzed, and the sampling strategy defined. Then the micropollutants extraction methods development in the different compartments will be mentioned. The non-target micropollutants screening method, using LC-HRMS/MS and GC-MS/MS and carried out the samples will also be specified. Finally, the data treatment to identify micropollutants will be brought up.

2.1.1. Study site description

All the samples on which the micropollutants non-target screening has been performed in this section were collected on the Falkwiller study site. Falkwiller is a small village located around 150 km south of Strasbourg as described in **Figure 18**.

Figure 18: Study site location in Falkwiller village (from Google maps).

This study site is a full-scale CW coupled to a tertiary treatment wetland. This CW collects wastewater from Falkwiller, Gildwiller and Hecken and has a capacity around 1450 people equivalent and has been set up in 2010. The CWs designed in Falkwiller is a two-stage vertical flow constructed wetlands. (VFCW) described in **Figure 19**. The location of this VFCW in the treatment system could be found in the water treatment global scheme represented in **Figure 20.**

Figure 19: Bed filter planted with reeds from the 2nd stage Constructed wetland in Falkwiller (Grand Est, France).

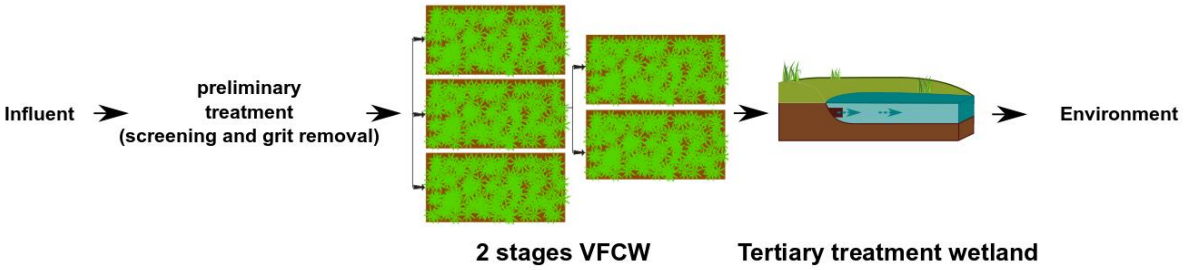

Figure 20: Falkwiller's water treatment system global scheme.

The two-stage VFCW was designed to receive 269 m^3/j (wastewater and infiltration to sewers). All design characteristics are described in the report *Controle techniques et fonctionnement des stations d'épuration* from LORraine Eau Assistance Technique (LOREAT). Hydraulic load and pollutants load used to design the VFCW are shown in the **Table 1**.

Table 1: Design parameters for the Falkwiller CW based on the hydraulics and pollutant flows. Where BOD_5: Biochemical Oxygen Demand 5 days, COD: Chemical Oxygen Demand, TSS: Total suspended solids, TKN: Total Kjedhal Nitrogen, TP: Total phosphorus.

Parameters	Falkwiller
Dry weather wastewater flow (m^3/j)	174
Dry weather Inflow/infiltration water (m^3/j)	95
Dry weather water flow (m^3/j)	269
Hydraulic load (m^3/j)	1080
Organic load (kg/j)	85 kg BOD_5/j
	174 COD/j
Suspended solid load (kg/j)	130.5 kg TSS/j
Nutrient load (kg/j)	21.8 kg TKN/j
	4.4 kg TP/j

On the other hand, tertiary treatment wetland has been set up to obtain a complementary treatment. These complementary treatment systems are built, when the environment (river that collects the treated wastewater) is highly sensitive to nitrogen or phosphorus issues. Furthermore, these systems could be an alternative to pipes, and connect WWTP to the environment. Nevertheless, no rules have been defined to create these wetlands. In this way, wetlands were designed depending on the field constraints and the operators' sensitivity. The Falkwiller wetland could be described as a ditch wetland with a length of 95 m in **Figure 21**.

Figure 21: Tertiary treatment wetland (ditch) in Falkwiller (Grand Est, France).

All the tertiary treatment wetland characteristics could be described in the **Table 2**.

Table 2: Design characteristics of Falkwiller tertiary treatment wetlands.

Wetland type	Ditch
Bank slope	1 by 1
Length (m)	95
Width (m)	1.70
Depth (m)	0.1
Surface (m^2)	140
Volume (m^3)	60

The treated wastewater is released in a small river called the Soultzbach which flows into the Largue and then into the Ill as shown in **Figure 22**.

Figure 22: Rivers maps where the constructed wetlands releases the effluent (Google maps).

The waterbodies quality defined in the Water framework is checked in the measurement station located downstream in Spechbach-Le-Bas on the Largue river. The results highlight a medium waterbodies quality found in the **supplementary data (1)**. In this way, considering the water framework, the waterbody quality should be improved.

2.1.2. Environment compartments analyzed and sampling strategy

As it has been described in the previous section, the study site is composed of two main system compartments, the 2 stage VFCW as secondary treatment and a vegetated ditch tertiary treatment wetland. These two treatment systems are based on the ecological engineering principles mentioned by Mitsch 2012. Thus, the non-target screening of micropollutants has been performed on the compartments composing the treatment system, i.e., wastewater, sediments and plants growing near or in these treatment systems. These compartments were chosen to visualize distribution in the ecosystems. Indeed, this distribution could be highlighted by the direct interactions processes such as sorption between micropollutants and solid matrix or micropollutants release from one compartment to another.

Concerning the sampling strategy, the methods used to collect the samples could be developed for each compartment.

2.1.2.1. Wastewater sampling strategy

The wastewater was sampled in two ways depending on the aims of the study. Except for one case, wastewater was collected by automatic samplers, as it has been described in Nuel et al., 2017.

Figure 23: Automatic samplers (Avalanche Teledyne ISCO) used to collect wastewater.

Briefly, a flow rate-controlled sampling was performed using refrigerated samplers (Avalanche TELEDYNE ISCO, Lincoln, Nebraska) found in **Figure 23**. The pooled samples are collected in a glass bottle and all the sampler elements (pipes and glass) were adapted for micropollutants sampling as mentioned in Nuel 2017. Indeed, these samples will provide an overview of the daily water quality integrated peaks and troughs of wastewater releases. This refrigerated samples will be kept at 4 °C before the sample preparation and limit the degradation of heat-sensitive xenobiotics. This sampling was controlled by flow rate using ultrasonic sensors (IJINUS, Mellac, France). Venturi flumes, described in **Figure 24** were located at the inlet and the outlet of the CW and the tertiary treatment wetland. Thus, ultrasonic sensors could measure the water depth. Furthermore, each Venturi flume is characterized by a law linking the water depth to flow rates. In our study case, the Venturi flume found at the inlet and outlet of the CW has the following law [11] provided by the constructors (Venturi flume with exponential opening type III ISMA, Forbach, France).

Figure 24: Venturi flume found at the outlet of Falkwiller's CW.

$$Q = -0.58461.h + 1156.085\,h^2 - 1125.h^3 + 6550.h^4 \quad [11]$$

At the tertiary treatment wetland outlet, a metallic weir with a triangular opening has been set up. Hager law could be used to find water flow using water levels. Hager law is described in equation [12] and Cd coefficient in equation [13].

$$Q = \frac{8}{15}.Cd.\tan\left(\frac{\propto}{2}\right).(2.g.h^5)^{\frac{1}{2}} \quad [12]$$

$$Cd = \frac{1}{\sqrt{3}}.\left[1 + \left(\frac{h^2.\tan\left(\frac{\propto}{2}\right)}{3.B.(h+w)}\right)\right].\left[1 + \left(\frac{0.66}{h^{\frac{3}{2}}.\tan\left(\frac{\propto}{2}\right)}\right)\right] \quad [13]$$

Where B: weir width (m), α: weir opening angle (rad), h: water level (m)

Control loop of the samplers will also be adjusted using the flow volume measured. Indeed, it was defined according to the methods introduced in Nuel 2017. Briefly, the sampling starts with a sampler cleaning (pipes and glass) using wastewater collected to limit the cross-contamination. On the other hand, an instantaneous flow rate is measured and has been used to calculate the daily flow rate in the sampling point. Then 150 samplings of 50 mL (to obtain the

most representative average samples) will be selected to perform the sampling. The sampling will be induced by pulse generated at regular flow intervals. Finally, these intervals were calculated using the samplings number and the flow rate measured.

On the other hand, wastewater was just collected specifically for one case. In order to visualize the distribution concerning the poplar study, wastewater was collected near the poplar roots. Therefore, in this study case, surface wastewater (0–15 cm) was directly collected in glass bottles (2L) near the poplar roots, as the samplers could not be placed in these areas.

2.1.2.2. Solids samples (sludge and plants) sampling strategy

Concerning the solid samples (sediments and plants), all samples were collected in the same square meter to visualize the potential distribution and interactions between the different compartments as described in **Figure 25**. Reed roots were collected in triplicates. Concerning the sediments, a composite sample was collected in the area around the water inlet and biological replicates of these samples were performed.

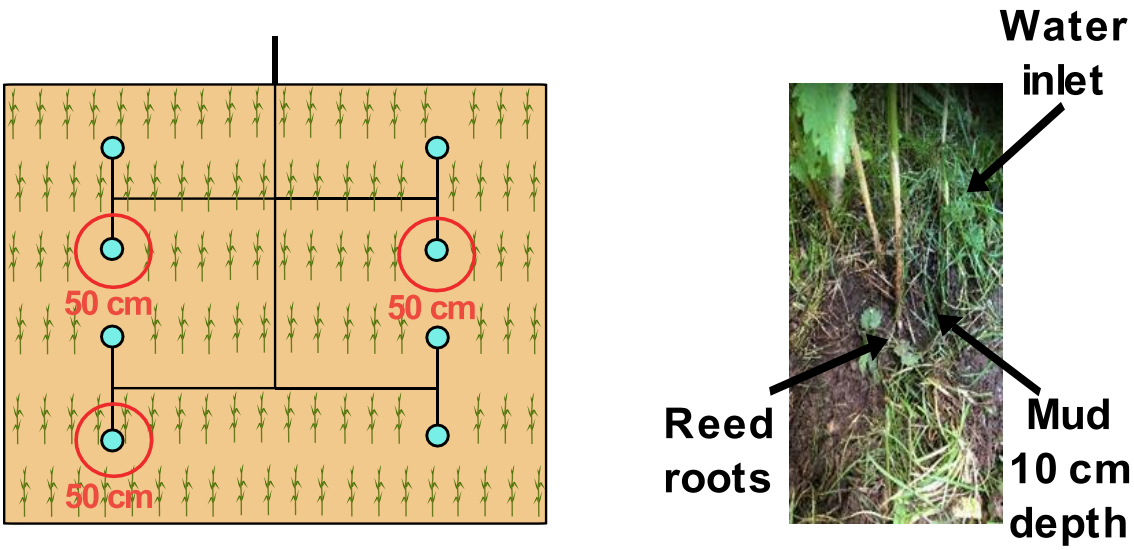

Figure 25: Sampling of the ecosystem compartment (water, reed roots and mud) in the CW.

Two strategies have been defined for each system, according to the different objectives defined for each study case. Therefore, in the tertiary treatment wetland sediments were collected in the

square meter around the plant to visualize the potential micropollutants releases or sources for each plant as described in **Figure 26**. For the plant growing in the tertiary treatment wetland, only the leaves were analyzed, as these tissues will also be used for MSI ant the plants were not sacrificed for further experiments.

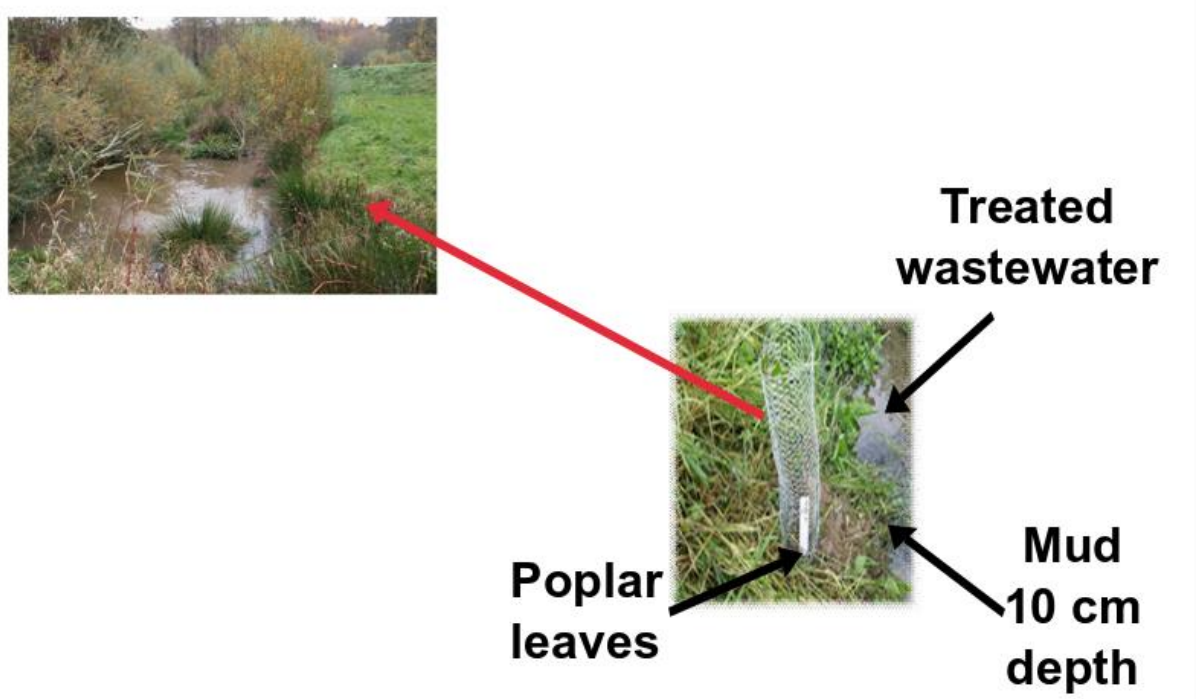

Figure 26: Compartment sampled in the tertiary treatment wetland.

2.1.2.3. Sludge vertical profile sampling strategy

On the other hand, the distribution in the different compartments is helpful to understand the fate of micropollutants, but it cannot be restricted to the sludge surface layer. Therefore, the study was also focused on the distribution of a sediment vertical profile. A coring in the CW was performed with three replicates using a manual auger as shown in **Figure 27**. The points selected for the coring were located around one meter near the wastewater inlet in the CW. And the different layers analyzed could be visualized in **Figure 28**.

Figure 27: Coring performed using a manual auger.

Figure 28: Coring performed in the CW. **A)** Manual auger used for the coring. **B)** CW mud vertical profile reconstructed after coring.

The coring was performed until 60 cm depth when the auger reached the gravels. In this coring sample, two layers were analyzed. The top layer which corresponds to the ten first cms and the bottom layer which correspond the last ten cms (50–60 cms) as shown in the **Figure 29.**

The same coring was carried out on the bank, which did not collect wastewater, to identify only compounds found in CW and eliminate the background contamination detected in the banks. Three reed rhizomes were also sampled in the same square meters to visualize the

micropollutants distribution in the wetland ecosystem. All the samples were kept à 4 °C before the extraction.

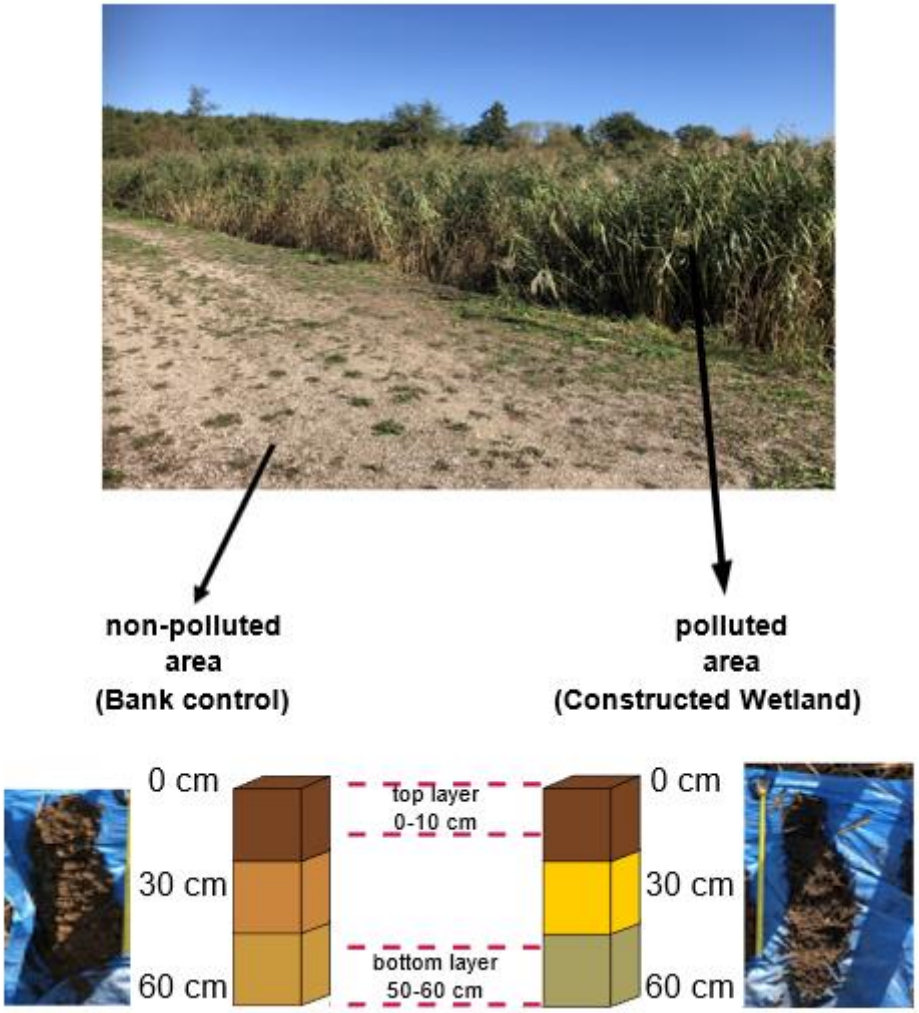

Figure 29: Scheme of the sampling strategy defined for the coring in the VFCWs.

2.1.3. Sludge layers physical properties

Micropollutants distribution in the sludge layers is probably linked both to compounds and to sludge properties through biotic and abiotic processes. Hence, the physical properties of the different sludge layers could not be neglected in this study as they influence the micropollutants distribution. Therefore, three parameters describing the sludge structure were measured: the granulometry, the bulk density and the porosity.

The granulometry distribution was performed according to the standard French NF EN 933-1. After drying sludge layers at 150 °C (until the sludge mass becomes stable), the samples layers

were passed through successive sieves of different mesh sizes under mechanical stirring as shown on **Figure 30**.

Figure 30: Sludge samples passed through different sized mesh under mechanical stirring.

Finally, the different sieves were weighted, and results of each sieves weight will be used to create a granulometry curve. Thus, distribution of the grain size for each layer could be characterized, effective diameter and uniformity coefficient are estimated.

Bulk density and porosity, for their parts were obtained by following the French standard NF P94-410-3. The porosity measurement was performed using a water pycometer.

2.1.4. Micropollutants extraction optimization

Once the sampling strategy defined and the samples collected, a micropollutants extraction must be performed. Concerning sediment and water samples, several protocols and methods described the micropollutants extraction. The major method used is based on an SPE extraction (Gros et al., 2017; Petrie et al., 2017; Hebert et al., 2018; Boonnorat et al., 2019; Tröger et al., 2020). Nevertheless, in the context of this PhD project with the micropollutants non-target screening several extraction methods with different conditions were compared to select the most adapted to the study case. The critical points of this optimization were focused on the sample

quantity, the extraction solvent, and the data acquisition. The main criteria used to select the most appropriate method were the reproducibility, the speed, the solvent dangers.

2.1.4.1. Initial weight or volume sample optimization

In this way, the first step of this optimization was to find the appropriate initial weight (for sediment) or volume (for wastewater). Therefore 2 sediment initial weights (10 g and 20 g) and 2 wastewater volumes were selected (10 mL and 50 mL) based on literature reviews (Bergé et al., 2018; Cotton et al., 2016).

Wastewater was previously filtered with paper filters to remove coarse particles, and sediments were also filtered to eliminate the aqueous phase (in excess). This first comparison was carried out using a single extraction method based on double extraction (for sediment only) and freeze drying. Then samples were solubilized in 1 mL of solvents and analyzed in positive mode using TASQ software and its Pesticides & ToxScreener database (Bruker). The details of the method, the acquisition and the data treatment will be introduced in the next section.

The results of this optimization could be described in the **Tables 3** and **4.**

Table 3: Results from micropollutants identified in the two wastewater volume conditions (10 and 50 mL).

	50 Ml	10 mL
Micropollutants found in water sample	**48**	**12**

Table 4: Results from micropollutants identified in the two sludge weight conditions (10 and 20 g).

	20 g	10 g
Micropollutants found in sludge sample	**76**	**82**

According to the results found in this optimization, the sediment weight used for the rest of the studies will be 10 g and the wastewater volume will be 50 mL.

2.1.4.2. Micropollutants extraction methods optimization

Once the initial weight or volume defined, the optimization could be focused on the extraction method. In this way, three methods have been compared. The most quoted method for micropollutants extraction (liquid extraction coupled with SPE), then a liquid extraction without SPE and finally the Bligh & Dyer extraction. Indeed, SPE cartridges are specific for some micropollutants (cartridge affinity). The comparison with the liquid extraction without SPE cartridges will highlight the potential micropollutants lost due to the cartridge specificity. On the other hand, the Bligh & Dyer method is a common method used in lipids extraction. As sludge are composed of greasy substances, this extraction could also be interesting in this way.

The liquid extraction will be the first method developed in this manuscript. A double extraction is performed on the 10 g of sediment samples. The first extraction used 40 mL of acetonitrile: water (90:10) with 1% acetic acid (on the total volume). Samples are shaking overnight at 4 °C using a magnetic stirrer. Then samples are centrifuged at 5500 rpm during 15 min. The supernatant is collected and a second extraction is carried out using 20 mL of isopropanol: acetonitrile (90:10) and shaking during 15 min. Samples are centrifuged again using the same conditions as those mentioned previously. The supernatant is collected and pooled with the first supernatant. Then, the supernatant is freeze-dried and the pellet is solubilized in 1 mL of acetonitrile: isopropanol: water (50:45:5). This process could be observed on **Figure 31**.

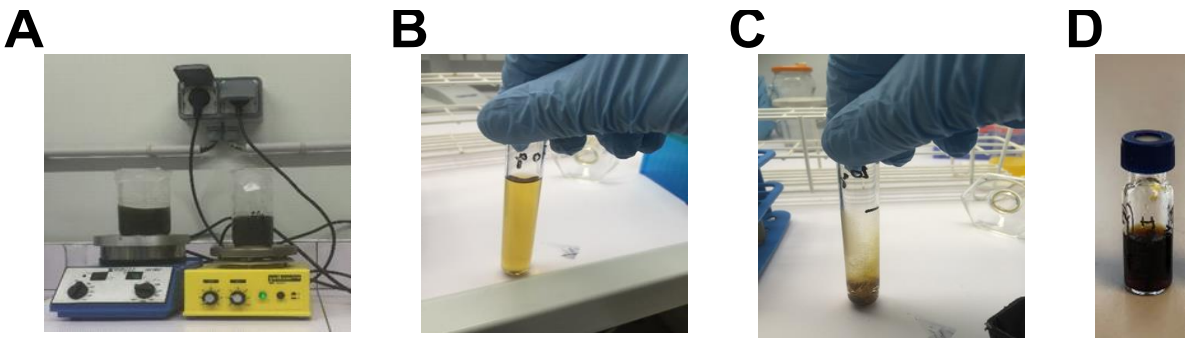

Figure 31: Micropollutants extraction from solid matrix using the liquid extraction method **A)** Overnight extraction using isopropanol: acetonitrile then isopropanol: water. **B)** Supernatant collected before the freeze-drying step. **C)** Pellet collected after the freeze-drying. **D)** Samples solubilized in 1 mL acetonitrile: isopropanol: water (50:45:5) before MS analysis.

Concerning the water samples, 50 mL are collected and directly freeze-dried. Then the pellet is solubilized in 1 mL of methanol: water (90: 10), as shown in **Figure 32**.

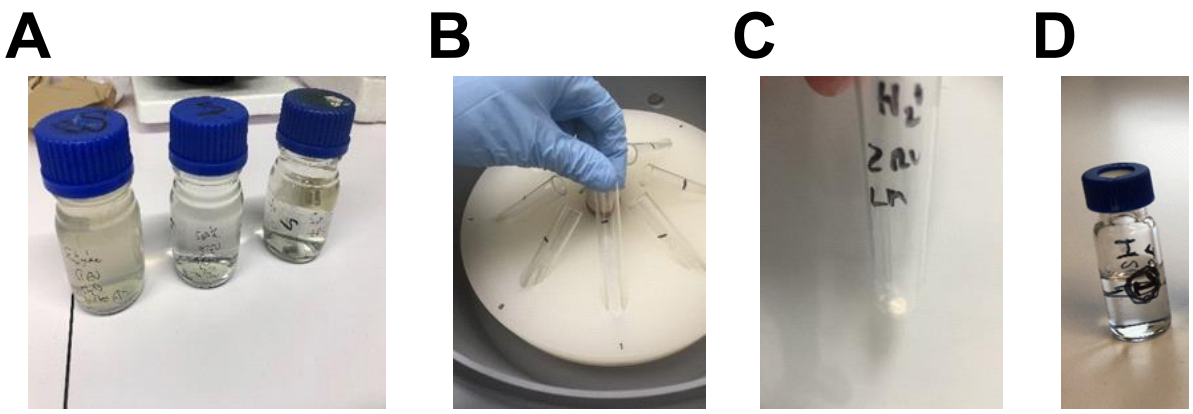

Figure 32: Micropollutants extraction in wastewater based on freeze drying and extracted by methanol: water (90:10). **A)** Wastewater samples. **B)** Freeze-drying step. **C)** Pellet collected after the freeze-drying. **D)** Sample solubilized in 1 mL methanol: water (90:10).

The second method compared was based on the SPE cartridge, which is widely used in the literature. The extraction was adapted from the method presented in Nuel, 2017. First the liquid extraction was carried out as it has been described in the previous method, followed by a cartridge elution phase. Briefly, a silica cartridge and C_{18} coupled with an HLB cartridge (mounted in tandem) have been used respectively for sediment and water samples extraction. The cartridges were activated using 5 mL of methanol, then they were equilibrated with 10 mL of water (MilliQ) with 0.5% of acetic acid for water samples and 10 mL of methanol: water (95:5) with 0.5% of acetic acid for sediment samples. Next, the sample extraction is added to the cartridge. The cartridges are eluted by 10 mL of methanol: water (80:20). Finally, the eluate is freeze-dried and the pellet is solubilized in 1 mL as it has been described previously. This SPE system could be described in the **Figure 33**.

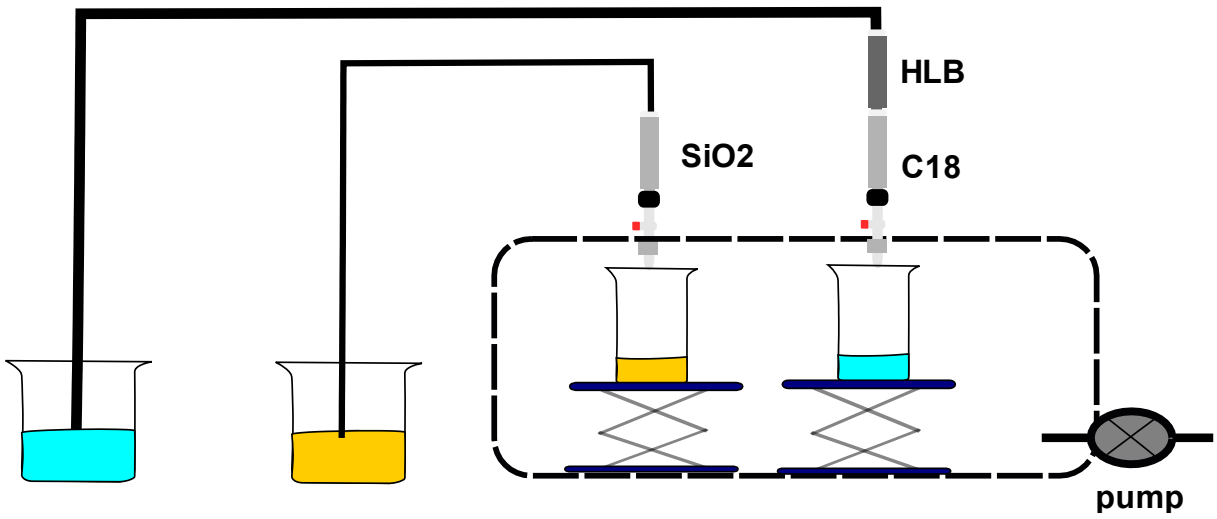

Figure 33: Scheme of the experimental set-up using SPE method for micropollutants extraction. Blue sample corresponds to water and orange sample corresponds to sludge.

The last method used in this comparison is the Bligh & Dyer (1959) method, that was initially used for lipids extraction. This method could be well adapted for hydrophobic xenobiotics but also to identify the sludge metabolome, according to the method developed in Bligh et Dyer 1959. 10 g of sediment were extracted using 37.5 mL of chloroform: methanol (2:1). Then the sample is stirring for five minutes and the extraction is performed overnight. Finally, liquid phases are found: the aqueous and the organic phase, which were both collected and analyzed separately. A scheme of the Bligh and Dyer principles could be described in the **Figure 34.**

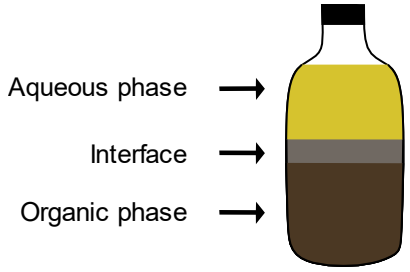

Figure 34: Scheme of the Bligh & Dyer method.

The results comparison was carried out in the same way, as mentioned for the weight or volume selection. The micropollutants identified in each method could be found in the **Tables 5** and **6**.

Table 5: Results from micropollutants identified in the three micropollutants extraction method applied on sludge samples (liquid extraction, SPE, and Bligh & Dyer).

	Liquid extraction without SPE	Liquid extraction with SPE	Bligh & Dyer
Micropollutants found in sludge sample	**82**	**33**	**51**

Table 6: Results from micropollutants identified in the two micropollutants extraction method applied on water samples (liquid extraction, SPE).

	Liquid extraction without SPE	Liquid extraction with SPE
Micropollutants found in water sample	**48**	**31**

In this way, a higher number of compounds could be found in the liquid extraction method without SPE. Furthermore, this method is faster than the SPE method and uses less toxic solvent than the Bligh & Dyer. Following these criteria, this method will be selected for the different studies, as the optimized method used to extract micropollutants.

2.1.4.3. Micropollutants extraction from plant samples

Concerning the plant extraction, the method used was developed in the laboratory and mentioned in Villette et al., 2019. 300 mg fresh weight of plant samples are collected and ground in liquid nitrogen as shown in **Figure 35**. Then a first extraction is performed using 1.5 mL cold MeOH containing $^{2}H_{6}$ abscisic acid (Olchemim) as an internal standard (10µg/mL). Then this solution is vortexed and the extraction is carried out overnight (16h) at -20 °C. Then the solution is centrifuged for 15 min at 13 000 rpm. The supernatant is collected and freeze dried using a speed vac concentrator (Savant SPD121P, Thermo Fisher). All the extraction is repeated once, and the supernatants are pooled in the same glass. Finally, the dried material is recovered in 300 µL of MeOH.

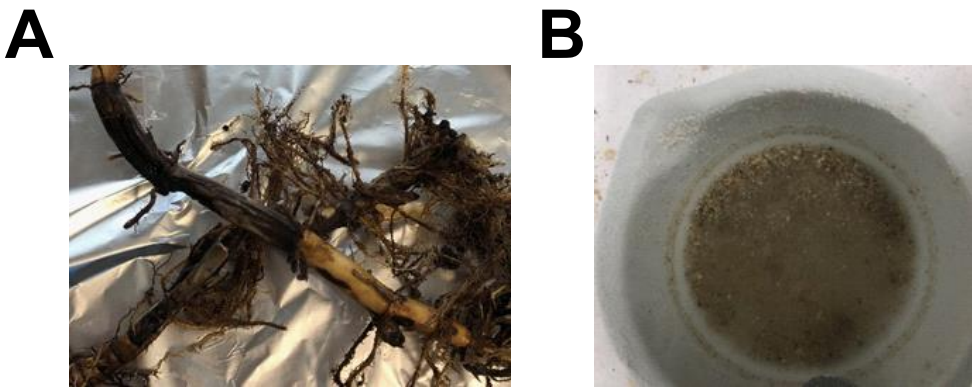

Figure 35: Reed rhizome extraction. **A)** reed rhizome samples. **B)** reed rhizome ground using liquid nitrogen.

2.1.4.4. Method limits characterization

The final step of this optimization is focused on the characteristic of this method. This method has been characterized by the reproducibility and the identification of limits of detection (LOD), limit of quantification (LOQ) and finally the matrix effect. Deuterated compounds have been used to figure out the limits and the reproducibility. The compounds used were acetaminophen-d4, sulfamethoxazole-d4, N-Desmethyl sildenafil d8, gemfibrozil-d6, diclofenac-d4, bezafibrate-d4, as mentioned in Boleda et al., 2013. Indeed, water and sludge samples were spiked with these standards from 1 ng/mL to 10 µg/mL. The signal-to-noise ratio (S/N) has been used to determine the LOD (S/N lower than 3) and LOQ (S/N lower than 5). According to the results found in the **supplementary datas (2)**, LOD could be fixed at 1 µg/mL. As the extraction was performed on 10 g of sediments and 50 mL of wastewater, LOD could be 100 ng/g in the sediment samples and 20 ng/mL in the water samples. On the other hand, the matrix effects in water and sludge could also be calculated as described in Alygizakis et al., 2016. [14]

$$Matrice\ effect = 1 - \frac{Area\ of\ compound\ in\ the\ matrix}{Area\ of\ the\ compound\ in\ methanol} \quad [14]$$

The results for matrix effects and LOD and LOQ could be described in the **Table 7**.

Table 7: Characteristics of the extraction method: LOD, LOQ, and matrix effect adapted from Villette et al., 2019a.

	LOD (µg/mL)	LOQ (µg/mL)	Water matrix effect	Sediment matrix effect
Acetaminopher-d4	**10**	**10**	**97%**	**98%**
Gemfibrozil-d6	**1**	**1**	**98%**	**98%**
N-Desmethyl sildenafil-d8	**1**	**10**	**94%**	**96%**
Sulfamethoxazole-d4	**10**	**10**	**97%**	**98%**
Diclofenac-d4	**1**	**10**	**97%**	**98%**
Bezafibrate-d4	**1**	**10**	**98%**	**97%**

Matrix effect results underline the difficulties to identify compounds in complex samples as water or sludge, due to the extinction coefficient around 95%. These results suggest that a part of the micropollutants are hardly detected and highlights the importance to consider this matrix effect.

The last parameter studied in this optimization concerns the repeatability of the extraction process. To qualify this repeatability, three technical replicates for each matrix were performed and the standard deviation was studied. A summary could be found in the **Table 8** and the area details are found in the **supplementary datas (3).**

Table 8: Repeatability of the extraction method using deuterated compounds in water and sludge samples using average area, standard deviation and coefficient of variation (CV).

	Water			**Sediment**		
	Average area	Standard deviation	**CV**	Average area	Standard deviation	**CV**
Acetaminophen-d4	1.45E+07	1.32E+06	**9%**	7.70E+06	2.27E+06	**29%**
Sulfamethoxazole-d4	1.69E+08	4.37E+06	**3%**	9.26E+07	6.57E+06	**7%**
N-desmethyl sildenafil-d8	3.01E+05	9.37E+04	**31%**	1.59E+04	1.07E+03	**7%**
Gemfibrozil-d6	6.19E+08	8.34E+07	**13%**	4.20E+08	4.40E+06	**1%**
Diclofenac-d4	4.39E+08	6.79E+06	**2%**	6.51E+08	3.03E+07	**5%**
Bezafibrate-d4	3.97E+08	3.25E+07	**8%**	5.87E+08	5.96E+07	**10%**

The coefficient of variation observed is in agreement with the range defined by Boleda et al., 2013 or Cotton et al., 2016) (2 to 18%), except for acetaminophen-d4 in sediment and N-desmethyl-sildenafil-d8 in water. As deviation seems to agree with the results mentioned in the literature, this method could be validated to extract the micropollutants.

The extraction process has been optimized considering the sample quantity, and the development of a new method adapted to extract micropollutant in this study. Furthermore, repeatability, LOD, LOQ and matrix effect have been determined for this extraction. In this way, once the extraction process has been determined, the sample analysis in mass spectrometry must be introduced.

The final step of the extraction optimization was focused on the dilution rate used to inject the samples. Indeed, the concentration process performed to identify micropollutants in the samples can lead to the spectrometer saturation. To deal with this saturation but also with the low-intensity compounds, the samples collected before the analysis were diluted in different dilution rates (2; 10; 20; 100; 200; 1000) or concentrated (10 fold) to obtain the most global overview of compounds content.

2.1.5. Sample analysis in mass spectrometry

Micropollutants class is a heterogeneous class of compounds. Polar, apolar, volatile, non-volatile compounds, compounds with diverse chemical structures or molecular weight could be found in the micropollutants. But this micropollutants non-target screening was achieved using mass spectrometry. Yet, to detect the most global overview of compounds, GC-MS and LC-HRMS/MS analyses were combined. Indeed, GC-MS is well adapted to analyze volatile, apolar compounds such as PAHS or some pesticides. Besides, GC-MS method is widely used to analyze sludge or sediment samples. On the other hand, LC-HRMS/MS is better suited for polar organic compounds such as drugs. Therefore, samples were analyzed using these two types of analytical tools.

The samples were first analyzed in GC-MS/MS coupled to triple quadrupole (SCION TQ, Bruker; 70eV, mass to charge ratio 50 to 700 Da). The gas chromatography is carried out on a HP-5-MS column (30-m, 0.25-mm, 0.25 µm; 436-GC, Bruker) and uses helium as a carrier gas. The injector temperature was set at 230 °C. Samples injected were kept at 60 °C for the first minute, then a temperature ramp (5 °C/min) has been programed and raised to 320 °C. This temperature is kept for 10 min. On the other hand, a constant flow of 1 mL/min with a pressure pulse of 30 psi during 1 min has been set up.

Furthermore, samples were also analyzed using LC-HRMS/MS on a Dionex Ultimate 3000 (Thermo) coupled to a Q-TOF (Impact II, Bruker), using the TargetScreener method developed by Bruker (Bremen, Germany) and mentioned in Villette et al., 2019a. Briefly, two solvents were used solvent A (water: methanol (90:10) with 0.01% formic acid and 314 mg/L of ammonium formate) and solvent B (methanol with 0.01% formic acid and 314 mg/L of ammonium formate). The run last 20 min. The compounds separation is carried out on a C18 column (Acclaim TM RSLC 120 C18, 2.2 µm 120 A 2.1x 100 nm, Dionex bonded silica products). Briefly, solvent is first injected with a flow at 0.2 mL/min and 1% B for 3 minutes, then the B rate increases to 39%. Next the flow increases to 0.4 mL/min at 14 min and B rate is about 99.9%, and finally the flow reaches to 0.48 mL/min after 16 minutes. The final stage at 19.1 min decreases the flow to 0.2 mL/min with B ratio about 1% and the run ends up at 20 min. This gradient program is also found in the **supplementary datas (4)**. All the samples were analyzed using the positive ion mode of the spectrometer with a spectra rate of 2 Hz and a mass range from 30 to 1000 Da. The capillary voltage was set at 2500 V, the nebulizer at 2 Bars and

the dry gas at 8 L/min, with a dry temperature of 200 °C. Fragments were obtained via broadband collision-induced dissociation (bbCID) with an MS/MS collision energy set at 30 eV.

2.1.6. Data processing

2.1.6.1. Analyte of interest extraction

The final step of this method optimization is focused on the data processing. Indeed, non-target screening generates a huge number of data, which need to be processed to obtain micropollutants identification. As it has been described in the state of art, the identifications were performed following the method mentioned in Schymanski et al., 2014 and the 5 levels defined in this study.

First the compounds annotated in GC-MS/MS were obtained using MS DataReview. The compounds identification is based on the comparison with spectral libraries. In this PhD project, large spectral databases were used to obtain a global overview with NIST 17 or Wiley 14 but also specific databases for toxic compounds with the example of Maurer, Pfleger, Weber 2011. These spectral libraries are useful to reach the level 3 (molecules names) in the Schymanski classification. To perform this annotation only compounds with the following criteria were extracted from the mass spectra, as recommended in Sumner et al., 2007:

- peak width lower than two seconds,
- slope sensitivity higher than three,
- peak intensity higher than 1000 cps.

Finally, only compounds with a RMatch higher than 800 were considered as compounds annotated (level 3) (Lange et al., 2019) and used in the study. The confirmation of compounds annotations requires the analysis and the match with an analytical standard. In this way, the identification reaches to the level 1.

On the other hand, the samples were also analyzed in LC-HRMS/MS. A similar method using spectral libraries could be used to identify compounds. Nevertheless, spectral libraries are less suited for LC-HRMS/MS. GC-MS/MS used an electron ionization (EI) as ion sources. Identical operating conditions were applied for all EI sources and thus facilitate the comparison with spectral libraries. However, EI sources are not coupled with LC-MS systems. In our case, the

ion source used in the LC-HRMS is electrospray ionization (ESI). Nevertheless, this ion sources could have different operating conditions, depending on the constructors or the applications. In this way, the use of spectral libraries does not seem to be the most appropriate to identify compounds in LC-HRMS or would be high time consuming. To solve this issue, another method could be used. This method is based on the raw formula generation from exact mass, isotopic pattern but also of the fragment ions. To achieve these annotations, the software Metaboscape 3.0 (Bruker) and SmartFormula 3D from Bruker were used. Therefore, the samples injected for a study could be imported in the Metaboscape software. The data selected (with the corresponding ionization mode, positive in our case) will be used to create groups and define the most representative value. To obtain this group, first an intensity threshold as well as the value count of each group should be defined. The optimization of intensity threshold, described in the next section, has suggested setting the threshold at 1000 and only compounds found in 80% of the individuals from at least one group sample were selected as mentioned in Villette et al., 2018. Then the compounds of interest were selected based on the non-parametric Wilcoxon rank sum test (p-value <0.05) and the fold changes ≥ 2 (absolute value).

Metaboscape detects all the adducts forms for a mass of interest. Then it creates a pool of these adducts, called “buckets”, which is representing a single metabolite feature (Villette et al., 2019). Then all the buckets could be found in the software and be annotated as shown in **Figure 36.**

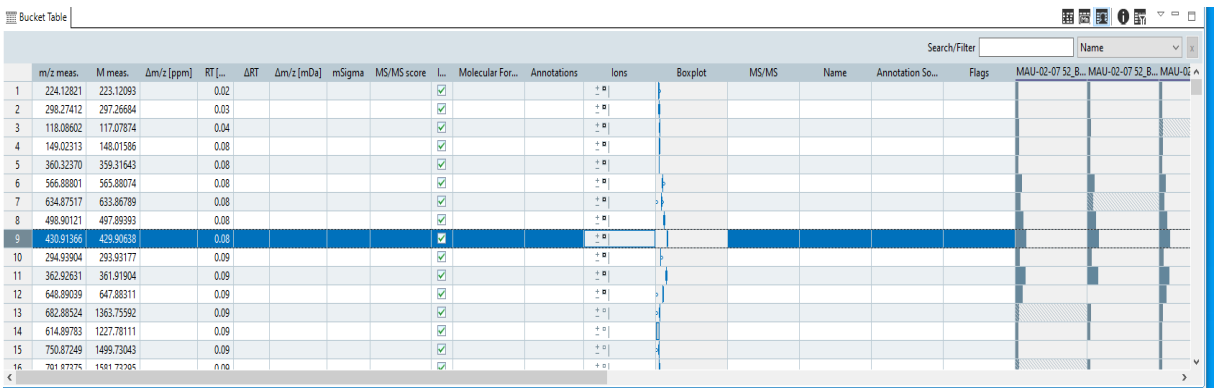

Figure 36: Bucket table from Metaboscape representing the different buckets found in a sample.

This pool corresponds to the level 5 (exact mass) in the Schymanski classification. An intensity threshold has been optimized to obtain a global overview. Then the intensity threshold for features extractions parameters should be chosen. Therefore, three thresholds have been tested to visualize the impact on the extraction and compared to the peaks detected. The results from this optimization could be observed in **Figure 37**.

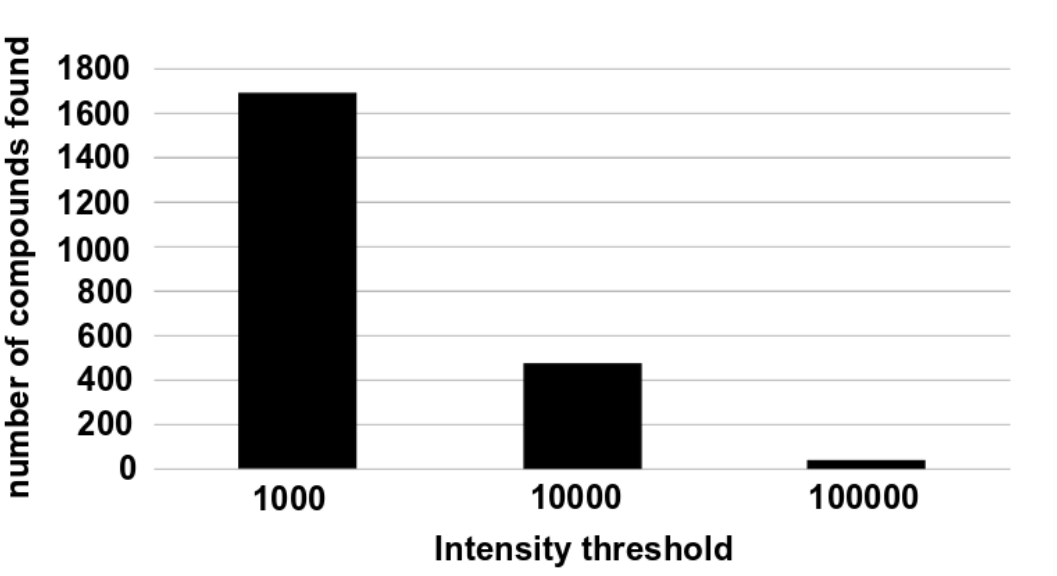

Figure 37: Intensity threshold sensitivity optimization for compounds annotations.

2.1.6.2. Molecular formula generation and tentative annotations

Regarding the results found in **Figure 37**, it seems that intensity threshold should be introduced at 1000 as it represents the higher number of mass of interest (level 5). Once the bucket table created and all the features found, identifications could be performed. The first step is dedicated to the raw formula generation. As it has been described in the previous section, SmartFormula will be used to obtain this raw formula. SmartFormula is based on the exact mass and the isotopic patterns of fragment ions to generate a formula. The software will combine the data from MS and MS/MS data to find a restricted list of formulae. The most elements found in the micropollutants were selected, i.e., C, H, N, O, P, S, Cl, Br, F and I. The following criteria have been set up to generate raw formulae:

- a mass deviation (Δm/z) under 3ppm,
- a mSigma (fitting between measured and theoretical isotope patterns) under 30.

Once the raw formula generated, the following objectives are to identify the compounds. Therefore, these raw formulae must be compared with data included in several databases. The classical way could be the interrogations of each database. Indeed, in metabolomics, no single database containing all the micropollutants or all the plant metabolites is existing. Therefore, each database of interest should be used separately. Nevertheless, this option has several drawbacks. Due to the lack of a single database for micropollutants or plant metabolites, this

option will be time consuming. Furthermore, the use of online databases could cause several issues. The access is depending on the servers and databases could disappear and working on an online database with sensitive data would not be safe. Therefore, a home-made database has been created by importing the raw formula found in the online database. This home-made database could be used in Metaboscape 3.0. Indeed, the software has serval options to annotate compounds, and the most appropriate option in this case is called “Analyte list”. These “Analyte list” can contain a list of compounds that can be compared with the buckets found in the samples. The compound lists (restricted to 60,000 compounds) could be imported in Mestaboscape and raw formula to calculate the exact mass and compared with the data contained in the bucket. The identification fitting could be checked with the same criteria as those applied for SmartFormula (Δm/z, mSigma). An example of Analyte list will be found in the **supplementary datas (5)**. Then if the raw formula generated by Smart Formula 3D and the raw formula containing in the Analyte list match, in this way, the compounds could be annotated and reach the level 3 in the Schymanski classification. Finally, the different annotations found for a feature were compared, thanks to a home-made program developed in Visual Basic. In the same way as GC-MS annotation, the confirmation of compounds annotations requires the analysis and the match with an analytical standard. The databases used for the identification and the compounds number contained in the databases could be observed in the **Table 9** and were available online in July 2018.

Table 9: Different databases used for the compounds identification. a (http://foodb.ca/), b (http://kanaya.naist.jp/KNApSAcK/), c (https://www.plantcyc.org/), d (http://phenol-explorer.eu/), e (http://www.swisslipids.org/), f (https://www.norman-network.net/), g (http://www.t3db.ca/), h (http://www.swgdrug.org/), i (http://www.eurl-pesticides.eu), j (http://www.ymdb.ca/), k (http://www.ecmdb.ca/). The other databases were commercially available.

Database type				
Global database	**NIST14** 242,477 compounds	**Wiley 10** 620,000 compounds	**FoodDB**[a] 15,959 compounds	
Plant database	**KNApSAck**[b] 40,053 compounds	**PlantCyc**[c] 2,837 compounds	**Phenol Explorer**[d] 488 compounds	
Lipids database	**Swiss Lipids**[e] 570,677 compounds			
Toxic database	**Norman**[f] 40,053 compounds	**TargetScreener** 2,246 compounds	**T3DB**[g] 3,003 compounds	**Maurer, Pleger, Weber** 8,650 compounds
Drugs database	**SWGDRUGS**[h] 2,672 Compounds			
Pesticides database	**EURL-FV**[i] 761 compounds			
Bacteria/Yeast database	**YMDB**[j] 1,652 compounds	**ECMD**[k] 3,722 compounds		

Finally, the buckets of interest were selected based on the non-parametric Wilcoxon rank sum test (p-value <0.05) and the fold changes set at 2.

Furthermore, all these databases contained parent molecules and few micropollutants metabolites. Nevertheless, the distribution of micropollutants in the environment must also

focus on the fate of these micropolluants, and thus of micropollutants metabolites. In this way, the software Metabolite Predict 2.0 (Bruker, Germany) has been used to generate drugs metabolites (catabolites and conjugates) from drugs detected in the samples. The drugs structure is drawn or imported using the SDF file from Pubchem in the software then 79 biotransformation rules found in the **supplementary datas (6)** were selected for *in silico* prediction. A mass list is then generated based on the raw formulae found, and this list could be imported as an "Analyte list" described in the previous section.

This material and method section have defined the context of the study with the main objectives and the study site. Furthermore, all the sampling strategy and the different compartments analyzed were introduced. Then the optimization of micropollutant has been introduced. This optimization suggests the use of 10 g of sediment, 50 mL of water and a method based on freeze-drying and liquid extraction without SPE. On the other hand, the method limits have also been defined with the LOD, LOQ, the matrix effect and the reproducibility. To obtain the largest view of micropollutants, samples were both analyzed in GC-MS/MS and LC-HRMS/MS. Finally, this section was focused on data treatment with the use of spectral libraries for the GC-MS/MS analysis. On the other hand, compounds identified in LC-HRMS/MS were identified thanks to a method using raw formula and a home-made annotation based on several online databases imported. These methods could now be applied on the different studies to obtain the micropollutants distribution in the tertiary treatment wetland ecosystems and the constructed wetland.

2.2. Results and discussions

2.2.1. Large scale micropollutants screening in the wetland ecosystem

The first part of the results will be dedicated to the large screening of micropollutants in the wetland (vegetated ditch) ecosystem. The three main compartments composing this ecosystem were wastewater, plants and sludge. In the tertiary treatment wetland, poplar leaves were studied, while reed roots were analyzed in the constructed wetland.

Concerning the results, the non-target screening was first performed on the tertiary treatment wetland located at the outlet of the CW. Results found in this wetland could represent the micropollutants widespread in the environment near an urban wastewater release. The **Figure 38** represents the metabolites distribution found in the tertiary treatment wetland.

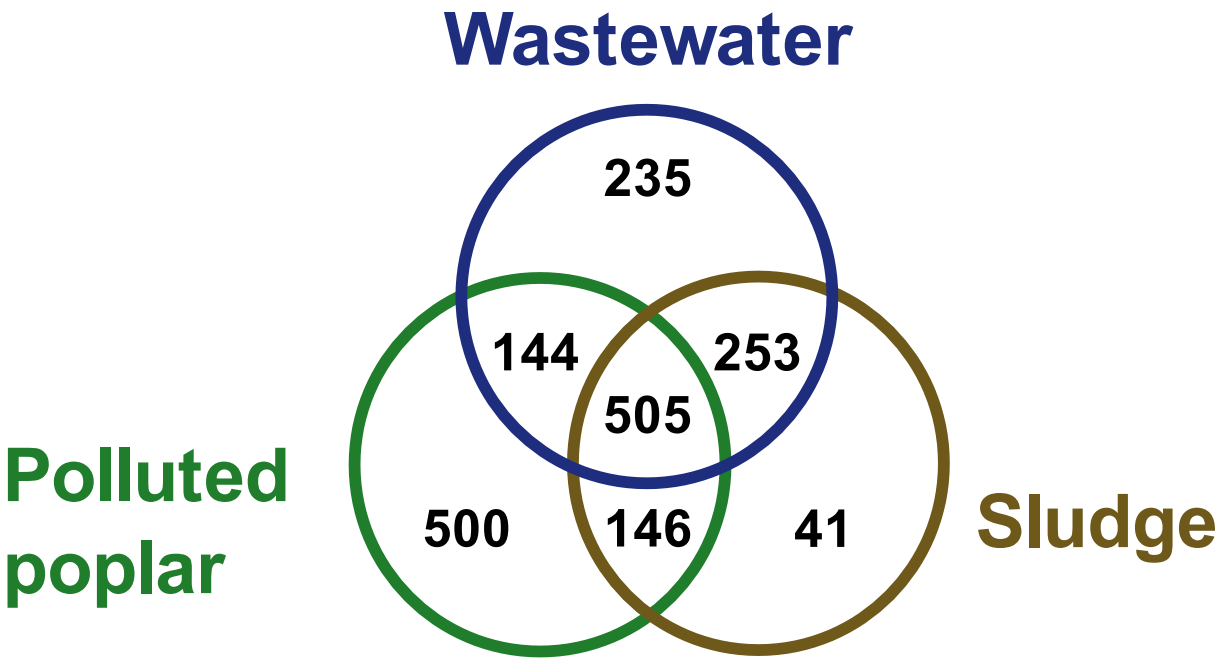

Figure 38: Metabolites distribution in the ecosystem of the tertiary treatment wetland (wastewater, sludge and polluted poplar) adapted from Villette et al., 2019a.

First, a wide diversity of metabolites could be noticed in the different compartments. The compounds could be distinguished as compounds found specifically in a compartment and those detected at least in two compartments. All the details of the compounds are mentioned in the supplementary data from the publication Villette et al.,2019 a. Concerning the specific compounds, they are mainly found in the polluted poplar (500 annotations) then in wastewater

(235 annotations). The interface role of sludge could partly explain that few compounds (41 annotations) are specific to sludge. Indeed, sludge analyzed was not dried so water could remain in sludge pores. Therefore, sludge clearly contains compounds found in the wastewater, as underlined by the huge number of compounds found both in these two compartments. It is well known that micropollutants taken up by plants were mainly found in the water pores from the soil (Chuang et al., 2019; Li et al., 2019). Besides, even if a large part of compounds could be sorbed, most of them could be detected in equilibrium in the water and solid phase. Therefore, it is not surprising to find a large number of compounds in the interface of the three compartments. About half of the annotations (1048 annotations on 1824 total annotations) were found at least in two compartments and almost one third (505 annotations) could be detected in all the compartments. Indeed, 144 common annotations are detected for the poplar and wastewater, 253 for sludge and wastewater and finally, 146 for sludge and poplar. The comparison with the constructed wetland suggests a similar trend with strong interactions between the different compartments. However, a higher compartment specificity could be observed, only 20% of the compounds are found at least in two compartments (275 annotations on 1392 total annotations) and the results are detailed in the article Maurer et al., 2020.

These results could highlight the compounds wide spreading in the different compartments of this ecosystem. Nevertheless, this distribution, based only on the metabolites number, could hide some diversity as only the metabolites annotations are shown in this **Figure 38**. The metabolites cover compounds naturally present in the environment such as plant, animal, bacteria metabolites but also xenobiotics and lipids. Therefore, the metabolites classes were investigated in each compartment. The results are shown in **Figure 39**.

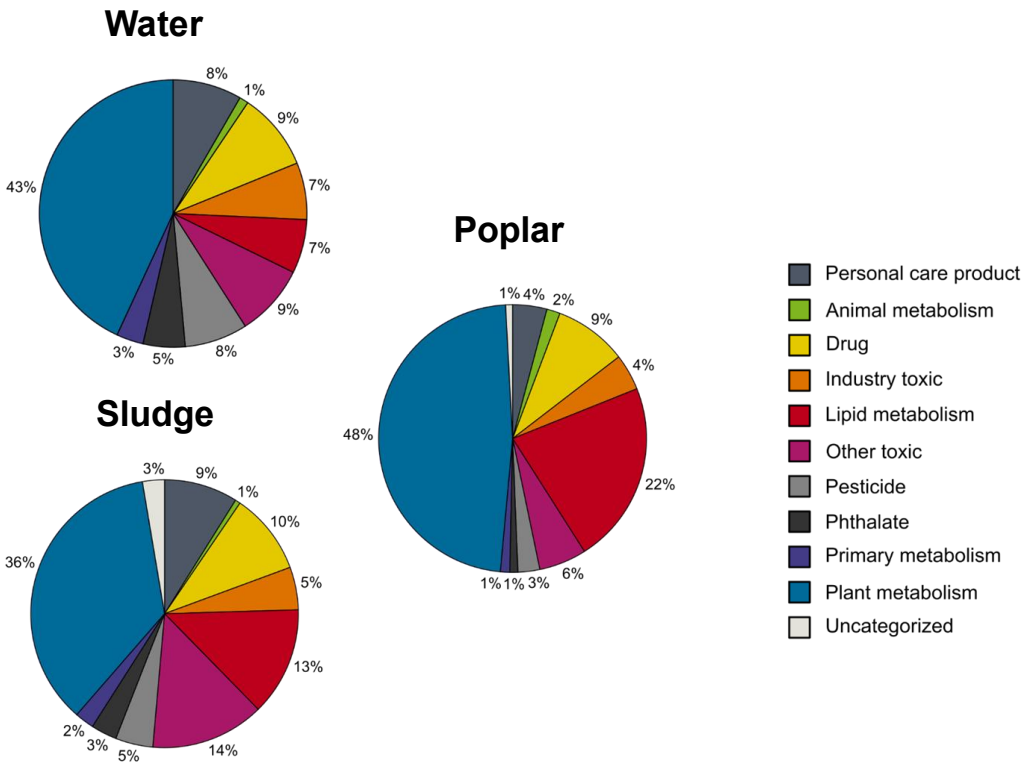

Figure 39: Distribution of metabolite classes observed in the different wetland ecosystem compartments (water, plants and sludge, adapted from Villette et al., 2019a).

Concerning the compounds classes, the classes naturally found in the environment are predictably detected in each compartment. Indeed, the plant and microorganisms growing in this system, the animals living there (worms, tadpoles, birds) will generate some metabolites during their development (growth and death). These metabolites are not surprisingly found in a system based on natural processes. But the interesting result is that drugs, industry toxics, pesticides, phthalates or personal care products are also detected in the different compartments. Besides, the xenobiotics fraction in the metabolites profile observed in each compartment could not be neglected. These xenobiotics represent between 28% and 46% of the metabolic profile, depending on the compartment considered. Among these xenobiotics, drugs, other toxics and personal care products are the main classes detected. Besides, the same classes are detected in each compartment, suggesting the wide spread of each xenobiotics class in all the compartments, as it has already been demonstrated in the literature (Carvalho et al., 2014; Li et al., 2019). Results underline the interactions that can occur between the different compartments (Nuel et al., 2018; Petrie et al., 2018). As described in several studies, the physicochemical properties are not the driving force governing the distribution. The distribution of the most intense compounds detected in each compartment has been studied using the distribution factor

(Kd, BCF factor…) but also their physico-chemical properties as found in the **supplementary datas (7)**. This observation has already been made for selected compounds to understand the transport in soil layers (Gros et al., 2019) or in different compartments (Chuang et al., 2019; Li et al., 2019). Nevertheless, the literature mentions that ionic fraction could be used to find compounds preferably found in plants (Li et al., 2019; Chuang et al., 2019), but the link is not clearly obvious in this study. Indeed, only the compounds detected in the three compartments seem to have a higher ionic proportion. This result suggests that compounds transferred and found in equilibrium in the environment compartment may be influenced by these parameters. To illustrate this distribution, venlafaxine was quantified in the three compartments (with concentration about 860 µg/kg in the mud, 531 µg/kg in the plant and 24 µg/L in wastewater) and Kd = 35.19 (partage coefficient) and BCF (bioconcentration factor) = 22.15 were calculated. The Kd has also been calculated for acebutolol also observed in raw wastewater (Kd=1.55). Nevertheless, these parameters, as described in Li et al., 2019, combined with predicted Henry law parameters (for photovolatilization), could not be related to the distribution.

On the other hand, the most surprising result is that a plant growing in a polluted area could survive with almost one third of its metabolic profile that is composed of xenobiotics. The different micropollutants taken up by plants is widely discussed in the literature and could explain a part of their fate (Picó et al., 2017). This transport from water and soil to plant could be influenced by the sorption of micropollutants in mud and by bioprocesses that can transform the micropollutants. (Miller et al., 2016; Uddin et al., 2020).

As mentioned previously, this uptake is mainly related to the compounds found in pore water (Li et al., 2019) and water and sludge content mainly influence the micropollutants detected in plants (Carvalho et al., 2014; Li et al., 2019; Nuel et al., 2018). But the use of single physicochemical or fate parameters could not by itself explain the distribution. On the other hand, the molecule size is also mentioned as a discriminative parameter for compounds found in planta. Nevertheless, in their study Chuang et al., 2019 mentioned that large size molecules could be transferred using both apoplastic and symplastic ways. The symplastic pathway is just slower (Chuang et al., 2019). However, as we investigated plant chronically exposed to micropollutants, the results could provide an integrative view of the contamination and the impact of pharmaceuticals size seems to be limited. This transfer using several ways could also explain the difference of xenobiotics found in poplar leaves or in reed roots and the other compartments. The detection in the aerial parts has for example been performed by Bartrons

and Peñeulas who described the micropollutants detection in stem or leaves (Bartrons and Peñuelas, 2017). Indeed, the detection of micropollutants in the shoots and this transport could be explained by the transpiration stream, generating the micropollutants movements (Chuang et al., 2019; Li et al., 2019). The translocation factor (TF) could estimate the distribution (Li et al., 2019; Gong et al., 2020 Liu et al., 2019; W. Wang et al., 2019) but it has not been investigated in this study as only specific organs were analyzed. An estimation of this parameter will be done in the chapter dedicated to the mass spectrometry imaging. Besides these transfer processes are not class dependent as Pullagurala et al., 2018 underline in their review that different classes of emerging contaminants could be found. Nevertheless, no single xenobiotics behavior concerning this translocation could be highlighted.

Nevertheless, this micropollutants accumulation could create a stress response from the plants, as described in **Figure 40**. Indeed, this plant stress is underlined with the pigment degradation and plant metabolite involved in tissues degradation found in the poplar leaves. The chlorophyll a was observed in higher amounts in the polluted plant. This result could highlight the process set up by the plants to deal with the contamination. Indeed, precursor production is coupled to catabolites production. Therefore, the plant should activate a rapid turnover to counter the loss of chlorophyll and produce biomass, as the gibberellin A7 (GA_7) (plant hormone promoting growth and elongation cells) seems to indicate, to prevent biomass loss potentially induced by the micropollutants stress. In addition to this turnover, plant defense mechanisms are also set up. These defense mechanisms could be supported by the detection of IBA (indole-butyric acid) or azelaic acid (AzA) in the polluted plant. IBA is involved in the abiotic stress response (Tognetti et al., 2010) and AzA in the systemic acquired resistance. This stress metabolites found should indicate that plants set a defense mechanism against this chronic exposure (Villette et al., 2019,a).

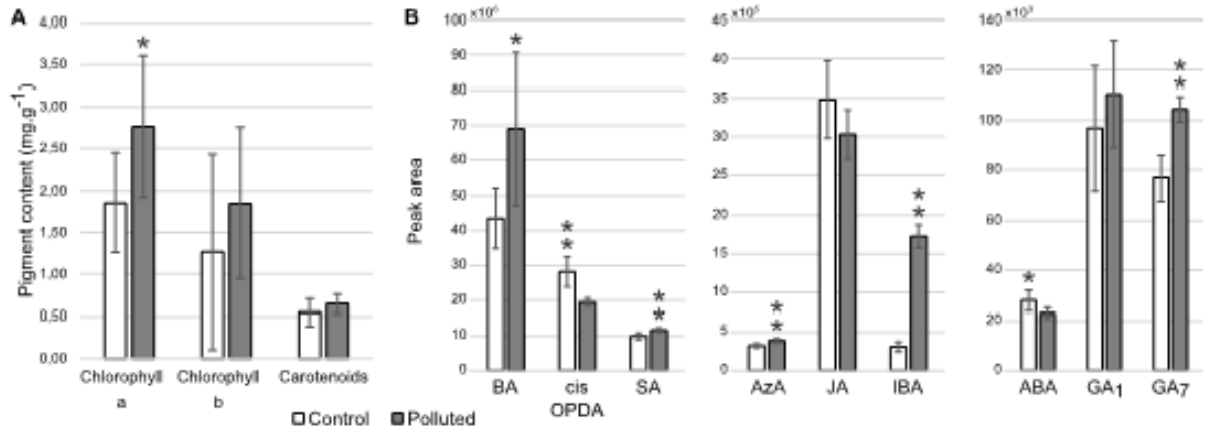

Figure 40: Pigments concentration and hormones and azelaic acid found in the poplar leaves (control and polluted). The analysis showed that chlorophyll a is found in higher concentration in the polluted leaves. ABA and cis-OPDA are found in higher proportion in the control leaves, while BA, SA and GA7 were found in higher amount in polluted leaves from Villette et al., 2019a.

The plant sets up mechanisms as stress responses, storage (as shown in the next chapter) or biodegradation to deal with these micropollutants. Using the plants defense mechanism combined with storage processes and biotransformation the plant could deal with these micropollutants. This biotransformation could also explain why some parent compounds are not detected. Indeed, enzymes present inside the plants could generate micropollutants biotransformation as mentioned by Klampfl 2019. These biotransformations will be mentioned in the next chapter.

The results found in this section showed that the micropollutants detected in this ecosystem are a global issue for this system and for the environment located in the outlet of the CW. The results found here highlight that the micropollutants issue could not be restricted to some classes and the non-target approach should be performed to obtain an overview of this contamination. Moreover, this contamination is not restricted to the wastewater but is widespread in all the compartment, where plants could play a key role. Nevertheless, this first section was only focusing on compartments with direct interactions with wastewater. But the water infiltration could also contaminate lower soil layers. Therefore, a vertical profile of soil in the constructed wetland was also investigated, using the same approach.

2.2.2. Large scale micropollutants screening in the sludge layers in a constructed wetland

The last part of this non-target screening in the ecosystem will investigate the vertical profile of soil layers in the CW. Indeed, wastewater could contaminate the soil at various depths. To

estimate this contamination, a coring should be performed and analyzed using the non-target approach. To obtain the micropollutants results coming only from wastewater, a control coring was also carried out in the bank of the CW to remove the background as mentioned in the materials and methods section. Therefore, in this section only the micropollutants specific to the CW will be discussed. This approach will provide a close up view of micropollutants only coming from the wastewater. The xenobiotics and lipids annotations number have been summarized in the **Table 10**.

Table 10: Annotations found in the sludge layers.

	Top layer	Both	Bottom layer
Annotations (level 3 in Schymanski classification)	**191**	**319**	**38**

The main results underlined by these annotations performed in the coring show that the main part of the lipids and micropollutants investigated will diffuse through the entire depth (319 single names annotated), suggesting the xenobiotics transport by wastewater. On the other hand, regarding the results found in a specific layer, a higher specificity could be noticed in the top layer with 191 single names while 38 single names were identified in the bottom layer.

This sequestration in the top layer has already been mentioned in the literature, suggesting the key role of the first soil layer. (Biel-Maeso et al., 2019; Gros et al., 2019). As mentioned in the previous section, the number of micropollutants hides the diversity of compounds. Indeed, even if the same micropollutants classes have been detected, different trends of micropollutants distribution could be observed as shown in **Figure 41**.

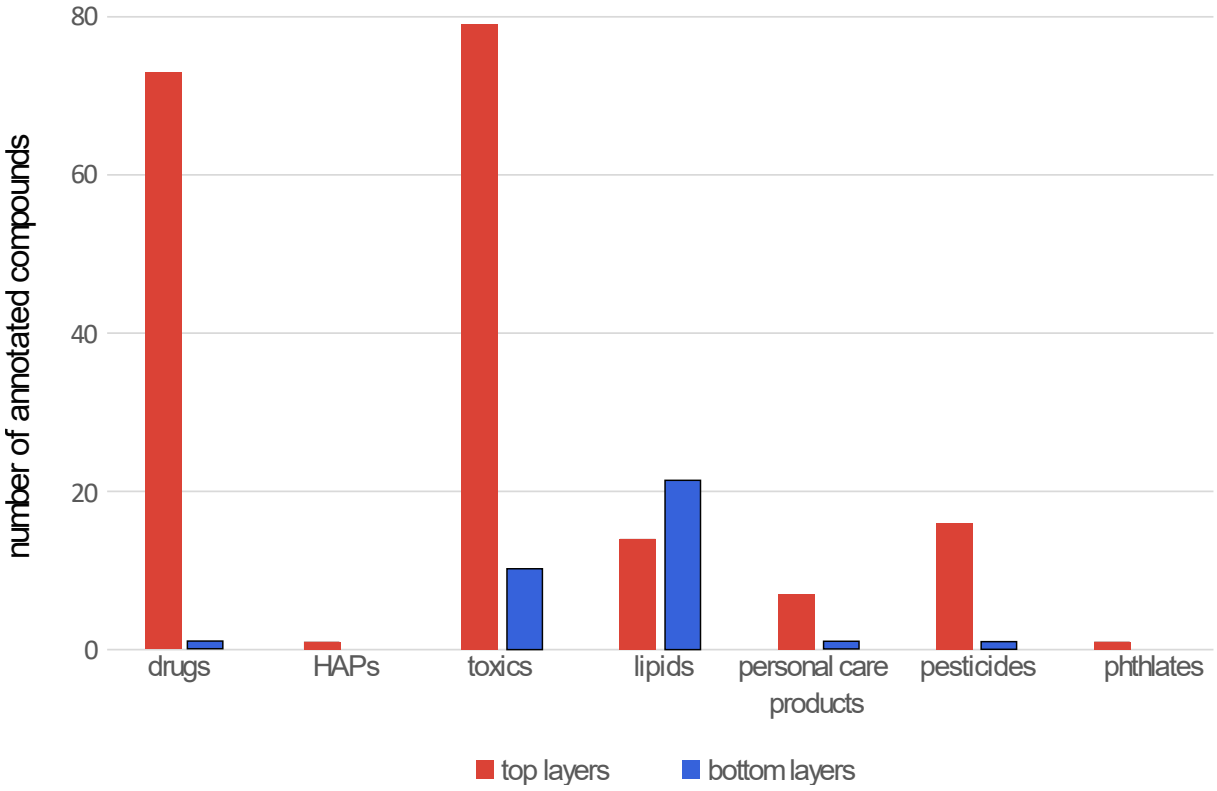

Figure 41: Xenobiotics and lipids distribution in the sludge layers.

73 drugs, 79 toxics, 7 personal care products, 16 pesticides are found in the top layer, while 1 drug, personal care product, pesticide and 10 toxics were detected in the bottom layer. The drugs and pesticides are mainly polar compounds, and could diffuse in the entire depth or will be stored in the top layer as mentioned for pharmaceuticals in the study from Gros et al., (2019) based on soil contaminated by slurry. Indeed, in our micropollutants study these two xenobiotics behaviors has been observed. In general terms, all the micropollutants quantified were found in higher concentrations in the top layer.

This distribution through the different layers could be linked with water transport through the sludge layers. Nevertheless, some sludge physical properties and their content in carbon, nitrogen and phosphorus should be investigated to understand the specificity observed in each layer. The texture layers analysis indicates a sandy-like texture with fine grain size promoting the water infiltration through the layers. Nevertheless, the top layer seems to have a higher proportion of finer grain size in the top layer (D10 180 µm versus 550 µm) as the granulometry represented in **Figure 42** indicated.

A

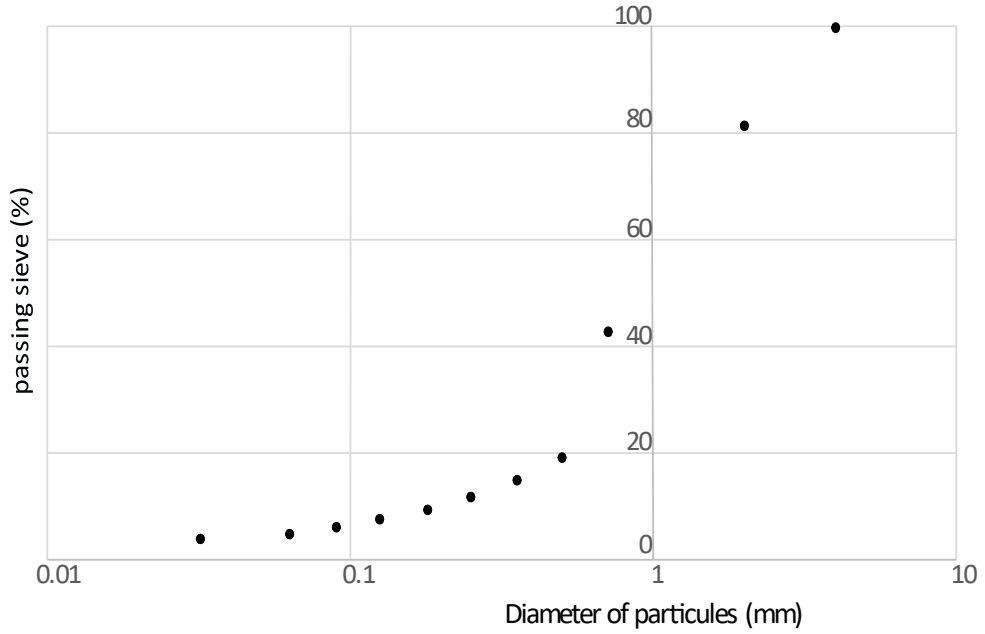

B

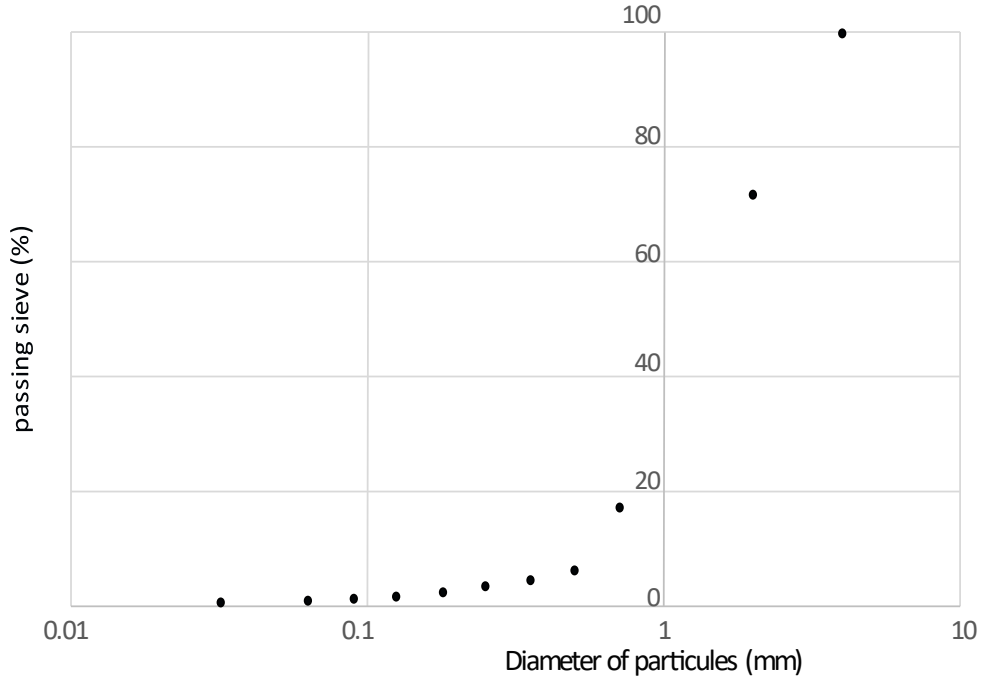

Figure 42: Granulometry curve from the two CW's sludge layers. **A)** top layer granulometry curve. **B)** Bottom layer granulometry curve adapted from Maurer et al., 2020.

This finer grain size could lead to slow water flow and increase the residence time and the interactions with sludge or rhizomes (Stefanakis and Tsihrintzis, 2012). Besides, the other characteristics such as porosity analysis could highlight a higher soil sorption ability, by increasing specific surface per unit of volume and enhance the water storage (Ávila et al., 2014). In our study, a high porosity has been found in both layers (92% in the top layer and 70% in the bottom layer), suggesting the high pollutants storage abilities in accordance with the micropollutants results found in the different layers. But physical sludge properties and structure should also be combined with their carbon, nitrogen and phosphorus content. Indeed, organic matter could improve sorption capacity in this layer (Cottin and Merlin, 2008; Brunsch et al., 2018; Biel-Maeso et al., 2019). Therefore, the higher total organic carbon (TOC) content (94.93 ± 23.24 mg/kg in the top layer versus 57.03 ± 10,92 mg/kg in the bottom layer) in the top layer could also partly explain this higher micropollutants content in the top layer. The literature mentioned that a higher organic matter content could promote sorption capacity (Cottin and Merlin, 2008; Brunsch et al., 2018) (Macht et al., 2011; Liu et al., 2019) and will enhance the interactions with wastewater. This high organic matter content will also promote the development of more animal and bacterial life or biofilms. Therefore, the sludge should also be investigated as a biological compartment. In this way, the different classes of lipids have been described and could be observed in the **Figure 43.**

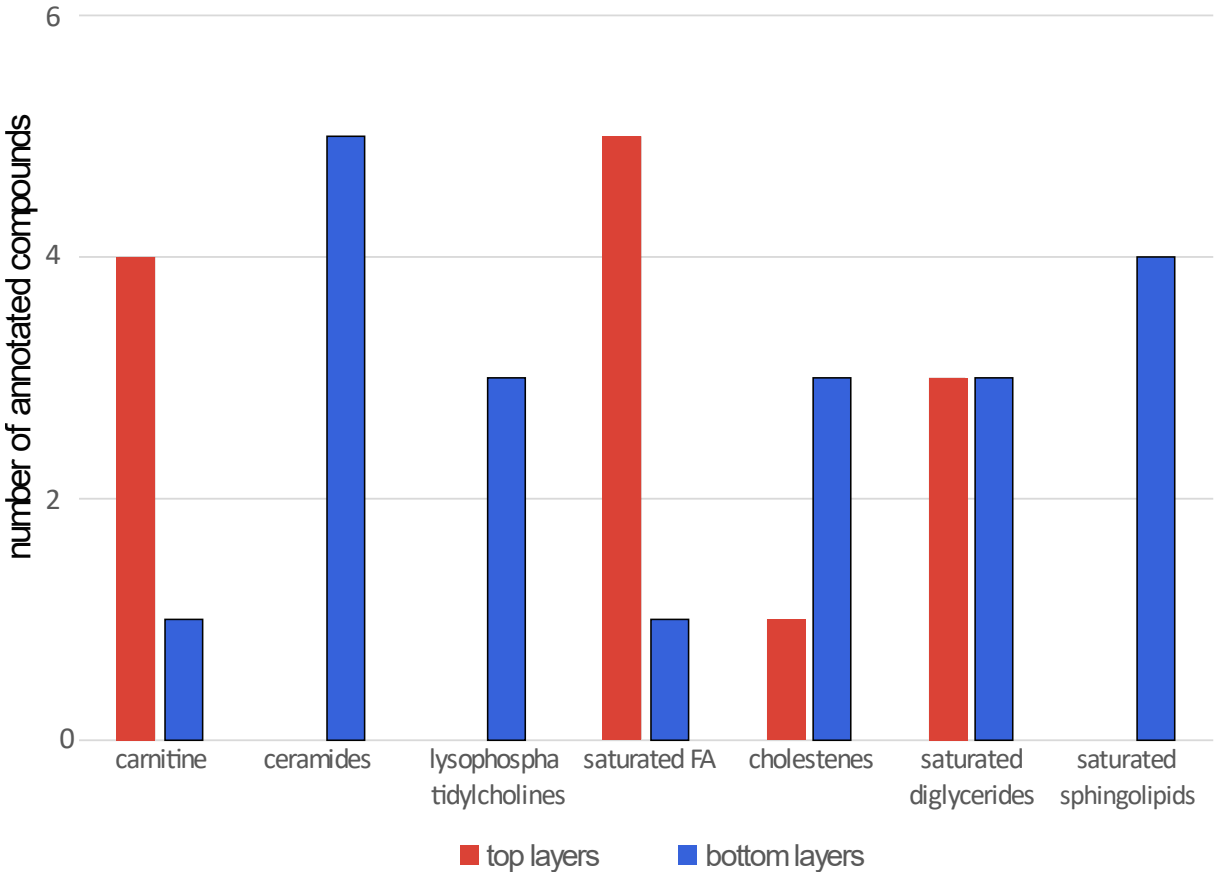

Figure 43: Profile of lipids found in the CW's sludge layers.

The lipids classes investigation underlines that cellular lipids such as ceramides, sphingolipids and lysophosphatidylcholines could be specifically found in the bottom layer. At the opposite, carnitines, and saturated fatty acids (FA) were mainly found in the top layer. Physico chemical properties could partly explain the lipids distribution. By definition lipids are hydrophobic compounds and could be easily sorbed to sludge, but fatty acids and carnitines are very hydrophobic compounds and could easily be caught in the top sludge layers and cannot reach the lower layers. On the contrary, sphingolipids or lysophosphatidylcholines are amphiphilic compounds, promoting their transport to the bottom layer. Their amphiphilic characteristics will enhance the water affinity and help them to reach the lower layers. However, their distribution could also be investigated using their biological function. Indeed, the fatty acids are considered as a substrate for microorganisms (Zhu et al., 2017). Fatty acids are widely detected in raw wastewater which leads to their detection in the top layer then support the microorganisms' growth. Therefore, according to these results the main microbial activity seems to be found in the top layer as mentioned in Tietz et al., 2008 and contributes to the pollutants removal. This layer will have a key role in this process. This microbial activity could

also explain the few xenobiotics specifically found in the bottom layer. Indeed, a part of xenobiotics could be degraded thanks to these microorganisms and the other will be distributed in the whole vertical profile. Besides, ceramides which have been found in the bottom layer are also detected in activated sludge system (Tsuge et al., 2008). But bacteria producing this kind of lipids in activated sludge can degrade emergent pollutants (Tsuge et al., 2008; White et al., 1996). The other classes detected in the bottom layer could also be linked to the variety of origins (animal, plant microbes degradation products) (Zhu et al., 2017).

All these results suggest that micropollutants only found in the top layer could be degraded or sorbed by these organisms (Ávila et al., 2014; Falås et al., 2018; Liu et al., 2019), degraded by photodegradation in surface water (Rühmland et al., 2015; Mathon et al., 2019) or transport in the other environment compartments.

2.3. Chapter conclusion

This second chapter dedicated to the non-target screening of micropollutants in wetland ecosystem has highlighted the large spreading of micropollutants. Indeed, the method developed in this section underlines that micropollutants are found in each compartment from the constructed wetlands. Besides even if different trends could be observed in the different compartment, the same classes are detected in each compartment. Yet the physicochemical properties and the transfer factors such as translocation factor, bioconcentration factor could not fully explain the distribution between the different compartments. The analyses made on the wetland systems underline that micropollutants are both found in a CW and the environment located at its outlet. Besides these micropollutants will also diffuse in a mud vertical profile and contaminate the lower layers. In this way, these results could provide an overview of micropollutants contamination in a polluted area. This sludge contamination in the vertical profile but also in the treated wastewater could create a risk for living organisms. As it has been mentioned in the literature, these micropollutants could contaminate living organisms and these organisms must deal with them. Then living organisms chronically exposed to micropollutants will take up and transform them from the environment. Besides as wetlands are plant-based systems, the analysis of plants could help to understand the fate of micropollutants. However, the non-target analysis as performed in this section could not provide spatial information in plant tissues. But this spatial informational could be crucial to understand bioprocesses. Therefore, the next section will be dedicated to the spatial distribution and metabolization of micropollutants using mass spectrometry imaging (MSI).

Chapter 3:

Spatial distribution and metabolization of micropollutants

The previous section has provided an overview of the contamination found in the wetland ecosystem using the non-target approach in LC-HRMS/MS. The distribution has shown that plant could take up micropollutants from the environment. And literature underline that plants set up mechanisms to deal with these pollutants. Yet, this LC-HRMS/MS method could be combined with MSI to visualize the micropollutants distribution in organisms living in this polluted environment. This method will be helpful to understand the stress factors detected in plants. On the other hand, the mechanisms induced in the plant (storage, biodegradation) to deal with these pollutants should be investigated. This approach will be developed in this chapter and applied on two compartments. First, MSI will be used on plants growing in the tertiary treatment wetland (vegetated ditch) and constructed wetlands (two stage VFCWs) to understand the mechanisms (storage, biotic and abiotic transformations) that could occur in these plants. Then the MSI will also be used to visualize spatial distribution in sludge, as it has been done in the previous chapter with the non-target screening in the different sludge layer. Therefore, this chapter will be structured as follows. First, the material and the methods used and developed will be described. This section will be dedicated to the sampling strategy, the samples preparation for MSI, the MSI acquisition and finally the data processing. Then these methods developed will be applied on three examples. First, the leaves of plant growing in the tertiary treatment wetland will be investigated to understand the fate and distribution of micropollutants in plants. Then a whole plant (*Phragmites australis* the common reed) will be studied to visualize the micropollutants distribution in the whole plant and its different organs. Finally, MSI will be used to visualize the distribution of micropollutants in different sludge samples.

3.1. Materials and Methods

3.1.1. Samples and sampling strategy

All the samples were collected in the same study site mentioned in the previous chapter. Indeed, the micropollutants distribution was investigated in plants growing in the constructed wetland and the tertiary treatment wetland. These areas are considered as polluted area in the Falkwiller study site.

3.1.1.1. Plants from vegetated ditch

First, the analysis was focused on plants growing in the tertiary treatment wetland, to visualize the impact of micropollutants release on plants located at the outlet of CWs. Therefore, the leaves of two plants growing in the wetland bank were collected. These two plants were *Salix alba (*willow) and *Populus nigra* (poplar) are described in **Figures 44** and **45**.

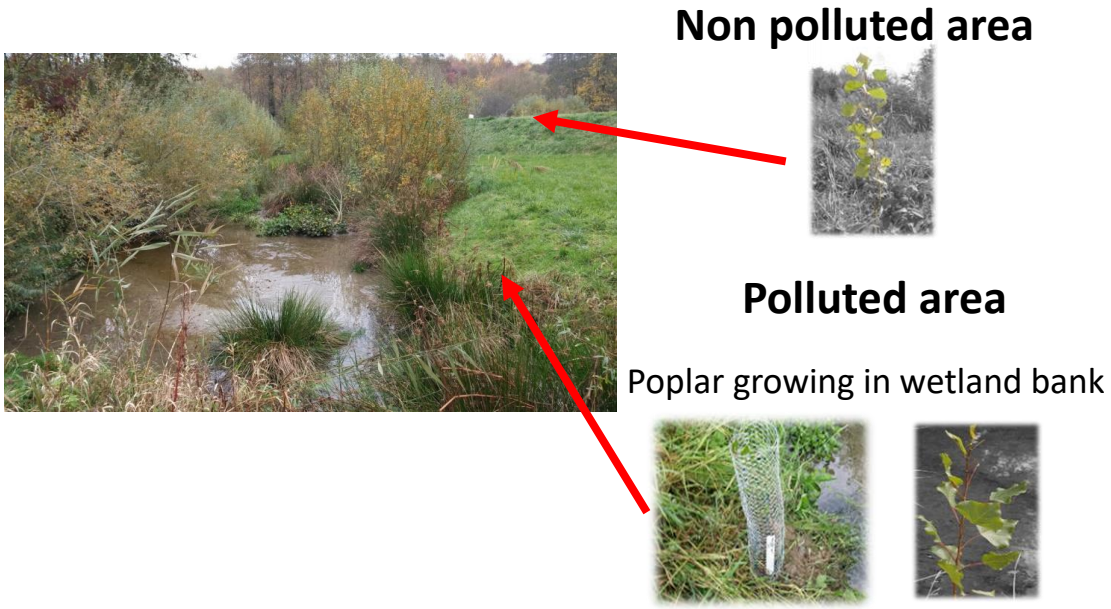

Figure 44: Poplars where leaves were collected to MSI analysis. A control plant was selected in the area considered in the non-polluted area and a poplar growing in wetland bank considered as polluted area.

Figure 45: Willow where leaves were collected for MSI analysis.

Concerning the poplar, two poplars were planted in the study site. The first one is located on the tertiary treatment wetland banks considering as polluted area and another one in the field were no wastewater could be collected. Therefore, this second poplar could be used as a control. In these poplars, leaves were collected and immediately store at 4 °C. Then, once the samples are brought back to the laboratory, they have been frozen at -20 °C before the analysis. In the same vein, a willow has been growing in the bank and leaves were collected, stored at 4 °C before being frozen at—20 °C. The leaves collected and used for MSI analysis could be observed in **Figure 46**.

Figure 46: Leaves collected from plant growing in the tertiary treatment wetland. **A)** poplar leaves **B)** Willow leaves.

3.1.1.2.Phragmites australis from VFCWs

On the other hand, plants growing in the CW were also sampled. As the CW were planted with *Phragmites australis* (common reed), this plant was selected. Indeed, the *Phragmites australis* is a plant used worldwide in wastewater treatment. In the study focused on the reed, the whole plant has been collected and analyzed. Therefore, three reeds replicates were selected with similar age and size as shown in **Figure 47** in the first stage of the VFCWs. Besides replicates were collected in the same area, near the water inlet (around 50 cm) as shown in the **Figure 48**. But the manuscript will illustrate the distribution using only the first reed replicates.

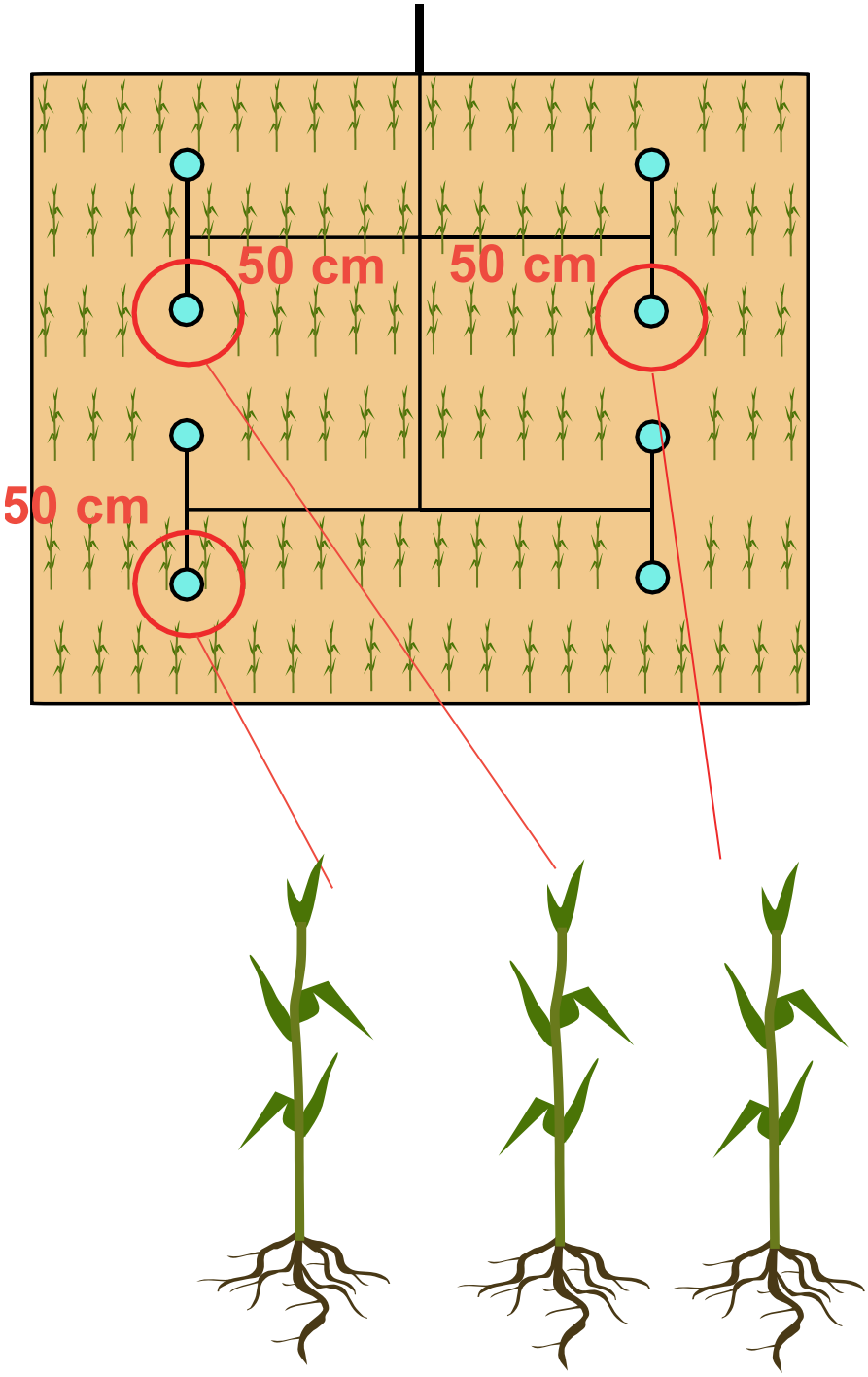

Figure 47: Sample strategy to collect the three reeds replicates in the first stage of the VFCW located in Falkwiller. These replicates were all collected in 50 cm radius of the water inlet.

Figure 48: The three reeds replicates collected in the study site.

3.1.2. Plant samples preparation

Once the samples are brought back to the laboratory, two strategies have been defined. For the study focused on the leaves of plants growing in the tertiary treatment wetland, the samples were immediately frozen at -20 °C before the cutting and the analyzing. Concerning the study focused on the whole reed, another approach has been set up. Indeed, the analysis of a whole plant has generated other constraints (for example samples storage in the freezer) then the plant samples preparation strategy has been adapted. The first step has been to separate the different organs of plants as shown in the **Figure 49**.

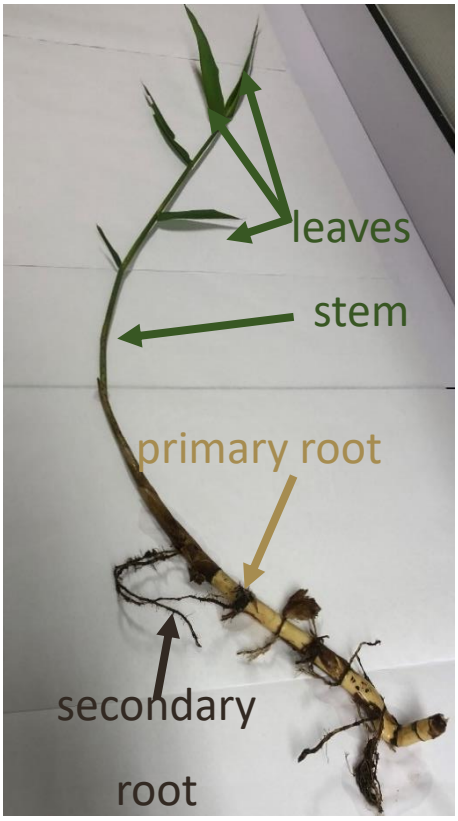

Figure 49: Reed (*Phragmites australis*) with its different organs before the analysis.

Samples preparation for mass spectrometry imaging acquisition

Once the different organs separated, the aerial part (stem and leaves) has been cut in regular intervals (each 3cms). Concerning the roots, the same method could not be applied due to the networked roots system. Therefore, a cut of the primary roots (3 cm), a secondary root associated, and tertiary roots were collected. All these samples were directly embedded in an M-1 solution and flash frozen in liquid nitrogen after the cutting. An example of samples flash frozen could be found in **Figure 50**. Then these samples were directly stored at -80 °C before the analysis.

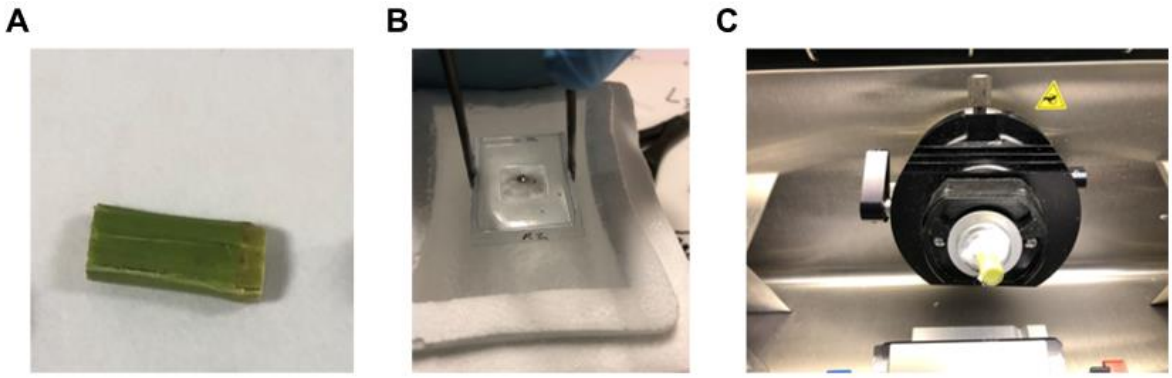

Figure 50: Plant sample preparation for cryosectionning. **A)** Stem cut used for the analysis. **B)** Flash freezing of the sample. **C)** Sample embedding and placed in the cryomycrotome for the cryosectionning.

The following step will be the samples cut and deposit in slides to perform the MALDI Imaging acquisition. After an optimization stage on the cryomycrotome, the optimal cut parameters for these samples were defined as a thickness about 30 µm at -20 °C as shown in **Figure 51**. Then the sections were deposited on indium-tin oxide (ITO) coated slides (Bruker, Germany) as shown in **Figure 52**.

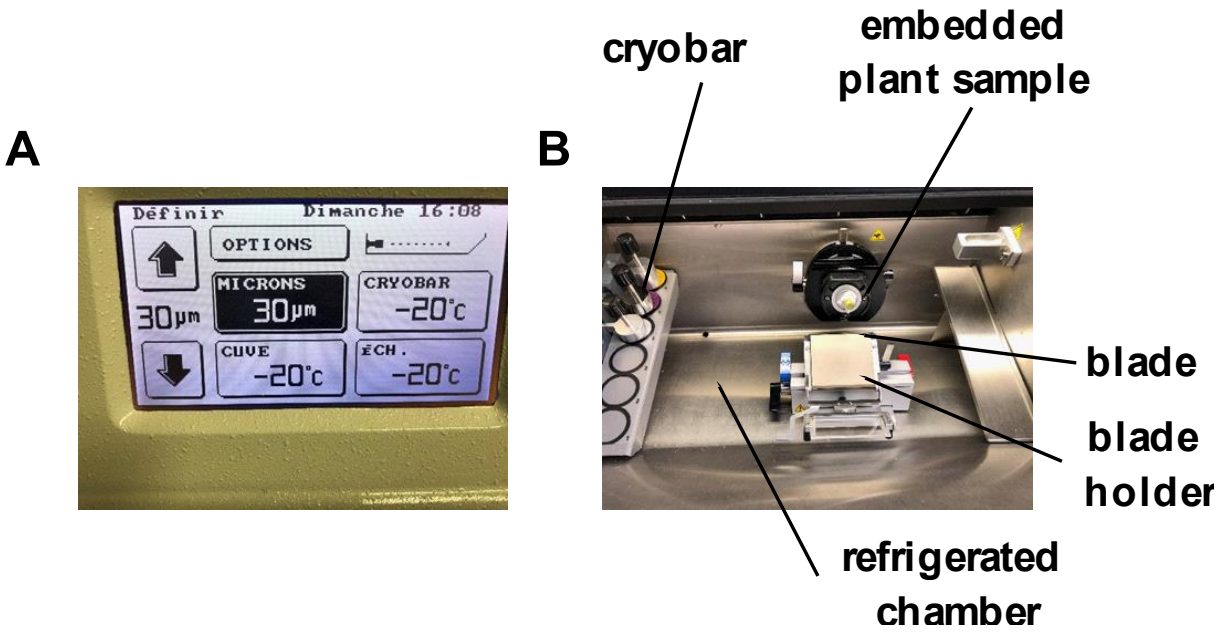

Figure 51: Samples cuts using the cryomycrotome and its parameters. **A)** Parameters optimized for the plants samples cutting. **B)** Sample embedding and placed in the cryomycrotome for the cryosectionning.

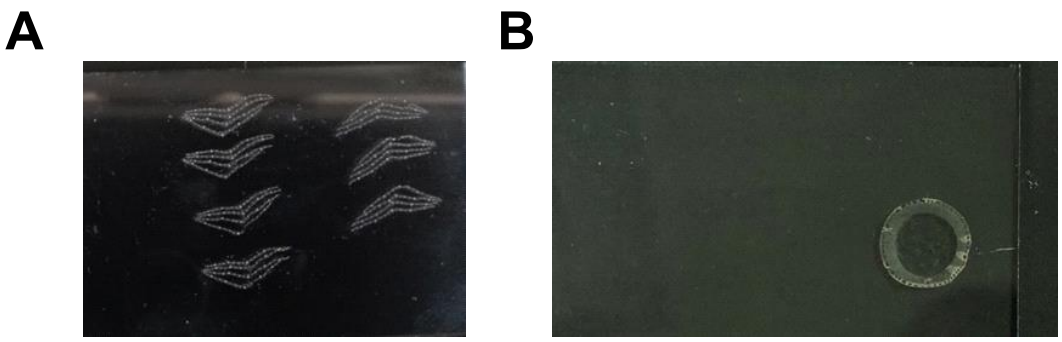

Figure 52: Cut of samples before matrix application. **A)** Willow leaves cuts. **B)** Reed stem cuts.

Then, the slides are immediately sprayed with α-cyano-4-hydroxycinnamic acid matrix (HCCA, Sigma Aldrich, USA) at 7 g L−1 in 50/50 MeOH/H2O, 0.2% TFA (Sigma Aldrich, USA) using the ImagePrep spotter (Bruker, Germany) found in the **supplementary datas (8)**.

3.1.3. Sludge samples preparation

As mentioned in the previous chapter with the sludge layers, a spatial distribution could be observed in the sludge compartments. Therefore, the MALDI Imaging approach has also been applied in this compartment.

Figure 53: Sludge samples placed in bucket with similar size used for MSI experiments.

In this study the sludge from constructed wetlands were analyzed. Then, once the samples have brought back to the laboratory, a small cube of sludge about 1 cm^3 has been frozen at -20 °C. The samples were placed in a small bucket with similar size in order to repeat the same sample preparation conditions as shown in **Figure 53**. Then the samples cutting could generate slices with similar areas and could be compared with each other. Slices have been carried using the cryomycrotome as shown in **Figure 54**.

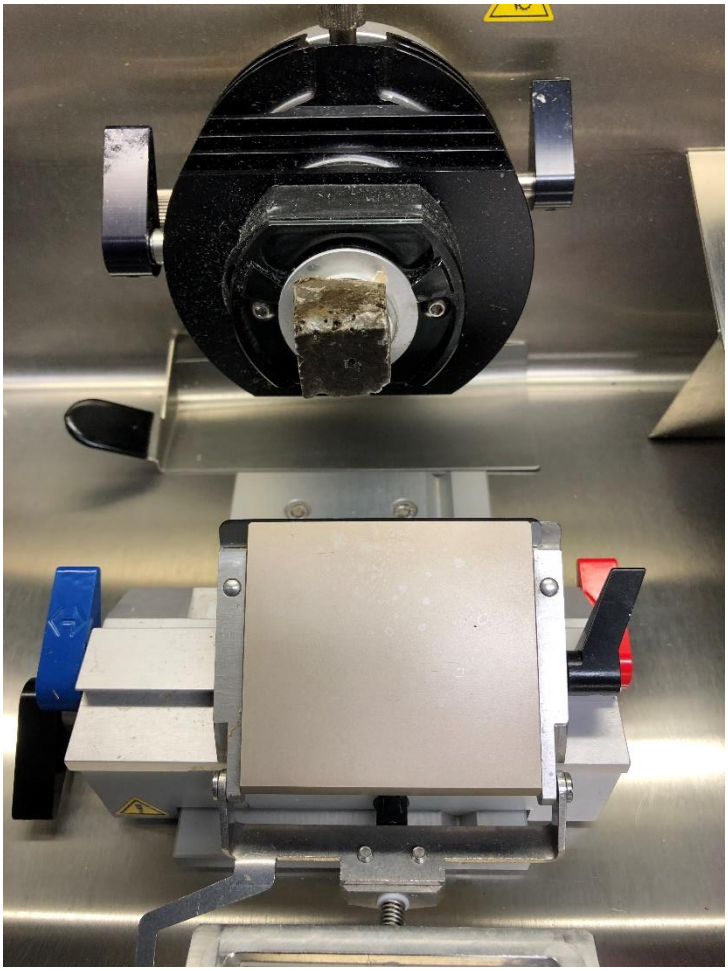

Figure 54: Sludge samples cut using the cryomycrotome.

Then, as it has been done for the plant samples, an optimization stage was carried out to obtain the optimal parameters. The parameters obtained were a thickness about 15 µm and at -20 °C. An example of sludge cut could be observed on **Figure 55.**

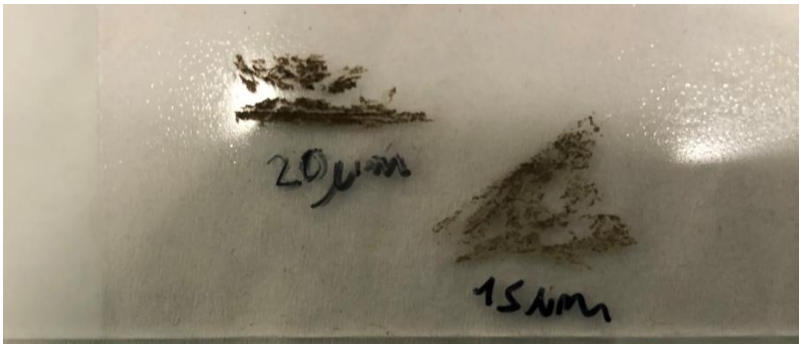

Figure 55: Sludge cut after the optimization stage.

Then, as it has been done for the plant samples, α-cyano-4-hydroxycinnamic acid matrix (HCCA, Sigma Aldrich, USA) at 7 g L−1 in 50/50 MeOH/H2O, 0.2% TFA (Sigma Aldrich, USA) was applied in the same conditions. The ITO slides found in **Figure 56** could be analyzed.

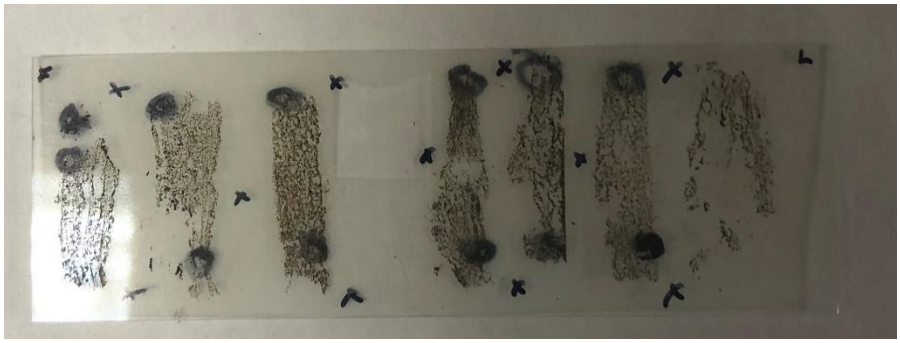

Figure 56: ITO slide containing sludge samples before the MSI analysis.

3.1.4. Mass spectrometry imaging acquisition

All the plants and sludge section deposited on ITO slides were loaded in the dual source of a 7 T Fourier transform ion cyclotron mass spectrometer (FT-ICR-MS) SolariX XR (Bruker, Germany) equipped with a Paracell at resolving power R = 120,000 at m/z = 400. The FT-ICR-MS used for the analysis could be found in **Figure 57**. The detailed scheme of the FT-ICR could be found in the **supplementary datas (9)**.

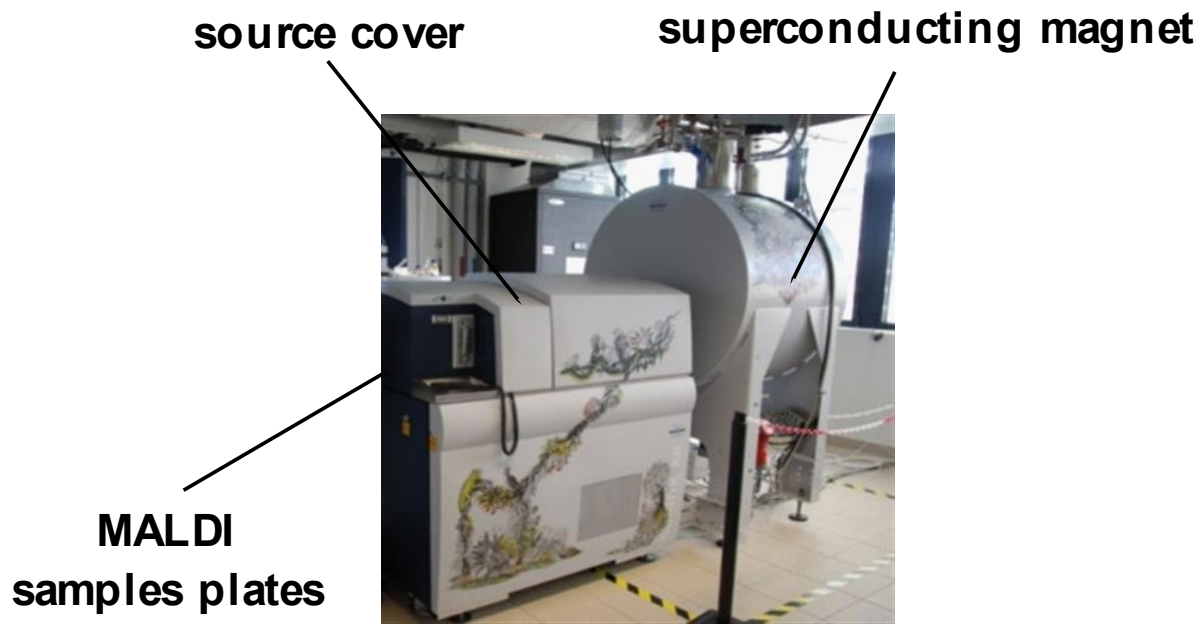

Figure 57: FT-ICR-MS (SolariX XR (Bruker, Germany)).

Then MSI acquisition was performed following the method mentioned in Villette et al., 2019a. A 50 µm x-y raster width was set using Smartbeam-II laser optics with the laser focus set to small (20–30 µm) and laser power at 18%. The region of interest and the teaching used to the sections on slide and the target position in the instruments were defined in flexImaging 5.0 (Bruker, Germany). Each pixel provides a spectrum accumulated from 50 laser shots. This laser was run at 1000 Hz and the ions were accumulated externally (hexapole) before being transferred into the ICR cell for a single scan.

The spectra were internally calibrated using a matrix cluster of HCCA ($C_{20}H_{14}N_2O_6 + H^+$, m/z = 379.0925) with a maximum deviation of 0.200 ppm. Besides, the mass range used for data acquisition was 100 <m/z <2000 and all the samples were analyzed using the positive ion mode with a transient size of 2 M. Online feature reduction was performed in ftmsControl software 2.1.0 (Bruker, Germany) to return only the peak centroids and intensities.

3.1.5. Data processing

The final step of this Material and methods section will be dedicated to the data processing and was based on the method mentioned in Villette et al., 2019a, b. SQLite data were imported in raw data convolution mode and the peak list data were used to create the dataset. The data were treated using the SCiLS Lab2016b software. The segmentation process could provide the compounds specifically found in a sample. Then, the dataset was exported in.csv file. Concerning the reed cuts samples, the whole dataset containing was exported then treated using Microsoft Access to visualize all the data points found in the spectra (approximately 2 million data points). This file was separated in csv containing 60,000 data points to annotate the all data observed in the datasets.

Then the annotations were carried out in two ways:

- using the Metaspace platform with HMDB, CHEBI, Swiss Lipids databases,
- using the Metaboscape software (3.0. for *Salix alba* and *Populus nigra* and 4.0 for *Phragmites australis*).

The second method was based on the method using analyte list and SmartFormula that have been mentioned in the chapter 1. After the peak list extraction, all the features obtained were annotated with these analyte lists using the same criteria of mass deviation (Δm/z under 3ppm). Then the peak fitting has been checked to ensure that annotations correspond to the peak identified.

Finally, the drug metabolites (conjugated and catabolites) were also generated using Metabolites Predict 2.0 (Bruker, Germany) using *in silico* prediction. These *in silico* predictions from the chemical structures of the parent compounds were based on 79 biotransformation rules found in **supplementary data (6)**. These metabolites generation was performed in two generations. The biotransformation rules were first applied on the parent compounds and the results will provide the first-generation metabolites. Then, the same method has been applied on the first-generation metabolites to obtain the second-generation metabolites. The results could be exported in a mass list and used as analyte list in Metaboscape as mentioned in the chapter 1.

On the other hand, to compare the results found in the different cut of the reed samples, the intensities were normalized using the following equation [15]:

$$\frac{\sum I_C\, pixel_c}{I_t\, pixel_t} \quad [15]$$

Where I_c sum of compound intensities in a single cut, $pixel_c$ pixels containing the compound in the single cut; I_t sum of compound intensities in the whole plant; $pixel^t$ pixels containing the compound in the whole plant.
In this way, all the cut intensities could be compared.

3.1.6. Methods limits identification

Then the acquisition method has been evaluated using the limits of detection (LOD), quantification (LOQ) and the matrix effect on the samples annalyzed in MSI. Therefore, sildenafil-d3 was used as model compounds to obtain the order of magnitude for the micropollutants detected. The LOQ defined at 100 µg/mL and the LOD at 10 µg/mL in the reeds, and 100 ng/mL when the sildenafil is spiked in the slides. The matrix effect in reed was about 99.5% and 98.5% in the sludge samples the details could be found in the **supplementary datas (10).**

3.1.7. Tracer experiment: a model for micropollutants movement

Finally, to understand the micropollutants distribution in the whole plants, model compounds were used to simulate this distribution. Therefore, reeds were collected in the study site with some sludge surrounding the reed rhizome in the same conditions from those collected for micropollutants distribution. In the laboratory, the reed was potted and 1 g/L of fluorescein (also called uranine) and sulforhodamine solution have been added. The combination of fluorescein (photosensitive) and sulforhodamine (sorptive compound) could model several micropollutants behavior and then those taken up by plants. Indeed, these fluorescent dyes were used in the literature as model (Vanderborght et al., 2002; Schuetz et al., 2012) to understand the distribution or fate of herbicides in several constructed wetlands (Lange et al., 2011; Durst et al., 2013; Maillard et al., 2016). Besides, these dyes have already been used to mimic herbicides sorption or plant uptake (Dollinger et al., 2017). Dollinger et al., (2017) have underlined that fluorescein could be used as model for hydrophobic herbicides and sulforhodamine for hydrophilic herbicides.

The reed has been sacrificed ten days after the injection of the solution. The **Figure 58** described the cuts, which have been selected to visualize the tracer distribution inside the whole plant.

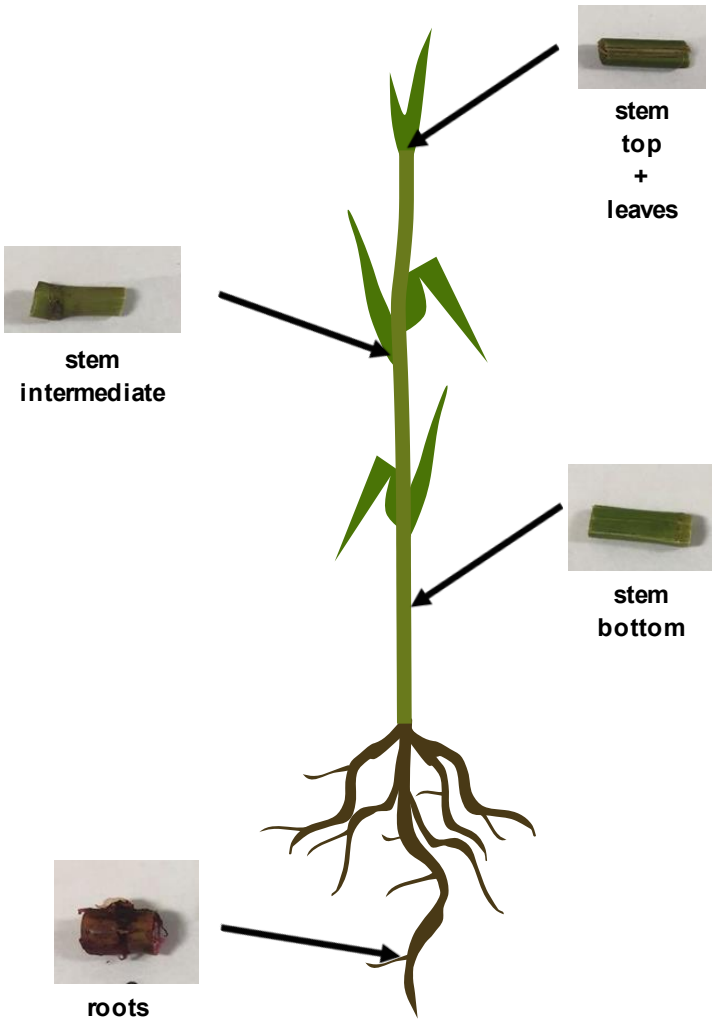

Figure 58: Reed cuts analyzed to investigate the fluorescein and sulforhodamine distribution in the whole plant.

The different cuts were analyzed using a confocal microscope to visualize the fluorescent compounds.

3.2. Results and discussions

3.2.1. Organic micropollutants and plant metabolites *in situ* location and metabolization in a poplar and willow growing in the tertiary treatment wetland

First results were focused on the distribution of compounds in plant leaves. As mentioned in chapter 2, two main compounds classes could be distinguished in plant samples, the endogenous compounds and the xenobiotics. Therefore, these two classes were investigated in this section with the plant metabolites (all plant small molecules which could be intermediate or end product of the metabolism). Chronic exposure to micropollutants has led to the transfers

of some micropollutants in the shoot part as mentioned in the previous chapter. But leaves have also been studied according to technical reasons. First, plants (poplar and willow) were not sacrificed to use for potential further experiments. Besides, the leaves samples are composed of soft tissue that are better suited to MSI than stem or roots with “wood section.” Therefore, the first results will be focused on leaves, and further optimization should be done to optimize the stem or root analysis.

First results will be focused on the compounds distribution inside the leaves of the two plants studied. This distribution seems to indicate that specific distribution should be found in the poplar leaves. The examples of six plants metabolites found in **Figure 59** and three micropollutants found in Figure 60, confirmed by commercial standards (retention time, exact mass and MS/MS profile if available) in the poplar leaves could illustrate this distribution. Plant metabolites distribution seems to be heterogeneous with no general trend could be observed. Some compounds are preferably detected in the outer tissues (Salicin or neurine), pheophorbide a, was mainly detected in inner tissues and piperidine could represent compounds evenly distributed in the leaves. The plants metabolites cover different functions (development, reproduction, signaling, enhancing, inhibition, defense or other interactions) and for some of them, these functions classification is unclear. In these results, this ambiguous classification could be illustrated by the example of salicin. Indeed, salicin is naturally detected in poplar but it is also well known that these compounds are used as anti-inflammatory (Mahdi 2010), and therefore could have a similar distribution than xenobiotics found in the leaves. Concerning pheophorbide a, a chlorophyll degradation product, the compound is mainly found in the inner tissue. But the literature mentioned that pheophoride screening could be used to detect chloroplast in the plant tissues (Jun, 2012.). And chloroplasts are mainly found in the mesophyll then in the inner tissue. Other plant metabolites distribution is less surprising as plant metabolites could be detected in the different tissues.

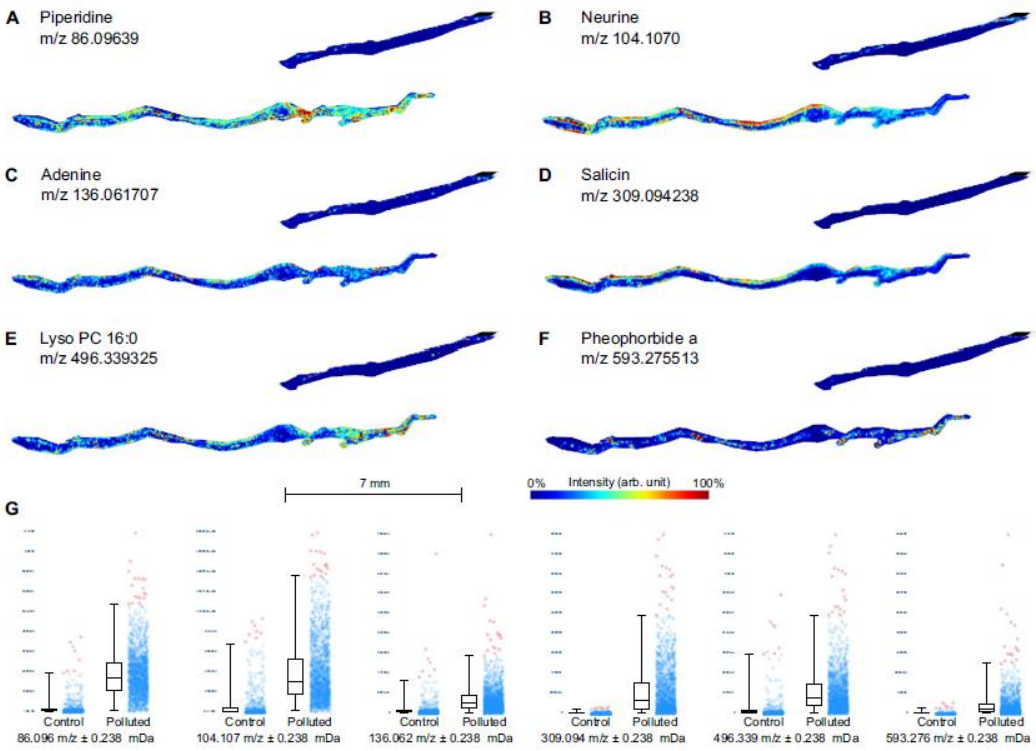

Figure 59: Distribution of plant metabolites annotated in poplar leaves (polluted the longest leaf and non-polluted the shortest). Different distribution could be observed in the leaves. Salicin (D) and neurine (B) seems to be preferably found in the outer tissue while pheophorbide a (F) are mainly found in the inner tissue. Piperidine (A), adenine (C), lyso PC 16:0 (E) are found in the different tissues. The boxplot (G) suggests that these compounds are found in higher proportion in the polluted leaves (Villette et al., 2019a).

Micropollutants distribution observed in **Figure 60** underline that they were mostly detected in the outer tissue. The micropollutants found in these leaves have hydrophobicity characteristic that can generate their uptake (log between 0.5 and 3) (Zhang and Wang, 2014). Nonetheless, their physicochemical properties found in the **supplementary datas (11)**, could not but themselves explained the distribution differences observed. Nevertheless, this specific distribution found for different micropollutants classes could suggest a mechanism set up by the plant to isolate these toxic compounds. An active transport to the peripheric tissues should be adopted to confine compounds in less sensitive areas for plants or to optimize the degradation processes that could occur *in planta*.

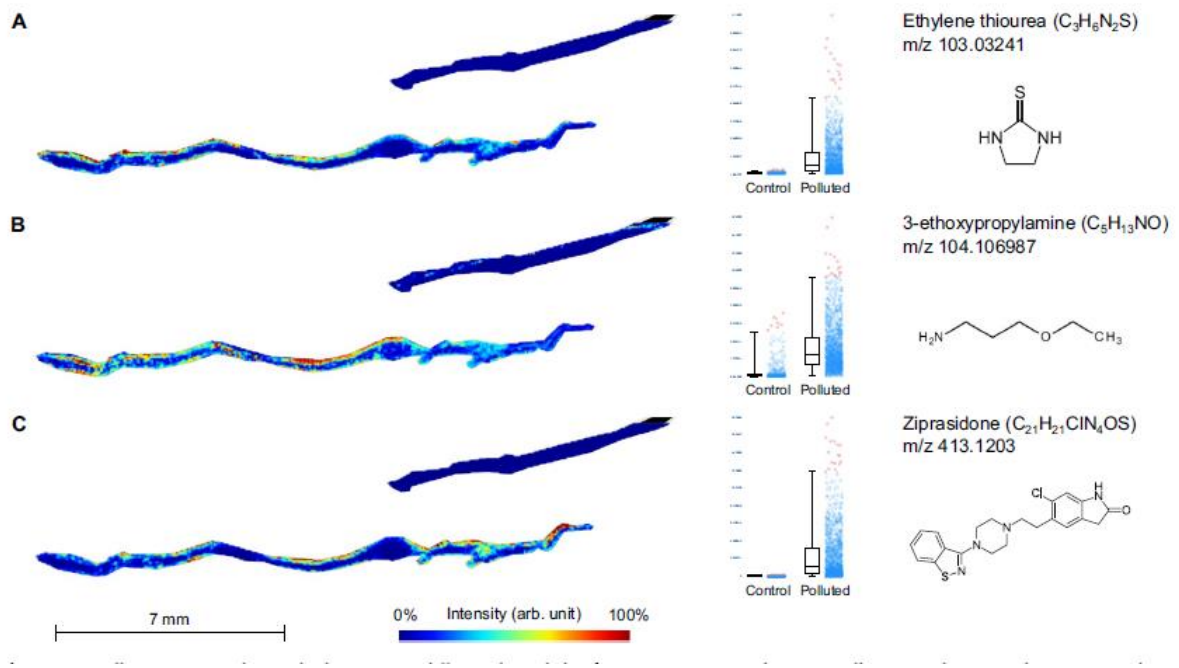

Figure 60: Micropollutants annotated in poplar leaves. Some differential metabolite features were annotated as micropollutants used as pesticides (A), personal care product derivatives (B) or drugs (C). The images (left) show a preferential localization in the peripheral tissues of the polluted leaves. Boxplots confirm that these metabolite features are differential between control and polluted leaves from Villette al., 2019a.

On the other hand, these micropollutants will impact the plant health and induce stress factors, as discussed in the previous chapter, and then promote some plant metabolites detection in polluted leaves. In MSI data, Lyso PC 16:0 and phephorbide a detection could illustrate this stress factor. The pheophorbide a mentioned in the previous section as chlorophyll degradation products could highlight a chlorophyll disruption. And Parween et al., 2013 have shown that this disruption could occur in plant exposed to pesticides. Besides, phosphatidylcholine (Lyso PC 16:0) detected in plant during their stress phase (Sarabia et al., 2018) have also been found in these leaves.

Furthermore, this micropollutants distribution observed in plant growing in the tertiary treatment wetland is not specific to the poplar. Indeed, Nuel et al., 2018 have shown that micropollutants could be widespread in different plants growing in this tertiary treatment wetland. The willow located in the tertiary treatment wetland has also accumulated micropollutants which were different from those detected in the poplar. Therefore, the micropollutants distribution was also investigated in the willow as found in the **Figure 61**.

.

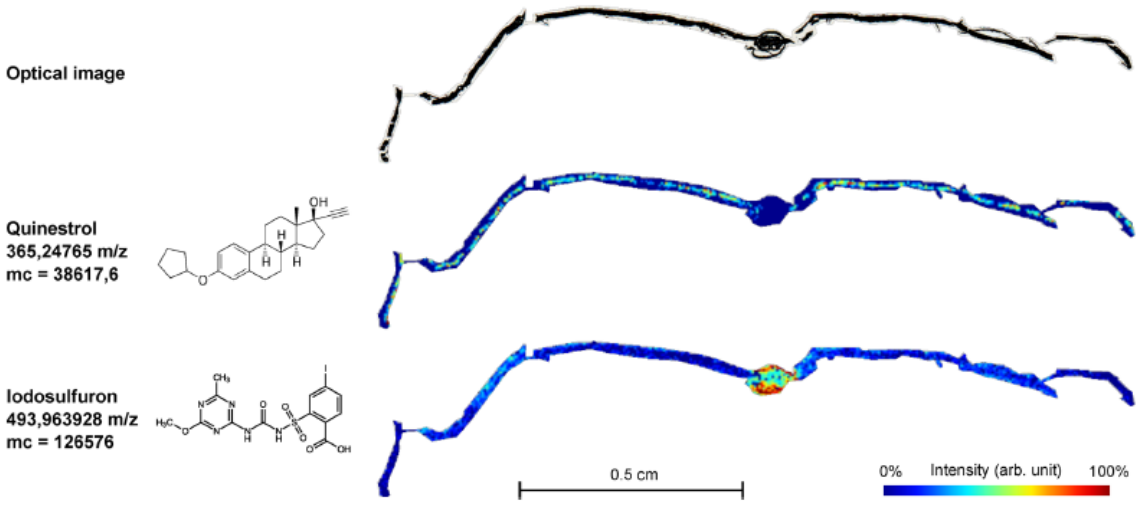

Figure 61: Micropollutants distribution in willow tissue. Quinestrol was mainly found in internal tissues while iodosulfuron is sequestered in the vascular tissues from Villette et al., 2019a.

Micropollutants distribution observed in the willow leaves suggests that no preferential transport way is occurring in this plant. This different transport ways could be illustrated by the micropollutants localization found in leaves tissues. Quinestrol is found in inner tissue and iodosulfuron is detected in the vascular tissue. Nevertheless, *in planta* transport of micropollutants is mainly described by the transpiration stream (Bartrons and Peñuelas, 2017; Petrie et al., 2018; Chuang et al., 2019) then, it is not surprising to find iodosulfuron in the vascular tissue. But Chuang et al., mentioned that this preferentially flow is not the single way to found micropollutants in plant tissues. By studying their translocations, they described their movement in two ways; the symplastic and the apoplastic way. This apoplastic way could therefore, partly explain their detection in inner tissues. On the other hand, quinestrol with log P = 6.13 should not be found in the plants according to the criteria mentioned in Zhang et al., 2014. Nevertheless, this detection in leaves could be explained by several hypotheses. Indeed, growing in this environment, micropollutants, microorganisms and plants have interactions, that could lead to the uptake by plants (W. C. Li et Wong 2012; Zeilinger et al., 2016). Besides, the similar structure with plants metabolites could also promote their uptake (Bucheli 2014). On the other hand, it cannot be neglected that these compounds could also be sorbed as micropollutants metabolites then a back conversion (Fu et al., 2018) could occur as a demethylation.

This back conversion could also suggest that micropollutants storage is only a part of the processes occurring in the different plants. As mentioned in the previous chapter, these plants should deal with this chronic exposure of organic pollutants. Therefore, plants have set up

mechanisms to degrade or transform the micropollutants (Marsik et al., 2017) by their own metabolism.

Therefore, two processes could explain micropollutants metabolites found in the willow leaves could be explained by two main processes. Indeed, metabolites generated in the environment by several processes such as metabolites generated by animal digestion, biodegradation by microorganisms, photodegradation or other oxidation processes could generate these metabolites that could be directly taken up by the plants.

On the other hand, other mechanisms will concern the metabolites only detected in plant tissues. Concerning these compounds, the "green liver" concept (Sandermann 1999) could be mentioned explaining the metabolite generated in planta. This concept is close the one occurring in mammals liver to degrade compounds. As liver, plant will use diverse enzymes to degrade organic micropollutants. Micropollutants transformation in willow leaves is mainly due to cytochrome P450 for the first generation. Previous results found in the literature have already highlighted the main role of cytochrome P450. Indeed, it is well documented that cytochromes P450 have a key role in the phase I metabolism for several herbicides (Cañameras et al., 2015). Besides, these cytochromes P450, found in wide diversity of organisms, can degrade a wide variety of micropollutants due to their low specificity (Cañameras et al., 2015). Then, the second generation of metabolites that can be related to phase II degradation, are linked to large diversity of enzymes found as described in Claire Villette et al., 2019b.
This compounds metabolization could be illustrated using the example of telmisartan found in willow leaves. Metabolites generated and detected in the willow were described in **Figure 62** and their spatial distribution in willow leaves are shown in **Figure 63**.

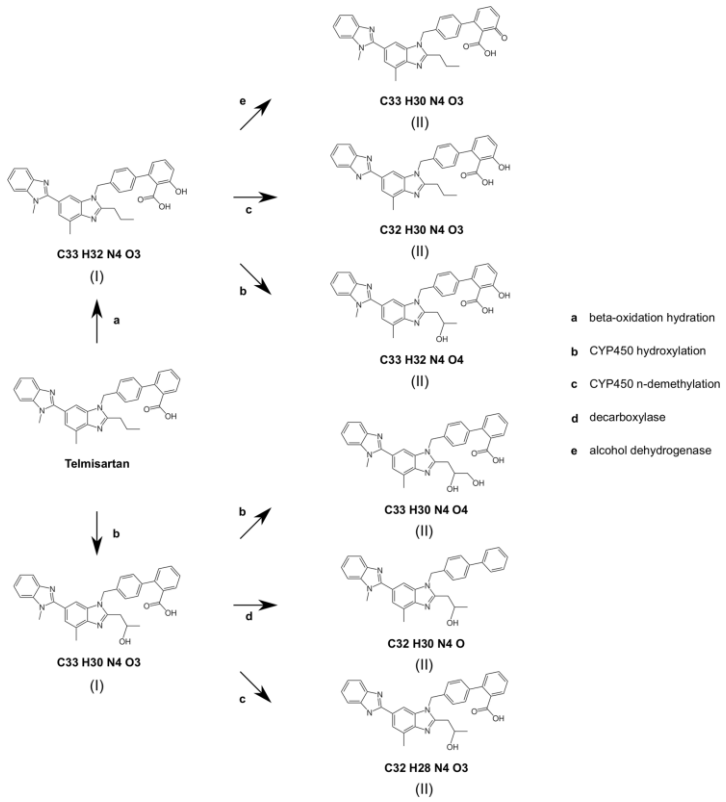

Figure 62: Metabolism of telmisartan in willow leaves. First (I) and second (II) generation metabolites identified in the willow leaves. All these compounds were found in the leaves using MSI, except $C_{33}H_{30}N_4O_3$ (Villette et al., 2019b).

Green liver concept could be well illustrated using the telmisartan example. Indeed, most of its metabolites detected in MSI were only found in leaves and not in sludge or water samples analyzed in LC-HRMS/MS (except for C33H30N4O3 and C33H32N4O4). Water samples are for sure not an integrative sample, then the interpretation concerning metabolites should be tempered. Nevertheless, it seems that telmisartan is mostly degraded by enzymatic reaction and not by chemical oxidation or UV radiation in accordance with the green liver concept.

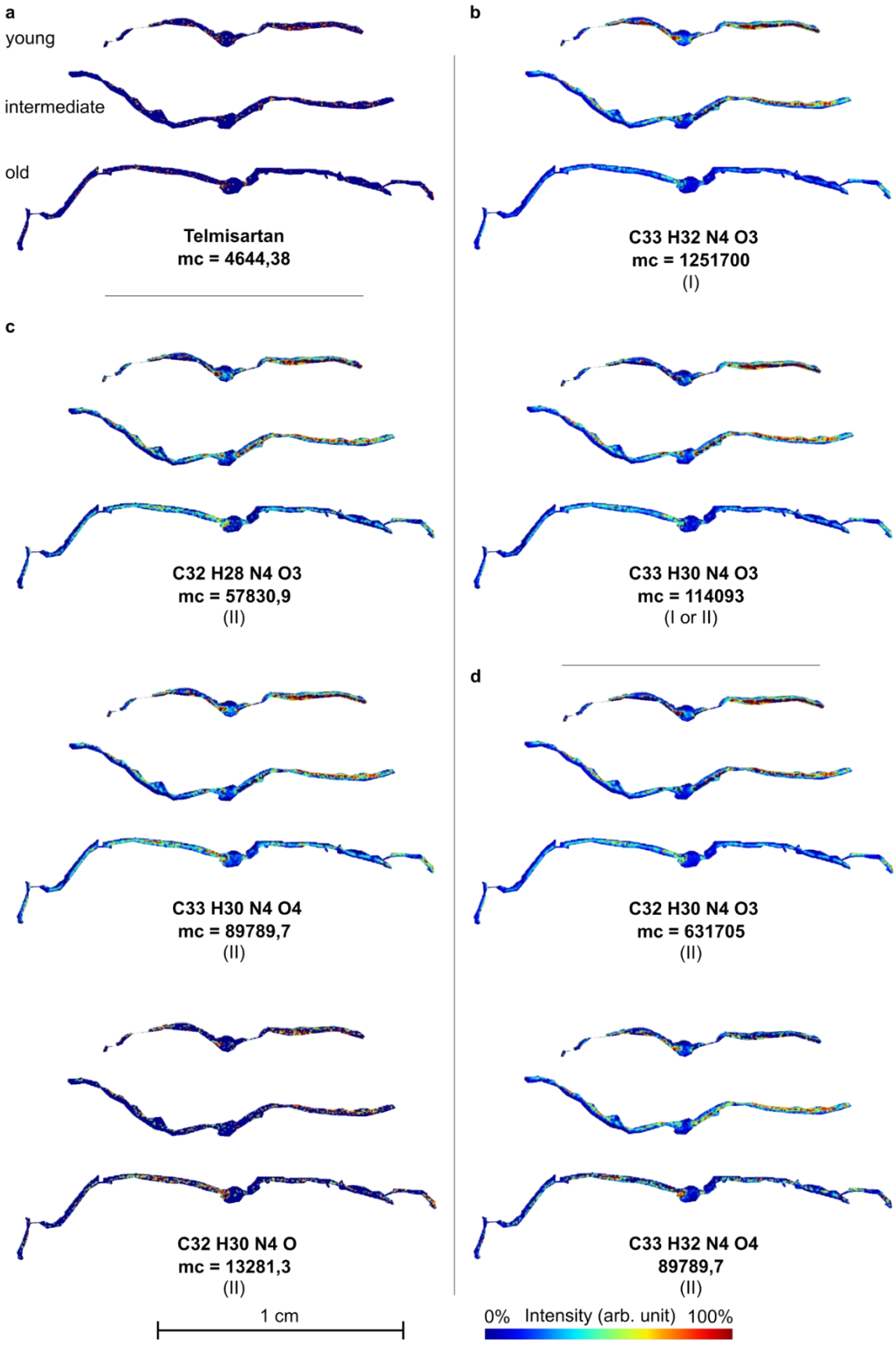

Figure 63: MSI images of telmisartan and some of its first- and second-generation metabolites in *S. alba* leaves from Villette et al., 2019b.

Concerning the telmisartan and its metabolites distribution in the different leaves, few intensity differences have been observed between old and young leaves. The chronic exposure could probably renew the micropollutant content in plants.

On the other hand, the comparison between the telmisartan and its metabolites show that its metabolites are found in higher intensity. These results agree with those mentioned in the study from Marsik et al., 2017. Indeed Marsik et al., have shown that the parent compound of ibuprofen represents around 1% of ibuprofen form detected in *Arabidopsis thaliana*. The telmisartan results combined with those from Marsik et al., highlight the key role of plants in micropollutants degradation and the importance of examining parent compounds but also the different potential forms of metabolites.
Besides these metabolites could also have a different location, impacting by the enzyme involved. For example, in these results, compounds obtained after a beta oxidation were mainly found in inner tissue. Beta oxidation will generate more hydrophilic compounds. These compounds could be stored in inner tissues instead being stored in outer tissue where more hydrophobic compounds could be located (lipid barriers).

All these results have underlined the different processes occurring in the plants (storage, degradation) using the shoot parts. In these processes, it has been shown that specific distribution could be observed in the different tissues, suggesting an active process set up by the plant to deal with these pollutants. This accumulation and distribution in shoots should also be related to other mechanisms non investigated in this section. Indeed, plants have interactions with the water, soil but also air compartment. Besides the final step of compounds degradation is the volatilization. Therefore, further analysis (with volatile compounds for example) should be investigated to understand their fate in the air compartment. Nevertheless, these observations are only focused on a single organ of plants: the leaves. And distribution in the leaves is not necessarily relevant to the one detected in a whole plant. As mentioned in the previous chapter, most of the compounds found in a plant coming from water or soil then are transferred to the shoots part, following several mechanisms. Therefore, to investigate the distribution in the different organs and evaluated the translocation, the micropollutants distribution has been studied in a whole plant (a reed).

3.2.2. Organic micropollutants *in situ* location and metabolization in a whole reed growing in the constructed wetland

The whole plant investigation has led to the identification of some micropollutants distributed in the different organs. The results introduced in the **Figure 64** represent micropollutants identified in the first biological replicates. The distribution introduced in the following figures will concern the micropollutants found with a specific distribution. Therefore, two drugs (carbamazepine and metoprolol) and six pesticides (parathion-ethyl, mecarbam, propachlor, flamprop methyl, dodemorph and fuberidazole) were investigated respectively in **Figure 64** and **Figure 66**.

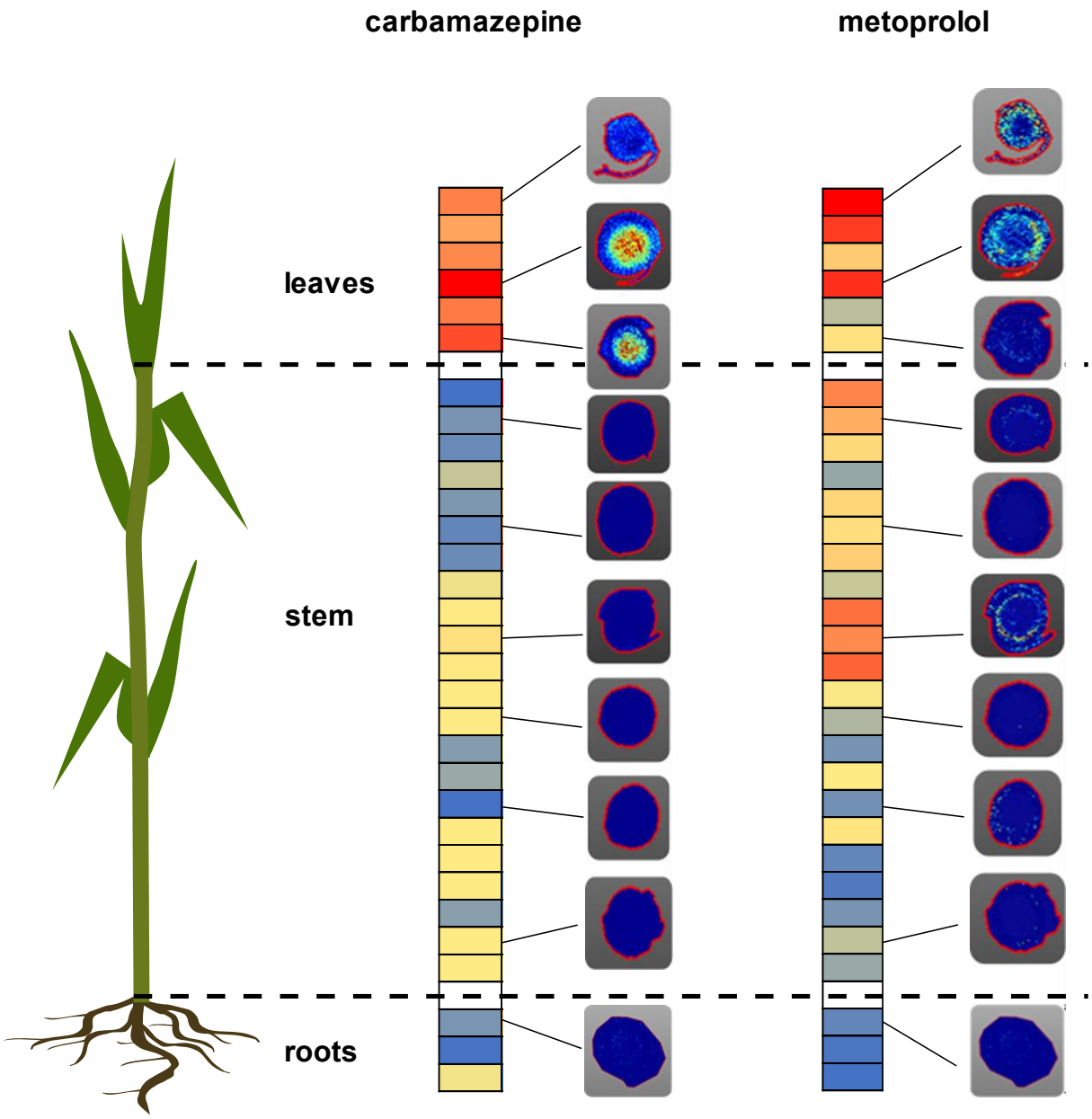

Figure 64: Carbamazepine and metoprolol distribution in the whole reed. The two compounds were analyzed in the different organs (roots, stem, leaves). The box represents the relative drugs intensity (according to the equation 15) found in each cut (a box is equivalent to a plants segment (3 cm) used for the MSI analysis) and representative MSI image were added to illustrate the distribution inside the different tissue.

The two drugs investigated, are detected in higher intensity in leaves. Indeed, the intensity maps show this higher detection in the leaves. Regarding the results of carbamazepine, it seems that this drug is almost only found in the leaves. The metoprolol is mainly observed in the leaves, but a more homogeneous distribution seems to appear between the top part of the stem and the leaf apex. Therefore, as mentioned in the previous chapter, this distribution in the shoots parts is related to the transpiration stream then the water flow found in the plant (Chuang et al., 2019; Li et al., 2019), as drugs should mainly come from the wastewater. Distribution difference could be partly explained by a temporal difference. As the plant is chronically exposed to

micropollutants and have accumulated micropollutants for eight months, the distribution could be influenced by this temporal difference. The plant sacrificed has stopped transpiration stream and downward flow (from the leaves to roots), and an instantaneous view is obtained. On the other hand, the affinity with plants could also be discussed, but for example the ionic fraction of the two compounds are less than 0.1%. Besides, the translocation factor was calculated for these two drugs using the mean intensity found in the cuts. Roots cuts, leaves cut, stem cuts (6 top stem cuts and 6 bottom stem cuts) were compared. Results found in **Table 11** can quantify the transfer. These results suggest the high transfers from roots to the leaves (TF = 468 for carbamazepine and TF = 317 for metoprolol). Therefore, the different organs should be studied and as mentioned previously, the transpiration stream seems to guide mainly compounds to the shoots (the leaves for carbamazepine and the leaves and the top stem for metoprolol).

Table 11: Translocation factor calculated for carbamazepine and metoprolol considering the different reed sections.

Translocation factor	Leaves vs roots	Bottom stem vs Roots	Top stem vs roots	Leaves vs Bottom stem	Top stem vs bottom stem	Leaves Vs top stem
Carbamazepine	**468**	**3.4**	**0.7**	**139**	**0.21**	**654**
Metoprolol	**317**	**9.3**	**114**	**34**	**12**	**2.8**

Nevertheless, compounds structure was also compared to structure of compounds found in plant database (Knapsack). The higher structure similarity was about 74% for the carbamazepine and 56% for metoprolol. Besides the carbamazepine have a structure similarity higher than 50% with 140 compounds contained in Knapsack, while metoprolol with only 25.

Finally, using the Kegg pathway, the carbamazepine could be found in the sodium pump pathways, which is also present in *planta*. At the opposite metoprolol were not detected in any pathways in plants. In addition to the temporal difference, these structure differences but also the pathways found could probably be a part of the few differences observed.

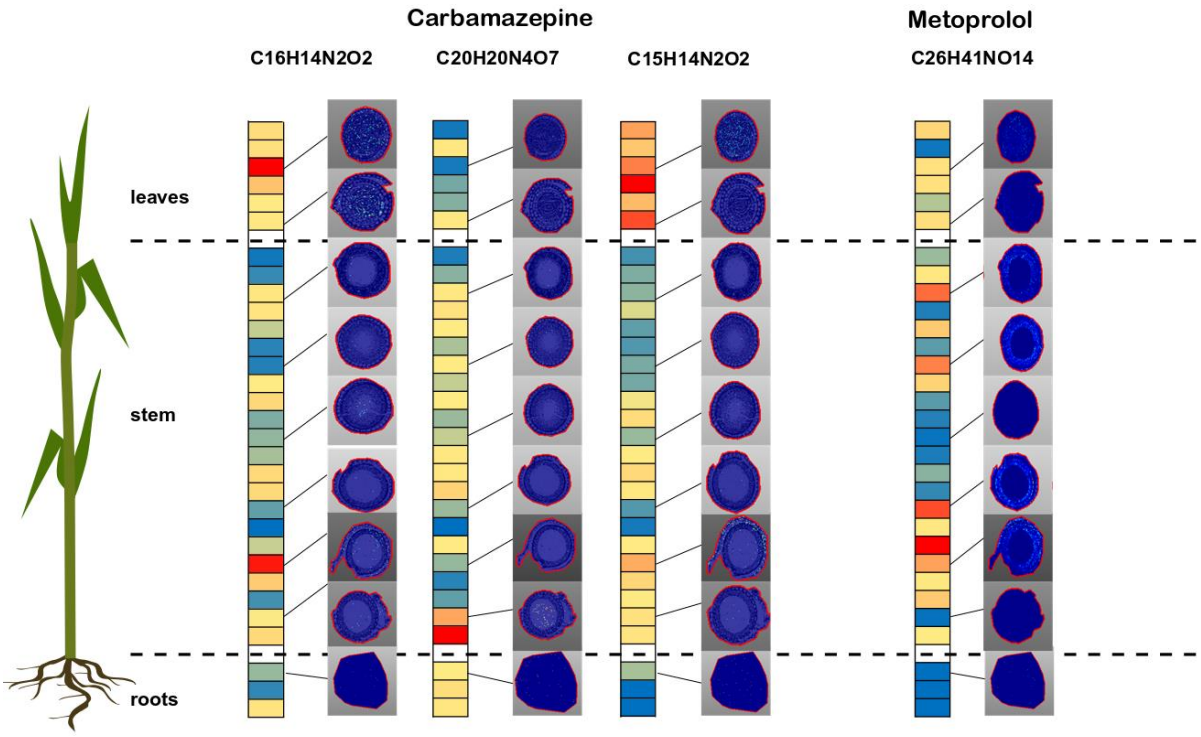

Figure 65: Carbamazepine and metoprolol metabolites distribution in the whole reed. The metabolites were analyzed in the different organs (roots, stem, leaves). The box represents the relative intensity found in each cut and representative.

On the other hand, translocation is only a part of the fate of this micropollutants. As mentioned for the willow, biotransformation could also occur *in planta* (phytodegradation or phytovolatilization). Indeed, as the drugs were mainly detected in shoots parts. This location is probably related to the potential final step of their degradation. Indeed, these compounds should be volatilized and then excrete them to the atmosphere by stomates. To visualize degradation processes occurring *in planta*, the metabolites of these drugs were investigated in **Figure 65**. Nevertheless, their intensities were lower than the parent compounds, at the opposite of results found in the willow leaves. Their distribution was also not fully related to the transpiration stream of water flow, as no clear gradient (top bottom) for all compounds could be distinguished.

Besides, these two drugs were also compared to pesticides found in the reed as shown in the **Figure 66.** Their distribution is even more heterogeneous regarding the different compounds. This could probably be linked to the upward and downward flow occurring in plants. At the opposite of drugs which are coming almost exclusively from wastewater, pesticides could also

be found in the air compartments. Then the downward flow could probably influence the transfers to the bottom stem or the roots.

Propachlor and fuberidazole seem to have a similar behavior that the one mentioned in the previous section. Parathion ethyl was poorly detected in leaves, but a similar trend seems to appear with a main flow in the top part of leaves. As mentioned for metoprolol, a temporal difference could probably explain this distribution. However, mecarbam and flamprop methyl seems to more evenly distributed in plants and hotspots of dodemorph could be detected in the stem near stem-leaf interface. Therefore, this distribution is fully not related to the pesticides classes or of its physicochemical properties, according to the data found in **supplementary data (12)**. The chronic exposure limits the impacts of compounds size (Chuang et al., 2019).

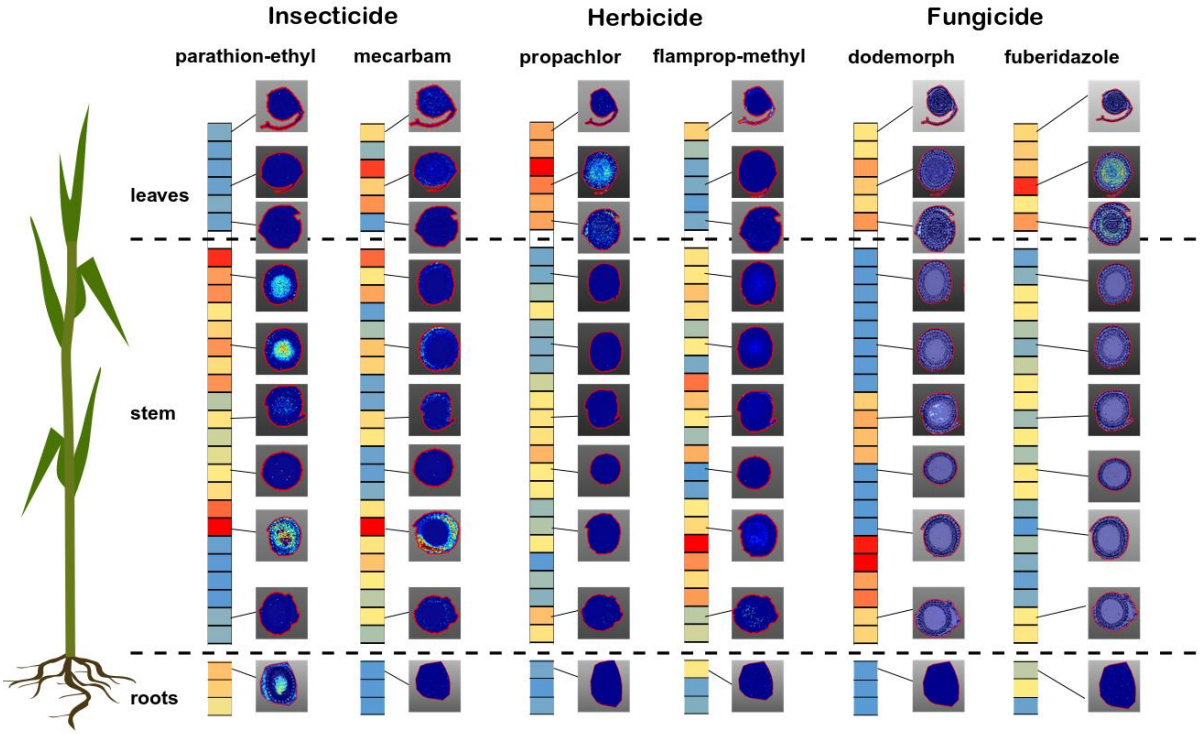

Figure 66: Pesticides distribution in the whole reed. The pesticides (parathion-ethyl, mecarbam, propachlor, flamprop-methyl, dodemorph, fuberidazole) were analyzed in the different organs (roots, stem, leaves). The box represents the relative intensity found in each cut and representative MSI image were added to illustrate.

On the other hand, different tissue distribution could also be observed. For example, parathion ethyl is mainly detected in the pith while mecarbam or fuberidazole could be observed in the peripheral tissues. The main process seems to be linked to transpiration streams and therefore a large part of them could be detected in the shoots or in the lateral leaves. Therefore, the distribution does not seem to be classes dependent, even if pesticides are compounds designed to protect plants and must have a specific process. But these compounds could also be degraded and then their metabolites should be investigated as performed for the drugs. The **Figure 67** described the pesticides metabolites detected in the reed.

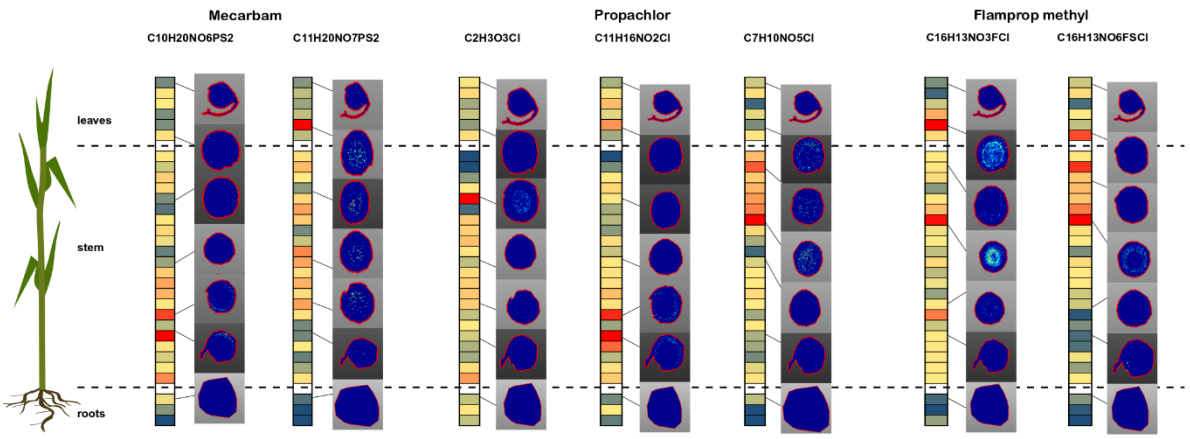

Figure 67: Pesticides metabolites distribution in the whole reed. The metabolites were analyzed in the different organs (roots, stem, leaves). The box represents the relative intensity found in each cut and representative.

Nevertheless, as mentioned for drugs metabolites their intensities were lower than the parent compounds. Only a flamprop methyl metabolite ($C_{16}H_{13}NO_3FCl$) was detected in higher intensity in some cuts. But as mentioned with the drugs metabolites, their distribution also was not related by the transpiration stream of water flow, as no clear gradient (top bottom) for all compounds could be distinguished.

.

On the other hand, in the literature, micropollutants or their metabolites are widely studied in roots. But the results found in this study underline that few compounds are detected in roots. The compounds found in roots tissue, where analyzed with low intensity. The rhizodegradation occurring in the rhizosphere could partly explain this low intensity. Indeed, the pollutants store in these areas where microbial activity is enhanced (Ouvrard et al., 2014) could be easily degraded (rhizodegradation). But chronic exposure and reed age could have a benefit impact

on the micropollutants translocation and then partly explain this low distribution. Indeed, these results could not be compared by mesocosm experiments as few studies are focused on a daily exposure of micropollutants as it seems to appear in the full-scale study site. These conditions could promote the translocation and then compounds mainly detected in the shoots part. Nevertheless, to understand and visualize the uptake and the potential role of transpiration stream, the tracer experiment performed in laboratory conditions could simulate the micropollutants uptake. Indeed, two fluorescent tracers (sulforhodamine and fluorescein), considered thus as xenobiotics, used in process engineering to determine residence time distribution were injected in the water feeding the plants. Then plant was feeding for ten days then it has been sacrificed. The analysis of the different sections using a confocal microscope as mentioned in the materials and methods section will provide the distribution of micropollutants over a shorter period of exposition. The results are observed in **Figure 68**.

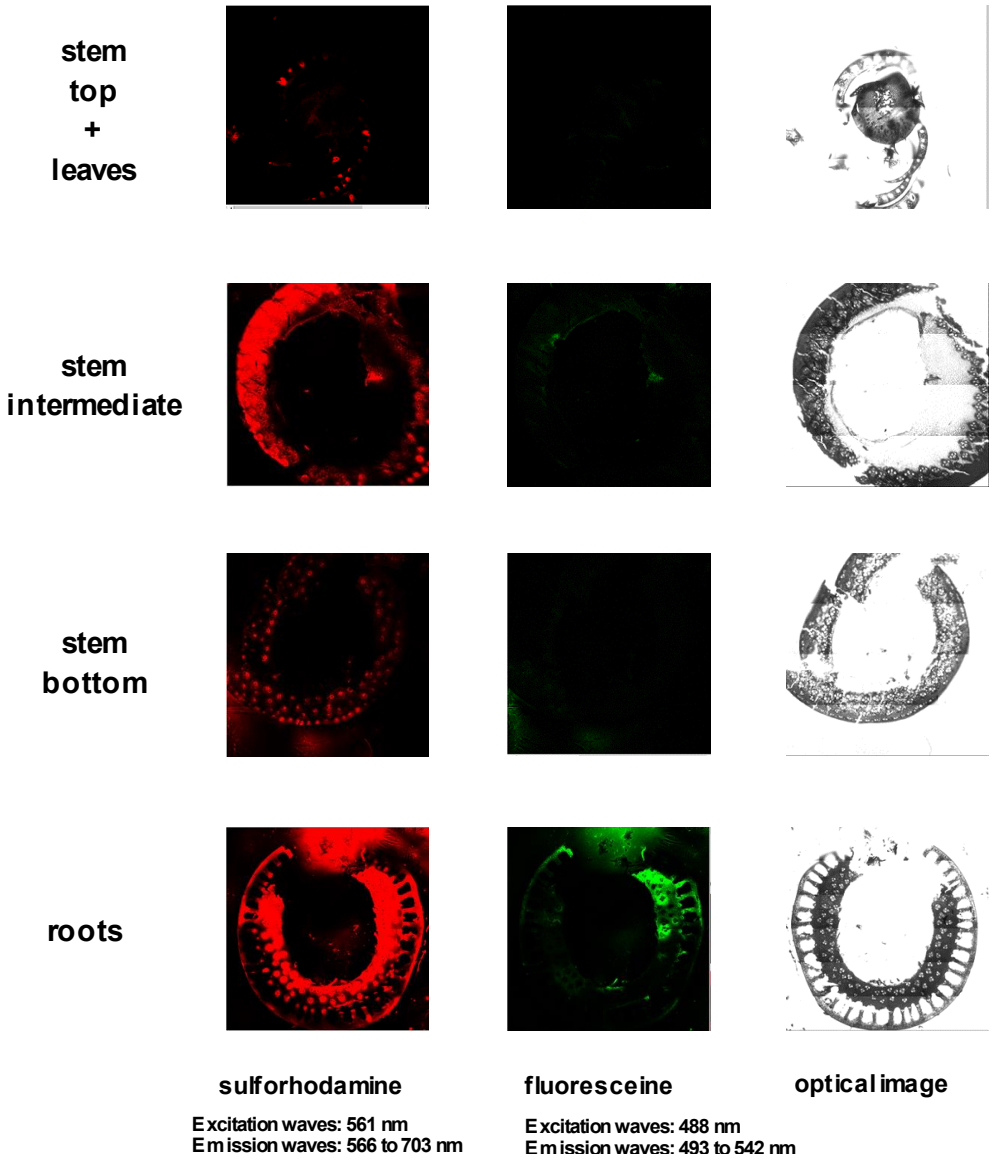

Figure 68: Sulforhodamine and fluorescein detected in the different organs of the reed.

These results, sulforhodamine experiment could underline the transpiration stream role in micropollutants transport. Sulforhodamine is highly detected in the roots but a transfer to the stem is observed, especially in the intermediate cut of the stem. The high photosensitivity of fluorescein could partly explain the poor detection of these compounds in plant. Besides, as fluorescein should represent hydrophobic compounds, it is not really surprising to find fluorescein in the roots. As fluorescein, sulforhodamine have high sorptive properties (Dollinger et al., 2017); therefore this compound is obviously found at the interface between plants and the solution; the roots. But sulfhorhodamine should represent more hydrophilic compounds (Dollinger et al., 2017). In this way, sulforhodamine could be easily transported in

the transpiration stream and be evenly distributed in the whole as shown in the figure 68. On the other hand, the difference observed with micropollutants distribution could be partly explained by the exposure time. Indeed, the tracer experiment was carried out in a shorter injection time (ten days). Tracer was accumulated in the roots and these results will be in accordance to those mentioned in the literature. The translocation was not yet fully set up. But an extended experiment time would lead to results similar to those mentioned in micropollutants distribution in our works. Therefore, these results also suggest the importance of exposure time to select the organs to investigate and the lack of chronic exposure during 8 months led the authors to investigate mainly the roots.

3.2.3. Compounds distribution in the sludge layers

The analysis of the CW sludge samples in MSI was performed using the Metaspace platform. Indeed, this sludge should be mainly composed of lipids and the platform. Metaspace contain several lipids databases. To evaluate, the acceptable mass error, an internal standard (sildenafil-d3) was applied on the slide and in the sludge samples as shown in **Figure 69**. The mass deviation was fixed at 2 ppm as the sildenafil-d3 spiked and found in the sludge samples was detected with an error of 0.9 ppm.

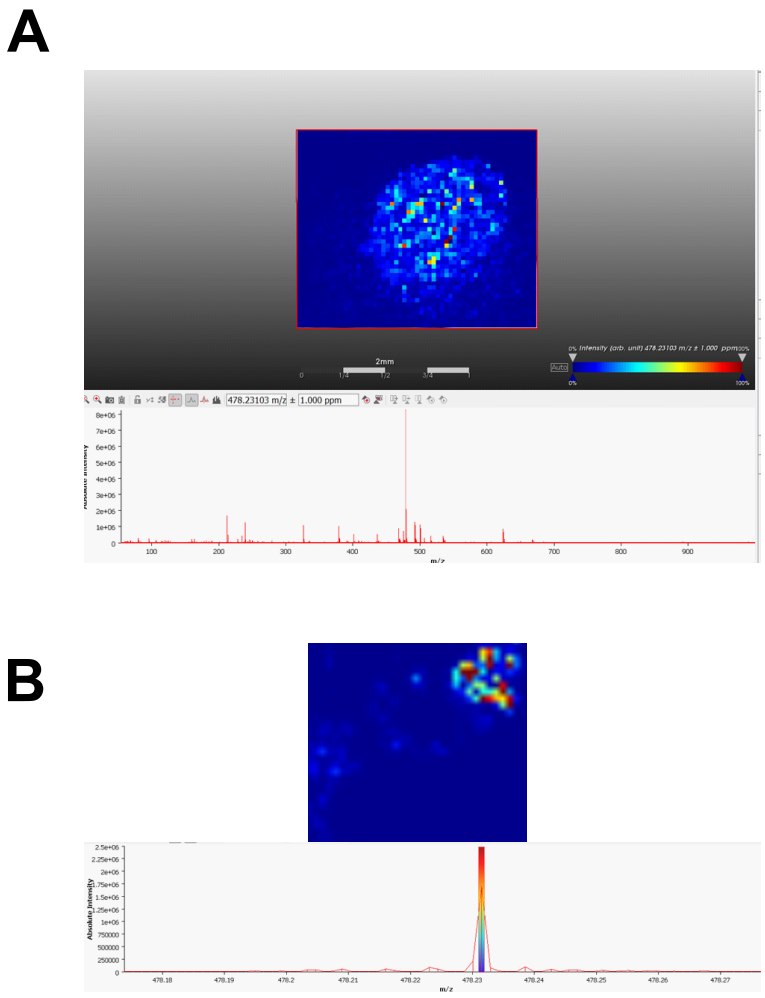

Figure 69: Sildenafil-d3 spiked in the sludge matrix using MSI.

Results found in the Metaspace platform underline the presence of two lipids evenly distributed in the whole slides (ceramide (iso:d17:1 (4E)/25:0:20H) and ceramide (iso:d17:1 (4E)/30:0:20H)), as described in **Figure 70**. The homogenous distribution is not surprising as sludge is mainly composed of lipids. But as it has been mentioned for plant samples, these annotations should not represent the distribution of the different compounds detected in the samples. Indeed, the use of Metascape could only investigate some databases available in the platform and a large part of micropollutants will not be annotated. Therefore, another method should be used to annotate the sludge samples and visualized the different analytes distribution in order to obtain a broader view.

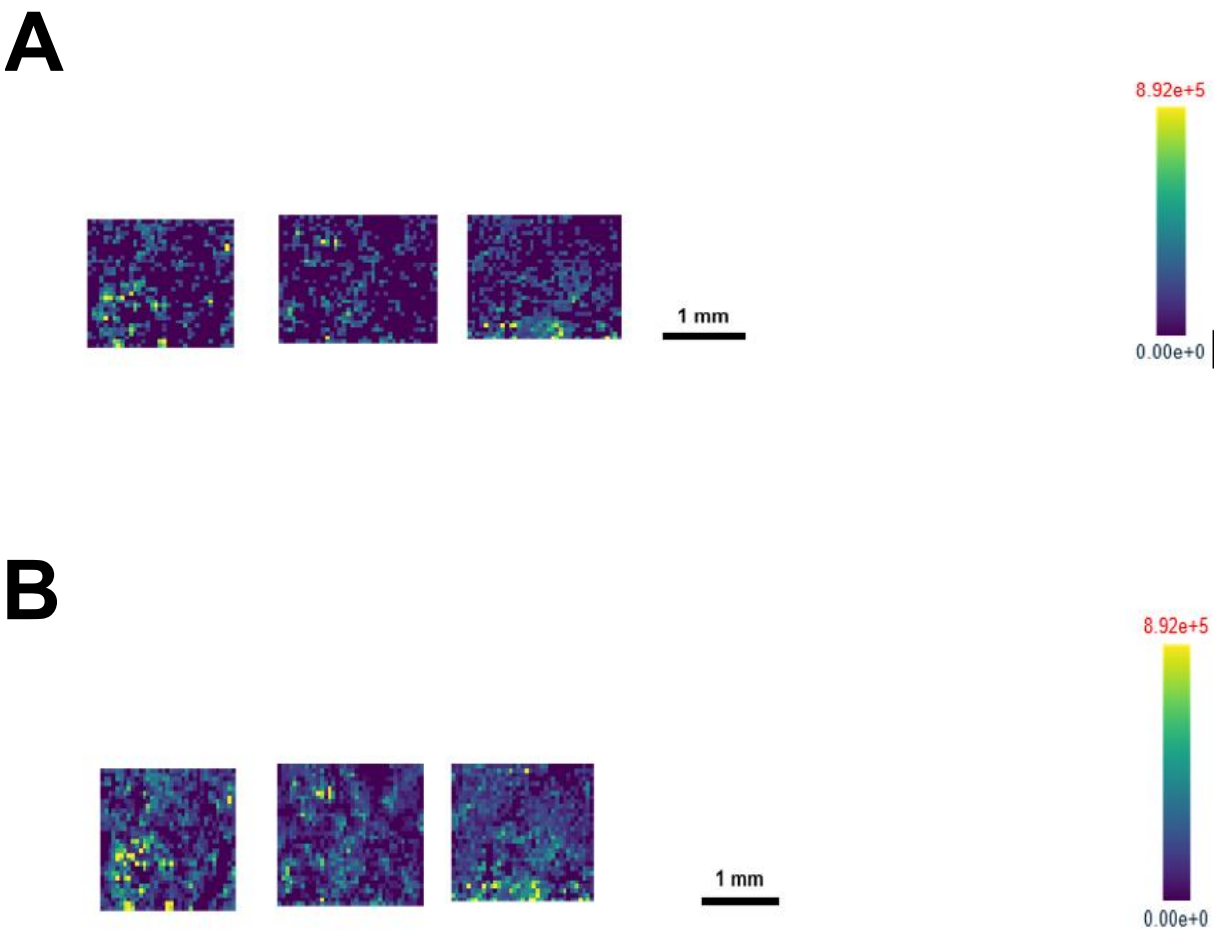

Figure 70: Lipids identified by MSI in sludge samples **A)** ceramide (iso:d17:1 (4E)/25:0:20H) **B)** ceramide (iso:d17:1 (4E)/30:0:20H).

To overcome this lack of annotations, our current works are focused on the annotations of the whole spectra using Data Analysis 5.0., SmartFormula and the different analyte lists, mentioned in the previous chapter to obtain a non-target approach on the sludge samples. But the main issues was to obtain the general mass list coming from the MSI acquisition.

Therefore, the MALDI Imaging data could be analyzed using Data Analysis. The raw datas will be represented as a chromatogram and from these raw datas, a mass list could be generated. as shown in **Figure 71**.

A

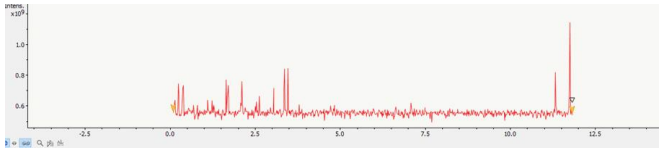

B

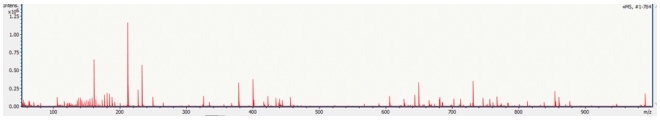

C

#	m/z	I
227415	408.01…	2926
227416	408.01…	3001
227417	408.01…	2986
227418	408.03…	3678
227419	408.06…	2902
227420	408.07…	2991
227421	408.07…	2957
227422	408.07…	2971
227423	408.10…	2877
227424	408.12…	2882
227425	408.12…	2751
227426	408.13…	3120
227427	408.13…	3037
227428	408.16…	2731
227429	408.18…	2856
227430	408.19…	3638
227431	408.20…	3264
227432	408.21…	3485
227433	408.23…	2722
227434	408.23…	2791
227435	408.25…	3232
227436	408.26…	2921
227437	408.27…	2980
227438	408.28…	2783
227439	408.29…	4372
227440	408.31…	3422
227441	408.33…	2723
227442	408.35…	4224
227443	408.37…	3178
227444	408.37…	3248
227445	408.37…	3226
227446	408.38…	3912
227447	408.43…	3169
227448	408.45…	3575
227449	408.46…	3199
227450	408.48…	3236
227451	408.49…	3213
227452	408.49…	3343
227453	408.49…	3728
227454	408.53…	3262
227455	408.55…	3395
227456	408.55…	3326
227457	408.55…	2710
227458	408.56…	3044
227459	408.57…	3449
227460	408.58…	3628
227461	408.62…	2905
227462	408.62…	2988
227463	408.63…	3110
227464	408.64…	3124

Figure 71: Alternative process to annotate compounds in sludge samples analyzed by MSI. **A)** Raw data represented as a chromatogram in DataAnalysis. **B)** Mass spectra generated from raw data. **C)** Mass list representing the different m/z found in the samples.

Then a similar process as mentioned in the first chapter could be applied. Indeed, the mass list generated in Data Analysis could also be annotated with Smart Formula using the same

parameters as mentioned in the first chapter. Then using the analyte list developed, a putative annotations could be obtained by associating a single name to the formula generated.

3.3. Chapter conclusion

After underlining the micropollutants widespread in the environment in the previous chapter, this chapter was focused on the micropollutants uptake in plant compartments. This plants chronically exposed to micropollutants must deal with them, as the plant response detected seems to indicate. To survive and limit micropollutants impacts, specific mechanisms seems to be set up inside the plant. For example, a specific storage in outer tissue has been observed in the poplar leaves. This storage suggests that plants guide the micropollutants in area to confine them and limit their impacts. On the other hand, some biodegradation processes have also been investigated in willow leaves. Indeed, drugs metabolism was studied and for two of them, the metabolites were only detected in leaves suggesting enzymatic reactions occurring in plant tissue. In these two plants only, the leaves were studied. Nevertheless, to understand the mechanisms which could occur in plants, a whole plant should be investigated. The reed was used as a model. The chronic exposure to micropollutants led to different micropollutant behavior in the plants. As plant grew for 10 months in the polluted area, most of the compounds have already migrated to the top part of the plants and thus the leaves. The other observation could also be linked to different temporal distribution, as the compounds classes could not explain the specific distribution.

Nevertheless, micropollutants found inside the plants come mainly from sludge and water compartments. Besides compounds detected in sludge are directly linked with the micropollutants water content. Nonetheless, the water distribution is not homogeneous due to the water introduction and its velocity field in this kind of system. This heterogeneity of velocity could also generate areas with heterogeneous micropollutants content. Therefore, to visualize the heterogeneity, found the area with higher micropollutants concentration then optimize the process, water flow inside wetlands must be studied. Thus, the water flow heterogeneity will be used to distinguished area where sludge could be samples. Finally, the micropollutants analyzed in sludge samples will indicate if water flow could influence the micropollutants distribution in this system.

Chapter 4:

Computational Fluid Dynamics coupled with micropollutants distribution in an artificial pond wetland

The two previous sections have introduced the distribution of micropollutants in the wetland ecosystem but also a spatial distribution in plants growing in these polluted areas. As mentioned in this chapter, the micropollutants found in these compartments come mainly from wastewater. Therefore, the influence of wastewater distribution should be investigated to understand the potential origins of micropollutants found in other compartments. Indeed, it is well known that long residence time could improve nutrient and carbon removal in this kind of system. But the influence is not so obvious concerning the micropollutants. Nevertheless, residence time distribution is a global indicator and cannot distinguish an area, with specific low velocity field in a whole system. But a detailed knowledge of water flow distribution could also be helpful to understand the micropollutants distribution inside the wetland. Therefore, a water flow process modeling should be performed to distinguish the different water flow areas in the wetland and obtain the detailed knowledge of water flow, as the velocity field, the residence time distribution, the dead and recirculation zones. To represent the most precisely the study site, the model was based on GPS coordinates and then the water flow was simulated using a 3D model based on computational fluid dynamics and the open-source software OpenFoam. The results from this hydrodynamics model could provide areas where the samples should be collected to visualize the different water flow. This model will be used to define a sample strategy where sludge will be collected. The sludge could provide an integrative view and visualize micropollutants found chronically in this wetland. And finally, this sludge samples will be analyzed using the non-target approach in LC-HRMS/MS, to find if a relationship between the micropollutants distribution and the water flow process is existing.

4.1. Materials and methods

4.1.1. Study site: the artificial pond description

This last part of this PhD project will be focused on another study site. The artificial pond is located in Lutter (Grand Est France) around 150 km from Strasbourg.as described in **Figure 72**. As the Faklwiller study site, a full-scale two stages VFCWs is coupled with a tertiary treatment wetland, an artificial pond. VFCW is working under actual conditions with a capacity around 950 people equivalent. The artificial pond wetland located in the study site is the first tertiary treatment wetland set up in Alsace in 2009. For further details, characteristics of the VFCW, which has not been studied here could be found in the Maximilien Nuel thesis (2017). This artificial pond wetland was set up by excavating area available at the outlet of the VFCWs.

Figure 72: Study site location in Lutter village (from Google maps).

In this chapter, only the hydraulic behavior of the tertiary treatment wetland and the potential link with micropollutants distribution have been investigated. Indeed, as mentioned in the first chapter, these systems are directly connected to the secondary treatment wetland and release wastewater to the environment. But micropollutants have already been detected in this wetland

(Nuel 2017). As an affinage treatment, the influence of hydraulics could probably impact the micropollutants distribution. This artificial pond is found on **Figure 73** and have a maximum length about 40 m and a maximum width about 20 m. Detailed characteristics are described in **Table 12**.

Figure 73: Tertiary treatment wetland (pond) in Lutter (Grand Est, France).

The water treatment system global scheme is similar to the one described in the Falkwiller study site in **Figure 20**.

Table 12: Design characteristics of Lutter wetlands.

Wetland type	Pond
Bank slope	1 by 4
Maximum length (m)	40
Maximum width (m)	20
Depth (m)	0.1-0.9
Surface (m^2)	750
Volume (m^3)	425

Once the wastewater has passed through the system. The treated wastewater is released in a small river called Le Briquelée which flows into the Lutterbach then into Ill.

4.1.2. Geometry building and meshing

The current paragraph aims to represent the most precisely the artificial pond to understand its hydraulics behavior. Therefore, the geometry data points should be measured to create a geometry model. The study site has been bounded as shown in **Figure 74** and GPS coordinates was collected. Once the geometry limit of the pond has been defined, the pond depth could be investigated. To measure this depth, a bathymetry campaign was carried out using an inflatable boat found in the **Figure 74**.

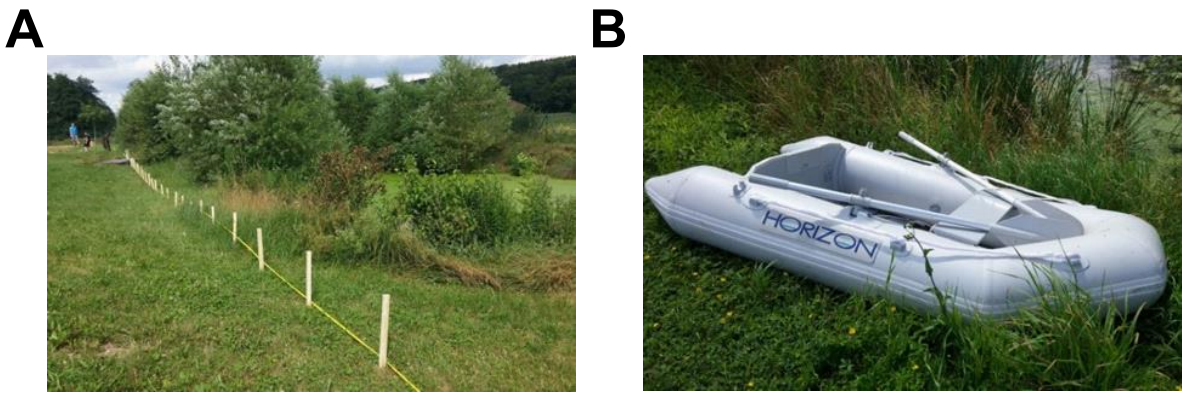

Figure 74: Material used to collect the geometry data. **A)** Bounds used to bound the system **B)** Inflatable boat used to measure the water depth.

Then to investigate the depth inside the whole pond, a virtual surface grid has been set up and the domain was split in one square meter subdomains. Then using the inflatable boat and a graduated stick the depth was measured manually each meter with the virtual grid as shown in **Figure 75**.

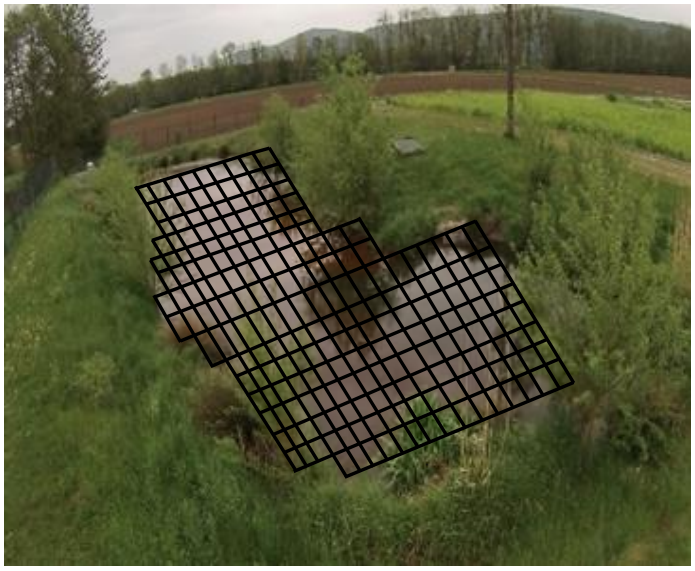

Figure 75: Virtual grid applied on the study site to collect the water depth.

Once the data collected, they were extracted and imported in a design software (SALOME) to create the geometry model. The coordinates were linked to build the whole geometry. Indeed, using the coordinates found in **Figure 76A**, the general shape has been built as found **Figure 76B**.

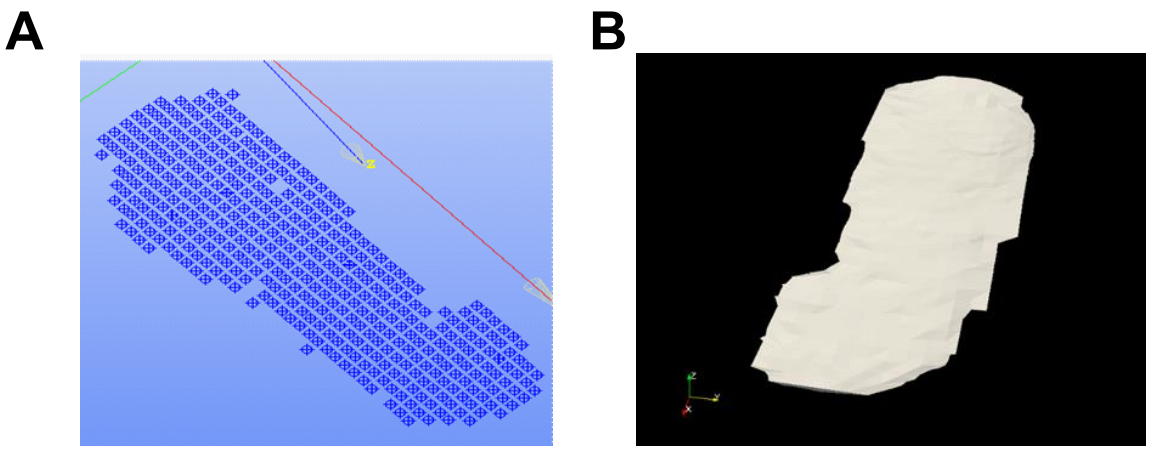

Figure 76: Data used to build the numerical geometry. **A)** Coordinates imported from the data collected in the study site. **B)** General shape of the numerical model.

Nevertheless, after several simulations, the result simulated was not fitting with the experimental data. This fitting will be developed in a following section. To reduce this issue, generate a meshing and obtain a convergent result, a geometry specificity was also considered. Indeed, a check valve has been set up in the inlet of the wetland. But this check valve has an inclination that can influence the inlet water flow. In the study site, the average inclination was measured at 25°. But this inclination is not well adapted with meshing methods applied (developed in the following section). To overcome the meshing issue, the water depth in the inlet pipe was determined using hydraulics diameter. This hydraulics diameter will simulate this check valve. Therefore, water depth was calculated using the following equation [16] and considering the check valve as the pipe as circular:

$$D_h = R\ (1 - \cos\delta)\ [16]$$

Where D_h: hydraulics diameter, R: pipe radius (50 mm) and δ angle

Therefore, this check valve simulation will be carried out using a water depth translation in the valve location. The 25° valve opening will generate a water depth under the valve that could be calculated using the trigonometric formula. This valve issue could be illustrated in **Figure 77**.

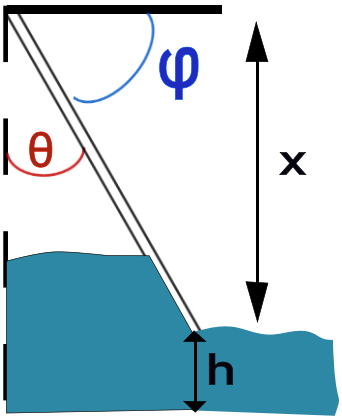

Figure 77: Scheme of the check valve inclination issue.

This water depth found in the pipe was calculated correspond to h = 9.37 mm. This water depth in the pipe will be used to estimate the valve translation. Translation could be illustrated in the **Figure 78**.

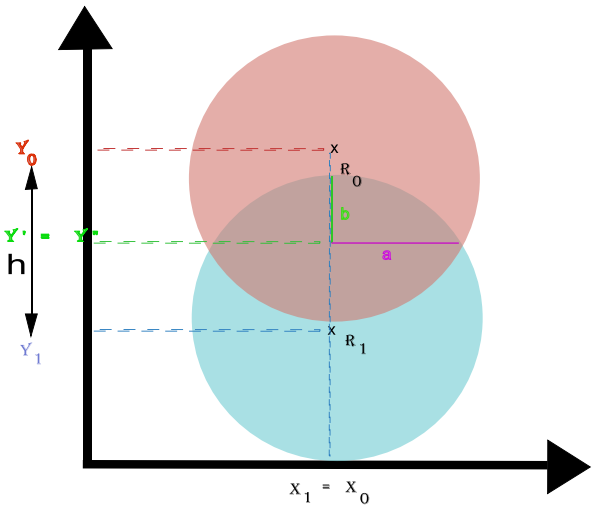

Figure 78: Scheme of the check valve translation used to determine the hydraulics perimeter. Blue ring represents the pipes and the red ring represent the check valve.

In the **Figure 78**, the red ring will represent the valve and the blue one the inlet pipe. This opening area in the pipe (only the blue part of the ring) will be calculated using this translation. This opening area could be estimated by the difference between the pipe area, and the ellipse generated by the intersection valve pipes. Therefore, ellipse center must be defined using the circle equation [17] and by resolving the second-degree polynomial [18–21]. The following equations were used:

$$(x_0 - x')^2 + (y_0 - y')^2 = R^2 \qquad [17]$$

$$A = \left(\frac{x_0 - x_1}{y_0 - y_1}\right)^2 + 1 \qquad [18]$$

$$B = 2y_0\left(\frac{x_0 - x_1}{y_0 - y_1}\right) - 2N\left(\frac{x_0 - x_1}{y_0 - y_1}\right) - 2x_0 \qquad [19]$$

$$C = y_0^2 + x_0^2 + N^2 - R_0^2 - 2y_0 N \qquad [20]$$

$$N = \frac{R_1^2 - R_0^2 - x_1^2 + x_0^2 - y_1^2 + y_0^2}{2(y_0 - y_1)} \qquad [21]$$

The resolution has led to find the ellipse center placed at a height about 54.7 mm from the pipe bottom. Then the opening area could be calculated and will be considered as the wetted perimeter. Assuming that the area corresponds to a circular pipe, the wetted perimeter could be found using the following equation [22].

$$P_{wet} = \frac{D^2}{4}(\delta - \sin\delta\cos\delta) \qquad [22]$$

Using this equation, δ was found (δ =0.8) and water depth in the pipes correspond to 15 mm, according to the hydraulics diameter equation.

Once the geometry has been built, all this geometry should be meshed. To resolve Navier-Stokes equations, all the domain should be divided in subunits. This meshing step is one of the most crucial part in the modeling. This meshing optimization was performed using two ways. First, the meshing was created in Salome and then be imported in OpenFoam 4.0. Nevertheless, the meshing quality was not adequate to perform the simulation. Therefore, snappyHexMesh (the mesh generator found in Open Foam) was used. Indeed, snappyHexMesh is well adapted to create high quality three-dimensional meshes and has the advantage being included in OpenFoam. OpenFoam is a free CFD software that uses the finite volume method to resolve the partial differential equations. This software could be used for pre-processing (meshing), solving (mathematical equations) and post processing (ParaView) to visualize the results as underline in **Figure 79.**

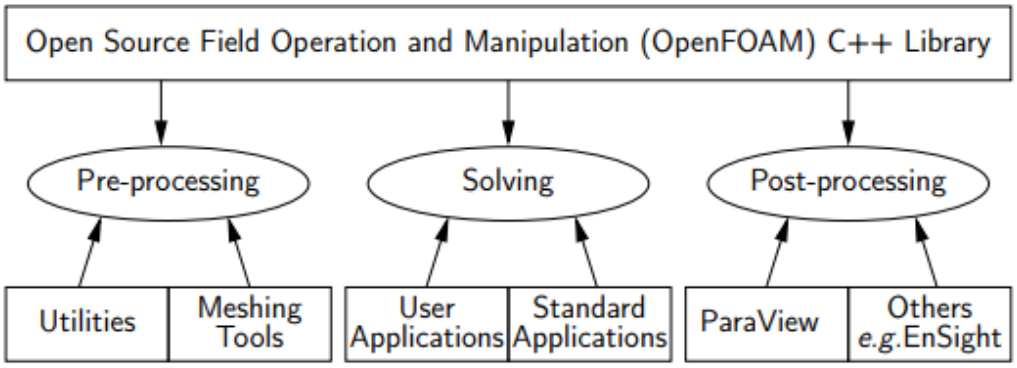

Figure 79: OpenFoam structure ("OpenFoam User Guide" 2007).

Then the first part concerning the meshing was carried out in three main steps:

- BlockMesh: The model is split in small blocks (preferably cubic or rectangular),
- Castellation: The BlockMesh is refinement locally in smaller blocks and the refinement is based on the features, surfaces…,
- Snapping: The mesh is snapped to the surface or edges.

Therefore, several mesh sizes were tested to find the most adapted model. Besides the meshing was refined in critical points of the model (the inlet/outlet pipe, the check valve and the pond border).

The final mesh model was chosen using the Y+ criterion following the standard k-Ɛ model. Indeed, these criteria calculated following the equation [23] described below should be found between 30 and 500 as recommended by Versteeg et Malalasekera 2007.

$$\Delta s = \frac{\left(\frac{2}{0.026}\right)^{\frac{1}{2}} Y^{+} \mu^{\frac{13}{14}}}{(\rho u)^{\frac{13}{14}} L^{-\frac{1}{14}}} \qquad [23]$$

Where u is the averaged velocity m/s, ρ the water density (kg.m-3), μ the dynamic viscosity (kg.m-1.s-1), L the average water depth (m) and Δs the mesh size in cm.

Using this criterion, the mesh size must be between 1.1 cm and 11 cm. Considering the calculation costs, the mesh size was defined at 10 cm. Using this mesh size, the model has 1.5 million grid cells. Finally, the mesh quality was checked using the checkMesh solver found in OpenFoam.

4.1.3. Governing equations and boundary conditions

Once the preprocessing step has been completed, the water flows simulation and the equation solving could be performed. This simulation was also carried out using OpenFoam 4.0. The method applied is conservative (inlet flux in a cell is the same as the one leaving in the adjacent cell). Therefore, this method is well adapted to solve the Navier-Stokes equation that governing the hydrodynamics in this kind of system. To obtain the velocity field inside the artificial pond, the continuity and the momentum equations [24–25], respectively and have been solved.

$$\nabla . u = 0 \qquad [24]$$

$$\frac{\partial u}{\partial t} + u\,\nabla u = -\nabla p + \upsilon \Delta u \qquad [25]$$

Where u is the velocity, p the pressure, υ the kinematic viscosity and t the time.

However several hypotheses are required to solve these equations. First, even if wastewater was the fluid consider in the model without particles transport. Besides, as the fluid is wastewater it has been studied as an incompressible fluid. Furthermore, the boundary conditions indicate a turbulence flow (at least in the inlet pipes). Therefore, the equations were solved using an unsteady mode. The solver pimpleFoam was selected. Indeed, pimpleFoam is a large time step transient solver and could be well adapted to the present case. Besides, to solve the equations, a RANS method has been used and the k—Ɛ standard model was selected to as turbulence model. This model is well adapted for water flow simulations more precisely in ponds systems (Alvarado et al., 2013; Ouedraogo et al., 2016). Then the simulation was solved using second order discretization schemes. The Euler scheme was used for the time discretization and the Gauss Linear for the space derivative. Finally, the model has been considered as converged, when the residuals value was lower than 10^{-7} and the velocity field does change over times' step, it was considered that the model had converged.

Nevertheless, this solving step should also consider the boundary conditions. The external conditions could also influence the result found in the model. Therefore, the following conditions have been considered.

Inlet flow rate: Flow rate was measured in the study site for each simulation (Nuel et al., 2017). The average inlet flow rate was used as no significant difference could be observed in the

maximum and minimum flow rate as described in the results found in Nuel et al., 2017. On the other hand, a zero gradient in pressure has been applied.

Outlet pressure: An atmospheric pressure and zero gradient concerning the velocity were set up to impact the water flow direction.

Water free surface: A symmetry condition has been applied. This condition will consider the normal component at zero, and no exchange with external conditions could be done.

Pond banks and bed: The velocity was set up at zero and a zero gradient in pressure has been applied.

4.1.4. Water model validation by tracer experiments

Results obtain by the simulation could be observed using the post-processing software included in OpenFoam and called Paraview. Nevertheless, the results do not necessarily represent the real case. Therefore, the water flow model must be validated. This validation was performed by comparing experimental data from full-scale tracer experiment with numerical results simulating water flows and passive scalar transport processes. Indeed, a sulforhodamine was injected in the wetland to determine the residence time distribution as mentioned in Nuel et al., 2017. Tracer experiments performed in the study site could be found in **Figure 80**.

Figure 80: Tracer experiment using sulforhodamine in the artificial pond.

Tracer intensity was detected in the wetland outlet using a fluorimeter and used to determine the residence time distribution (Nuel 2017).

Therefore, tracer experiment should also be simulated. The velocity field from the converged water flow model was used for the simulation of the conservative solute transport largely known as passive scalar transport. In this way, an inlet mass flow rate (100 mg/s) was defined and injected as done in the study site. Then a passive scalar has been applied on this velocity field. The equation [26] governing the passive scalar transport found below will be used to simulate a conservation experiment movement.

$$\frac{\partial C}{\partial t} + \nabla.(uC) - \nabla^2(D_m C) = q_m \qquad [26]$$

Where C is tracer concentration, u velocity, t time and D_m tracker diffusion coefficient (sulforhodamine D_m = 3.6 10^{-6} m²/s), qm pollutant source term. To solve these equations a Reynolds-Averaged Navier-Stokes (RANS) method was used.

Then residence time distribution could be calculated by integrated the results found in the outlet of the wetland. These two-residence time distribution (modeled and experimental) will be compared to validate the water flow model. Indeed, Alvarado et al., (Alvarado et al., 2013) and Coggins et al., (Coggins et al., 2017) already suggested the use of residence time to validate a waste stabilization pond (WSP) water flow mode. The comparison was investigated using the NAE (normalized absolute error). The NAE equation [27] could be found below:

$$NAE = \frac{|\overline{C_m - C_e}|}{0.5\,(\overline{C_m} + \overline{C_e})} \qquad [27]$$

The validated model will be finally used to define areas were sludge will be collected. The aims of this study were

- to have a full understanding of water flow dynamics through the artificial pond wetland,
- to determine low and fast water flow regions,
- to understand if hydraulics could influence micropollutants distribution in sludge (integrative view).

Therefore, using velocity field distribution, areas where sludge will be collected has been defined. Then, the micropollutants will be analyzed in the areas defined.

4.1.5. Micropollutants analysis

Micropollutants found in sludge samples were analyzed using the LC-HRMS/MS, on a Dionex Ultimate 3000 (Thermo) coupled to a Q-TOF (Impact II, Bruker), with the Targetscreener method developed by Bruker (Bremen, Germany). The details of micropollutants extraction and analysis are described in the sections micropollutants extraction optimization and sample analysis in mass spectrometry from the chapter 1 and in the supplementary data. Then the data analyses were carried out in two ways. The study was first focused on micropollutants found in the TargetScreener database (2200 drugs and pesticides). Therefore, all the samples were analyzed using TASQ 1.4. (Bruker Daltonics) software, to identify these micropollutants. Using standards analyzed in the same operating condition, the identification can reach the level 1 of the Schymanski classification (Schymanski et al., 2014). The compounds were selected following the criteria found below:

- exact mass variation lower than 3 ppm,
- retention time variation lower than 0.3 min,
- signal-to-noise ratio higher than three.

Besides only compounds detected in the three replicates were considered. Then non-target screening approach was performed to obtain a boarder spectrum of compounds found in these samples and identify some metabolites. The method applied is similar as the one mentioned in the data processing from Chapters 1 and 2.

4.2. Results and discussions

4.2.1. Water flow simulation and velocity field in the tertiary treatment wetland

Thanks to the previous PhD thesis in this study site, the residence time distribution has been determined in this system (Nuel et al., 2017). Nevertheless, these results could only define general parameters about hydraulics efficiency found in the wetland and did not provide a detailed knowledge of water flow distribution. Results described in this previous study will be used to simulate the inlet flow rate and validate the model. To represent the water flow distribution, the two extreme water flow found in the wetland during our measurement campaign were selected. Besides the residence time distribution measured in the experimental field were used to validate the model. The results found in **Figure 81** represent the two extreme flow rates detected.

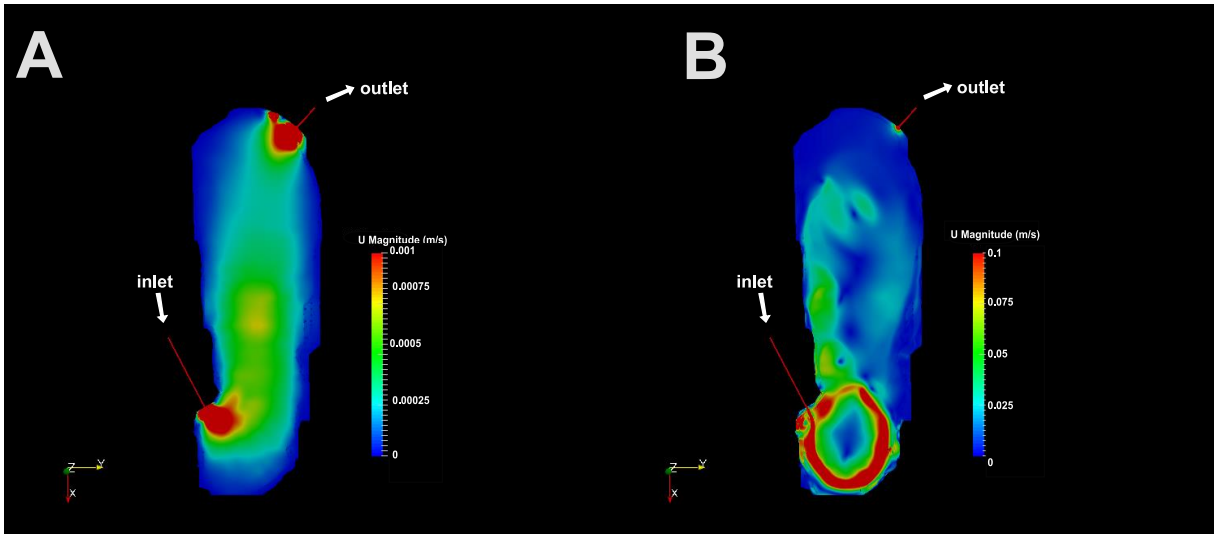

Figure 81: Velocity field in the tertiary treatment wetland obtained by CFD modeling. **A)** lowest inlet flowrate (4.1 m^3/h) simulation. **B)** Highest inlet flowrate simulation (21.1 m^3/h).

In general terms, the velocity observed in the wetland and shown in **Figure 81** suggest a low velocity field. Shallow water and rough sides could slow the velocity and generate this low velocity. The impact of water depth on hydraulic efficiency using numerical model has already been studied in the literature. Coggins et al., have suggested the loss of hydraulic efficiency related to the filling of a waste stabilization pond. (Coggins et al., 2017).

Nevertheless, the flow rate observed in the two simulation cases suggest different hydraulic behavior in the wetland. In both cases, a high velocity field is observed near the boundary conditions, probably due to the constrictions. Then, very low velocity field is detected near the

bank, where wastewater hardly flows. Therefore, these areas should be distinguished from other areas where wastewater is constantly flowing. The lowest velocity areas could be helpful for micropollutants removal. Indeed, lowest velocity field will generate an increasing residence time. The impact of higher hydraulic residence time has already been underlined in the literature for nutrients removal (Akratos and Tsihrintzis, 2007; Huang, 2000).

Despite global similarities found in the two simulations, the results also underline that a higher inlet flow rate could influence the velocity field inside the wetland. Regarding the results found in the lowest simulation, the inlet and outlet are directly connected by a preferential flow. This connection is less obvious with an increase of water flow. The results of the highest flow rate suggest the vortices presence inside the wetland. Results found in the **Figure 81** could suggest an impact of inlet water on its distribution in the wetland. However, it should be noticed that the velocity fields detected in the wetland are composed of very low velocities. Therefore, the influence of inlet flow rate is to be tempered. Besides, in general terms four main areas could be distinguished in both cases:

- the two areas near the boundary conditions (inlet and outlet) with a high velocity field,
- the areas near the banks where water hardly flows,
- areas where flow constantly flow inside the wetland.

Besides, the model has been validated using the residence time distribution as mentioned in the materials and methods section and found in Alvarado et al., 2013 and Coggins et al., 2017. The comparison between the experimental and simulated of residence time could be observed in **Figure 82**.

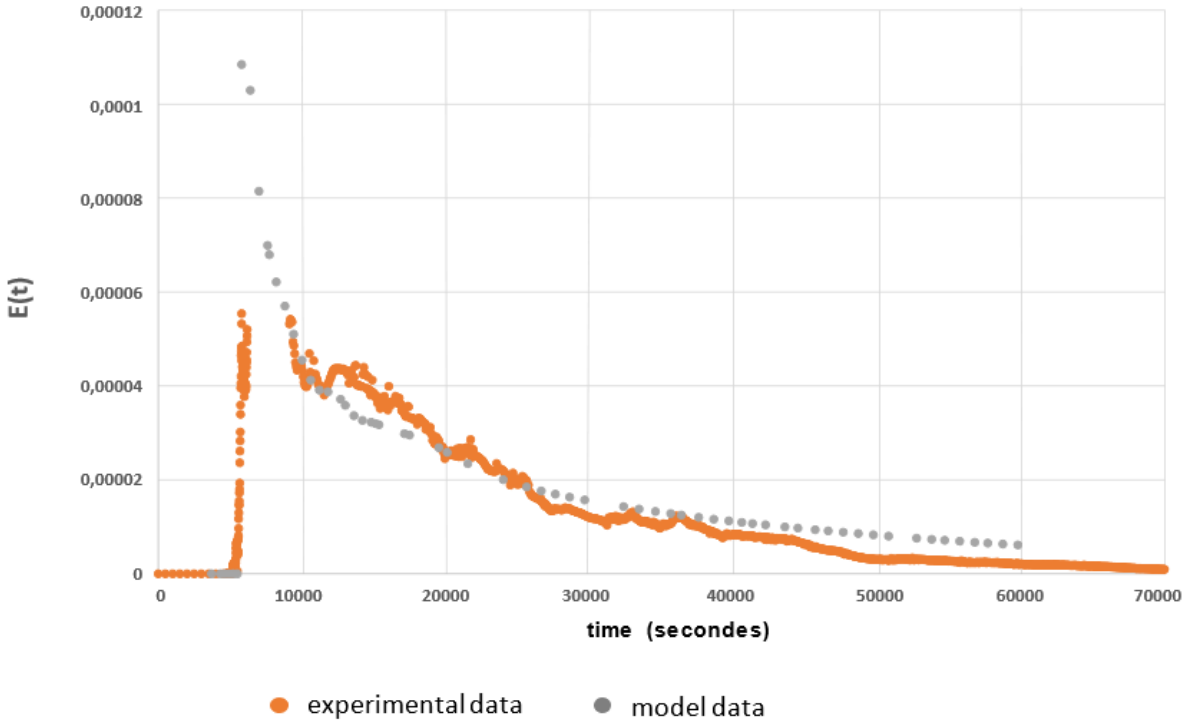

Figure 82: Experimental and modeled residence time distribution comparison to validate the model.

The general trends of the two curves indicated a good fitting by comparing experimental and modeled curve. In addition, to obtain a quantitative evaluation of the curve difference. Difference was calculated using the NAE as mentioned in the material and methods section. Results concerning the NAE indicate an average NAE about 29%. This NAE could be impacted that differences found at the end of the simulation. Nevertheless, regarding this result combined with the good fitting of the two curves, the model could be validated.

4.2.2. Sludge sampling areas

The validated model could now be used to define a sampling strategy. Indeed, the main aim of this study was to investigate if a link between water flow and micropollutants distribution is existing. To visualize this potential link, sludge sampling strategy has been defined using the numerical modeling. The four areas mentioned in the previous section (area 1: inlet, area 4: outlet, area 3: areas where water hardly flows and the one where water constantly flows; area 2) were selected. The areas were sampled to create a composite sample could be found in **Figure 83**.

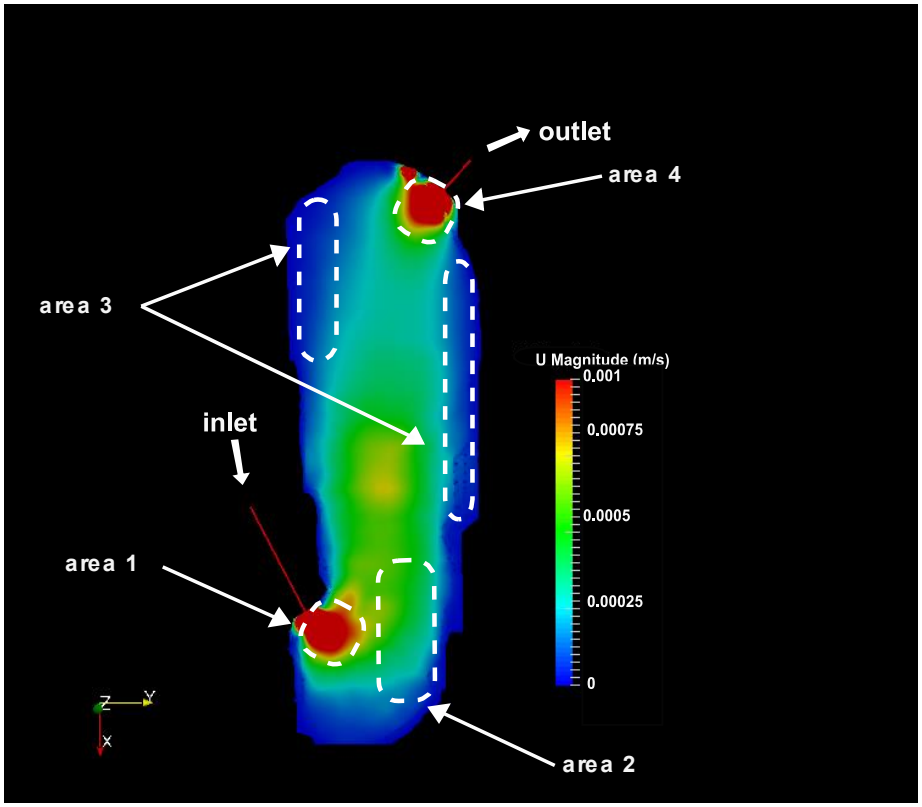

Figure 83: Sludge sampling area defined according to the velocity field simulated. Four areas were selected to represent fast and low flow rates but also the areas near the boundary conditions.

In this **Figure 83**, area 1 represents the inlet area with a high velocity filed. Then area 2 corresponds to the area where water constantly flows, and area 3 where water hardly flows. Finally, area 4 could be referred as the outlet sludge area.

4.2.3. Compounds and micropollutants distribution in wetlands

The areas defined by numerical modeling were used to collect sludge samples during four campaigns on the study site. A sampling campaign was carried out each season on the study site in the different water flow areas. The results from each season could be found in the **Figure 84**.

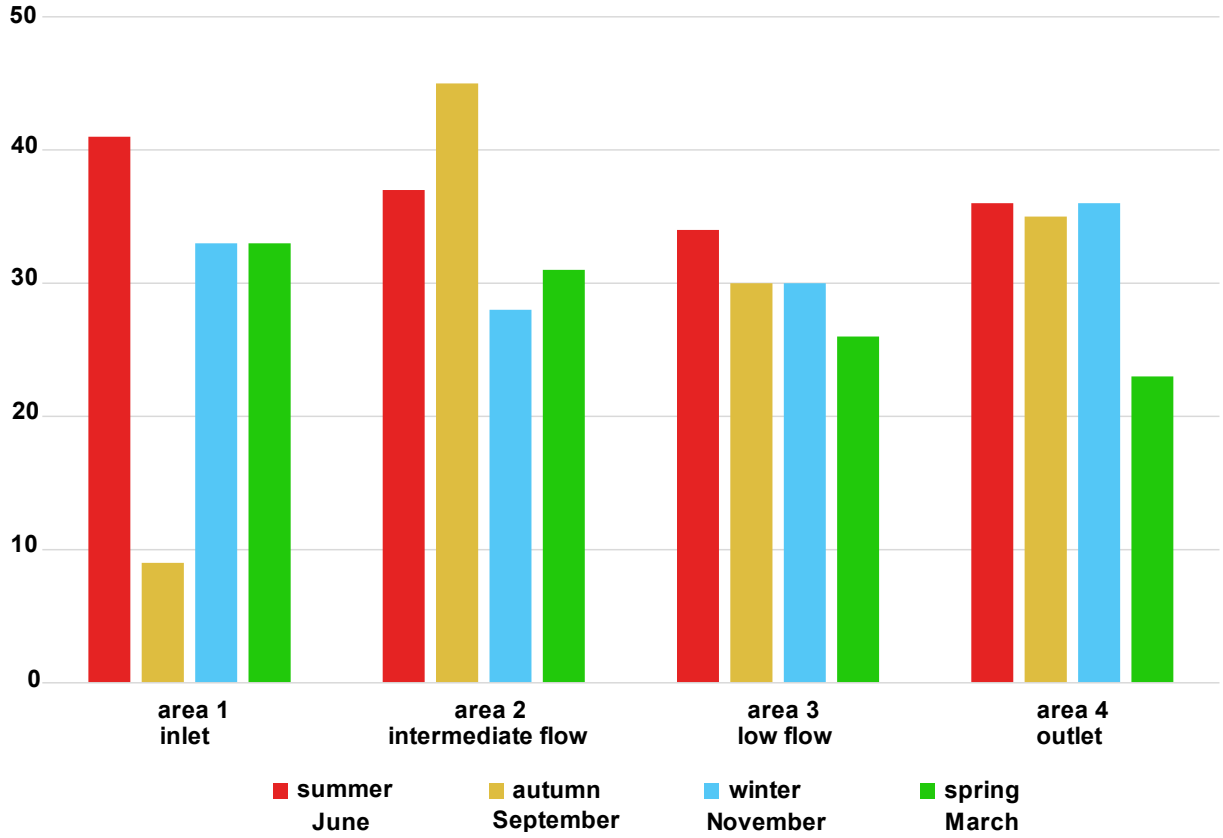

Figure 84: Micropollutants number found in the different water flow areas depending on the seasons.

The **Figure 84** shows micropollutants found in triplicates in the sludge areas over the different seasons. The detailed results from micropollutants in each area could be found in the **supplementary data (13)**. The results indicate that most of the samples contain between 25 and 35 micropollutants. Therefore, seasons have a limited impact on micropollutants number found in the different samples, especially in the areas 3 and 4, where only few decreases could be observed in Spring. This micropollutants decreased could be partly related to the microorganisms' productivity. Indeed, the environmental conditions in this season could promote the microorganism development. On the other hand, in the areas 1 and 2, the autumn simulation provides surprising results. Very few compounds were detected in the area 1 and at the opposite, this season sampling has the high number of micropollutants in the area 2. These two areas are probably linked but unclear reasons could explain the translation to the area 2. The leaching from area 1 to area 2 in this autumn could probably explain this movement.

Nevertheless, the analysis performed on different seasons could create heterogeneous results, due to the potential impact of environmental conditions. To overcome this influence, only the compounds found in each season were considered. Indeed, these results could provide a most

adapted and general view of sludge content and sludge quality. Results could be found in the **Table 13.**

Table 13: Micropollutants number found each season in the different water flow areas.

Area 1	Area 2	Area 3	Area 4
Celiprolol	**Diflufenicane**	**Acebutolol**	**Amiodaron**
Irbesartan	**Etofenprox**	**Celiprolol**	**Climbazole**
Oxadiazon	**Irbesartan**	**Etofenprox**	**Diflufenicane**
Tramadol	**Oxadiazon**	**Irbesartan**	**Etofenprox**
	Permethrim	**Isoconazole**	**Irbesartan**
	Propafenone	**Venlafaxine**	**Oxadiazon**
	Tramadol		**Venlafaxine**

These global results underline that micropollutants distribution does not seem related to the water flow. Indeed, 4 micropollutants were detected in area 1 (inlet), 6 in area 3 (low flow rate) and 7 in areas 2 (intermediate flow) and 4 (outlet) each season. Therefore, the difference does not seem significant. On the other hand, a large part of them are detected at least in two sampling areas, as found in **Figure 85**.

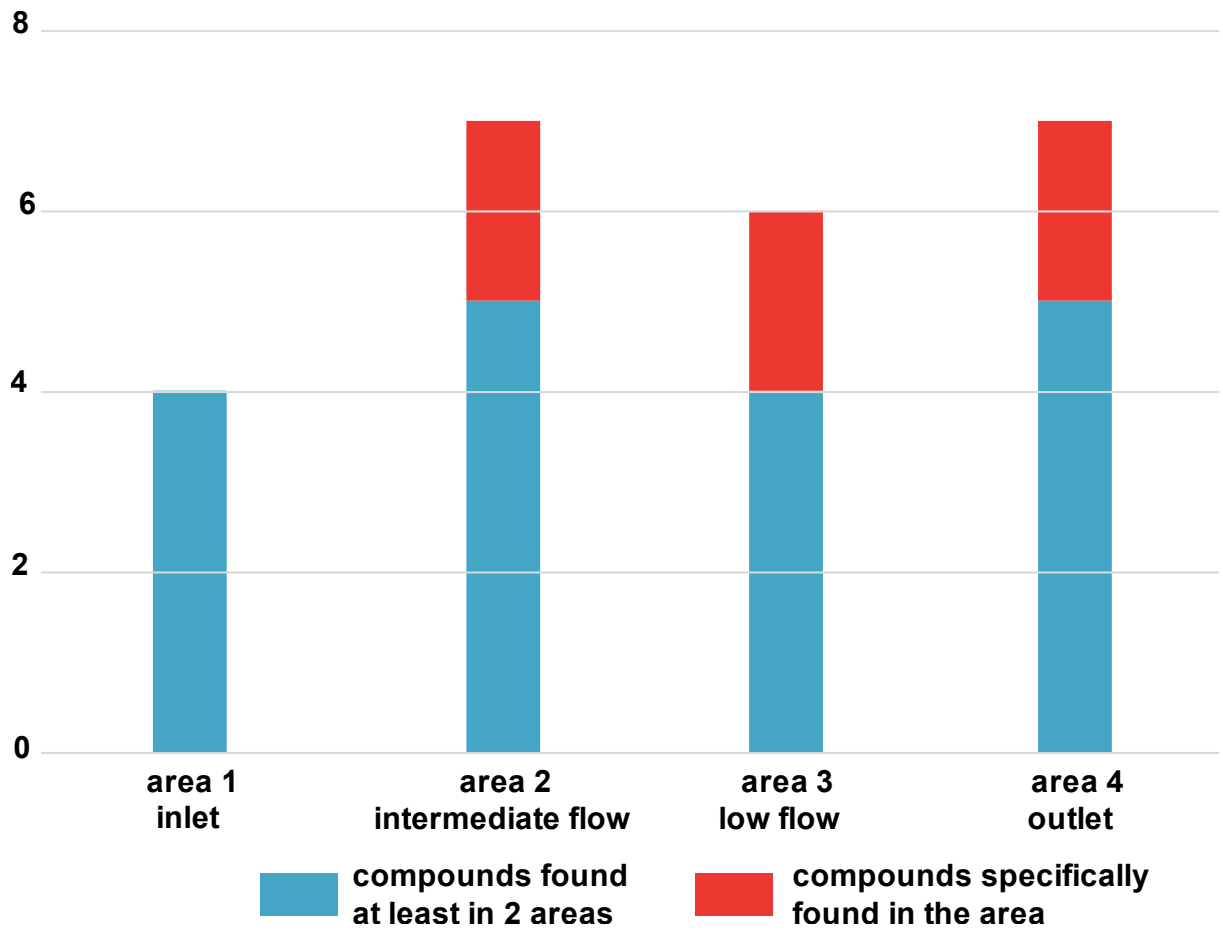

Figure 85: Distribution of micropollutants found specifically or in different areas.

Indeed, the **Figure 85** and **Table 13** highlight that a large part of micropollutants detected each season were also found at least in two areas. These compounds represent more than a half in each area (four out four in area 1, five out seven in areas 2 and 4 and four out six in area 3). Therefore, micropollutants will be diffused in the whole wetland and only few compounds were detected in a specific area. Nevertheless, micropollutants distribution in the wetland could not be restricted to micropollutants number found in these areas. Indeed, the water flow could probably generate a distribution of micropollutants in the different areas, but the compounds number cannot indicate if the distribution is homogeneous or not. Therefore, the micropollutants concentration should also be investigated. This investigation was carried out on compounds detected at least in two areas and could be observed in the **Figure 86**.

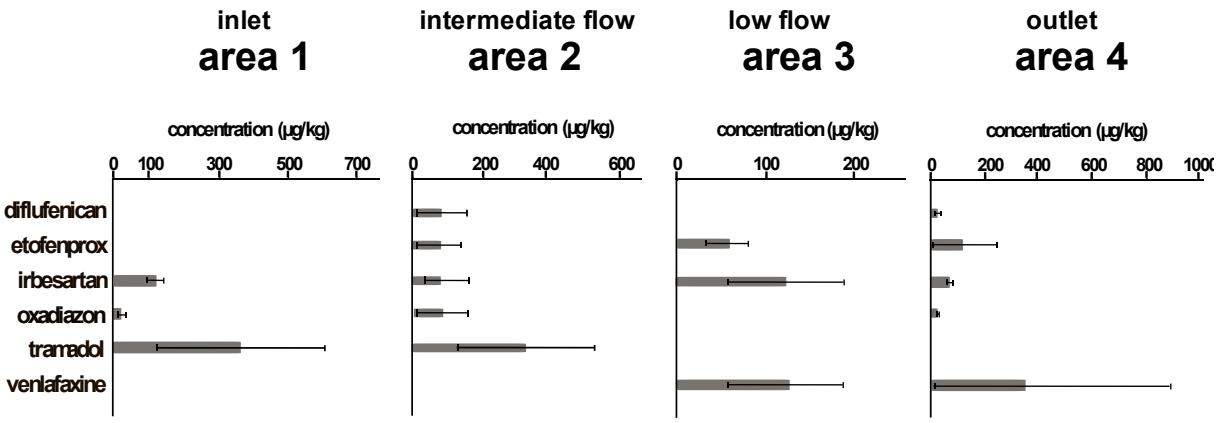

Figure 86: Concentration of compounds found at least in 2 areas, celiprolol was removed from the figure due to scale issues.

The results described in **Figure 86** could highlight that micropollutants which have been detected in several areas were found with similar concentration. The example of irbesartan mentioned in the **Figure 87**, and which has been detected in each area illustrates this homogeneous distribution in the different areas. Nevertheless, these results do not agree with those found in the literature.

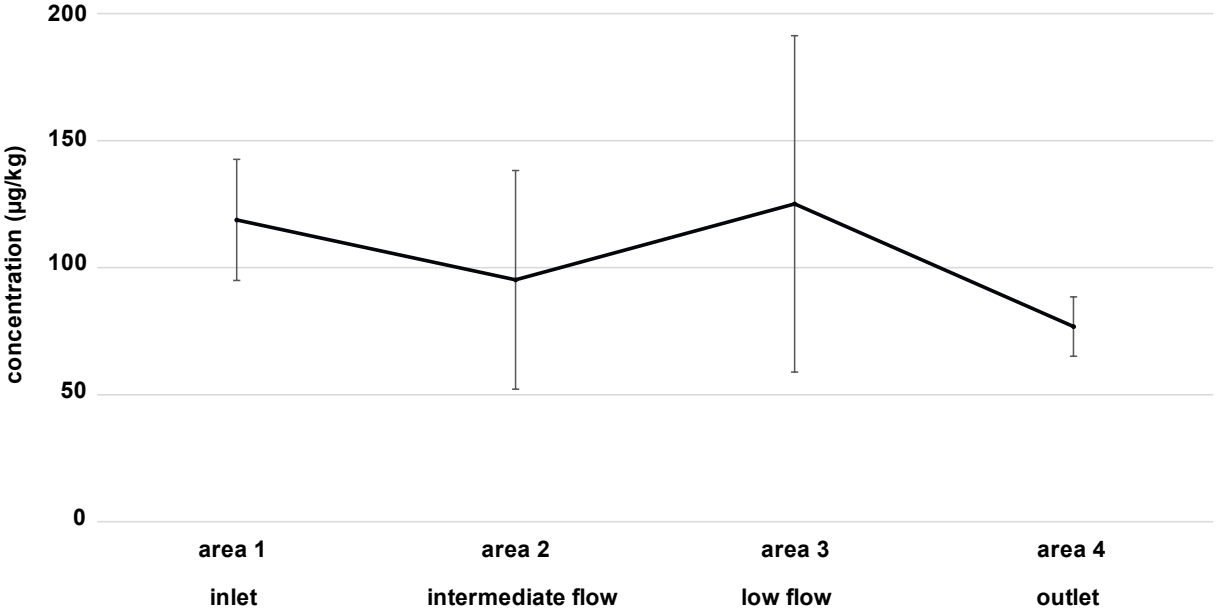

Figure 87: Irbesartan concentration found in the different water flow areas.

A lower flow rate will usually enhance general a higher sedimentation and micropollutants will be sequestered in this phase (Montiel-León et al., 2019). Therefore, it seems that water flow is not the key parameters that influence micropollutants distribution in the system. Several hypotheses could be done to explain this lack of differences observed in the results. First, the general velocity field is very low velocity (≤0.1 m/s). These low velocities could reduce the differences. This low difference will therefore impact the low difference in micropollutants content. The studies from the literature that shown an impact of water flow in micropollutants

distribution was based on system using higher velocity, for example in a port as found in (Mali et al., 2018). This higher velocity could, therefore, probably impact the distribution. A higher velocity field will generate higher differences and help to distinguish micropollutants samples composition.

Nevertheless, this correlation could also be impacted by the fact that only water flow process was considered at this stage in the model. Indeed, solid transport including conservative and non-conservative processes such as sediment or sludge deposit, sorption and other biotic and abiotic phenomena. But this solid transport could also impact the micropollutants content. The sludge deposit then its renewal is affected by sedimentation (of plant degradation products or solid particles from wastewater) and thus by the solid transport. The solid transport would help to estimate the sludge renew and its impact of micropollutants content. The lack of this parameter consideration in this study could also bias the areas selection.

On the other hand, this sludge samples should also be considered as a compartment where living organisms are growing. Indeed, worms have been found in this sludge and microorganisms are living in these compartments. All these living organisms could transform micropollutant into degradation products and the parent compounds found in the areas were not degraded. In this study, The example of permethrim could illustrate this comment. Permethrim is an insecticide poorly soluble. Therefore, it will be difficult for microorganisms to assimilate it and will be found in the sludge. Besides permethrim could have a negative impact on microorganisms living in aquatic systems (Muturi et al., 2017). Therefore, degradation processes are reduced, and it is not surprising to find these compounds in these areas.

Nevertheless, the lack of difference could be hidden by the generation of transformation products (catabolites or conjugated). In this study, the example of irbesartan found in the **Table 14** could also illustrate this comment. The irbesartan decrease is related to an increase of metabolites detection, suggesting a transformation of this drug.

Table 14: Irbesartan and its metabolites found in the different areas.

Compounds	Area 1	Area 2	Area 3	Area 4
Irbesartan (µg/kg)	118.81 ±23.84	95.21 ±43.05	125.12 ±66.22	76.82 ±11.69
C25H26N6O2 (area AU)		1466.33 ±480.72		
C25H28N6O2 (area AU)		22862.17 ±7059.86		
C26H30N6O2 (area AU)		5038.83 ±1993.28		
C25H30N6O3 (area AU)				5816.33 ±2482.14

Finally, the analysis of micropollutants should also be compared with a broader analysis focused on the general identification detected in the non-target analysis. As mentioned in the chapter 1, these putative identification covers both micropollutants but also lipids or plants metabolites. Therefore, the raw formulae (level 4) and putative identifications (level 3) distribution in the different areas were also investigated. The results could be found in **Figure 88**.

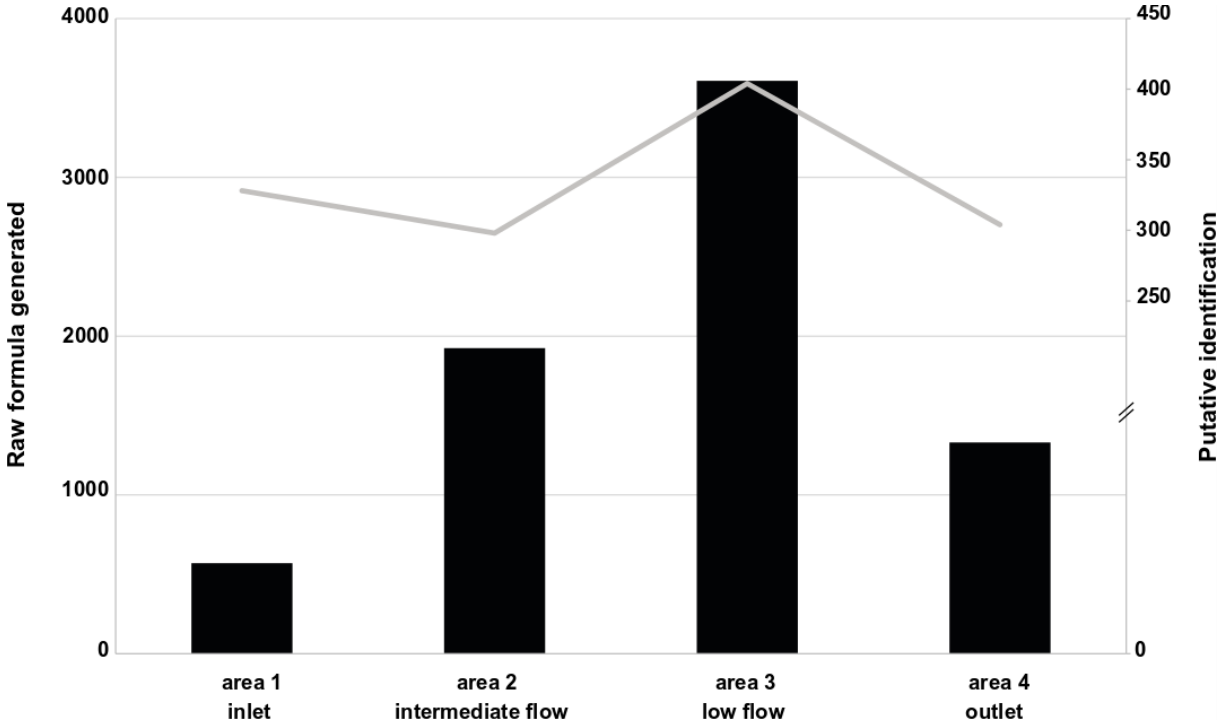

Figure 88: Raw formula and putative identification found in the different water flow areas.

The distribution of these putative identification underlines a higher identification number in the areas with lower flow rate. Therefore, in general terms the lower water flow seems to promote the sedimentation and deposits of compounds in these areas in accordance with results found in the literature, at the opposite of the observation made for micropollutants. Nevertheless, in this study, only the parent compounds were considered in this study. But micropollutants could be complex compounds that can be degraded and the absence of a global metabolites investigation could also bias the study. Therefore, their fate should be further investigated to understand if a correlation is existing between the micropollutants distribution, degradation and the water flow areas. This investigation should study both the biodegradation and the physico-chemical transformation that can be induced by oxidation or photodegradation.

Besides the study was only conducted on a single study site. Therefore, the results should be compared with different systems operating in different geographical areas and different flow rates to strengthen the results.

4.3. Chapter conclusion

The two previous chapters have underlined the widespread of micropollutants in the environment and the spatial distribution in specific compartment. In both cases, the results highlight the key role of wastewater as vectors of micropollutants in the system. Therefore, this chapter has investigated its distribution in the wetland to detect a potential correlation between the water flow and micropollutants distribution. The use of numerical modeling could predict the areas with different velocity fields and define a sampling strategy. Suspect screening of micropollutants in these different areas did not lead to correlate the micropollutants distribution and the water flow areas. Regarding the results concerning the number of micropollutants or their concentration, water flow process seems not be in this case a sufficient key parameter governing the distribution. This lack of correlation could be partly explained by several hypotheses. First it can be noticed that low velocities are found in the wetland. These low velocities could generate few differences between the different areas. Besides, the model does not consider the solid transport. And this solid transport could influence the sludge deposit. Finally, to understand the global distribution, the drugs metabolites should also be considered. Indeed, organic micropollutants could be degraded and their metabolites could also be transported following the water flow.

Concluding remarks

This work led to investigate the micropollutants distribution in a wetland ecosystem. This distribution analysis was carried out by combining a metabolomic approach and hydrodynamics. Each part of the approach could provide complementary data useful to understand the distribution.

A global approach was first carried out, using a non-target approach in the wetland ecosystem. This approach could provide a contamination overview of the different wetland's compartments. Indeed, the compartment investigation has highlighted the widespread of micropollutants in the different compartments. This widespread was not "classes" dependent, as the main xenobiotics classes were found in all the compartments. This distribution could not be fully explained by the physicochemical properties or their fate factor (i.e., translocation factor, Kd, Henry law…). Besides, the analysis performed in the CW and the tertiary treatment wetland suggest the widespread is not restricted to the treatment systems. However, the first analysis was only focused on the surface layer in direct interactions with wastewater and plants growing in these systems. But the distribution of xenobiotics could not be restricted to the analysis of the ecosystem's compartments. Spatial distribution could also be observed in different compartments. Therefore, a vertical profile of sludge has been investigated. The results detected in this sludge coring suggest that micropollutants could diffuse in the entire depth, even if a large part of them are specifically found in the top layer. The analysis of sludge content (physicochemical properties but also lipids analysis) could partly explain this distribution. Indeed, the physicochemical properties in the top layers will promote micropollutants sorption (porosity, dryness, granulometry analysis). However, a complete analysis should combine the structure and the biological component of a sludge samples. In this way, the lipids study suggests that the main microorganisms productivity is found in the top layer. Therefore, this microbial activity combined with the polar characteristics for many micropollutants and the sludge structure will explain the few compounds detected specifically in the bottom layer. All the results described in the first part of this manuscript could therefore provide an overview of the contamination found in these kinds of systems.

On the other hand, the results have suggested that this micropollutants could also affect living organisms and create and environmental but also a health risk. The analysis of hormones has underlined that plant generates a stress response to deal with these pollutants. And living organisms growing in these areas are chronically exposed to micropollutants and could develop strategies to manage these pollutants. Plants will take up and then transform micropollutants from the environment. Nevertheless, the non-target analysis should be combined with spatial

information to understand the bioprocesses occurring in the plants. Therefore, the micropollutants distribution and metabolization were investigated using mass spectrometry imaging (MSI).

The MSI results have underlined that specific mechanisms have been established in the plants to deal with the micropollutants. For example, a storage in outer tissue, to confine micropollutants, in poplar leaves have been described. In addition to this active storage, biodegradation processes were also found in plants leaves. Indeed, metabolites from two drugs were only found in poplar leaves with a higher intensity that the parent compounds. The results described in this study underline that enzymatic reactions are occurring in plants and the "green liver" process is set up to degraded micropollutants. Nevertheless, the analysis of leaves in MSI or roots in LC non-target screening is not sufficient to understand the bioprocesses that can be set up. The literature mentioned that micropollutants are transfers from roots to leaves using the transpiration stream. This transpiration stream could therefore also investigate using MSI in a whole plant. Therefore, a reed mainly used in CW was considered as a model plant chronically exposed to micropollutants. The pollutants migration has been highlighted by the different location of micropollutants inside the reed stem. This location difference could be related to a temporal distribution. As the plant grew for 10 months in the polluted area, and plant sacrifice has stopped the transfer process. Even if a large part of micropollutants are already detected in the top parts, specific distribution could also be found describing the different step of the transport linked to the transpiration stream.

Nevertheless, micropollutants found inside the plants come from sludge and water compartments. As mentioned in the previous section, the water flow could directly impact the micropollutants distribution. The observations described in a living organism could also be applied to the treatment system. Indeed, water distribution in the wetland is not homogeneous and the heterogeneous velocity field could impact the micropollutants distribution. Therefore, the last part of this manuscript has been dedicated to investigate if a correlation between the micropollutants distribution and the velocity field is existing. The velocity field has been obtained by numerical modeling based on study site measurement. These simulations have predicted different areas according to the velocity field. Then a sampling strategy has been defined to select the lower and higher velocity field area. The suspect analysis performed on the sludge collected in these areas do not provide a correlation between micropollutants distribution and water flow. Regarding the results concerning the number of micropollutants or their concentration, water flow seems not be in this case a key parameter governing the

distribution. The lack of correlations could partly be explained by the hypothesis done in this study (no transport solid simulation, general low velocity found in the systems). Besides, only the parent compounds were considered in this study that can bias the general conclusion.

To conclude, this work has highlighted the distribution of micropollutants in wetland ecosystems using several methods. The micropollutants from wastewater reach each compartment of the wetland ecosystem. But the fate of micropollutant could not be limited to the study of their distribution. Indeed, these systems based on natural processes could degrade micropollutants using oxidation or living organisms. Therefore, the micropollutants metabolites should also be investigated to understand the micropollutants fate. Some metabolites have been investigated in this study using biodegradation rules. Nevertheless, they do not fully represent the micropollutants degradation products. As perspectives, the metabolites generated by oxidation but also those found in the gas phase should be studied. Indeed, the final stage of degradation products will produce volatile compounds. Therefore, it would be interesting to study compounds found in the gas compartment (atmosphere) in this kind of system. Indeed, the final step of compounds degradation lead to generate volatile compounds. Therefore, the analysis of volatile compounds excreted by the organisms could probably help us to understand the mechanisms set up to deal with micropollutants. On the other, the combination between modeling and micropollutants distribution should probably improve by simulated the solid transport in the pond and considering all the micropollutants metabolites.

Summary of this thesis work
(French version)

Introduction Générale

Le développement d'activités anthropiques accompagné par l'accroissement de l'industrie de synthèse a favorisé l'émergence de contaminants au sein des différents milieux de l'environnement. Tous composés introduits dans l'environnement et pouvant générer un risque ou un problème peuvent être évoqués sous la dénomination de contaminants ou polluants. En effet, le rejet de contaminants au sein de l'environnement et plus particulièrement dans les milieux aquatiques a entrainé la mise en place de système de traitement afin de préserver la ressource. Il faut cependant attendre les années 1960-1970 pour que de tels systèmes soient mis en place en France et la loi de 1992 pour fixer des objectifs de traitement. Ces filières de traitement ont tout d'abord été concentrées sur les zones urbaines générant le plus grand flux de polluants. Mais la directive cadre sur l'eau de 2000 a fixé le bon état des masses d'eau en Europe. C'est pourquoi les zones rurales nécessitent également la mise en œuvre de filières de traitement. Cependant le contexte rural avec des moyens financiers moins importants a conduit à l'introduction de filières extensives tel que les filtres plantés de roseaux (FPR) ou des lagunes.

L'ensemble des filières mis en œuvre en France a été conçu sur les problématiques du XX^{ème} siècle et la macropollution (carbone, azote et phosphore). Ainsi les polluants émergents et donc les micropolluants n'ont pas ou très peu été pris en compte lors de la conception de ces ouvrages. Ces micropolluants sont issus de sources diverses, mais rejoignent l'environnement majoritairement par les eaux usées, faisant des stations d'épuration un point de rejet majeur vers l'environnement. Or, ils représentent un risque pour l'environnement, mais également pour la santé humaine. Au cours des dernières années, cette problématique a été prise en compte comme le montre l'exemple des Watch list dans la législation européenne.

Malgré l'absence de prise en compte de ces micropolluants dans les ouvrages de traitement, l'étude de la littérature montre que les FPR ont une certaine efficacité pour abattre une partie des micropolluants issus des eaux usées. Cependant, la plupart des études se concentrent sur une catégorie ou un nombre restreint de composés servant de modèle pour comprendre les mécanismes se déroulant dans ces ouvrages. Mais cette approche avec un choix de composés peut biaiser les conclusions. Or les avancées technologiques des dernières années, notamment en spectrométrie de masse à haute résolution, ont permis d'étudier un spectre large de composés, présents même à de très faibles concentrations. Ces avancées permettent également de ne plus se concentrer uniquement sur les molécules mères, mais également les produits de dégradation qui eux aussi peuvent présenter un risque majeur pour l'environnement.

Au sein de ces filières de traitement, l'un des sous-produits présentant un enjeu majeur est la boue accumulée. En effet, leur gestion est un point crucial pour les exploitants et demande ainsi une connaissance fine de leur contenu pour choisir la filière de traitement adaptée à ce sous-produit. Mais l'analyse ne peut pas être réduite au seul compartiment boues, car celui possède des interactions avec les plantes et les eaux présentes dans ce système. Lors d'une précédente thèse (Maximilien Nuel, 2017), il a été démontré que les résidus médicamenteux peuvent être retrouvés au sein des différents compartiments de l'environnement. Étant concentré sur une seule famille de polluants, il parait essentiel pour comprendre le devenir de ces micropolluants, d'étudier leur distribution en utilisant un spectre large dans les eaux et les plantes se développant dans ces systèmes. En effet, les micropolluants accumulés au sein des boues sont un enjeu majeur pour leur gestion. Pour comprendre cette répartition, différentes méthodes peuvent être combinées. Au sein de ce mémoire, cette étude de la distribution des micropolluants a été menée selon trois axes majeurs :

- une étude en spectre large des micropolluants dans les différents compartiments de l'environnement (eau, boues, plantes) à l'aide de la LC-HRMS/MS,
- une distribution spatiale des polluants réalisée à l'aide du MALDI-Imaging,
- une étude de la distribution des micropolluants en couplant les flux modélisés numériquement en CFD avec une analyse en spectre large.

Démarche expérimentale

L'approche expérimentale s'est déroulée en plusieurs phases suivant les axes mentionnés dans l'introduction générale. Tout d'abord ces travaux se sont concentrés sur la visualisation d'un spectre large de micropolluants au sein des différents compartiments de l'écosystème du FPR et de la zone de rejet végétalisé (ZRV). Pour étudier la distribution des micropolluants au sein des écosystèmes, une stratégie d'échantillonnage a été développée. Elle visait à collecter les échantillons dans un périmètre de 1 m². Dans ce périmètre, les compartiments en interactions ont été prélevés (eau, boues de la couche supérieure et plantes (roseau, peuplier)). Puis une méthode d'extraction des micropolluants a été mise au point et optimisée. Pour cela, différentes méthodes ont été comparées (extraction liquide-liquide, SPE, Bligh & Dyer). Suite à cette phase d'optimisation, la méthode d'extraction liquide-liquide a été retenue en utilisant 10 g de boues et 50 mL d'eau. Les échantillons ont ensuite été analysés en LC-HRMS/MS en mode d'ionisation positive et en utilisant la méthode TargetScreener développée par Bruker pour l'identification de micropolluants. Or l'analyse non ciblée de composés conduit à un large spectre de composés. Il a donc été nécessaire de définir une stratégie d'identification des

composés. Celle-ci fut basée sur la classification mentionnée par Schymanski (Schymanski et al., 2014). Pour cela, une méthodologie d'identification sur l'ensemble des échantillons a également été développée. Cette identification a été permise par l'utilisation du logiciel Metaboscape 3.0. (Bruker) et l'optimisation de ces paramètres afin d'extraire le plus grand nombre de composés. À partir du jeu de données extrait, l'outil SmartFormula a été utilisé pour générer les formules brutes de composés. Puis les composés possédant une formule brute ont été annotés afin d'obtenir une identification putative. L'identification est un défi important pour la métabolomique en mode non ciblée, car il n'existe pas de bases de données uniques regroupant l'ensemble des composés d'intérêt recherchés dans cette étude. Pour cela, les bases de données d'intérêt ont été importées localement et une méthode d'identification basée sur l'outil « Analyte list » a été menée. À l'aide de la méthode développée, les différents compartiments ont donc pu être analysés. Ces premiers résultats ont permis d'obtenir une vision des compartiments en interaction. Cependant, la boue qui demeure l'un des problèmes majeurs de gestion des exploitants ne peut être restreinte à sa couche superficielle. Pour optimiser la gestion de l'enlèvement des boues, il est nécessaire d'obtenir une vision sur le profil vertical de ces boues. Pour cela, un carottage au sein des ouvrages a été réalisé. L'analyse de la structure, mais également du contenu en macro et micropolluants a été réalisée afin de conclure sur la diffusion de ces micropolluants sur le profil vertical.

Ces résultats peuvent fournir une première information sur une distribution spatiale des polluants dans ces systèmes. Mais dans ces systèmes alliant plantes, eaux et boues, les plantes peuvent jouer un rôle essentiel dans le devenir des micropolluants. Or une localisation précise des micropolluants au sein de ces dernières peut avoir une importance cruciale pour comprendre les bioprocédés se déroulant au sein de ces dernières. Ces travaux se sont donc ensuite concentrés sur cette analyse spatiale des micropolluants à l'aide de l'imagerie par spectrométrie de masse. Pour cela, les différents organes de plantes ont été analysés. En effet, l'approche a tout d'abord été menée sur des feuilles de plantes ayant grandi dans la ZRV (peuplier et saule). Une fois les feuilles de ces derniers collectées, une optimisation de la coupe des échantillons a été réalisée afin de conserver l'intégrité des tissus. Ces échantillons ont ensuite été analysés en utilisant le MALDI Imaging et l'ultra haute résolution grâce à un FT-ICR (SolariX 7T, Bruker Daltonics). La distribution spatiale a été obtenue avec une résolution de 50 µm et les spectres ont été calibrés en utilisant les pics de la matrix HCCA. L'analyse des données s'est ensuite déroulée en plusieurs temps. Les données ont été importées dans le logiciel SCiLs Lab2016b pour visualiser la distribution des polluants. Or pour obtenir l'identification des composés les

données ont été exportées vers la plateforme open source Metaspace et vers le logiciel Metaboscape. De plus, les plantes pouvant être au cœur de procédés de dégradation, les métabolites (conjugués et catabolites) des micropolluants ont également été étudiés. Pour cela, ils ont été générés sur deux générations en utilisant les prédictions *in silico* à l'aide du logiciel Metabolites Predict 2.0 (Bruker). Mais l'analyse des seules feuilles des plantes peut introduire un biais sur les processus se déroulant au sein des plantes. Ainsi, une plante entière (un roseau) a été analysée en utilisant la méthode mentionnée précédemment. Pour cela, le roseau a été sectionné à intervalles réguliers et l'ensemble des organes ont été analysés. Cette analyse d'une plante entière permet de visualiser les localisations préférentielles, mais également d'étudier les translocations se déroulant au sein des plantes. En effet, la littérature évoque le flux de transpiration comme l'un des vecteurs du mouvement des micropolluants au sein des plantes.

Ce flux d'eau semble être l'un des vecteurs des micropolluants dans les plantes. Mais leur présence au sein des plantes est liée à celle dans les eaux usées et les boues. La distribution des eaux usées pourrait avoir un impact majeur sur la répartition spatiale des micropolluants dans les ouvrages et donc dans les boues. Or les flux d'eau dans ces ouvrages (FPR et ZRVs) ne sont pas homogènes et vont donc provoquer une hétérogénéité dans le contenu des micropolluants. Ainsi l'analyse des flux d'eau dans les ouvrages semble primordiale pour comprendre la distribution des micropolluants. Cette distribution peut être obtenue par la création d'un modèle numérique simulant les flux au sein d'un ouvrage. Pour cela, les conditions expérimentales retrouvées sur le site d'étude ont été relevées (géométrie de l'ouvrage par coordonnées GPS, mesures du débit d'entrée, prise des conditions aux limites…). Une fois le relevé de ces conditions aux limites effectuées, un modèle numérique a été créé. Ce dernier a permis de simuler les écoulements au sein de la ZRV en considérant les équations de Navier-Stokes dans un régime transitoire. Une fois la simulation convergée, des zones de prélèvements ont été définies sur la base des différences de champs de vitesse et de zones d'intérêt (entrée, sortie). Ces zones de prélèvements ont été utilisées pour collecter des boues et analyser le contenu en micropolluants. Ainsi les résultats obtenus permettront de visualiser si un lien entre la vitesse d'écoulement au sein d'une ZRV et la distribution de micropolluants existe.

Principaux résultats

Les résultats obtenus sur la distribution des micropolluants montrent la dispersion de ces derniers au sein de l'ensemble de l'écosystème. En effet, l'ensemble des classes des polluants recherchés a été retrouvé dans les différents compartiments (eau, boues, plantes). La comparaison du profil métabolomique suggère néanmoins une distribution hétérogène selon le compartiment considéré. Même si la répartition ne dépend pas de la classe des composés, il n'en demeure pas moins que certaines molécules ont une affinité plus forte avec les phases liquides, ou se sorbe mieux sur certaines matrices. Néanmoins, ces propriétés physico-chimiques ainsi que les paramètres gouvernant le devenir de ces micropolluants ne permettent pas à eux seuls d'expliquer totalement la distribution observée. De plus, l'analyse effectuée à la fois dans le FPR et la ZRV montre que cette distribution est observée dans la filière de traitement, mais également dans la zone réceptionnant son rejet et donc dans l'environnement. Ces résultats montrent bien une contamination globale des compartiments présents à la surface. Mais ces micropolluants peuvent également contaminer des éléments se situant dans des horizons plus profonds. C'est pourquoi un profil vertical de boues a également été analysé. Cette analyse a porté à la fois sur les micropolluants, la macropollution mais également la structure des boues pouvant expliquer la distribution des micropolluants. Concernant ces résultats, une large diffusion de micropolluants a été retrouvée sur l'ensemble de la profondeur du profil suggérant une contamination sur l'ensemble de la profondeur. Néanmoins, l'analyse des composés retrouvés spécifiquement dans un horizon de boues, montre que les micropolluants sont majoritairement présents dans la couche supérieure et peu d'entre eux sont détectés spécifiquement dans la couche inférieure. Le contact direct avec les eaux usées non traitées, la composition en carbone, mais également la porosité et la taille des grains favorisent la sorption des polluants dans ces couches. De plus, l'analyse des lipides menée dans ce profil montre que l'activité microbienne se situe principalement au sein de l'horizon supérieur. Ainsi une dégradation de ces composés pourrait se dérouler dans cet horizon et expliquer le faible nombre de composés retrouvés spécifiquement dans l'horizon inférieur. Ces résultats ont pu montrer la large dispersion des micropolluants dans l'ensemble de l'écosystème et même au sein des organismes vivants. Ces derniers doivent mettre en place des mécanismes pour faire face aux micropolluants et notamment pour les plantes se développant dans ces systèmes. Or pour comprendre les mécanismes mis en œuvre au sein d'une plante une localisation précise de ces micropolluants peut être nécessaire. Ainsi la seconde partie de ces travaux s'est concentrée

sur la distribution spatiale de composés au sein de différents compartiments obtenue à l'aide de l'imagerie par spectrométrie de masse (IMS).

L'analyse de la distribution spatiale des micropolluants au sein des feuilles du peuplier souligne une localisation spécifique de ces derniers. Au vu des résultats observés, il semble que le peuplier séquestre les micropolluants dans les tissus extérieurs des feuilles. Ce mécanisme qui semble être actif a probablement été mis en place par la plante pour confiner les micropolluants dans un espace moins toxique pour cette dernière et favoriser leur dégradation. Cette présence de micropolluants au sein de ces feuilles s'accompagne par une réponse de stress de la plante. Mais le stockage au sein d'espace spécifique n'est pas le seul processus mis en place par une plante. Une dégradation des micropolluants par voie métabolique peut également se dérouler au sein de ces dernières. L'exemple du telmisartan au sein des feuilles du saule peut parfaitement l'illustrer. En effet, les métabolites du telmisartan sont retrouvés avec des intensités plus fortes que ce dernier au sein des feuilles. Or ces métabolites ne sont pas retrouvés dans la boue ou l'eau environnante. Ces résultats suggèrent donc la dégradation de ces polluants par le biais du processus nommé « green liver ». Mais ces analyses effectuées sur les feuilles ne permettent pas d'obtenir une vision globale des processus se déroulant dans une plante. C'est pourquoi l'analyse spatiale a ensuite été effectuée sur une plante entière le roseau. En effet, le roseau, qui est la plante modèle utilisée dans les filières extensives de traitement des eaux usées avec les FPR, subit de manière chronique une exposition aux micropolluants. Les phénomènes de translocations peuvent ainsi être visualisés. Les résultats obtenus montrent qu'une large partie des micropolluants sont retrouvés dans les parties supérieures de la tige ou dans les feuilles. Ces résultats montrent bien un mouvement des micropolluants vers les parties aériennes suivant le flux de transpiration. Les différences de localisation ne s'expliquent pas par la classe de polluants ni entièrement par les propriétés physico-chimiques. Les différences de localisation peuvent montrer une différence temporelle de transfert au sein de la plante. La plante étant soumise de manière chronique aux micropolluants et le processus de transfert étant stoppé lors du sacrifice de la plante, différentes phases de transfert peuvent être observées.
Néanmoins ces résultats montrent l'importance du flux d'eau dans la distribution des micropolluants. Or ces derniers retrouvés dans les boues ou les plantes proviennent des eaux usées. Les filières de traitement extensives ne présentent pas un flux d'eau homogène au sein de la filière de traitement. C'est pourquoi afin de comprendre la distribution des micropolluants dans de tels systèmes, l'analyse de l'écoulement dans des filières extensives semble primordiale. La modélisation numérique réalisée sur la ZRV a pu mettre en évidence une

hétérogénéité du champ de vitesse. Elle a donc été utilisée pour définir des zones de prélèvements de boues afin de faire état de la diversité d'écoulement dans la ZRV. Cependant l'analyse des micropolluants retrouvés dans les différentes zones ne permet pas de conclure de l'influence de l'écoulement sur la distribution des micropolluants. Plusieurs hypothèses peuvent être apportées pour exprimer le manque de corrélation, comme les faibles vitesses observées dans l'ouvrage, l'absence de prise en compte du transport solide ou encore de la métabolisation des micropolluants.

Conclusion

Ces travaux ont donc permis de visualiser la distribution d'un spectre large de micropolluants dans l'écosystème de filière de traitement extensive. Ils mettent en évidence la contamination de l'ensemble des compartiments, ce qui pourrait générer des risques environnementaux, mais également pour la santé humaine. Les organismes présents dans ces systèmes et en état de stress mettent en place des mécanismes pour faire face à cette pollution. Une compartimentation ou encore des phénomènes de dégradation peuvent néanmoins être mis en place par ces organismes vivants. Enfin, la distribution des micropolluants au sein des filières extensives ne peut être résumée aux processus hydrauliques qui gouvernent le dimensionnement de filières extensives. En effet, les faibles vitesses observées dans ces ZRVs ne permettent pas une répartition préférentielle des micropolluants au sein de ces ouvrages.

Communications

Articles in International peer review Journal

In situ localization of micropollutants and associated stress response in Populus nigra leaves, C Villette*, **L Maurer***, J Delecolle, J Zumsteg, M Erhardt, D Heintz Environment international 126, 523–532

Xenobiotics metabolization in Salix alba leaves uncovered by mass spectrometry imaging, C Villette*, **L Maurer***, A Wanko, D Heintz, Metabolomics 15 (9), 122

Investigation of Xenobiotics Metabolism In Salix alba Leaves via Mass Spectrometry Imaging, C Villette, **L Maurer**, D Heintz, JoVE (Journal of Visualized Experiments), e61011

Large scale micropollutants and lipids screening in the sludge layers and the ecosystem of a vertical flow constructed wetland, STOTEN, **L.Maurer**, C. Villette , J. Zumsteg, A. Wanko, D. Heintz in press

Monitoring of road runoff micropollutants from surface to groundwater during infiltration, **L. Maurer**, C.Villette, J. Zumsteg, C. Lutz, M.P. Ottermatte, A.Wanko, M. Malfroy-camine, Y. Dabrowski, M. Pomies, D. Heintz, submitted to Water research

***co-first authors**

Oral in International conference

Maurer, L., Villette, C., Wanko, A. & Heintz, D. (2019). Large scale micropollutants screening in a wetland ecosystem using a non targeted high resolution mass spectrometry approach, RFMF, Clermont – Ferrand, France

Maurer, L., Villette, C., Laurent, J., Bois, P., Wanko, A. & Heintz, D. (2019)., Non-Targeted Micropollutants identification by High Resolution Mass Spectrometry in a Tertiary Treatment wetland ecosystem, WETPOL 2019, Aarhus Denmark

Villette C., **Maurer L.,** Wanko A., Heintz D., Large scale micropollutants inventory and potential migration in stormwater constructed wetland, WETPOL 2019, Aarhus Denmark

Maurer L., Villette C., Wanko A., Heintz D., MALDI Imaging micropollutants screening in Salix alba and Phragmites australis growing in a polluted environment, OURCON VII, 2019, Saint- Malo, France

Oral in National conference

Maurer L., Suivi des boues de FPR et ZRV, Journées techniques EPNAC,2019, Strasbourg, France

Poster in International conference

Maurer, L., Villette C., Delecolle, J., Zumsteg, J., Erhardt, M., & Heintz, D. (2019). In situ localization of micropollutants and associated stress response in Populus nigra leaves. OURCON VII, 2019, Saint-Malo, France

Supplementary datas

Supplementary datas 1: Water quality found in the Largue at Spechbach- Le -Bas.

.A LARGUE À SPECHBACH-LE-BAS(02003800)

Etat écologiqueEtat chimiqueAutres substances chimiquesSédiments

Paramètres	Année(s)										Etat écologique 2016-2018	
	2009	2010	2011	2012	2013	2014	2015	2016	2017	2018	2016-2018	Classes d'état
Invertébrés (IBGN ou IBGN équivalent)		15	16	15	15		16	15	16		15.5	Biologie
Diatomées (IBD 2007)	14	14	15.1	14.3		13.8		14	13.8		13.9	
Poissons (IPR)												
Macrophytes (IBMR)												
Température (P90, °C)	18.9	19	19.7	17.7	18	18.4	17.1	17.5	19.6	19.3	19.6	Température
pH (min)	7.8	7.85	7.85	7.8	7.9	7.8	7.7	7.9	7.9	7.8	7.9	Acidification
pH (max)	8.1	8.15	8.15	8.05	8.2	8.2	8	8.2	8.2	8.1	8.2	
Conductivité (P90, µS/cm)	505	510	520	498	508	491	483	497	522	512	505	salinité
Chlorures P90 (mg Cl/l)	32	26	26	25	23.3		26	23.6	29.9	29	29	
Sulfates P90 (mg SO4/l)	13	13	14	16	13.7		13.1	15.6	13.8	13	13.8	
O_2 dissous (P10, mgO_2/l)	8	8.3	7.6	7.1	8.6	8.6	8.6	8	7.7	6.9	7.6	Bilan de l'oxygène
Tx Sat, O2 (P10, %)	81	78	83	80	88	89	91	84	84	75	83	
DBO5 (P90, mg O_2/l)	3	3	3	3	2.9	4	2.9	4	2.5	3.8	3.8	
Carb, Org, (P90, mg C/l)	5.2	4.4	4.5	5.6	5.6	7.8	4.9	5.7	3.7	6.3	4.3	
Phosphates (P90, mg PO_4^{3-}/l)	0.72	0.56	0.84	0.49	0.61	0.85	0.64	0.57	0.8	0.865	0.8	Nutriments
Phosphore total (P90, mg P/l)	0.31	0.32	0.3	0.22	0.24	0.39	0.4	0.36	0.3	0.38	0.33	
Ammonium (P90, mg NH4+/l)	0.19	0.32	0.17	0.18	0.26	0.22	0.29	0.21	0.21	0.39	0.34	
Nitrites (P90, mg NO2-/l)	0.28	0.34	0.26	0.22	0.17	0.29	0.17	0.19	0.18	0.28	0.25	
Nitrates (P90, mg NO3-/l)	16	16	14	17	14.1	19.8	14.6	17.2	17.4	18	17.4	
Chlortoluron (moy, µg/L)	<0.02	<0.02	<0.02	<0.02	<0.02	<0.02	<0.02	<0.02	<0.02	0.0303	<0.02	Polluants spécifiques
Oxadiazon (moy, µg/L)	<0.05	<0.05	<0.02	<0.02	<0.02	0.0061	<0.005	<0.005	<0.005	<0.005	<0.005	
Thiabendazole (moy, µg/L)	<0.02	<0.02	<0.02	<0.02	<0.005	<0.02	<0.02	<0.02	<0.02	<0.002	<0.02	
2,4 D (moy, µg/L)	0.0082	0.0237	<0.02	<0.02	<0.02	<0.02	<0.02	<0.02	<0.02	0.0097	<0.02	
2,4 MCPA (moy, µg/L)	0.068	0.051	<0.02	0.124	<0.02	<0.02	<0.02	0.0245	0.055	0.0107	0.0299	
Arsenic dissous (moy, µg/L)						2.08	1.83					
Chrome dissous (moy, µg/L)						<0.5	<0.5					
Cuivre dissous (moy, µg/L)						1.27	1.13					
Zinc dissous (moy, µg/L)						1.58	1.2					
Métazachlore (moy, µg/L)	<0.02	<0.02	<0.02	<0.02	<0.02	<0.005	<0.005	<0.005	<0.005	<0.002	<0.005	
Aminotriazole (moy, µg/L)	<0.1	<0.1	<0.1	<0.1	<0.1	<0.02	<0.02	<0.02	<0.02	0.02	<0.02	
Nicosulfuron (moy, µg/L)	<0.02	<0.02	<0.02	<0.02	<0.02	0.0253	<0.02	0.033	<0.02	0.0204	0.0233	
AMPA (moy, µg/L)	0.48	<0.1	0.4	0.169	0.145	0.36	0.249	0.296	0.46	0.45	0.4	
Glyphosate (moy, µg/L)	<0.1	<0.1	<0.1	<0.1	0.037	0.083	0.06	0.13	0.066	0.125	0.107	
Diflufénicanil (moy, µg/L)	<0.05	<0.05	<0.02	<0.02	<0.02	0.009	0.0071	0.0056	0.0052	0.00283	<0.005	
Tébuconazole (moy, µg/L)	<0.05	<0.05	<0.02	<0.02	<0.02	<0.02	<0.02	0.0237	<0.02	0.007	<0.02	
Bentazone (moy, µg/L)	<0.05	<0.05	<0.02	<0.02	<0.02	0.023	<0.02	0.0242	<0.02	0.0085	<0.02	Polluants spécifiques non pertinents pour le bassin Rhin-Meuse
Cyprodinil (moy, µg/L)	<0.05	<0.05	<0.02	<0.02	<0.005	<0.005	<0.005	<0.005	<0.005	<0.002	<0.005	
Imidaclopride (moy, µg/L)	<0.05	<0.05	<0.02	<0.02	<0.005	<0.02	<0.02	<0.02	<0.005	<0.005	<0.02	
Iprodione (moy, µg/L)	<0.05	<0.05	<0.02	<0.02	<0.005	<0.005	<0.005	<0.005	<0.005	<0.005	<0.005	
Azoxystrobine (moy, µg/L)	<0.02	<0.02	<0.02	<0.02	<0.02	<0.02	<0.02	<0.02	<0.02	<0.002	<0.02	
Toluene (moy, µg/L)										<0.1	<0.1	
Phosphate de tributyle (moy, µg/L)	<0.5	<0.5	<0.1	<0.1	<0.1	<0.005	<0.005	<0.005	<0.005	<0.03	<0.03	
Biphényle (moy, µg/L)	<0.05	<0.05	<0.05	<0.05	0.0125	<0.005	<0.005	<0.005	<0.005	<0.01	<0.01	
Boscalid (moy, µg/L)							<0.02	<0.02	<0.02	0.0082	<0.02	
Métaldéhyde (moy, µg/L)	<0.05	<0.05	<0.02	<0.02	<0.02			0.0247	<0.02	<0.02	<0.02	
Chlorprophame (moy, µg/L)	<0.1	<0.1	<0.02	<0.02	<0.02	<0.005	<0.005	<0.005	<0.005	<0.01	<0.01	
Xylène (moy, µg/L)												
Linuron (moy, µg/L)	<0.02	<0.02	<0.02	<0.02	<0.02	<0.02	<0.02	<0.02	<0.02	<0.005	<0.02	
Chlordécone (moy, µg/L)												
Pendiméthaline (moy, µg/L)	<0.05	<0.05	<0.02	<0.02	<0.02	<0.005	<0.005	<0.005	<0.005	0.0053	<0.005	

Parametres généraux

Etat écologique

L'état écologique est calculé selon les critères de l'arrêté du 27 juillet 2015 modifiant l'arrêté du 25 janvier 2010 relatif aux méthodes et critères d'évaluation de l'état écologique. Pour les métaux, la moyenne a été calculée sans retrancher le fond géochimique et la fraction biodisponible du cuivre et du zinc n'a pas pu être évaluée. La totalité de la fraction dissoute a été prise en compte pour le calcul de la moyenne.du cuivre,du zinc, de l'arsenic et du chrome. Le diagnostic d'état pour ces quatre paramètres est probablement plus pénalisant qu'il ne l'est en réalité.

Légende :
Etat/Potentiel écologique

	Très bon
	Bon
	Moyen

Supplementary datas 2: Compounds used to determine the LOD and LOQ in the different matrices from Villette et al., 2019a.

Matrix	Quantity (µg)	Standard	Area 1	Area 2	Area 3	Average area	S/N 1	S /N2	S/N 3	Average S/N	standard deviation	error %
Methanol	10	Acetominophen-d4	2.86E+07	2.69E+07	1.66E+07	2.40E+07	8.00	5.00	3.00	5.33	6.50E+06	27%
	1	Acetominophen-d4	2.21E+06	2.28E+06	1.35E+06	1.94E+06	6.00	5.00	2.00	4.33	5.18E+05	27%
	0,1	Acetominophen-d4	2.68E+05	1.92E+05	1.64E+05	2.08E+05	3.00	2.00	1.00	2.00	5.41E+04	26%
	0,01	Acetominophen-d4	1.34E+04	7.71E+03	4.26E+03	8.47E+03	3.00	3.00	2.00	2.67	4.64E+03	55%
	0,001	Acetominophen-d4	0.00	0.00	0.00	0.00	0.00	0.00	0.00	0.00	0.00	-
	0,0001	Acetominophen-d4	0.00	0.00	0.00	0.00	0.00	0.00	0.00	0.00	0.00	-
Water	10	Acetominophen-d4	9.51E+06	1.14E+07	1.07E+07	1.05E+07	6.00	4.00	1.00	3.67	9.52E+05	9%
	1	Acetominophen-d4	1.48E+06	1.93E+06	1.60E+06	1.67E+06	4.00	1.00	3.00	2.67	2.34E+05	14%
	0,1	Acetominophen-d4	2.04E+05	1.83E+05	1.85E+05	1.90E+05	1.00	1.00	1.00	1.00	1.15E+04	6%
	0,01	Acetominophen-d4	1.03E+04	1.01E+04	1.04E+04	1.03E+04	1.00	1.00	3.00	1.67	1.26E+02	1%
	0,001	Acetominophen-d4	0.00	0.00	0.00	0.00	1.00	1.00	2.00	1.33	0.00	-
Sludge	10	Acetominophen-d4	5.25E+06	5.07E+06	5.65E+06	5.32E+06	9.00	5.00	3.00	5.67	2.95E+05	6%
	1	Acetominophen-d4	4.85E+05	5.72E+05	7.51E+05	6.03E+05	5.00	5.00	1.00	3.67	1.36E+05	23%
	0,1	Acetominophen-d4	4.65E+04	3.63E+04	5.79E+04	4.69E+04	5.00	2.00	1.00	2.67	1.08E+04	23%
	0,01	Acetominophen-d4	1.88E+03	1.11E+03	1.15E+03	1.38E+03	1.00	2.00	1.00	1.33	4.34E+02	32%
	0,001	Acetominophen-d4	0.00	0.00	0.00	0.00	0.00	0.00	0.00	0.00	0.00	-
Methanol	10	Gemfibrozil-d6	9.27E+08	6.70E+08	5.69E+08	7.22E+08	1.01E+02	7.90E+01	1.05E+02	9.50E+01	1.85E+08	26%
	1	Gemfibrozil-d6	7.04E+07	5.74E+07	4.35E+07	5.71E+07	7.00	9.00	8.00	8.00	1.34E+07	24%
	0,1	Gemfibrozil-d6	4.86E+06	3.63E+06	3.04E+06	3.84E+06	1.00	1.00	1.00	1.00	9.29E+05	24%
	0,01	Gemfibrozil-d6	3.64E+05	3.11E+05	2.43E+05	3.06E+05	1.00	1.00	1.00	1.00	6.03E+04	20%
	0,001	Gemfibrozil-d6	2.22E+04	2.58E+04	1.62E+04	2.14E+04	1.00	1.00	1.00	1.00	4.85E+03	23%
	0,0001	Gemfibrozil-d6	7.99E+02	4.72E+03	2.35E+03	2.62E+03	1.00	1.00	1.00	1.00	1.97E+03	75%
Water	10	Gemfibrozil-d6	4.49E+08	4.15E+08	4.33E+08	4.32E+08	9.50E+01	8.10E+01	1.17E+02	9.77E+01	1.69E+07	4%
	1	Gemfibrozil-d6	4.65E+07	4.77E+07	4.80E+07	4.74E+07	9.00	1.40E+01	1.50E+01	1.27E+01	8.01E+05	2%
	0,1	Gemfibrozil-d6	4.04E+06	3.15E+06	2.88E+06	3.36E+06	1.00	1.00	2.00	1.33	6.11E+05	18%
	0,01	Gemfibrozil-d6	3.11E+05	2.35E+05	2.95E+05	2.81E+05	1.00	1.00	1.00	1.00	4.04E+04	14%
	0,001	Gemfibrozil-d6	2.57E+04	1.65E+04	2.55E+04	2.26E+04	1.00	1.00	3.00	1.67	5.29E+03	-
Sludge	10	Gemfibrozil-d6	2.00E+08	1.96E+08	2.23E+08	2.06E+08	3.70E+01	5.30E+01	3.60E+01	4.20E+01	1.45E+07	7%
	1	Gemfibrozil-d6	2.95E+07	3.08E+07	3.89E+07	3.31E+07	6.00	6.00	5.00	5.67	5.09E+06	15%
	0,1	Gemfibrozil-d6	2.58E+06	2.39E+06	2.92E+06	2.63E+06	2.00	1.00	1.00	1.33	2.68E+05	10%
	0,01	Gemfibrozil-d6	2.31E+05	2.27E+05	2.16E+05	2.25E+05	2.00	1.00	1.00	1.33	8.04E+03	4%
	0,001	Gemfibrozil-d6	1.67E+04	1.28E+04	1.52E+04	1.49E+04	1.00	1.00	1.00	1.00	1.95E+03	13%

Matrix	Quantity (µg)	Standard	Area 1	Area 2	Area 3	Average area	S/N 1	S /N2	S/N 3	Average S/N	standard deviation	error %
Methanol	10	N-Desmethyl sildenafil-d8	9.14E+07	5.40E+07	2.01E+07	5.52E+07	9.00	7.00	4.00	6.67	3.57E+07	65%
	1	N-Desmethyl sildenafil-d8	1.28E+07	7.95E+06	3.53E+06	8.09E+06	3.00	4.00	2.00	3.00	4.64E+06	57%
	0,1	N-Desmethyl sildenafil-d8	1.43E+06	7.26E+05	3.60E+05	8.37E+05	2.00	1.00	2.00	1.67	5.41E+05	65%
	0,01	N-Desmethyl sildenafil-d8	8.33E+04	5.79E+04	1.78E+04	5.30E+04	1.00	3.00	1.00	1.67	3.30E+04	62%
	0,001	N-Desmethyl sildenafil-d8	2.96E+03	8.12E+02	0.00	1.26E+03	1.00	1.00	1.00	1.00	1.53E+03	122%
	0,0001	N-Desmethyl sildenafil-d8	0.00	0.00	0.00	0.00	0.00	0.00	0.00	0.00	0.00	-
Water	10	N-Desmethyl sildenafil-d8	1.05E+07	4.20E+06	2.13E+06	5.60E+06	2.00	2.00	1.00	1.67	4.35E+06	78%
	1	N-Desmethyl sildenafil-d8	2.33E+06	9.74E+05	4.54E+05	1.25E+06	3.00	2.00	1.00	2.00	9.69E+05	77%
	0,1	N-Desmethyl sildenafil-d8	2.91E+05	7.77E+04	2.96E+04	1.33E+05	2.00	2.00	2.00	2.00	1.39E+05	105%
	0,01	N-Desmethyl sildenafil-d8	1.36E+04	3.92E+03	0.00	5.85E+03	1.00	1.00	1.00	1.00	7.02E+03	120%
	0,001	N-Desmethyl sildenafil-d8	0.00	0.00	0.00	0.00	0.00	0.00	0.00	0.00	0.00	-
Sludge	10	N-Desmethyl sildenafil-d8	7.31E+05	3.66E+05	4.24E+05	5.07E+05	3.00	1.00	3.00	2.33	1.96E+05	39%
	1	N-Desmethyl sildenafil-d8	9.14E+04	3.83E+04	5.19E+04	6.05E+04	1.00	1.00	1.00	1.00	2.76E+04	46%
	0,1	N-Desmethyl sildenafil-d8	4.12E+03	7.21E+02	1.27E+03	2.04E+03	1.00	1.00	1.00	1.00	1.83E+03	90%
	0,01	N-Desmethyl sildenafil-d8	0.00	0.00	0.00	0.00	0.00	0.00	0.00	0.00	0.00	-
	0,001	N-Desmethyl sildenafil-d8	0.00	0.00	0.00	0.00	0.00	0.00	0.00	0.00	0.00	-
Methanol	10	Sulfamethoxazole-d4	2.05E+08	1.69E+08	1.17E+08	1.63E+08	1.10E+01	1.40E+01	1.60E+01	1.37E+01	4.39E+07	27%
	1	Sulfamethoxazole-d4	2.42E+07	1.51E+07	1.25E+07	1.73E+07	2.00	2.00	2.00	2.00	6.14E+06	36%
	0,1	Sulfamethoxazole-d4	2.57E+06	1.74E+06	1.44E+06	1.92E+06	3.00	2.00	1.00	2.00	5.85E+05	31%
	0,01	Sulfamethoxazole-d4	1.12E+05	1.45E+05	1.02E+05	1.20E+05	1.00	4.00	1.00	2.00	2.22E+04	19%
	0,001	Sulfamethoxazole-d4	3.55E+03	3.14E+03	2.30E+03	3.00E+03	1.00	1.00	1.00	1.00	6.35E+02	21%
	0,0001	Sulfamethoxazole-d4	0.00	0.00	0.00	0.00	0.00	0.00	0.00	0.00	0.00	-
Water	10	Sulfamethoxazole-d4	1.30E+08	1.30E+08	1.37E+08	1.32E+08	1.80E+01	1.80E+01	2.20E+01	1.93E+01	3.81E+06	3%
	1	Sulfamethoxazole-d4	1.67E+07	1.67E+07	1.68E+07	1.68E+07	6.00	6.00	3.00	5.00	5.65E+04	0%
	0,1	Sulfamethoxazole-d4	1.62E+06	1.62E+06	1.53E+06	1.59E+06	1.00	1.00	1.00	1.00	5.20E+04	3%
	0,01	Sulfamethoxazole-d4	1.29E+05	1.29E+05	1.07E+05	1.22E+05	1.00	1.00	1.00	1.00	1.25E+04	10%
	0,001	Sulfamethoxazole-d4	3.70E+03	3.70E+03	2.29E+03	3.23E+03	2.00	1.00	2.00	1.67	8.16E+02	25%

Matrix	Quantity (µg)	Standard	Area 1	Area 2	Area 3	Average area	S/N 1	S /N2	S/N 3	Average S/N	standard deviation	error %
Sludge	10	Sulfamethoxazole-d4	5.25E+07	1.50E+07	5.53E+07	4.09E+07	1.20E+01	9.00	2.00E+01	1.37E+01	2.25E+07	55%
	1	Sulfamethoxazole-d4	5.35E+06	6.74E+06	5.16E+06	5.75E+06	4.00	5.00	2.00	3.67	8.63E+05	15%
	0,1	Sulfamethoxazole-d4	5.29E+05	6.15E+05	5.75E+05	5.73E+05	1.00	2.00	2.00	1.67	4.34E+04	8%
	0,01	Sulfamethoxazole-d4	4.52E+04	5.16E+04	5.31E+04	4.99E+04	1.00	2.00	1.00	1.33	4.18E+03	8%
	0,001	Sulfamethoxazole-d4	9.99E+02	0.00	2.36E+03	1.12E+03	1.00	0.00	1.00	6.67E-01	1.18E+03	106%
Methanol	10	Diclofenac-d4	5.39E+08	3.80E+08	3.34E+08	4.18E+08	3.50E+01	4.40E+01	4.10E+01	4.00E+01	1.08E+08	26%
	1	Diclofenac-d4	5.09E+07	4.07E+07	3.52E+07	4.23E+07	5.00	4.00	7.00	5.33	7.98E+06	19%
	0.1	Diclofenac-d4	4.42E+06	3.28E+06	2.79E+06	3.50E+06	1.00	3.00	1.00	1.67	8.37E+05	24%
	0.01	Diclofenac-d4	3.77E+05	3.10E+05	2.52E+05	3.13E+05	1.00	1.00	1.00	1.00	6.22E+04	20%
	0.001	Diclofenac-d4	3.24E+04	3.37E+04	1.84E+04	2.82E+04	1.00	1.00	1.00	1.00	8.49E+03	30%
	0.0001	Diclofenac-d4	0.00	0.00	4.15E+03	1.38E+03	0.00	0.00	1.00	3.33E-01	2.40E+03	173%
Water	10	Diclofenac-d4	2.64E+08	2.63E+08	2.65E+08	2.64E+08	3.80E+01	4.00E+01	4.50E+01	4.10E+01	1.35E+06	1%
	1	Diclofenac-d4	3.74E+07	3.32E+07	3.49E+07	3.52E+07	8.00	8.00	7.00	7.67	2.13E+06	6%
	0.1	Diclofenac-d4	3.79E+06	2.76E+06	2.91E+06	3.15E+06	1.00	1.00	1.00	1.00	5.59E+05	18%
	0.01	Diclofenac-d4	3.17E+05	3.13E+05	2.31E+05	2.87E+05	1.00	2.00	1.00	1.33	4.84E+04	17%
	0.001	Diclofenac-d4	2.88E+04	2.82E+04	2.27E+04	2.66E+04	1.00	1.00	1.00	1.00	3.36E+03	13%
Sludge	10	Diclofenac-d4	2.07E+08	2.41E+08	2.34E+08	2.28E+08	4.80E+01	6.40E+01	3.70E+01	4.97E+01	1.79E+07	8%
	1	Diclofenac-d4	2.82E+07	3.44E+07	2.81E+07	3.02E+07	9.00	9.00	6.00	8.00	3.59E+06	12%
	0.1	Diclofenac-d4	2.55E+06	2.76E+06	2.36E+06	2.56E+06	2.00	2.00	1.00	1.67	2.00E+05	8%
	0.01	Diclofenac-d4	2.55E+05	2.21E+05	2.42E+05	2.39E+05	1.00	1.00	1.00	1.00	1.70E+04	7%
	0.001	Diclofenac-d4	1.98E+04	1.70E+04	1.50E+04	1.73E+04	1.00	1.00	1.00	1.00	2.38E+03	14%
Methanol	10	Bezafibrate-d4	5.24E+08	3.82E+08	3.25E+08	4.10E+08	4.20E+01	4.00E+01	3.70E+01	3.97E+01	1.02E+08	25%
	1	Bezafibrate-d4	4.20E+07	3.54E+07	3.01E+07	3.58E+07	6.00	5.00	4.00	5.00	5.97E+06	17%
	0.1	Bezafibrate-d4	4.02E+06	2.96E+06	2.63E+06	3.21E+06	1.00	2.00	1.00	1.33	7.25E+05	23%
	0.01	Bezafibrate-d4	3.21E+05	2.70E+05	2.19E+05	2.70E+05	2.00	1.00	1.00	1.33	5.08E+04	19%
	0.001	Bezafibrate-d4	1.28E+04	1.54E+04	4.40E+03	1.09E+04	1.00	1.00	1.00	1.00	5.76E+03	53%
	0.0001	Bezafibrate-d4	0.00	6.28E+02	6.14E+02	4.14E+02	0.00	1.00	1.00	6.67E-01	3.59E+02	87%
Water	10	Bezafibrate-d4	2.48E+08	2.39E+08	2.52E+08	2.46E+08	4.30E+01	4.80E+01	5.60E+01	4.90E+01	6.38E+06	3%
	1	Bezafibrate-d4	3.50E+07	3.22E+07	3.52E+07	3.41E+07	9.00	9.00	7.00	8.33	1.64E+06	5%
	0.1	Bezafibrate-d4	3.62E+06	2.51E+06	2.92E+06	3.02E+06	1.00	2.00	1.00	1.33	5.59E+05	19%
	0.01	Bezafibrate-d4	2.75E+05	2.93E+05	2.15E+05	2.61E+05	1.00	1.00	2.00	1.33	4.09E+04	16%
	0.001	Bezafibrate-d4	1.68E+04	1.91E+04	1.30E+04	1.63E+04	1.00	1.00	1.00	1.00	3.08E+03	19%

Matrix	Quantity (µg)	Standard	Area 1	Area 2	Area 3	Average area	S/N 1	S /N2	S/N 3	Average S/N	standard deviation	error %
Sludge	10	Bezafibrate-d4	2.27E+08	2.07E+08	2.35E+08	2.23E+08	4.00E+01	5.50E+01	3.30E+01	4.27E+01	1.47E+07	7%
	1	Bezafibrate-d4	2.66E+07	2.20E+07	3.00E+07	2.62E+07	6.00	5.00	6.00	5.67	4.03E+06	15%
	0.1	Bezafibrate-d4	2.55E+06	1.81E+06	2.50E+06	2.28E+06	1.00	1.00	1.00	1.00	4.15E+05	18%
	0.01	Bezafibrate-d4	2.27E+05	1.69E+05	1.93E+05	1.96E+05	1.00	1.00	2.00	1.33	2.94E+04	15%
	0.001	Bezafibrate-d4	7.22E+03	6.37E+03	5.14E+03	6.24E+03	1.00	1.00	1.00	1.00	1.04E+03	17%

Methanol	10	Sildenafil-d3	no data	no data	no data	no data	no data	no data	no data	no data	no data	no data
	1	Sildenafil-d3	no data	no data	no data	no data	no data	no data	no data	no data	no data	no data
	0.1	Sildenafil-d3	no data	no data	no data	no data	no data	no data	no data	no data	no data	no data
	0.01	Sildenafil-d3	no data	no data	no data	no data	no data	no data	no data	no data	no data	no data
	0.001	Sildenafil-d3	no data	no data	no data	no data	no data	no data	no data	no data	no data	no data
	0.0001	Sildenafil-d3	no data	no data	no data	no data	no data	no data	no data	no data	no data	no data
Water	10	Sildenafil-d3	no data	no data	no data	no data	no data	no data	no data	no data	no data	no data
	1	Sildenafil-d3	no data	no data	no data	no data	no data	no data	no data	no data	no data	no data
	0.1	Sildenafil-d3	no data	no data	no data	no data	no data	no data	no data	no data	no data	no data
	0.01	Sildenafil-d3	no data	no data	no data	no data	no data	no data	no data	no data	no data	no data
	0.001	Sildenafil-d3	no data	no data	no data	no data	no data	no data	no data	no data	no data	no data
Sludge	10	Sildenafil-d3	no data	no data	no data	no data	no data	no data	no data	no data	no data	no data
	1	Sildenafil-d3	no data	no data	no data	no data	no data	no data	no data	no data	no data	no data
	0.1	Sildenafil-d3	no data	no data	no data	no data	no data	no data	no data	no data	no data	no data
	0.01	Sildenafil-d3	no data	no data	no data	no data	no data	no data	no data	no data	no data	no data
	0.001	Sildenafil-d3	no data	no data	no data	no data	no data	no data	no data	no data	no data	no data

Supplementary datas 3: Repeatability found in the micropollutants extraction from Villette et al., 2019a.

	Area1	Area2	Area3	Average area	Standard deviation	**CV**	Area1	Area2	Area3	Average area	Standard deviation	**CV**
Acetaminophen-d4	1.30E+07	1.49E+07	1.56E+07	1.45E+07	1.32E+06	**9%**	6.33E+06	1.03E+07	6.46E+06	7.70E+06	2.27E+06	**29%**
Sildenafil-d3	no data	no data	no data	no data	no data	**no data**	no data	no data	no data	no data	no data	**no data**
Sulfamethoxazole-d4	1.66E+08	1.74E+08	1.69E+08	1.69E+08	4.37E+06	**3%**	9.51E+07	9.76E+07	8.52E+07	9.26E+07	6.57E+06	**7%**
N-desmethyl sildenafil-d8	2.06E+05	3.04E+05	3.93E+05	3.01E+05	9.37E+04	**31%**	1.47E+04	1.67E+04	1.64E+04	1.59E+04	1.07E+03	**7%**
Gemfibrozil-d6	5.67E+08	5.75E+08	7.15E+08	6.19E+08	8.34E+07	**13%**	4.25E+08	4.21E+08	4.16E+08	4.20E+08	4.40E+06	**1%**
Diclofenac-d4	4.31E+08	4.44E+08	4.40E+08	4.39E+08	6.79E+06	**2%**	6.62E+08	6.16E+08	6.74E+08	6.51E+08	3.03E+07	**5%**
Bezafibrate-d4	3.76E+08	4.34E+08	3.80E+08	3.97E+08	3.25E+07	**8%**	5.85E+08	5.28E+08	6.47E+08	5.87E+08	5.96E+07	**10%**

Supplementary datas 4: TargetScreener Method.

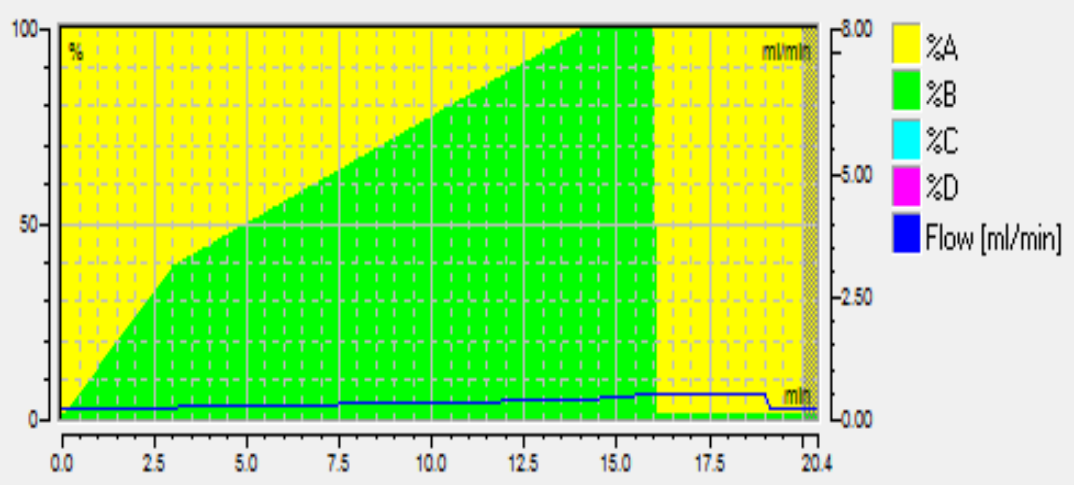

Supplementary datas 5: Example of analyte list used in the Metaboscape software.

Mass	RT	Formula	Name	MainPositiveAdduct	MainNegativeAdduct	KEGG	CAS	PubChem	ChemSpider	HMDB	BioCyc	Metlin	UserID
138.0549549	0.35	C7H7NO2	N-Methylnicotinate	[M+H]+	[M-H]-	C01004	535-83-1	5570	5369	HMDB00875	methylnicotinate	273	MTBLC18123
99.04405588	0.4	C5H6O2	Furfuryl alcohol	[M+H]+	[M-H]-	C20441							
103.0389705	0.48	C4H6O3	Succinate semialdehyde	[M+H]+	[M-H]-	C00232							
112.0393049	0.53	C5H5NO2	Dihydroxypyridine	[M+H]+	[M-H]-	C01059							
117.0182351	0.55	C4H4O4	Fumarate	[M+H]+	[M-H]-	C00122							
117.0182351	0.55	C4H4O4	Maleic acid	[M+H]+	[M-H]-	C01384							
123.0552893	1.36	C6H6N2O	Nicotinamide	[M+H]+	[M-H]-	C00153							
124.0393049	0.57	C6H5NO2	Nicotinate	[M+H]+	[M-H]-	C00253							
127.0389705	1.43	C6H6O3	Pyrogallol	[M+H]+	[M-H]-	C01108							
129.0546206	1.54	C6H8O3	Dihydrophloroglucinol	[M+H]+	[M-H]-	C06719							
140.0342195	0.58	C6H5NO3	6-Hydroxynicotinate	[M+H]+	[M-H]-	C01020							
142.0498695	0.633	C6H7NO3	6-Oxo-1_4_5_6-tetrahydronicotinate	[M+H]+	[M-H]-	C04226							
143.0702706	2.14	C7H10O3	4-Oxocyclohexanecarboxylate	[M+H]+	[M-H]-	C03767							
145.0495352	1	C6H8O4	2_3-Dimethylmaleate (?)	[M+H]+	[M-H]-	C00922							
145.0495352	0.4	C6H8O4	2-Methyleneglutarate (?)	[M+H]+	[M-H]-	C02930							
147.0440559	2.12	C9H6O2	Coumarin	[M+H]+	[M-H]-	C05851							
153.0546206	1.87	C8H8O3	Vanillin	[M+H]+	[M-H]-	C00755							
163.039	1.82	C9H6O3	Hydroxycoumarin	[M+H]+	[M-H]-	C20414							
163.0600999	0.4	C6H10O5	2-(Hydroxymethyl)glutarate	[M+H]+	[M-H]-	C16390							
165.0546206	1.77	C9H8O3	4-Coumarate	[M+H]+	[M-H]-	C00811							
177.055	2.22	C10H8O3	4-Methylumbelliferone	[M+H]+	[M-H]-	C03081							
181.0859207	2.67	C10H12O3	Coniferyl alcohol	[M+H]+	[M-H]-	C00590							
182.0811697	0.63	C9H11NO3	Tyrosine	[M+H]+	[M-H]-	C00082							
193.0495352	2.31	C10H8O4	Scopoletin	[M+H]+	[M-H]-	C01752							
193.0706646	0.361	C7H12O6	Quinic acid	[M+H]+	[M-H]-	C00296							
209.0808353	2.95	C11H12O4	Sinapoyl aldehyde	[M+H]+	[M-H]-	C05610							
321.0968793	2.47	C16H16O7	4-Coumaroylshikimate	[M+H]+	[M-H]-	C02947							
337.0917939	2.15	C16H16O8	5-O-Caffeoylshikimic acid	[M+H]+	[M-H]-	C10434							
339.107444	2.13	C16H18O8	p-Coumaroyl quinic acid	[M+H]+	[M-H]-	C12208							

Supplementary datas 6: Biotransformation rules used for the metabolites *in silico* predictions.

001_Alcohol Dehydrogenase_A
002_Aldehyde Dehydrogenase_A
003_beta-Oxidation Hydrogenation 1_A
004_beta-Oxidation Hydration_A
005_beta-Oxidation Hydrogenation 2_A
006_beta-Oxidation Cleavage_A
007a_CYP450 Hydroxylation_A
007b_CYP450 Hydroxylation_A
008_CYP450 N-Demethylation_A
009_CYP450 O-Demethylation_A
010_CYP450 S-Demethylation_A
011_CYP450 Epoxidation 1_A
012_CYP450 Epoxidation 2_A

013_CYP450 Acetylene Oxidation_A
014_CYP450 N-Oxidation_A
015_CYP450 S-Oxidation_A
016_CYP450 Sulfoxide Oxidation_A
017_CYP450 Phosphine Sulfide_A
018_Xanthine Oxidase_A
019_Carboxylesterase_A
020_Sulfatase Monoester_A
021_Sulfatase Diester_A
022_Phosphatase Monoester_A
023_Phosphatase Diester_A
024_Amidase_A
025_Peptidase_A

026_Peptidase N-Terminus_A
027_Peptidase C-Terminus_A
028_Glycosidase_A
029_S-Glycosidase_A
030_Epoxide Hydrolase_A
031_GSH Thiol_M
032a_GSH Epoxide_M
032b_GSH Epoxide_M
033a_GSH Addition_M
033b_GSH Addition_M
034_GSH Substitution_M
035_GSH Substitution aromatic_M
036_Glutathione-gamma-glutamylpeptidase_M

037_Cysteinylglycinase_M
038_N-Acetyltransferase Cystein_M
039_S-Methyltransferase_B_M
040_O-Methyltransferase_P
041_O-Methyltransferase_M
042_Cysteinyl-beta-lyase._M
043_Hydrolysis 1 Anhydride_H
044_Hydrolysis Acylhalogenide_H
045_Hydrolysis oxidative Dehalogenation_H
046_Hydrolysis oxidative Deamination_H
047_Hydrolysis Diol_H
048_oxidative HCN cleavage_H
049_Hydrolysis Ketenehydration_H
050_Hydrolysis Phenolisomerisation_H

051_Hydrolysis Imine_H
052_Tautomer Iminoalcohol_H
053_Tautomer Enol_H
054_Tautomer Oxime_H
055_Decarboxylation Carbamate_A
056_Decarboxylase_A
057_Nitrilreductase_B
058_Nitroreductase NO2_B
059_Nitroreductase NO_B
060_Nitroreductase NHOH_B
061_Azoreductase_B
062_N-Acetyltransferase_M
063_Glycine Transferase_M
064_Glutamate Transferase_M

065_Glycosyl Transferase_P
066_Glycosyl Transferase Aromatic Alcohol_P
067_Glucuronyl Transferase Alcohol_M_P
068_Glucuronyl Transferase Aromatic Alcohol_M_P
069_Glucuronyl Transferase Aromatic Amine_M_P
070_Glucuronyl Transferase Aromatic Thiol_M_P
071_Glucuronyl Transferase Carboxylic Acid_M_P
072_Glucuronyl Transferase Thiocarboxylic Acid_M_P
073_Glucuronyl Transferase Aromatic Hydroxylamine_M_P
074_Glucuronyl Transferase Tert Amine_M_P
075_Glucuronyl Transferase Sulfonic Acid Aminoester._M_P
076_Glucuronyl Transferase 1-3-Diketone_M_P
077_Sulfotransferase_Alcohol_M_P
078_Sulfotransferase Aromatic Hydroxylamine_M_P

079_Sulfotransferase Aromatic Amine_M_P

Supplementary datas 7: Physico-chemical properties of the most intense compounds found in the wetland ecosystems. From Maurer et al., 2020.

compounds found in higher proportion	top layer	bottom layer	water	Reed
1	1- (9Z,12 Z-hexadecadienoyl)-sn-glycerol	2-octadecanoyl-sn-glycerol	2- (9Z-hexadecenoyl)-sn-glycerol	3-ethoxypropylamine
2	Norverapamil	Ceramide (d28:0)	Metoprolol	Methyl L-threoninate
3	Bis [4-(diethylamino) phenyl] methanone	4 alpha-hydroxymethyl-4beta-methyl-5alpha-cholesta-8,24-dien-3beta-ol	N-eicosanoylethanolamine	2- ((3-(Dodecyloxy) propyl) (2-(2-hydroxyethoxy) ethyl) amino) ethanol
4	O-tetradecanoyl-(R)-carnitine	Ceramide (d29:0)		(1S,3'R,4'S,5'S,6'R)-6-[(4-ethylphenyl) methyl]-3',4',5',6'-tetrahydro-6'-(hydroxymethyl)-Spiro[isobenzofuran-1 (3H), 2'-[2H] pyran]-3',4',5'-triol
5	Methyl1,2,2,6,6 pentamethyl-2,4piperidyl sebacate	2-octadecanoyl-sn-glycerol	Glycerol 2-hexadecanoate	4alpha-hydroxymethyl-5alpha-cholest-8-en-3beta-ol
6	O-(9Z-tetradecenoyl)-(R)-carnitine	4 alpha-hydRoxymethyl-4beta-methyl-5alpha-cholesta-8,24-dien-3beta-ol	Di-n-butyl phthalate	SPIROXAMINE
7	Metformin	1- O-hexadecyl-sn-glycerol	N-Isobutyl-2,4,8-decatrienamide	(10E)-9-Hydroxy-13-oxo-10-octadecenoic acid
8	orphenadrine	ergosta-5,7,22,24(28)-tetraen-3beta-ol	Tetrahydro-harmine	Episterol
9	Dinonyl phthalate	Ceramide (t20:0)	Di-n-butyl phthalate	Cyclopropanecarboxylic acid, 2-[1-(3,3-dimethylcyclohexyl)ethoxy]-2-methylpropyl ester
10	Verapamil	Ceramide (t25:0)	Tramadol	2,2'-((3-(Dodecyloxy) propyl) imino)bisethanol

log P	top layer	bottom layer	water	Reed
1	8,1	15,1	11,1	-0,1
2	4,11		1,78	-1,33
3	4,84	7,7	8,3	3,97
4	6,6			
5	4,46	17,3	6,1	7,8
6	5,7	7,7	4,6	4,98
7	-1,37	6,5	3,6	
8	3,67	7,7	1,9	8,4
9	9,29		4,6	4,5
10	3,8		2,44	4,7

water solubility	top layer	bottom layer	water	reed
1				
2	0,000000278		0,147	4,88
3	0,0000231	0,00214		0,000664
4				
5				
6		0,00214	0,0000323	0,000783
7	0,276			
8	0,00828			
9	0,000000246		0,0000323	
10	0,0000399		0,0303	

henry constant	top layer	bottom layer	water	reed
1				
2	3,08 E-09		0,000000126	1,06 E-08
3	5,24 E-08			1,21 E-10
4				
5				
6			0,0000012	0,00000077
7	3,46 E-09			
8	0,00000156			
9	0,000000129		0,0000012	
10	0,000000428		0,00000117	

Pharmaceutical	compartment	MW (g/mol) pubmed	molecular volume comptox (cm3)	water solubility comptox (mol/L)	log Kow	log Dow	pKa	Neutral fraction	(%) i Ionic fraction (%)
Ethotoin	Reed	204.089878	171	1.23e-2	1.05		11.29	100%	
kebuzone	Reed	322.131742	260	3.15e-3			4,17	0%	100%
Bisoprolol	Sludge	325.225308	315	7.97e-2	2.15		9,5	100%	
fenethylline	Sludge	341.185175	271	4.43e-3	2.04		10.03	100%	
irbesartan	Sludge	428.23246	328	4.06e-6	5.31		4,12	0%	100%
Telmisartan	Sludge	514.236876	415	3.00e-6	8.42		3,65		50%
Tramadol	Sludge	263.188529		3.03e-2	3.01		9,23	99%	1%
CARBETAMIDE	sludge reed	236.116092	201	9.81e-3	1.75		11,3	100%	
Galaxolidone	sludge reed	272.17763		1.70e-6	5.9				
dodemorph	sludge reed water	281.271865	315	3.02e-4	2.52		8,08	89%	
Doxapram	sludge reed water	378.230728	343	1.42e-4			7,23	53%	
THIOCYCLAM-HYDROGENOXALATE	sludge reed water	271.000671	142	5.80e-2			7	40%	60%
Acebutolol	sludge/water	336.204907	301	6.12 10-3	1.71	1.71	9,6	100%	
Venlafaxine	sludge/water	277.204179	262	2.14e-3	3.2		8,91	98%	2%
Diethofencarb	Water	267.147058	243	2.55e-4	3.02		12,8	100%	
metaldehyde	Water	176.104859			0.85		-3,9	0%	
metoprolol	Water	267.183444	259	0.147	1.88		9,7	100%	
methomyl	water reed	162.046299	138	0.209	1.24		3,48	0%	
N, N-dibutylformamide	water reed	157.146664	182	6.61e-2	A- 1.01		-0,065	0%	
alprenolol	water sludge	249.172879	247	2.79.10-2	3.1	3.1	9,6	100%	
O-desmethylvenlafaxine	water sludge	263.188529	236	7.08e-2	3.2		2,96	0%	100%
TRIPHENYL-PHOSPHATE	water sludge	326.070796	258	2.06e-5	4.59				

Supplementary datas 8: Imageprep (Bruker).

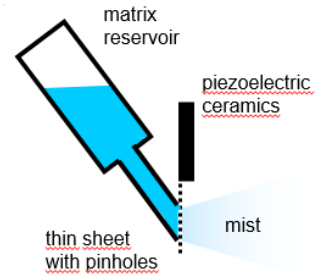

Supplementary datas 9: Detail scheme of the SolarIX (FT-ICR) (user manual SolariX, Bruker Daltonics).

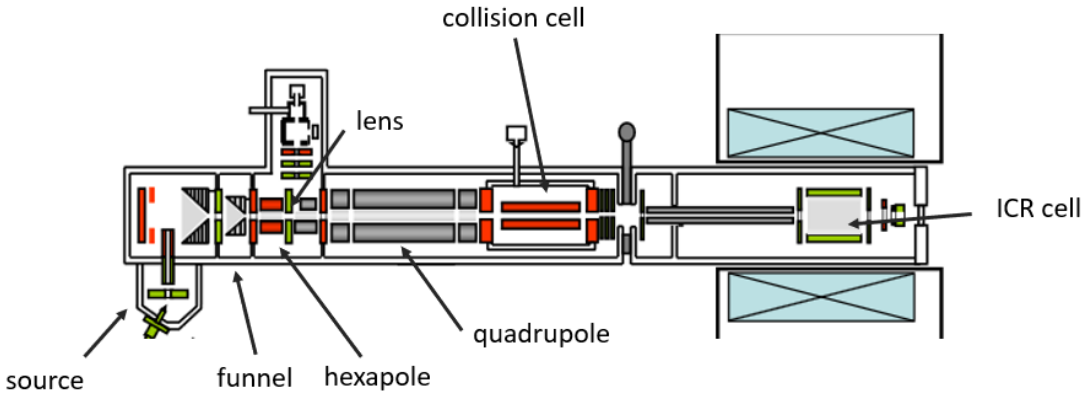

Supplementary datas 10: LOQ, LOD and matrix effect of sildenafil-d3 found for the MSI experiment.

Concentration (µg/mL)	Intensity in ITO slides	Intensity in reed samples	Plant Matrix effect	Intensity in sludge samples	Sludge Matrix effect
1000	$1.09\ 10^{8}$	462739	99.5%	$1.7.10^{6}$	98.5%
100	$1.19.10^{7}$	46740			
10	$5.3.10^{6}$	16647			
1	5.10^{6}				
0.1	$3.7.\ 10^{6}$				

Supplementary data 11: Chemical properties of the compounds mostly found in polluted poplar leaves. Yellow, molecules mostly located in outer tissues; green, generally distributed; blue, mostly located in inner tissues, from Vilette et al.,2019a.

PROPERTY	UNIT	3-ethoxy propylamine	Salicin	Ethylene thiourea	Neurine	Ziprasidone	Piperidine	Adenine	LysoPC 16:0	Pheopho
N°CAS	-	6291-85-6	138-52-3	96-45-7	463-88-7	146939-27-7	110-89-4	73-24-5	9008-30-4	15664-
Molecular formula	-	$C_5H_{13}NO$	$C_{13}H_{18}O_7$	$C_3H_6N_2S$	$C_5H_{13}NO$	$C_{21}H_{21}ClN_4OS$	$C_5H_{11}N$	$C_5H_5N_5$	$C_{24}H_{50}NO_7P$	$C_{35}H_{36}$
Molecular weight	g/mol	103.099165	286.104704	102.024621	103.099165	412.111912	85.088601	135.053947	495.331941	592.26
LogP: Octanol-Water	-	0.13	-0.95	-0.597	3.49	-2.12	0.87	-0.32	1.83	4.9
Melting point	°C	-42.40	181	134	200	264	-17.40	223	-	16
Boiling point	°C	131	349	284	452	546	114	381	-	40
Water solubility	mol/L	4.05	0.03	0.719	1.20e-5	6.24e-3	4.38	0.03	0.00	0.0
Vapor pressure	mmHg	27.00	0.00	1.29	2.56e-9	2.29e-9	27.10	0.00	-	0.0
Flash point	°C	37.10	-	49.5	308	-	13.70	309	-	-
Surface tension	dyn/cm	26.60	-	61.1	61.5	-	26.90	123	-	-
Index of refraction	-	1.42	-	1.63	1.68	-	1.43	1.84	-	-
Molar refractivity	cm^3	30.50	-	28.3	114	-	26.40	37.00	-	-
Polarizability	$Å^3$	12.10	27.89	11.2	45.2	-	10.50	14.70	-	-
Density	g/cm^3	0.87	-	1.24	1.39	-	0.86	1.58	-	-
Molar volume	cm^3	121	-	80.0	301	-	102	83.80	-	-
Thermal conductivity	mW/(m*K)	177	-	-	-	-	153	-	-	-
Viscosity	cP	1.24	-	-	-	-	1.38	-	-	-
Henry's law	atm-m^3/mole	0.00	0.00	5.44e-9	6.31e-9	1.64e-11	0.00	0.00	-	0.0
LogKoa: Octanol-Air	-	4.70	9.47	7.19	10.2	9.51	4.32	8.08	-	9.5
LogS	-	-	-1.10	-	-	-	-	-	-6.20	-
pKa (Strongest Acidic)	-	-	12.20	-	-	-	-	-	1.86	-
pKa (Strongest Basic)	-	-	-2.90	-	-	-	-	-	-3.40	-

Supplementary data 12: Chemical properties of the pesticides mostly found in the reed.

		Dodemorph	Flamprop methyl	Fuberidazole	Mecarbam	Parathion ethyl	Propachlor
LogP: Octanol-Water	-	5.57	3.21	2.42	2.66	3.69	2.28
Melting Point	°C	58.9	109	161	35.2	35.4	67.8
Boiling Point	°C	337	396	359	367	358	296
Water Solubility	mol/L	3.02e-4	3.12e-4	3.67e-3	7.24e-4	1.49e-4	3.64e-3
Vapor Pressure	MmHg	1.28e-5	4.72e-6	1.96e-6	3.37e-6	1.17e-5	7.27e-4
Flash Point	°C	114	237	183	210	174	136
Surface Tension	dyn/cm	31.4	47.9	56.3	49.2	52.8	40.8
Index of Refraction	-	1.46	1.59	1.67	1.52	1.56	1.55
Molar Refractivity	cm^3	86.4	86.1	53.5	79.5	71.0	59.3
Polarizability	$Å^3$	34.3	34.1	21.2	31.5	28.1	23.5
Density	g/cm^3	0.891	1.34	1.28	1.27	1.33	1.10
Molar Volume	cm^3	315	256	143	260	220	186
Henry's Law	$atm\text{-}m^3/mole$	5.03e-6	3.63e-9	6.94e-8	9.59e-10	3.18e-7	1.24e-7
LogKoa: Octanol-Air	-	8.99	10.8	9.38	10.9	9.33	7.38
Viscosity	Cp	10.0					8.85
Thermal Conductivity	mW/(m*K)	145					145
Bioaccumulation Factor	-					134	10.7
Bioconcentration Factor	-	239	240	271	16.7	121	16.1
Soil Adsorp. Coeff. (Koc)	L/kg	1.62e+3	1.68e+3	4.99e+3	255	1.43e+3	187
Atmos. Hydroxylation Rate	$cm^3/molecule*sec$	1.65e-11	1.82e-11	4.31e-11	1.83e-11	1.59e-11	1.45e-11
Biodeg. Half-Life	Days	18.4	3.35	3.36	25.0	4.30	3.36
Fish Biotrans. Half-Life (Km)	Days	43.2	0.747	0.128	0.443	0.500	0.491

Supplementary data 13: Micropollutants detected each season in the different artificial pond areas.

area 1 inlet			
summer	**spring**	**autumn**	**winter**
Acebutolol	Acebutolol	Benzethonium	4-Methyl-5-thiazoleethanol
Aliskiren	Alimemazine	Celiprolol	Acebutolol
Almitrine	Amiodarone	Flecainide	Alimemazine
Amiodarone	Azithromycin	Gemfibrozil	Almitrine
Benomyl (decomposed to Carbendazim) Fragm 192	Benzethonium	Irbesartan	Amiodarone
Benproperine	Benzoxonium	Isoconazole	Benzethonium
Benzoxonium	Celiprolol	O-Desmethylvenlafaxine. Desvenlafaxine	Celiprolol
Cannabidiol	Citalopram	Oxadiazon	Climbazole
Cannabinol	Climbazole	Tramadol	DEET (Diethyltoluamide)
Celiprolol	Clopidogrel		Desoxycortone enantate
Chlorpyriphos	Deacetyldiltiazem		Diflufenican
Cinnarizine	Diflufenican		Etofenprox (NH4)
Citalopram	Fipronil-sulfide		Fipronil-sulfide
Deacetyldiltiazem	Fipronilsulfone (NH4)		Fipronilsulfone (NH4)
Diflufenican	Imazalil		Furathiocarb
Dodemorph II	Irbesartan		Imazalil
Etofenprox (NH4)	Ketobemidone		Irbesartan
Fipronil-sulfide	Lamotrigine		Isoconazole
Gemfibrozil	Methadone		Lamotrigine
Imazalil	Methoprene Peak 1 Fragm 279		Methoprene Peak 1 Fragm 279
Irbesartan	Norverapamil		Norverapamil
Isoconazole	Octhilinone		Octhilinone
Ketobemidone	O-Desmethylvenlafaxine. Desvenlafaxine		O-Desmethylvenlafaxine. Desvenlafaxine
Memantine	Oxadiazon		Oxadiazon
Metformin	Proguanil		Permethrin Peak 3 (NH4)
Methadone	Pyrethrin I		Terbutryn
Nafronyl oxalate salt	Ticagrelor		Tiemonium
O-Desmethylnortramadol	Tiemonium		Tramadol
O-Desmethylvenlafaxine. Desvenlafaxine	Tramadol		Triclocarban
Oxadiazon	Triclocarban		Triphenylphosphate
Permethrin Peak 3 (NH4)	Triphenylphosphate		Venlafaxine
Propranolol	Venlafaxine		
Pyrethrins: Cinerin I	Verapamil		
Pyrethrins: Cinerin II			
Terbutryn			
Terodiline			
Ticagrelor			
Tramadol			
Tridemorph (main component) Peak2			
Venlafaxine			
Verapamil			

area 2 intermediate flow			
summer	**spring**	**autumn**	**winter**
Acebutolol	4-Methyl-5-thiazoleethanol	2.4 Dimethylphenyl-N-methylformamidine (metabolite Amitraz)	Acetochlor Fragm 224
Almitrine	Albendazole	Albendazole	Benzethonium
Amiodarone	Almitrine	Almitrine	Citalopram
Azithromycin	Benproperine	Amiodarone	Coumachlor
Benproperine	Benzethonium	Benzethonium	Cyamemazine
Bethanidine	Cannabinol	Cannabidiol	Diflufenican
Cannabinol	Celiprolol	Climbazole	Etofenprox (NH4)
Celiprolol	Climbazole	Clopidogrel	Fenpropimorph
Climbazole	Diflufenican	Deacetyldiltiazem	Fipronilsulfone (NH4)
DEET (Diethyltoluamide)	Etofenprox (NH4)	DEET (Diethyltoluamide)	Irbesartan
Desoxycortone enantate	Fenticonazole	Diflufenican	Isoconazole
Diflufenican	Gemfibrozil	Diphenhydramine	Isoproturon
Drofenine	Imazalil	Dipyridamole	Lidocaine
EDDP	Irbesartan	EDDP	Metformin
Etofenprox (NH4)	Memantine	Etofenprox (NH4)	Methoprene Peak 1 Fragm 279
Fipronilsulfone (NH4)	Methadone	Fenticonazole	Norverapamil
Flecainide	O-Desmethylvenlafaxine. Desvenlafaxine	Fipronilsulfone (NH4)	Octhilinone
Furathiocarb	Oxadiazon	Flecainide	Oxadiazon
Gemfibrozil	Permethrin Peak 3 (NH4)	Fluacrypyrim Fragm 205	Pendimethalin Fragm 212
Histamine	Proguanil	Gemfibrozil	Permethrin (cis-)
Imazalil	Propafenone	Irbesartan	Propafenone
Irbesartan	Propiconazole I	Isoconazole	Propiconazole I
Isoconazole	Pyrethrins: Cinerin II	Ketobemidone	Pyrethrins: Cinerin I
Metformin	Spirotetramate-mono-hydroxy	Lamotrigine	Siduron Peak 1
N.N-Diethyl-m-toluamide. DEET	Terbutryn	Maprotiline	Terbutryn
Norverapamil	Terodiline	Methadone	Terodiline
O-Desmethylvenlafaxine. Desvenlafaxine	Tiemonium	Naptalam (N-1-Naphthylphthalamicacid)	Tiemonium
Oxadiazon	Tramadol	O-Desmethylvenlafaxine. Desvenlafaxine	Tramadol
Permethrin Peak 3 (NH4)	Triclocarban	Oxadiazon	
Pheniramine	Tridemorph (main component) Peak2	Pendimethalin Fragm 212	
Proguanil	Venlafaxine	Permethrin (cis-)	
Propafenone		Pheniramine	
Pyrethrins: Cinerin II		Proguanil	
Sildenafil		Propiconazole I	
Terbutryn		Pyrethrins: Cinerin II	
Tramadol		Sertraline	
Tridemorph (main component) Peak2		Tebuconazole	
		Telmisartan	
		Terodiline	
		Tiapride	
		Tramadol	
		Triclocarban	
		Tridemorph (main component) Peak2	
		Trimipramine	
		Venlafaxine	

area 3 low flow

summer	spring	autumn	winter
Acebutolol	4-Methyl-5-thiazoleethanol	Acebutolol	4-Methyl-5-thiazoleethanol
Aliskiren	Acebutolol	Alimemazine	Acebutolol
Almitrine	Almitrine	Aliskiren	Alimemazine
Butoxycaine	Benzethonium	Benproperine	Amiodarone
Celiprolol	Celiprolol	Benzethonium	Benzethonium
Chlorpyriphos	Citalopram	Celiprolol	Celiprolol
Climbazole	Desoxycortone enantate	Citalopram	Citalopram
Deacetyldiltiazem	Diflufenican	Climbazole	Climbazole
Desoxycortone enantate	EDDP	Desoxycortone enantate	Desoxycortone enantate
Diflufenican	Etofenprox (NH4)	EtG (Na)	Diflufenican
Dodemorph II	Fipronil-sulfide	Etofenprox (NH4)	Dodemorph II
EDDP	Fipronilsulfone (NH4)	Fenticonazole	Etofenprox (NH4)
Etofenprox (NH4)	Flurtamone	Fipronilsulfone (NH4)	Fipronil-sulfide
Fipronilsulfone (NH4)	Irbesartan	Flecainide	Fipronilsulfone (NH4)
Furathiocarb	Isoconazole	Harman	Irbesartan
Histamine	JWH-018-M-7-OH-Ind	Irbesartan	Isoconazole
Irbesartan	Ketobemidone	Isoconazole	Metformin
Isoconazole	Memantine	Lidocaine	Methadone
Isothipendyl	O-Desmethylnortramadol	Methadone	Methoprene Peak 2 Fragm 279
JWH-018-M-7-OH-Ind	O-Desmethylvenlafaxine. Desvenlafaxine	Methoprene Peak 1 Fragm 279	Nandrolone phenylpropionate
Ketobemidone	Propafenone	Nortriptyline	Octhilinone
Metformin	Pyrethrins: Cinerin II	O-Desmethylvenlafaxine. Desvenlafaxine	O-Desmethylvenlafaxine. Desvenlafaxine
Metoprolol	Terbutryn	Oxadiazon	Oxadiazon
O-Desmethylnortramadol	Tiemonium	Pyrethrin I	Piperonylbutoxide Fragm 177
O-Desmethyltramadol	Tramadol	Terbutryn	Proguanil
Pheniramine	Triclocarban	Tiapride	Propafenone
Propranolol		Tramadol	Terbutryn
Rivaroxaban		Triclocarban	Tiemonium
Sertraline		Tridemorph (main component) Peak2	Tramadol
Sildenafil		Venlafaxine	Venlafaxine
Terbutryn			
Tiapride			
Tridemorph (main component) Peak2			
Venlafaxine			

area 4 outlet			
summer	**spring**	**autumn**	**winter**

Acebutolol	Acebutolol	3-Methylnorfentanyl	4-Methyl-5-thiazoleethanol
Amiodarone	Almitrine	Aliskiren	Acebutolol
Benproperine	Amiodarone	Almitrine	Almitrine
Bethanidine	Benzethonium	Amiodarone	Amiodarone
Bisoprolol	Celiprolol	Benproperine	Benomyl (decomposed to Carbendazim) Fragm 192
Celiprolol	Citalopram	Benzethonium	Carbendazim
Citalopram	Climbazole	Bethanidine	Climbazole
Climbazole	Deacetyldiltiazem	Carvone	Diflufenican
Deacetyldiltiazem	Diflufenican	Celiprolol	Diuron
Diflufenican	EDDP	Citalopram	Etofenprox (NH4)
EDDP	Etofenprox (NH4)	Climbazole	Fipronil-sulfide
Etofenprox (NH4)	Irbesartan	Desoxycortone enantate	Fipronilsulfone (NH4)
Flecainide	Methadone	Diflufenican	Flecainide
Gemfibrozil	Oxadiazon	Etofenprox (NH4)	Harman
Histamine	Propafenone	EtS (NH4)	Irbesartan
Irbesartan	Propiconazole II	Fenticonazole	Isoconazole
Lamotrigine	Pyrethrins: Cinerin II	Fipronil-sulfide	Memantine
Metformin	Terbutryn	Fipronilsulfone (NH4)	Metformin
Methadone	Tiemonium	Irbesartan	Methadone
Norcitalopram	Triclocarban	Isoconazole	Norfentanyl
O-Desmethyltramadol	Tris(2-chloroethyl)phosphate	Mexiletine	Nortetrazepam
O-Desmethylvenlafaxine. Desvenlafaxine	Venlafaxine	Norfentanyl	O-Desmethylnortramadol
Oxadiazon	Verapamil	O-Desmethyltramadol	O-Desmethyltramadol
Pheniramine		Orlistat (Na)	O-Desmethylvenlafaxine. Desvenlafaxine
Progesterone		Oxadiazon	Oxadiazon
Proguanil		Pendimethalin Fragm 212	Permethrin (cis-)
Propafenone		Propiconazole I	Piperonylbutoxide Fragm 177
Propranolol		Propranolol	Proguanil
Pyrethrins: Cinerin I		Tebuconazole	Propafenone
Rivaroxaban		Terbutryn	Propiconazole I
Terbutryn		Terodiline	Pyrethrins: Cinerin I
Terodiline		Tramadol	Tebuconazole
Tiapride		Triclocarban	Tramadol
Tridemorph (main component) Peak1		Tridemorph (main component) Peak2	Triclocarban
Venlafaxine		Venlafaxine	Tridemorph (main component) Peak2
Verapamil			Venlafaxine

Bibliography

Abdel-Shafy, H.I., Mansour, M.S.M., 2016. A review on polycyclic aromatic hydrocarbons: Source, environmental impact, effect on human health and remediation. Egyptian Journal of Petroleum 25, 107–123. https://doi.org/10.1016/j.ejpe.2015.03.011

Akratos, C.S., Tsihrintzis, V.A., 2007. Effect of temperature, HRT, vegetation and porous media on removal efficiency of pilot-scale horizontal subsurface flow constructed wetlands. Ecological Engineering 29, 173–191. https://doi.org/10.1016/j.ecoleng.2006.06.013

Albergamo, V., Schollée, J.E., Schymanski, E.L., Helmus, R., Timmer, H., Hollender, J., de Voogt, P., 2019. Nontarget Screening Reveals Time Trends of Polar Micropollutants in a Riverbank Filtration System. Environ. Sci. Technol. 53, 7584–7594. https://doi.org/10.1021/acs.est.9b01750

Alvarado, A., Vesvikar, M., Cisneros, J.F., Maere, T., Goethals, P., Nopens, I., 2013. CFD study to determine the optimal configuration of aerators in a full-scale waste stabilization pond. Water Research 47, 4528–4537. https://doi.org/10.1016/j.watres.2013.05.016

Alygizakis, N.A., Gago-Ferrero, P., Borova, V.L., Pavlidou, A., Hatzianestis, I., Thomaidis, N.S., 2016. Occurrence and spatial distribution of 158 pharmaceuticals, drugs of abuse and related metabolites in offshore seawater. Science of The Total Environment 541, 1097–1105. https://doi.org/10.1016/j.scitotenv.2015.09.145

Andersson, B. (Ed.), 2012. Computational fluid dynamics for engineers. Cambridge Univ. Press, Cambridge New York.

Andersson, J.T., Achten, C., 2015. Time to Say Goodbye to the 16 EPA PAHs? Toward an Up-to-Date Use of PACs for Environmental Purposes. Polycycl Aromat Compd 35, 330–354. https://doi.org/10.1080/10406638.2014.991042

Andreozzi, R., Raffaele, M., Nicklas, P., 2003. Pharmaceuticals in STP effluents and their solar photodegradation in aquatic environment. Chemosphere 50, 1319–1330. https://doi.org/10.1016/S0045-6535(02)00769-5

Arrêté du 22 juin 2007 relatif à la collecte, au transport et au traitement des eaux usées des agglomérations d'assainissement ainsi qu'à la surveillance de leur fonctionnement et de leur efficacité, et aux dispositifs d'assainissement non collectif recevant une charge brute de pollution organique supérieure à 1,2 kg/j de DBO5., n.d.

Ávila, C., Nivala, J., Olsson, L., Kassa, K., Headley, T., Mueller, R.A., Bayona, J.M., García, J., 2014. Emerging organic contaminants in vertical subsurface flow constructed wetlands: Influence of media size, loading frequency and use of active aeration. Science of The Total Environment 494–495, 211–217. https://doi.org/10.1016/j.scitotenv.2014.06.128

Azaroff, A., Miossec, C., Lanceleur, L., Guyoneaud, R., Monperrus, M., 2020. Priority and emerging micropollutants distribution from coastal to continental slope sediments: A case study of Capbreton Submarine Canyon (North Atlantic Ocean). Science of The Total Environment 703, 135057. https://doi.org/10.1016/j.scitotenv.2019.135057

Baek, S.O., Field, R.A., Goldstone, M.E., Kirk, P.W., Lester, J.N., Perry, R., 1991. A review of atmospheric polycyclic aromatic hydrocarbons: Sources, fate and behavior. Water Air Soil Pollut 60, 279–300. https://doi.org/10.1007/BF00282628

Bartrons, M., Peñuelas, J., 2017. Pharmaceuticals and Personal-Care Products in Plants. Trends in Plant Science 22, 194–203. https://doi.org/10.1016/j.tplants.2016.12.010

Batool, A., Saleh, T.A., 2020. Removal of toxic metals from wastewater in constructed wetlands as a green technology; catalyst role of substrates and chelators. Ecotoxicology and Environmental Safety 189, 109924. https://doi.org/10.1016/j.ecoenv.2019.109924

Bergé, A., Buleté, A., Fildier, A., Mailler, R., Gasperi, J., Coquet, Y., Nauleau, F., Rocher, V., Vulliet, E., 2018. Non-target strategies by HRMS to evaluate fluidized micro-grain activated carbon as a tertiary treatment of wastewater. Chemosphere 213, 587–595. https://doi.org/10.1016/j.chemosphere.2018.09.101

Besombes, J.-L., Maître, A., Patissier, O., Marchand, N., Chevron, N., Stoklov, M., Masclet, P., 2001. Particulate PAHs observed in the surrounding of a municipal incinerator. Atmospheric Environment 35, 6093–6104. https://doi.org/10.1016/S1352-2310(01)00399-5

Biel-Maeso, M., Corada-Fernández, C., Lara-Martín, P.A., 2019. Removal of personal care products (PCPs) in wastewater and sludge treatment and their occurrence in receiving soils. Water Research 150, 129–139. https://doi.org/10.1016/j.watres.2018.11.045

Bletsou, A.A., Jeon, J., Hollender, J., Archontaki, E., Thomaidis, N.S., 2015. Targeted and non-targeted liquid chromatography-mass spectrometric workflows for identification of transformation products of emerging pollutants in the aquatic environment. TrAC Trends in Analytical Chemistry 66, 32–44. https://doi.org/10.1016/j.trac.2014.11.009

Bligh, E.G., Dyer, W.J., 1959. A Rapid Method of Total Lipid Extraction and Purification. Can. J. Biochem. Physiol. 37, 911–917. https://doi.org/10.1139/y59-099

Blocken, B., Gualtieri, C., 2012. Ten iterative steps for model development and evaluation applied to Computational Fluid Dynamics for Environmental Fluid Mechanics. Environmental Modelling & Software 33, 1–22. https://doi.org/10.1016/j.envsoft.2012.02.001

Blum, K.M., Andersson, P.L., Renman, G., Ahrens, L., Gros, M., Wiberg, K., Haglund, P., 2017. Non-target screening and prioritization of potentially persistent, bioaccumulating and toxic domestic wastewater contaminants and their removal in on-site and large-scale sewage treatment plants. Science of The Total Environment 575, 265–275. https://doi.org/10.1016/j.scitotenv.2016.09.135

Boleda, M.R., Galceran, M.T., Ventura, F., 2013. Validation and uncertainty estimation of a multiresidue method for pharmaceuticals in surface and treated waters by liquid chromatography–tandem mass spectrometry. Journal of Chromatography A 1286, 146–158. https://doi.org/10.1016/j.chroma.2013.02.077

Boonnorat, J., Kanyatrakul, A., Prakhongsak, A., Honda, R., Panichnumsin, P., Boonapatcharoen, N., 2019. Effect of hydraulic retention time on micropollutant biodegradation in activated sludge system augmented with acclimatized sludge treating low-micropollutants wastewater. Chemosphere 230, 606–615. https://doi.org/10.1016/j.chemosphere.2019.05.039

Brix, H., 1994. Use of constructed wetlands in water pollution control: historical development, present status, and future perspectives. Water Science and Technology 30, 209–223. https://doi.org/10.2166/wst.1994.0413

Brunsch, A.F., ter Laak, T.L., Christoffels, E., Rijnaarts, H.H.M., Langenhoff, A.A.M., 2018. Retention soil filter as post-treatment step to remove micropollutants from sewage treatment plant effluent. Science of The Total Environment 637–638, 1098–1107. https://doi.org/10.1016/j.scitotenv.2018.05.063

Bucheli, T.D., 2014. Phytotoxins: Environmental Micropollutants of Concern? Environ. Sci. Technol. 48, 13027–13033. https://doi.org/10.1021/es504342w

Burkholder, J., Libra, B., Weyer, P., Heathcote, S., Kolpin, D., Thorne, P.S., Wichman, M., 2007. Impacts of Waste from Concentrated Animal Feeding Operations on Water Quality. Environ Health Perspect 115, 308–312. https://doi.org/10.1289/ehp.8839

Busch, W., Schmidt, S., Kühne, R., Schulze, T., Krauss, M., Altenburger, R., 2016. Micropollutants in European rivers: A mode of action survey to support the development of effect-based tools for water monitoring. Environmental Toxicology and Chemistry 35, 1887–1899. https://doi.org/10.1002/etc.3460

Buszka, P.M., Yeskis, D.J., Kolpin, D.W., Furlong, E.T., Zaugg, S.D., Meyer, M.T., 2009. Waste-indicator and pharmaceutical compounds in landfill-leachate-affected ground water near Elkhart, Indiana, 2000-2002. Bulletin of Environmental Contamination and Toxicology. https://doi.org/10.1007/s00128-009-9702-z

Cabello, F.C., 2006. Heavy use of prophylactic antibiotics in aquaculture: a growing problem for human and animal health and for the environment. Environ. Microbiol. 8, 1137–1144. https://doi.org/10.1111/j.1462-2920.2006.01054.x

Callender, E., 2003. Heavy Metals in the Environment-Historical Trends. Treatise on Geochemistry 9, 612. https://doi.org/10.1016/B0-08-043751-6/09161-1

Cañameras, N., Comas, J., Bayona, J.M., 2015. Bioavailability and Uptake of Organic Micropollutants During Crop Irrigation with Reclaimed Wastewater: Introduction to Current Issues and Research Needs, in: Fatta-Kassinos, D., Dionysiou, D.D., Kümmerer, K. (Eds.), Wastewater Reuse and Current Challenges, The Handbook of Environmental Chemistry. Springer International Publishing, Cham, pp. 81–104. https://doi.org/10.1007/698_2015_412

Candelone, J.-P., Hong, S., Pellone, C., Boutron, C., 1995. Post industrial revolution changes in large scale atmospheric pollution of the northern hemisphere for heavy metals as documented in central Greenland snow and ice. Journal of Geophysical Research 100, pp 16,605-16,616.
Caprioli, R.M., Farmer, T.B., Gile, J., 1997. Molecular Imaging of Biological Samples: Localization of Peptides and Proteins Using MALDI-TOF MS. Anal. Chem. 69, 4751–4760. https://doi.org/10.1021/ac970888i
Carballa, M., Omil, F., Lema, J.M., Llompart, M., García-Jares, C., Rodríguez, I., Gómez, M., Ternes, T., 2004. Behavior of pharmaceuticals, cosmetics and hormones in a sewage treatment plant. Water Research 38, 2918–2926. https://doi.org/10.1016/j.watres.2004.03.029
Carvalho, F.P., 2017. Pesticides, environment, and food safety. Food and Energy Security 6, 48–60. https://doi.org/10.1002/fes3.108
Carvalho, P.N., Basto, M.C.P., Almeida, C.M.R., Brix, H., 2014. A review of plant–pharmaceutical interactions: from uptake and effects in crop plants to phytoremediation in constructed wetlands. Environ Sci Pollut Res 21, 11729–11763. https://doi.org/10.1007/s11356-014-2550-3
Castiglioni, S., Bagnati, R., Fanelli, R., Pomati, F., Calamari, D., Zuccato, E., 2006. Removal of Pharmaceuticals in Sewage Treatment Plants in Italy. Environ. Sci. Technol. 40, 357–363. https://doi.org/10.1021/es050991m
Chaney, R.L., Malik, M., Li, Y.M., Brown, S.L., Brewer, E.P., Angle, J.S., Baker, A.J., 1997. Phytoremediation of soil metals. Curr. Opin. Biotechnol. 8, 279–284. https://doi.org/10.1016/s0958-1669(97)80004-3
Chen, Y., Vymazal, J., Březinová, T., Koželuh, M., Kule, L., Huang, J., Chen, Z., 2016. Occurrence, removal and environmental risk assessment of pharmaceuticals and personal care products in rural wastewater treatment wetlands. Science of The Total Environment 566–567, 1660–1669. https://doi.org/10.1016/j.scitotenv.2016.06.069
Chevreuil, M., Carru, A.-M., Chesterikoff, A., Boët, P., Tales, E., Allardi, J., 1995. Contamination of fish from different areas of the river Seine (France) by organic (PCB and pesticides) and metallic (Cd, Cr, Cu, Fe, Mn, Pb and Zn) micropollutants. Science of The Total Environment 162, 31–42. https://doi.org/10.1016/0048-9697(95)04335-X
Chiaia-Hernandez, A.C., Krauss, M., Hollender, J., 2013. Screening of Lake Sediments for Emerging Contaminants by Liquid Chromatography Atmospheric Pressure Photoionization and Electrospray Ionization Coupled to High Resolution Mass Spectrometry. Environ. Sci. Technol. 47, 976–986. https://doi.org/10.1021/es303888v
Chiaia-Hernandez, A.C., Schymanski, E.L., Kumar, P., Singer, H.P., Hollender, J., 2014. Suspect and nontarget screening approaches to identify organic contaminant records in lake sediments. Analytical and Bioanalytical Chemistry 406, 7323–7335. https://doi.org/10.1007/s00216-014-8166-0
Chuang, Y.-H., Liu, C.-H., Sallach, J.B., Hammerschmidt, R., Zhang, W., Boyd, S.A., Li, H., 2019. Mechanistic study on uptake and transport of pharmaceuticals in lettuce from water. Environment International 131, 104976. https://doi.org/10.1016/j.envint.2019.104976
Circulaire du 7 mai 2007 DCE/23 définissant les “normes de qualité environnementale provisoires (NQEp)” des 41 substances impliquées dans l’évaluation de l’état chimique des masses d’eau ainsi que des substances pertinentes du programme national de réduction des substances dangereuses dans l’eau, n.d.
Clara, M., Strenn, B., Gans, O., Martinez, E., Kreuzinger, N., Kroiss, H., 2005. Removal of selected pharmaceuticals, fragrances and endocrine disrupting compounds in a membrane bioreactor and conventional wastewater treatment plants. Water Research 39, 4797–4807. https://doi.org/10.1016/j.watres.2005.09.015
Code de la santé publique | Legifrance [WWW Document], n.d. URL https://www.legifrance.gouv.fr/affichCode.do?cidTexte=LEGITEXT000006072665 (accessed 7.13.20).
Coggins, L.X., Ghisalberti, M., Ghadouani, A., 2017. Sludge accumulation and distribution impact the hydraulic performance in waste stabilisation ponds. Water Research 110, 354–365. https://doi.org/10.1016/j.watres.2016.11.031

Commission Implementing Decision (EU) 2015/495 of 20 March 2015 establishing a watch list of substances for Union-wide monitoring in the field of water policy pursuant to Directive 2008/105/EC of the European Parliament and of the Council (notified under document C(2015) 1756) Text with EEA relevance, 2015. , OJ L.

Conn, K.E., Lowe, K.S., Drewes, J.E., Hoppe-Jones, C., Tucholke, M.B., 2010. Occurrence of Pharmaceuticals and Consumer Product Chemicals in Raw Wastewater and Septic Tank Effluent from Single-Family Homes. Environmental Engineering Science 27, 347–356. https://doi.org/10.1089/ees.2009.0364

Cornett, D.S., Frappier, S.L., Caprioli, R.M., 2008. MALDI-FTICR Imaging Mass Spectrometry of Drugs and Metabolites in Tissue. Anal. Chem. 80, 5648–5653. https://doi.org/10.1021/ac800617s

Corrigan, W.J., 1932. SANITATION UNDER THE ANCIENT MINOAN CIVILIZATION. Can Med Assoc J 27, 77–78.

Cotran, R.S., Kumar, V., Robbins, S.L., 1990. Robbins, patología estructural y funcional, cuarta edición. Interamericana/McGraw-Hill, Madrid.

Cottin, N., Merlin, G., 2008. Removal of PAHs from laboratory columns simulating the humus upper layer of vertical flow constructed wetlands. Chemosphere 73, 711–716. https://doi.org/10.1016/j.chemosphere.2008.06.060

Cotton, J., Leroux, F., Broudin, S., Poirel, M., Corman, B., Junot, C., Ducruix, C., 2016. Development and validation of a multiresidue method for the analysis of more than 500 pesticides and drugs in water based on on-line and liquid chromatography coupled to high resolution mass spectrometry. Water Research 104, 20–27. https://doi.org/10.1016/j.watres.2016.07.075

Deblonde, T., Cossu-Leguille, C., Hartemann, P., 2011. Emerging pollutants in wastewater: A review of the literature. International Journal of Hygiene and Environmental Health, The second European PhD students workshop: Water and health ? Cannes 2010 214, 442–448. https://doi.org/10.1016/j.ijheh.2011.08.002

Decision No 2455/2001/EC of the European Parliament and of the Council of 20 November 2001 establishing the list of priority substances in the field of water policy and amending Directive 2000/60/EC (Text with EEA relevance), 2001. , OJ L.

Derco, J., Valičková, M., Šilhárová, K., Dudáš, J., Luptáková, A., 2013. Removal of selected chlorinated micropollutants by ozonation. Chemical Papers 67, 1585–1593. https://doi.org/10.2478/s11696-013-0324-x

Directive 91/414/CEE du Conseil, du 15 juillet 1991, concernant la mise sur le marché des produits phytopharmaceutiques, n.d.

Directive 2008/105/EC of the European Parliament and of the Council of 16 December 2008 on environmental quality standards in the field of water policy, amending and subsequently repealing Council Directives 82/176/EEC, 83/513/EEC, 84/156/EEC, 84/491/EEC, 86/280/EEC and amending Directive 2000/60/EC of the European Parliament and of the Council, 2008. , 348.

Dollinger, J., Dagès, C., Voltz, M., 2017. Using fluorescent dyes as proxies to study herbicide removal by sorption in buffer zones. Environ Sci Pollut Res 24, 11752–11763. https://doi.org/10.1007/s11356-017-8703-4

Dordio, A., Carvalho, A.J.P., Teixeira, D.M., Dias, C.B., Pinto, A.P., 2010. Removal of pharmaceuticals in microcosm constructed wetlands using Typha spp. and LECA. Bioresource Technology 101, 886–892. https://doi.org/10.1016/j.biortech.2009.09.001

D. Scherson, Y., F. Wells, G., Woo, S.-G., Lee, J., Park, J., J. Cantwell, B., S. Criddle, C., 2013. Nitrogen removal with energy recovery through N 2 O decomposition. Energy & Environmental Science 6, 241–248. https://doi.org/10.1039/C2EE22487A

Dufresne, M., Vazquez, J., Terfous, A., Ghenaim, A., Poulet, J.-B., 2009. Experimental investigation and CFD modelling of flow, sedimentation, and solids separation in a combined sewer detention tank. Computers & Fluids, Advances in Computational Fluid Dynamics 38, 1042–1049. https://doi.org/10.1016/j.compfluid.2008.01.011

Durst, R., Imfeld, G., Lange, J., 2013. Transport of pesticides and artificial tracers in vertical-flow lab-scale wetlands. Water Resources Research 49, 554–564. https://doi.org/10.1002/wrcr.20080

Eggen, R.I.L., Hollender, J., Joss, A., Schärer, M., Stamm, C., 2014. Reducing the Discharge of Micropollutants in the Aquatic Environment: The Benefits of Upgrading Wastewater Treatment Plants. Environ. Sci. Technol. 48, 7683–7689. https://doi.org/10.1021/es500907n

Eggen, T., Moeder, M., Arukwe, A., 2010. Municipal landfill leachates: a significant source for new and emerging pollutants. Sci. Total Environ. 408, 5147–5157. https://doi.org/10.1016/j.scitotenv.2010.07.049

Falås, P., Jewell, K.S., Hermes, N., Wick, A., Ternes, T.A., Joss, A., Nielsen, J.L., 2018. Transformation, CO 2 formation and uptake of four organic micropollutants by carrier-attached microorganisms. Water Research 141, 405–416. https://doi.org/10.1016/j.watres.2018.03.040

Favas, P.J.C., Pratas, J., Varun, M., DSouza, R., Manoj, P., 2014. Phytoremediation of Soils Contaminated with Metals and Metalloids at Mining Areas: Potential of Native Flora, in: Hernandez Soriano, M.C. (Ed.), Environmental Risk Assessment of Soil Contamination. InTech. https://doi.org/10.5772/57469

Fergusson, J.E., 1990. The heavy elements: chemistry, environmental impact and health effects. Pergamon Press, Oxford [England.

Freyssinet, P., Piantone, P., Azaroual, M., Itard, Y., Clozel-Leloup, B., Guyonnet, D., Baubron, J.C., 2002. Chemical changes and leachate mass balance of municipal solid waste bottom ash submitted to weathering. Waste Management 22, 159–172. https://doi.org/10.1016/S0956-053X(01)00065-4

Fu, Q., Liao, C., Du, X., Schlenk, D., Gan, J., 2018. Back Conversion from Product to Parent: Methyl Triclosan to Triclosan in Plants. Environ. Sci. Technol. Lett. 5, 181–185. https://doi.org/10.1021/acs.estlett.8b00071

Gadd, G.M., 2001. Phytoremediation of toxic metals; using plants to clean up the environment. Edited by Ilya Raskin and Burt D Ensley, John Wiley & Sons, Inc, New York, 2000, 304 pp, price UK £58.80, ISBN 0 471 19254 6. Journal of Chemical Technology & Biotechnology 76, 325–325. https://doi.org/10.1002/jctb.374

Gago-Ferrero, P., Schymanski, E.L., Hollender, J., Thomaidis, N.S., 2016. Nontarget Analysis of Environmental Samples Based on Liquid Chromatography Coupled to High Resolution Mass Spectrometry (LC-HRMS), in: Comprehensive Analytical Chemistry. Elsevier, pp. 381–403. https://doi.org/10.1016/bs.coac.2016.01.012

García, J., Rousseau, D.P.L., Morató, J., Lesage, E., Matamoros, V., Bayona, J.M., 2010. Contaminant Removal Processes in Subsurface-Flow Constructed Wetlands: A Review. Critical Reviews in Environmental Science and Technology 40, 561–661. https://doi.org/10.1080/10643380802471076

Geissen, V., Mol, H., Klumpp, E., Umlauf, G., Nadal, M., van der Ploeg, M., van de Zee, S.E.A.T.M., Ritsema, C.J., 2015. Emerging pollutants in the environment: A challenge for water resource management. International Soil and Water Conservation Research 3, 57–65. https://doi.org/10.1016/j.iswcr.2015.03.002

Gil, Y., Sinfort, C., 2005. Emission of pesticides to the air during sprayer application: A bibliographic review. Atmospheric Environment 39, 5183–5193. https://doi.org/10.1016/j.atmosenv.2005.05.019

Godfrey, E., Woessner, W.W., Benotti, M.J., 2007. Pharmaceuticals in on-site sewage effluent and ground water, Western Montana. Ground Water 45, 263–271. https://doi.org/10.1111/j.1745-6584.2006.00288.x

Gong, W., Jiang, M., Zhang, T., Zhang, W., Liang, G., Li, B., Hu, B., Han, P., 2020. Uptake and dissipation of metalaxyl-M, fludioxonil, cyantraniliprole and thiamethoxam in greenhouse chrysanthemum. Environmental Pollution 257, 113499. https://doi.org/10.1016/j.envpol.2019.113499

Grice, K., Lu, H., Atahan, P., Asif, M., Hallmann, C., Greenwood, P., Maslen, E., Tulipani, S., Williford, K., Dodson, J., 2009. New insights into the origin of perylene in geological samples. Geochimica et Cosmochimica Acta 73, 6531–6543. https://doi.org/10.1016/j.gca.2009.07.029

Gros, M., Blum, K.M., Jernstedt, H., Renman, G., Rodríguez-Mozaz, S., Haglund, P., Andersson, P.L., Wiberg, K., Ahrens, L., 2017. Screening and prioritization of micropollutants in wastewaters

from on-site sewage treatment facilities. Journal of Hazardous Materials 328, 37–45. https://doi.org/10.1016/j.jhazmat.2016.12.055
Gros, M., Mas-Pla, J., Boy-Roura, M., Geli, I., Domingo, F., Petrović, M., 2019a. Veterinary pharmaceuticals and antibiotics in manure and slurry and their fate in amended agricultural soils: Findings from an experimental field site (Baix Empordà, NE Catalonia). Science of The Total Environment 654, 1337–1349. https://doi.org/10.1016/j.scitotenv.2018.11.061
Gros, M., Mas-Pla, J., Boy-Roura, M., Geli, I., Domingo, F., Petrović, M., 2019b. Veterinary pharmaceuticals and antibiotics in manure and slurry and their fate in amended agricultural soils: Findings from an experimental field site (Baix Empordà, NE Catalonia). Science of The Total Environment 654, 1337–1349. https://doi.org/10.1016/j.scitotenv.2018.11.061
Gruchlik, Y., Linge, K., Joll, C., 2018. Removal of organic micropollutants in waste stabilisation ponds: A review. Journal of Environmental Management 206, 202–214. https://doi.org/10.1016/j.jenvman.2017.10.020
Hao, T., Xiang, P., Mackey, H.R., Chi, K., Lu, H., Chui, H., van Loosdrecht, M.C.M., Chen, G.-H., 2014. A review of biological sulfate conversions in wastewater treatment. Water Research 65, 1–21. https://doi.org/10.1016/j.watres.2014.06.043
Harb, M., Lou, E., Smith, A.L., Stadler, L.B., 2019. Perspectives on the fate of micropollutants in mainstream anaerobic wastewater treatment. Current Opinion in Biotechnology, Energy Biotechnology • Environmental Biotechnology 57, 94–100. https://doi.org/10.1016/j.copbio.2019.02.022
Harms, H., Schlosser, D., Wick, L.Y., 2011. Untapped potential: exploiting fungi in bioremediation of hazardous chemicals. Nature Reviews Microbiology 9, 177–192. https://doi.org/10.1038/nrmicro2519
Haya, K., Burridge, L.E., Davies, I.M., Ervik, A., 2005. A Review and Assessment of Environmental Risk of Chemicals Used forthe Treatment of Sea Lice Infestations of Cultured Salmon, in: Hargrave, B.T. (Ed.), Environmental Effects of Marine Finfish Aquaculture, Handbook of Environmental Chemistry. Springer, Berlin, Heidelberg, pp. 305–340. https://doi.org/10.1007/b136016
He, Y., Langenhoff, A.A.M., Sutton, N.B., Rijnaarts, H.H.M., Blokland, M.H., Chen, F., Huber, C., Schröder, P., 2017. Metabolism of Ibuprofen by Phragmites australis: Uptake and Phytodegradation. Environ. Sci. Technol. 51, 4576–4584. https://doi.org/10.1021/acs.est.7b00458
Hebert, A., Feliers, C., Lecarpentier, C., Neale, P.A., Schlichting, R., Thibert, S., Escher, B.I., 2018. Bioanalytical assessment of adaptive stress responses in drinking water: A predictive tool to differentiate between micropollutants and disinfection by-products. Water Research 132, 340–349. https://doi.org/10.1016/j.watres.2017.12.078
Herrmann, M., Menz, J., Olsson, O., Kümmerer, K., 2015. Identification of phototransformation products of the antiepileptic drug gabapentin: Biodegradability and initial assessment of toxicity. Water Research 85, 11–21. https://doi.org/10.1016/j.watres.2015.08.004
Hijosa-Valsero, M., Matamoros, V., Sidrach-Cardona, R., Pedescoll, A., Martín-Villacorta, J., García, J., Bayona, J.M., Bécares, E., 2011. Influence of design, physico-chemical and environmental parameters on pharmaceuticals and fragrances removal by constructed wetlands. Water Science and Technology 63, 2527–2534. https://doi.org/10.2166/wst.2011.500
Hijosa-Valsero, M., Sidrach-Cardona, R., Martín-Villacorta, J., Bécares, E., 2010. Optimization of performance assessment and design characteristics in constructed wetlands for the removal of organic matter. Chemosphere 81, 651–657. https://doi.org/10.1016/j.chemosphere.2010.08.010
Hodson, M.E., 2004. Heavy metals—geochemical bogey men? Environmental Pollution 129, 341–343. https://doi.org/10.1016/j.envpol.2003.11.003
Hollender, J., Zimmermann, S.G., Koepke, S., Krauss, M., McArdell, C.S., Ort, C., Singer, H., von Gunten, U., Siegrist, H., 2009. Elimination of Organic Micropollutants in a Municipal Wastewater Treatment Plant Upgraded with a Full-Scale Post-Ozonation Followed by Sand Filtration. Environ. Sci. Technol. 43, 7862–7869. https://doi.org/10.1021/es9014629
Holm, J.V., Ruegge, Kirsten., Bjerg, P.L., Christensen, T.H., 1995. Occurrence and Distribution of Pharmaceutical Organic Compounds in the Groundwater Downgradient of a Landfill

(Grindsted, Denmark). Environ. Sci. Technol. 29, 1415–1420. https://doi.org/10.1021/es00005a039
Hong, S., Candelone, J.-P., Patterson, C.C., Boutron, C.F., 1994. Greenland Ice Evidence of Hemispheric Lead Pollution Two Millennia Ago by Greek and Roman Civilizations. Science 265, 1841–1843. https://doi.org/10.1126/science.265.5180.1841
Hopkins, J.N.N., 2007. THE CLOACA MAXIMA AND THE MONUMENTAL MANIPULATION OF WATER IN ARCHAIC ROME 15.
Hsieh, Y., Chen, J., Korfmacher, W.A., 2007. Mapping pharmaceuticals in tissues using MALDI imaging mass spectrometry. Journal of Pharmacological and Toxicological Methods 55, 193–200. https://doi.org/10.1016/j.vascn.2006.06.004
Huang, J., 2000. Nitrogen removal in constructed wetlands employed to treat domestic wastewater. Water Research 34, 2582–2588. https://doi.org/10.1016/S0043-1354(00)00018-X
Huber, C., Bartha, B., Harpaintner, R., Schröder, P., 2009. Metabolism of acetaminophen (paracetamol) in plants--two independent pathways result in the formation of a glutathione and a glucose conjugate. Environ Sci Pollut Res Int 16, 206–213. https://doi.org/10.1007/s11356-008-0095-z
Huber, M.M., Göbel, A., Joss, A., Hermann, N., Löffler, D., McArdell, C.S., Ried, A., Siegrist, H., Ternes, T.A., von Gunten, U., 2005. Oxidation of pharmaceuticals during ozonation of municipal wastewater effluents: a pilot study. Environ. Sci. Technol. 39, 4290–4299. https://doi.org/10.1021/es048396s
Hug, C., Ulrich, N., Schulze, T., Brack, W., Krauss, M., 2014. Identification of novel micropollutants in wastewater by a combination of suspect and nontarget screening. Environmental Pollution 184, 25–32. https://doi.org/10.1016/j.envpol.2013.07.048
Isenmann, G., 2016. Approche Euler-Lagrange pour la modélisation du transport solide dans les ouvrages de décantation 214.
Ivanová, L., Mackuľak, T., Grabic, R., Golovko, O., Koba, O., Staňová, A.V., Szabová, P., Grenčíková, A., Bodík, I., 2018. Pharmaceuticals and illicit drugs – A new threat to the application of sewage sludge in agriculture. Science of The Total Environment 634, 606–615. https://doi.org/10.1016/j.scitotenv.2018.04.001
Jansen, M., 1989. Water supply and sewage disposal at Mohenjo-Daro. World Archaeology 21, 177–192. https://doi.org/10.1080/00438243.1989.9980100
Jun, J.H., n.d. Development of high-spatial and high-mass resolution mass spectrometric imaging (MSI) and its application to the study of small metabolites and endogenous molecules of plants 164.
Jung, S., Chen, Y., Sullards, M.C., Ragauskas, A.J., 2010. Direct analysis of cellulose in poplar stem by matrix-assisted laser desorption/ionization imaging mass spectrometry. Rapid Communications in Mass Spectrometry 24, 3230–3236. https://doi.org/10.1002/rcm.4757
K Mohanarangam, D W Stephens, 2009. CFD MODELLING OF FLOATING AND SETTLING PHASES IN SETTLING TANKS. https://doi.org/10.13140/RG.2.1.5078.7686
Kadlec, R.H., Wallace, S.D., 2009. Treatment wetlands, 2nd ed. ed. CRC Press, Boca Raton, FL.
Karvelas, M., Katsoyiannis, A., Samara, C., 2003. Occurrence and fate of heavy metals in the wastewater treatment process. Chemosphere 53, 1201–1210. https://doi.org/10.1016/S0045-6535(03)00591-5
Kasprzyk-Hordern, B., Dinsdale, R.M., Guwy, A.J., 2009. The removal of pharmaceuticals, personal care products, endocrine disruptors and illicit drugs during wastewater treatment and its impact on the quality of receiving waters. Water Research 43, 363–380. https://doi.org/10.1016/j.watres.2008.10.047
Keith, L.H., 2015. The Source of U.S. EPA's Sixteen PAH Priority Pollutants. Polycyclic Aromatic Compounds 35, 147–160. https://doi.org/10.1080/10406638.2014.892886
Kern, S., Singer, H., Hollender, J., Schwarzenbach, R.P., Fenner, K., 2011. Assessing Exposure to Transformation Products of Soil-Applied Organic Contaminants in Surface Water: Comparison of Model Predictions and Field Data. Environ. Sci. Technol. 45, 2833–2841. https://doi.org/10.1021/es102537b
Kickuth, R., 1970. Ökochemische Leistungen höherer Pflanzen. Naturwissenschaften 57, 55–61. https://doi.org/10.1007/BF00590679

Kiefer, K., Müller, A., Singer, H., Hollender, J., 2019. New relevant pesticide transformation products in groundwater detected using target and suspect screening for agricultural and urban micropollutants with LC-HRMS. Water Research 165, 114972. https://doi.org/10.1016/j.watres.2019.114972
Klampfl, C.W., 2019. Metabolization of pharmaceuticals by plants after uptake from water and soil: A review. TrAC Trends in Analytical Chemistry 111, 13–26. https://doi.org/10.1016/j.trac.2018.11.042
Koli, A.K., Whitmore, R., Walden, B., 1980. Comparative analysis of inorganic elements in the muscle and liver of some fish species. Environment International 4, 261–263. https://doi.org/10.1016/0160-4120(80)90174-9
Kolpin, D.W., Furlong, E.T., Meyer, M.T., Thurman, E.M., Zaugg, S.D., Barber, L.B., Buxton, H.T., 2002. Pharmaceuticals, hormones, and other organic wastewater contaminants in US streams, 1999- 2000: A national reconnaissance. Environmental science & technology 36, 1202–1211.
Komives, T., Gullner, G., 2005. Phase I xenobiotic metabolic systems in plants. Zeitschrift fur Naturforschung—Section C Journal of Biosciences, 60, 179–185.
Kosjek, T., Heath, E., 2008. Applications of mass spectrometry to identifying pharmaceutical transformation products in water treatment. TrAC Trends in Analytical Chemistry, Advanced MS Analysis of Metabolites and Degradation Products - I 27, 807–820. https://doi.org/10.1016/j.trac.2008.08.014
Kouzayha, A., 2011. Développement des méthodes analytiques pour la détection et la quantification de traces des HAP et de pesticides dans l'eau. Application à l'évaluation de la qualité des eaux libanaises. (PhD Thesis). Université Sciences et Technologies-Bordeaux I.
Krauss, M., Singer, H., Hollender, J., 2010. LC–high resolution MS in environmental analysis: from target screening to the identification of unknowns. Analytical and Bioanalytical Chemistry 397, 943–951. https://doi.org/10.1007/s00216-010-3608-9
Kumar, M., Gogoi, A., Mukherjee, S., 2020. Metal removal, partitioning and phase distributions in the wastewater and sludge: Performance evaluation of conventional, upflow anaerobic sludge blanket and downflow hanging sponge treatment systems. Journal of Cleaner Production 249, 119426. https://doi.org/10.1016/j.jclepro.2019.119426
Lagarrigue, M., Caprioli, R.M., Pineau, C., 2016. Potential of MALDI imaging for the toxicological evaluation of environmental pollutants. Journal of Proteomics 144, 133–139. https://doi.org/10.1016/j.jprot.2016.05.008
Lah, L., Podobnik, B., Novak, M., Korošec, B., Berne, S., Vogelsang, M., Kraševec, N., Zupanec, N., Stojan, J., Bohlmann, J., Komel, R., 2011. The versatility of the fungal cytochrome P450 monooxygenase system is instrumental in xenobiotic detoxification. Molecular Microbiology 81, 1374–1389. https://doi.org/10.1111/j.1365-2958.2011.07772.x
Lange, J., Schuetz, T., Gregoire, C., Elsässer, D., Schulz, R., Passeport, E., Tournebize, J., 2011. Multi-tracer experiments to characterise contaminant mitigation capacities for different types of artificial wetlands. International Journal of Environmental Analytical Chemistry 91, 768–785. https://doi.org/10.1080/03067319.2010.525635
Lapworth, D.J., Baran, N., Stuart, M.E., Ward, R.S., 2012. Emerging organic contaminants in groundwater: A review of sources, fate and occurrence. Environ. Pollut. 163, 287–303. https://doi.org/10.1016/j.envpol.2011.12.034
Laurent, J., 2016. Modélisation du couplage de la dynamique des écoulements et des cinétiques réactionnelles : démarches appliquée aux bioprocédés de traitements des effluents. Strasbourg.
Le Bihanic, Fl., 2013. Effets des hydrocarbures aromatiques polycycliques sur les stades précoces de poissons modèles : développement de bioessais et étude comparée de mélanges. Université Bordeaux 1.
Lechat, P., 2006. Pharmacologie niveau DCEM 1.
Lee, Y., Gerrity, D., Lee, M., Bogeat, A.E., Salhi, E., Gamage, S., Trenholm, R.A., Wert, E.C., Snyder, S.A., von Gunten, U., 2013. Prediction of Micropollutant Elimination during Ozonation of Municipal Wastewater Effluents: Use of Kinetic and Water Specific Information. Environ. Sci. Technol. 47, 5872–5881. https://doi.org/10.1021/es400781r

Lee, Y.-S., Lee, S., Lim, J.-E., Moon, H.-B., 2019. Occurrence and emission of phthalates and non-phthalate plasticizers in sludge from wastewater treatment plants in Korea. Science of The Total Environment 692, 354–360. https://doi.org/10.1016/j.scitotenv.2019.07.301

Li, W.C., Wong, M.H., 2012. Interaction of Cd/Zn hyperaccumulating plant (Sedum alfredii) and rhizosphere bacteria on metal uptake and removal of phenanthrene. J. Hazard. Mater. 209–210, 421–433. https://doi.org/10.1016/j.jhazmat.2012.01.055

Li, Y., Sallach, J.B., Zhang, W., Boyd, S.A., Li, H., 2019. Insight into the distribution of pharmaceuticals in soil-water-plant systems. Water Research 152, 38–46. https://doi.org/10.1016/j.watres.2018.12.039

Lindqvist, N., Tuhkanen, T., Kronberg, L., 2005. Occurrence of acidic pharmaceuticals in raw and treated sewages and in receiving waters. Water Research 39, 2219–2228. https://doi.org/10.1016/j.watres.2005.04.003

Literáthy, P., 1975. Study of river pollution caused by micropollutants. Water Research 9, 1001–1003. https://doi.org/10.1016/0043-1354(75)90128-1

Liu, T., Xu, S., Lu, S., Qin, P., Bi, B., Ding, H., Liu, Y., Guo, X., Liu, X., 2019. A review on removal of organophosphorus pesticides in constructed wetland: Performance, mechanism and influencing factors. Science of The Total Environment 651, 2247–2268. https://doi.org/10.1016/j.scitotenv.2018.10.087

López-Jiménez, P.A., Escudero-González, J., Montoya Martínez, T., Fajardo Montañana, V., Gualtieri, C., 2015. Application of CFD methods to an anaerobic digester: The case of Ontinyent WWTP, Valencia, Spain. Journal of Water Process Engineering 7, 131–140. https://doi.org/10.1016/j.jwpe.2015.05.006

Luo, Y., Guo, W., Ngo, H.H., Nghiem, L.D., Hai, F.I., Zhang, J., Liang, S., Wang, X.C., 2014. A review on the occurrence of micropollutants in the aquatic environment and their fate and removal during wastewater treatment. Science of The Total Environment 473–474, 619–641. https://doi.org/10.1016/j.scitotenv.2013.12.065

Macht, F., Eusterhues, K., Pronk, G.J., Totsche, K.U., 2011. Specific surface area of clay minerals: Comparison between atomic force microscopy measurements and bulk-gas (N2) and -liquid (EGME) adsorption methods. Applied Clay Science 53, 20–26. https://doi.org/10.1016/j.clay.2011.04.006

Mahdi, J.G., 2010. Medicinal potential of willow: A chemical perspective of aspirin discovery. Journal of Saudi Chemical Society 14, 317–322. https://doi.org/10.1016/j.jscs.2010.04.010

Maillard, E., Lange, J., Schreiber, S., Dollinger, J., Herbstritt, B., Millet, M., Imfeld, G., 2016. Dissipation of hydrological tracers and the herbicide S-metolachlor in batch and continuous-flow wetlands. Chemosphere 144, 2489–2496. https://doi.org/10.1016/j.chemosphere.2015.11.027

Mali, M., Malcangio, D., Dell' Anna, M.M., Damiani, L., Mastrorilli, P., 2018. Influence of hydrodynamic features in the transport and fate of hazard contaminants within touristic ports. Case study: Torre a Mare (Italy). Heliyon 4, e00494. https://doi.org/10.1016/j.heliyon.2017.e00494

Marçais, J., 2017. Transferts des polluants organiques persistants de l'atmosphère aux milieux aquatiques de montagne (PhD Thesis). Université Grenoble Alpes.

Margot, J., Rossi, L., Barry, D.A., Holliger, C., 2015. A review of the fate of micropollutants in wastewater treatment plants. WIREs Water 2, 457–487. https://doi.org/10.1002/wat2.1090

Marsik, P., Sisa, M., Lacina, O., Motkova, K., Langhansova, L., Rezek, J., Vanek, T., 2017. Metabolism of ibuprofen in higher plants: A model Arabidopsis thaliana cell suspension culture system. Environmental Pollution 220, 383–392. https://doi.org/10.1016/j.envpol.2016.09.074

Martín, J., Santos, J.L., Aparicio, I., Alonso, E., 2015. Pharmaceutically active compounds in sludge stabilization treatments: Anaerobic and aerobic digestion, wastewater stabilization ponds and composting. Science of The Total Environment, Towards a better understanding of the links between stressors, hazard assessment and ecosystem services under water scarcity 503–504, 97–104. https://doi.org/10.1016/j.scitotenv.2014.05.089

Masclet, P., Mouvier, G., Nikolaou, K., 1986. Relative decay index and sources of polycyclic aromatic hydrocarbons. Atmospheric Environment (1967) 20, 439–446. https://doi.org/10.1016/0004-6981(86)90083-1
Masindi, V., Muedi, K.L., 2018. Environmental Contamination by Heavy Metals. Heavy Metals. https://doi.org/10.5772/intechopen.76082
Matamoros, V., Bayona, J.M., 2006. Elimination of Pharmaceuticals and Personal Care Products in Subsurface Flow Constructed Wetlands. Environmental Science & Technology 40, 5811–5816. https://doi.org/10.1021/es0607741
Matamoros, V., García, J., Bayona, J.M., 2008. Organic micropollutant removal in a full-scale surface flow constructed wetland fed with secondary effluent. Water Research 42, 653–660. https://doi.org/10.1016/j.watres.2007.08.016
Matamoros, V., García, J., Bayona, J.M., 2005. Behavior of selected pharmaceuticals in subsurface flow constructed wetlands: a pilot-scale study. Environmental science & technology 39, 5449–5454.
Matamoros, V., Rodríguez, Y., Albaigés, J., 2016. A comparative assessment of intensive and extensive wastewater treatment technologies for removing emerging contaminants in small communities. Water Res. 88, 777–785. https://doi.org/10.1016/j.watres.2015.10.058
Mathon, B., Coquery, M., Miège, C., Vandycke, A., Choubert, J.-M., 2019. Influence of water depth and season on the photodegradation of micropollutants in a free-water surface constructed wetland receiving treated wastewater. Chemosphere 235, 260–270. https://doi.org/10.1016/j.chemosphere.2019.06.140
Meijers, A.P., van der Leer, R.Chr., 1976. The occurrence of organic micropollutants in the river Rhine and the river Maas in 1974. Water Research 10, 597–604. https://doi.org/10.1016/0043-1354(76)90140-8
Mendis, L., 2016. Distribution of Lipids in the Human Brain and their Differential Expression in Alzheimer's Disease: A Matrix-Assisted Laser Desorption/Ionisation-Imaging Mass Spectrometry (MALDI-IMS) Study (Thesis). ResearchSpace@Auckland.
Meunier, B., de Visser, S.P., Shaik, S., 2004. Mechanism of Oxidation Reactions Catalyzed by Cytochrome P450 Enzymes. Chemical Reviews 104, 3947–3980. https://doi.org/10.1021/cr020443g
Michael, I., Rizzo, L., McArdell, C.S., Manaia, C.M., Merlin, C., Schwartz, T., Dagot, C., Fatta-Kassinos, D., 2013. Urban wastewater treatment plants as hotspots for the release of antibiotics in the environment: A review. Water Research 47, 957–995. https://doi.org/10.1016/j.watres.2012.11.027
Miller, E.L., Nason, S.L., Karthikeyan, K.G., Pedersen, J.A., 2016. Root Uptake of Pharmaceuticals and Personal Care Product Ingredients. Environ. Sci. Technol. 50, 525–541. https://doi.org/10.1021/acs.est.5b01546
Ministère de la transition ecologique, n.d. Plan micropolluants 2016-2021 pour préserver la qualité des eaux et la biodiversité.pdf [WWW Document]. URL https://www.ecologique-solidaire.gouv.fr/sites/default/files/Plan%20micropolluants%202016-2021%20pour%20pr%C3%A9server%20la%20qualit%C3%A9%20des%20eaux%20et%20la%20biodiversit%C3%A9.pdf (accessed 7.13.20).
Mitsch, W.J., 2012. What is ecological engineering? Ecological Engineering 45, 5–12. https://doi.org/10.1016/j.ecoleng.2012.04.013
Montiel-León, J.M., Munoz, G., Vo Duy, S., Do, D.T., Vaudreuil, M.-A., Goeury, K., Guillemette, F., Amyot, M., Sauvé, S., 2019. Widespread occurrence and spatial distribution of glyphosate, atrazine, and neonicotinoids pesticides in the St. Lawrence and tributary rivers. Environmental Pollution 250, 29–39. https://doi.org/10.1016/j.envpol.2019.03.125
Moriarty, F., 1983. , Academic Press. London.
Muturi, E.J., Donthu, R.K., Fields, C.J., Moise, I.K., Kim, C.-H., 2017. Effect of pesticides on microbial communities in container aquatic habitats. Scientific Reports 7, 44565. https://doi.org/10.1038/srep44565
Nakada, N., Shinohara, H., Murata, A., Kiri, K., Managaki, S., Sato, N., Takada, H., 2007. Removal of selected pharmaceuticals and personal care products (PPCPs) and endocrine-disrupting

chemicals (EDCs) during sand filtration and ozonation at a municipal sewage treatment plant. Water Research 41, 4373–4382. https://doi.org/10.1016/j.watres.2007.06.038
Neff, J.M., 1979. Polycyclic aromatic hydrocarbons in the aquatic environment: sources, fates and biological effects [WWW Document]. Polycyclic aromatic hydrocarbons in the aquatic environment: sources, fates and biological effects. URL http://bases.bireme.br/cgi-bin/wxislind.exe/iah/online/?IsisScript=iah/iah.xis&src=google&base=REPIDISCA&lang=p&nextAction=lnk&exprSearch=149062&indexSearch=ID (accessed 3.6.18).
Nikolaou, K., Masclet, P., Mouvier, G., 1984. Sources and chemical reactivity of polynuclear aromatic hydrocarbons in the atmosphere — A critical review. Science of The Total Environment 32, 103–132. https://doi.org/10.1016/0048-9697(84)90125-6
Nuel, M., 2017. Devenir de 81 substances médicamenteuses et de leurs métabolites au sein des Zones de Rejet Végétalisées (ZRV) (Génie des Procédés). Strasbourg, Strasbourg.
Nuel, M., Laurent, J., Bois, P., Heintz, D., Mosé, R., Wanko, A., 2017. Seasonal and ageing effects on SFTW hydrodynamics study by full-scale tracer experiments and dynamic time warping algorithms. Chemical Engineering Journal 321, 86–96. https://doi.org/10.1016/j.cej.2017.03.013
Nuel, M., Laurent, J., Bois, P., Heintz, D., Wanko, A., 2018. Seasonal and ageing effect on the behaviour of 86 drugs in a full-scale surface treatment wetland: Removal efficiencies and distribution in plants and sediments. Science of The Total Environment 615, 1099–1109. https://doi.org/10.1016/j.scitotenv.2017.10.061
OpenFoam User Guide, 2007. . URL: http://creativecommons. org/licenses/by-sa/3.0/(last accessed 07.08. 2012).
Ouedraogo, F.R., Zhang, J., Cornejo, P.K., Zhang, Q., Mihelcic, J.R., Tejada-Martinez, A.E., 2016. Impact of sludge layer geometry on the hydraulic performance of a waste stabilization pond. Water Research 99, 253–262. https://doi.org/10.1016/j.watres.2016.05.011
Ouvrard, S., Leglize, P., Morel, J.L., 2014. PAH Phytoremediation: Rhizodegradation or Rhizoattenuation? International Journal of Phytoremediation 16, 46–61. https://doi.org/10.1080/15226514.2012.759527
Parween, T., Jan, S., Mahmooduzzafar, Fatma, T., 2013. Differential Response of Vigna Radiata L. to Varied Doses of Chlorpyrifos. Journal of Plant Nutrition 36, 1565–1577. https://doi.org/10.1080/01904167.2013.799185
Pereira, A.M.P.T., Silva, L.J.G., Meisel, L.M., Lino, C.M., Pena, A., 2015. Environmental impact of pharmaceuticals from Portuguese wastewaters: geographical and seasonal occurrence, removal and risk assessment. Environmental Research 136, 108–119. https://doi.org/10.1016/j.envres.2014.09.041
Pérez-Lemus, N., López-Serna, R., Pérez-Elvira, S.I., Barrado, E., 2019. Analytical methodologies for the determination of pharmaceuticals and personal care products (PPCPs) in sewage sludge: A critical review. Analytica Chimica Acta 1083, 19–40. https://doi.org/10.1016/j.aca.2019.06.044
Persson, J., 2000. The hydraulic performance of ponds of various layouts 2.
Petrie, B., Barden, R., Kasprzyk-Hordern, B., 2015. A review on emerging contaminants in wastewaters and the environment: Current knowledge, understudied areas and recommendations for future monitoring. Water Research 72, 3–27. https://doi.org/10.1016/j.watres.2014.08.053
Petrie, B., Rood, S., Smith, B.D., Proctor, K., Youdan, J., Barden, R., Kasprzyk-Hordern, B., 2018. Biotic phase micropollutant distribution in horizontal sub-surface flow constructed wetlands. Science of The Total Environment 630, 648–657. https://doi.org/10.1016/j.scitotenv.2018.02.242
Petrie, B., Smith, B.D., Youdan, J., Barden, R., Kasprzyk-Hordern, B., 2017. Multi-residue determination of micropollutants in Phragmites australis from constructed wetlands using microwave assisted extraction and ultra-high-performance liquid chromatography tandem mass spectrometry. Analytica Chimica Acta 959, 91–101. https://doi.org/10.1016/j.aca.2016.12.042
Petrović, M., Hernando, M.D., Díaz-Cruz, M.S., Barceló, D., 2005. Liquid chromatography–tandem mass spectrometry for the analysis of pharmaceutical residues in environmental samples: a

review. Journal of Chromatography A 1067, 1–14. https://doi.org/10.1016/j.chroma.2004.10.110
Phillips, P.J., Chalmers, A.T., Gray, J.L., Kolpin, D.W., Foreman, W.T., Wall, G.R., 2012. Combined Sewer Overflows: An Environmental Source of Hormones and Wastewater Micropollutants. Environmental Science & Technology 46, 5336–5343. https://doi.org/10.1021/es3001294
Picó, Y., Alfarham, A., Barceló, D., 2017. Analysis of emerging contaminants and nanomaterials in plant materials following uptake from soils. TrAC Trends in Analytical Chemistry 94, 173–189. https://doi.org/10.1016/j.trac.2017.07.016
Pimentel, D., 1995. Amounts of pesticides reaching target pests: Environmental impacts and ethics. J Agric Environ Ethics 8, 17–29. https://doi.org/10.1007/BF02286399
Pleil, J.D., Isaacs, K.K., 2016. High-resolution mass spectrometry: basic principles for using exact mass and mass defect for discovery analysis of organic molecules in blood, breath, urine and environmental media. J. Breath Res. 10, 012001. https://doi.org/10.1088/1752-7155/10/1/012001
Pokorna, D., Zabranska, J., 2015. Sulfur-oxidizing bacteria in environmental technology. Biotechnology Advances, BioTech 2014 and 6th Czech-Swiss Biotechnology Symposium 33, 1246–1259. https://doi.org/10.1016/j.biotechadv.2015.02.007
Pól, J., Strohalm, M., Havlíček, V., Volný, M., 2010. Molecular mass spectrometry imaging in biomedical and life science research. Histochem Cell Biol 134, 423–443. https://doi.org/10.1007/s00418-010-0753-3
Portail d'informations sur l'assainissement communal - Services en ligne [WWW Document], 2020. URL http://assainissement.developpement-durable.gouv.fr/services.php (accessed 7.13.20).
PROST-BOUCLE, S., BOUTIN, C., 2012. Etat des lieux national des Zones de Rejet Végétalisées 58.
Radjenović, J., Petrović, M., Barceló, D., 2009. Fate and distribution of pharmaceuticals in wastewater and sewage sludge of the conventional activated sludge (CAS) and advanced membrane bioreactor (MBR) treatment. Water Research 43, 831–841. https://doi.org/10.1016/j.watres.2008.11.043
Raghoebarsing, A.A., Pol, A., van de Pas-Schoonen, K.T., Smolders, A.J.P., Ettwig, K.F., Rijpstra, W.I.C., Schouten, S., Damsté, J.S.S., Op den Camp, H.J.M., Jetten, M.S.M., Strous, M., 2006. A microbial consortium couples anaerobic methane oxidation to denitrification. Nature 440, 918–921. https://doi.org/10.1038/nature04617
Ravindra, K., Sokhi, R., Van Grieken, R., 2008. Atmospheric polycyclic aromatic hydrocarbons: Source attribution, emission factors and regulation. Atmospheric Environment 42, 2895–2921. https://doi.org/10.1016/j.atmosenv.2007.12.010
Reddy, K.R., D'Angelo, E.M., 1997. Biogeochemical indicators to evaluate pollutant removal efficiency in constructed wetlands. Water Science and Technology, Wetland Systems for Water Pollution Control 1996 35, 1–10. https://doi.org/10.1016/S0273-1223(97)00046-2
Reeves, R.D., Brooks, R.R., 1983. Hyperaccumulation of lead and zinc by two metallophytes from mining areas of Central Europe. Environmental Pollution Series A, Ecological and Biological 31, 277–285. https://doi.org/10.1016/0143-1471(83)90064-8
Rengers, E.E., da Silva, J.B., Paulo, P.L., Janzen, J.G., 2016. Hydraulic performance of a modified constructed wetland system through a CFD-based approach. Journal of Hydro-environment Research 12, 91–104. https://doi.org/10.1016/j.jher.2016.04.002
Richardson, S.D., 2009. Water Analysis: Emerging Contaminants and Current Issues. Anal. Chem. 81, 4645–4677. https://doi.org/10.1021/ac9008012
Rogers, H.R., 1996. Sources, behaviour and fate of organic contaminants during sewage treatment and in sewage sludges. Sci. Total Environ. 185, 3–26. https://doi.org/10.1016/0048-9697(96)05039-5
Römpp, A., Spengler, B., 2013. Mass spectrometry imaging with high resolution in mass and space. Histochem Cell Biol 139, 759–783. https://doi.org/10.1007/s00418-013-1097-6
Rühmland, S., Wick, A., Ternes, T.A., Barjenbruch, M., 2015. Fate of pharmaceuticals in a subsurface flow constructed wetland and two ponds. Ecological Engineering 80, 125–139. https://doi.org/10.1016/j.ecoleng.2015.01.036
Ruiz, H., 2017. Optimization of French Vertical Flow Treatment Wetlands applied to domestic wastewater treatment for different levels of performances 166.

Samstag, R.W., Ducoste, J.J., Griborio, A., Nopens, I., Batstone, D.J., Wicks, J.D., Saunders, S., Wicklein, E.A., Kenny, G., Laurent, J., 2016. CFD for wastewater treatment: an overview. Water Science and Technology 74, 549–563. https://doi.org/10.2166/wst.2016.249

Sandermann, H., 1999. Plant Metabolism of Organic Xenobiotics. Status and Prospects of the 'Green Liver' Concept, in: Altman, A., Ziv, M., Izhar, S. (Eds.), Plant Biotechnology and In Vitro Biology in the 21st Century: Proceedings of the IXth International Congress of the International Association of Plant Tissue Culture and Biotechnology Jerusalem, Israel, 14–19 June 1998, Current Plant Science and Biotechnology in Agriculture. Springer Netherlands, Dordrecht, pp. 321–328. https://doi.org/10.1007/978-94-011-4661-6_74

Sarabia, L.D., Boughton, B.A., Rupasinghe, T., van de Meene, A.M.L., Callahan, D.L., Hill, C.B., Roessner, U., 2018. High-mass-resolution MALDI mass spectrometry imaging reveals detailed spatial distribution of metabolites and lipids in roots of barley seedlings in response to salinity stress. Metabolomics 14, 63. https://doi.org/10.1007/s11306-018-1359-3

Schollée, J.E., Bourgin, M., von Gunten, U., McArdell, C.S., Hollender, J., 2018. Non-target screening to trace ozonation transformation products in a wastewater treatment train including different post-treatments. Water Research 142, 267–278. https://doi.org/10.1016/j.watres.2018.05.045

Schollée, J.E., Schymanski, E.L., Hollender, J., 2016. Statistical Approaches for LC-HRMS Data To Characterize, Prioritize, and Identify Transformation Products from Water Treatment Processes, in: Drewes, J.E., Letzel, T. (Eds.), ACS Symposium Series. American Chemical Society, Washington, DC, pp. 45–65. https://doi.org/10.1021/bk-2016-1241.ch004

Schuetz, T., Weiler, M., Lange, J., 2012. Multitracer assessment of wetland succession: Effects on conservative and nonconservative transport processes. Water Resources Research 48. https://doi.org/10.1029/2011WR011292

Schwarzenbach, R.P., Escher, B.I., Fenner, K., Hofstetter, T.B., Johnson, C.A., Gunten, U. von, Wehrli, B., 2006. The Challenge of Micropollutants in Aquatic Systems. Science 313, 1072–1077. https://doi.org/10.1126/science.1127291

Schymanski, E.L., Singer, H.P., Longrée, P., Loos, M., Ruff, M., Stravs, M.A., Ripollés Vidal, C., Hollender, J., 2014. Strategies to Characterize Polar Organic Contamination in Wastewater: Exploring the Capability of High Resolution Mass Spectrometry. Environ. Sci. Technol. 48, 1811–1818. https://doi.org/10.1021/es4044374

Schymanski, E.L., Singer, H.P., Slobodnik, J., Ipolyi, I.M., Oswald, P., Krauss, M., Schulze, T., Haglund, P., Letzel, T., Grosse, S., 2015. Non-target screening with high-resolution mass spectrometry: critical review using a collaborative trial on water analysis. Analytical and bioanalytical chemistry 407, 6237–6255.

Shilton, A., Harrison, J., Massey University, Institute of Technology and Engineering, 2003. Guidelines for the hydraulic design of waste stabilisation ponds. Institute of Technology and Engineering, Massey University, Palmerston North, N.Z.

Singhal, N., Perez-Garcia, O., 2016. Degrading Organic Micropollutants: The Next Challenge in the Evolution of Biological Wastewater Treatment Processes. Front. Environ. Sci. 4. https://doi.org/10.3389/fenvs.2016.00036

Sonntag, C. von, Gunten, U. von, 2012. Chemistry of Ozone in Water and Wastewater Treatment. IWA Publishing.

Stefanakis, A.I., Tsihrintzis, V.A., 2012. Effects of loading, resting period, temperature, porous media, vegetation and aeration on performance of pilot-scale vertical flow constructed wetlands. Chemical Engineering Journal 181–182, 416–430. https://doi.org/10.1016/j.cej.2011.11.108

Sukandar, S., Yasuda, K., Tanaka, M., Aoyama, I., 2006. Metals leachability from medical waste incinerator fly ash: A case study on particle size comparison. Environmental Pollution 144, 726–735. https://doi.org/10.1016/j.envpol.2006.02.010

Sumner, L.W., Amberg, A., Barrett, D., Beale, M.H., Beger, R., Daykin, C.A., Fan, T.W.-M., Fiehn, O., Goodacre, R., Griffin, J.L., Hankemeier, T., Hardy, N., Harnly, J., Higashi, R., Kopka, J., Lane, A.N., Lindon, J.C., Marriott, P., Nicholls, A.W., Reily, M.D., Thaden, J.J., Viant, M.R., 2007. Proposed minimum reporting standards for chemical analysis Chemical Analysis Working Group (CAWG) Metabolomics Standards Initiative (MSI). Metabolomics 3, 211–221. https://doi.org/10.1007/s11306-007-0082-2

Sweeney, D.G., Cromar, N.J., Nixon, J.B., Ta, C.T., Fallowfield, H.J., 2003. The spatial significance of water quality indicators in waste stabilization ponds--limitations of residence time distribution analysis in predicting treatment efficiency. Water Sci. Technol. 48, 211–218.
Taylor, D., Senac, T., 2014. Human pharmaceutical products in the environment - the "problem" in perspective. Chemosphere 115, 95–99. https://doi.org/10.1016/j.chemosphere.2014.01.011
Tchounwou, P.B., Yedjou, C.G., Patlolla, A.K., Sutton, D.J., 2012. Heavy Metals Toxicity and the Environment. EXS 101, 133–164. https://doi.org/10.1007/978-3-7643-8340-4_6
Ternes, T., Joss, A., 2007. Human Pharmaceuticals, Hormones and Fragrances. IWA Publishing.
Ternes, T.A., 1998. Occurence of drugs in German sewage treatment plants and rivers1. Water Research 32, 3245–3260.
Tietz, A., Langergraber, G., Watzinger, A., Haberl, R., Kirschner, A.K.T., 2008. Bacterial carbon utilization in vertical subsurface flow constructed wetlands. Water Res. 42, 1622–1634. https://doi.org/10.1016/j.watres.2007.10.011
Tognetti, V.B., Aken, O.V., Morreel, K., Vandenbroucke, K., Cotte, B. van de, Clercq, I.D., Chiwocha, S., Fenske, R., Prinsen, E., Boerjan, W., Genty, B., Stubbs, K.A., Inzé, D., Breusegem, F.V., 2010. Perturbation of Indole-3-Butyric Acid Homeostasis by the UDP-Glucosyltransferase UGT74E2 Modulates Arabidopsis Architecture and Water Stress Tolerance. The Plant Cell 22, 2660–2679. https://doi.org/10.1105/tpc.109.071316
Tröger, R., Köhler, S.J., Franke, V., Bergstedt, O., Wiberg, K., 2020. A case study of organic micropollutants in a major Swedish water source – Removal efficiency in seven drinking water treatment plants and influence of operational age of granulated active carbon filters. Science of The Total Environment 706, 135680. https://doi.org/10.1016/j.scitotenv.2019.135680
Tsuge, J., Hiratsuka, H., Kamimiya, H., Nozaki, H., Kushi, Y., 2008. Glycosphingolipids as a Possible Signature of Microbial Communities in Activated Sludge and the Potential Contribution of Fungi to Wastewater Treatment under Cold Conditions. Bioscience, Biotechnology, and Biochemistry 72, 2667–2674. https://doi.org/10.1271/bbb.80331
Uddin, M., Chen, J., Qiao, X., Tian, R., Zhu, M., 2020. Insight into dynamics and bioavailability of antibiotics in paddy soils by in situ soil moisture sampler. Science of The Total Environment 703, 135562. https://doi.org/10.1016/j.scitotenv.2019.135562
Van der Zee, F.P., Cervantes, F.J., 2009. Impact and application of electron shuttles on the redox (bio)transformation of contaminants: A review. Biotechnology Advances 27, 256–277. https://doi.org/10.1016/j.biotechadv.2009.01.004
Vanderborght, J., Gähwiller, P., Flühler, H., 2002. Identification of Transport Processes in Soil Cores Using Fluorescent Tracers. Soil Science Society of America Journal 66, 774–787. https://doi.org/10.2136/sssaj2002.7740
Verbruggen, N., Hermans, C., Schat, H., 2009. Molecular mechanisms of metal hyperaccumulation in plants. New Phytol. 181, 759–776. https://doi.org/10.1111/j.1469-8137.2008.02748.x
Verlicchi, P., Al Aukidy, M., Zambello, E., 2012. Occurrence of pharmaceutical compounds in urban wastewater: Removal, mass load and environmental risk after a secondary treatment—A review. Science of The Total Environment 429, 123–155. https://doi.org/10.1016/j.scitotenv.2012.04.028
Verlicchi, P., Zambello, E., 2015. Pharmaceuticals and personal care products in untreated and treated sewage sludge: Occurrence and environmental risk in the case of application on soil — A critical review. Science of The Total Environment 538, 750–767. https://doi.org/10.1016/j.scitotenv.2015.08.108
Versteeg, H.K., Malalasekera, W., 2007. An introduction to computational fluid dynamics: the finite volume method, 2nd ed. ed. Pearson Education Ltd, Harlow, England ; New York.
Villette, C., Maurer, L., Delecolle, J., Zumsteg, J., Erhardt, M., Heintz, D., 2019. In situ localization of micropollutants and associated stress response in Populus nigra leaves. Environment International 126, 523–532. https://doi.org/10.1016/j.envint.2019.02.066
Villette, Claire, Maurer, L., Wanko, A., Heintz, D., 2019. Xenobiotics metabolization in Salix alba leaves uncovered by mass spectrometry imaging. Metabolomics 15, 122. https://doi.org/10.1007/s11306-019-1572-8

Villette, C., Zumsteg, J., Schaller, H., Heintz, D., 2018. Non-targeted metabolic profiling of BW312 Hordeum vulgare semi dwarf mutant using UHPLC coupled to QTOF high resolution mass spectrometry. Scientific Reports 8, 13178. https://doi.org/10.1038/s41598-018-31593-1
Vogelsang, C., Grung, M., Jantsch, T.G., Tollefsen, K.E., Liltved, H., 2006. Occurrence and removal of selected organic micropollutants at mechanical, chemical and advanced wastewater treatment plants in Norway. Water Research 40, 3559–3570. https://doi.org/10.1016/j.watres.2006.07.022
Vymazal, J., 2010. Constructed wetlands for wastewater treatment. Ecological Engineering 25, 475–477. https://doi.org/10.1016/j.ecoleng.2005.07.002
Wallace, S., Knight, L., 2006. Feasibility, Design Criteria, and O&M Requirements for Small Scale Constructed Wetland Wastewater Treatment Systems. Water Intelligence Online 5, 9781780403991–9781780403991. https://doi.org/10.2166/9781780403991
Wang, J., Tian, Z., Huo, Y., Yang, M., Zheng, X., Zhang, Y., 2017. Monitoring of 943 organic micropollutants in wastewater from municipal wastewater treatment plants with secondary and advanced treatment processes. Journal of Environmental Sciences. https://doi.org/10.1016/j.jes.2017.09.014
Wang, X.-H., Lin, A.Y.-C., 2012. Phototransformation of Cephalosporin Antibiotics in an Aqueous Environment Results in Higher Toxicity. Environ. Sci. Technol. 46, 12417–12426. https://doi.org/10.1021/es301929e
Warner, W., Licha, T., Nödler, K., 2019. Qualitative and quantitative use of micropollutants as source and process indicators. A review. Science of The Total Environment 686, 75–89. https://doi.org/10.1016/j.scitotenv.2019.05.385
White, D.C., Sutton, S.D., Ringelberg, D.B., 1996. The genus Sphingomonas: physiology and ecology. Curr. Opin. Biotechnol. 7, 301–306. https://doi.org/10.1016/s0958-1669(96)80034-6
Wicklein, E., Batstone, D.J., Ducoste, J., Laurent, J., Griborio, A., Wicks, J., Saunders, S., Samstag, R., Potier, O., Nopens, I., 2016. Good modelling practice in applying computational fluid dynamics for WWTP modelling. Water Sci Technol 73, 969–982. https://doi.org/10.2166/wst.2015.565
Wilcke, W., Krauss, M., Amelung, W., 2002. Carbon Isotope Signature of Polycyclic Aromatic Hydrocarbons (PAHs): Evidence for Different Sources in Tropical and Temperate Environments? Environ. Sci. Technol. 36, 3530–3535. https://doi.org/10.1021/es020032h
Wither, E.D., Brooks, R.R., 1977. Hyperaccumulation of nickel by some plants of Southeast Asia. Journal of Geochemical Exploration 8, 579–583. https://doi.org/10.1016/0375-6742(77)90100-5
World Health Organization, 2010. The WHO recommended classification of pesticides by hazard and guidelines to classification 2009. WHO, Geneva.
World Health Organization Collaborating Centre for Drug Statistics Methodology, 1996. Guidelines for ATC classification and DDD assignment. World Health Organization.
Yao, L., Zhao, J.-L., Liu, Y.-S., Zhang, Q.-Q., Jiang, Y.-X., Liu, S., Liu, W.-R., Yang, Y.-Y., Ying, G.-G., 2018. Personal care products in wild fish in two main Chinese rivers: Bioaccumulation potential and human health risks. Science of The Total Environment 621, 1093–1102. https://doi.org/10.1016/j.scitotenv.2017.10.117
Yin, L., Wang, B., Yuan, H., Deng, S., Huang, J., Wang, Y., Yu, G., 2017. Pay special attention to the transformation products of PPCPs in environment. Emerging Contaminants 3, 69–75. https://doi.org/10.1016/j.emcon.2017.04.001
Zeilinger, S., Gupta, V.K., Dahms, T.E.S., Silva, R.N., Singh, H.B., Upadhyay, R.S., Gomes, E.V., Tsui, C.K.-M., Nayak S, C., 2016. Friends or foes? Emerging insights from fungal interactions with plants. FEMS Microbiol. Rev. 40, 182–207. https://doi.org/10.1093/femsre/fuv045
Zhang, M., Wang, H., 2014. Organic wastes as carbon sources to promote sulfate reducing bacterial activity for biological remediation of acid mine drainage. Minerals Engineering 69, 81–90. https://doi.org/10.1016/j.mineng.2014.07.010
Zhu, F., Wu, X., Zhao, L., Liu, X., Qi, J., Wang, X., Wang, J., 2017. Lipid profiling in sewage sludge. Water Research 116, 149–158. https://doi.org/10.1016/j.watres.2017.03.032
Zimmermann, S.G., Wittenwiler, M., Hollender, J., Krauss, M., Ort, C., Siegrist, H., von Gunten, U., 2011. Kinetic assessment and modeling of an ozonation step for full-scale municipal

wastewater treatment: Micropollutant oxidation, by-product formation and disinfection. Water Research 45, 605–617. https://doi.org/10.1016/j.watres.2010.07.080

Loïc MAURER

Mécanismes de transfert et dynamique d'accumulation d'un spectre large de micropolluants au sein de l'écosystème des filtres plantés et de zones de rejet végétalisées associées.

Résumé

Les filtres plantés de roseaux, filière de traitement privilégiée en France pour traiter les eaux usées en milieu rural, fait face à la problématique des micropolluants. L'étude menée vise à comprendre la distribution et le devenir d'un large spectre de micropolluants dans l'écosystème de ces filières extensives. Pour cela, le profil des micropolluants et du métabolome au sein des différents compartiments (eau, boues, plantes) a été établi par une analyse LC-MS/MS en spectre large. D'autre part pour évaluer, l'infiltration de ces polluants un profil métabolique a été décrit sur la profondeur des boues des filtres plantés. Mais cette distribution spatiale peut également être obtenue à l'échelle de l'organisme afin de comprendre certains bioprocédés. L'utilisation de l'imagerie par spectrométrie de masse a pu mettre en évidence ces localisations et les mécanismes mise en œuvre par les plantes pour faire face à ces polluants. Enfin l'eau demeure le principal vecteur des micropolluants dans l'environnement. Ainsi les données de micropolluants ont été couplées à une modélisation numérique d'écoulement pour comprendre leur distribution au sein de ces systèmes.

LC-HRMS/MS, Imagerie par spectrométrie de masses, ZRV, sludge, micropolluants, CFD, Analyse non ciblée, écosystèmes

Résumé en anglais

Constructed wetland are popular systems used to treat wastewater in rural areas in France. But these systems are facing to the micropollutants issues. This study aims to understand the micropollutants distribution in the wetland ecosystems. Therefore, micropollutants, lipids and plants large scale screening were performed in the wetland ecosystem, as well as in the different sludge layers from the constructed wetland. Nevertheless, the spatial distribution should also be investigated inside the organisms to understand the bioprocesses. The storage and degradation mechanisms to deal with micropollutants has been unveiled using mass spectrometry imaging. Nonetheless, water remains the key vector of micropollutants in the organisms or in the environment. The water distribution should in this way be investigated to explore the micropollutants distribution. Therefore, hydraulics numerical modelling was combined with micropollutants large scale screening to investigate their distribution.

LC-HRMS/MS, MSI, wetland, sludge, micropollutants, CFD, large-scale screening, ecosystems